TECHNISCHE UNIVERSITÄT WIEN
Vienna University of Technology

DISSERTATION

Cooling and Thermalization of One-Dimensional Bosonic Systems

ausgeführt zum Zwecke der Erlangung des akademischen Grades
eines Doktors der Naturwissenschaften

unter der Leitung von
Univ. Prof. Dipl. Ing. Dr. Hannes-Jörg Schmiedmayer
Atominstitut (E141)

und
Dr. Igor E. Mazets
Atominstitut (E141)

eingereicht an der
Technischen Universität Wien
Fakultät für Physik

von
MSc Pjotrs Grišins
Matrikelnummer 1029657
Stadionallee 2, 1020 Wien, Österreich

Wien, 2014

Pjotrs Grišins

Diese Dissertation haben begutachtet:

Jörg Schmiedmayer   Anatoli Polkovnikov

Zusammenfassung

Die Arbeit beschäftigt sich mit der Frage wie, im Fall eindimensionaler Vielteilchensysteme, die klassische Physik aus der Quantenphysik hervorgeht. Der erste Abschnitt klärt die Frage warum die experimentelle Technik des 'evaporativen' Kühlens in eindimensionalen Bose-Einstein Quasikondensaten so effektiv angewandt werden kann obwohl diese Systeme in sehr guter Näherung quantenmechanisch integrabel sind. Basierend auf dem Luttingerflüssigkeitsformalismus präsentiere ich hierfür ein neues Model welches keinen Thermalisierungsmechanismus benötigt und die experimentellen Daten gut beschreibt. Der zweite Teil der Arbeit beschäftigt sich mit der Thermalisierung nach einem Quanten-Quench in einer mesoskopischen eindimensionalen Bose-Hubbard Kette, welche bosonische Atome in einem optischen Gitter beschreibt. In numerischen Simulationen zeige ich wie sich die Thermalisierung am Übergang zu einem integrablen System verhält und versuche aufzuzeigen welche Rolle die Eigenzustandsthermalisierungshypothese, die Verschränkung in der Eigenbasis, Quantenchaos, das verallgemeinerte Gibbs-Ensemble sowie die kinetische Boltzmann-Gleichung spielen.

Abstract

The thesis is structured around the question of how classical physics emerges from the quantum in the case of one-dimensional many-body systems. The first part of the thesis resolves the long-standing issue of why the experimental technique of 'evaporative' cooling is so effective in application to the one-dimensional Bose-Einstein quasicondensate, despite the fact that the latter represents a quantum integrable system to a high degree of accuracy. I present a novel theory based on the Luttinger liquid formalism that explains cooling without any need of thermalization. The theory agrees with experimental data well. The second part concerns thermalization after a quantum quench in a mesoscopic one-dimensional Bose-Hubbard chain, which describes bosonic atoms in optical lattices. Using numerical simulations I show how thermalization proceeds at integrability crossover and try to reveal the role played by the eigenstate thermalization hypothesis, entanglement in the eigenbasis, quantum chaos, generalized Gibbs ensemble, and kinetic Boltzmann equation.

Preface

We know that at the very fundamental level physics is described by the linear equations of quantum mechanics, with the evolution being unitary and time-reversal symmetric. On the other hand, classical world is governed by irreversibility, clearly defining the arrow of time. So a fundamental question arises, how can we recover the classical from the quantum? How does thermodynamics and statistical description emerge from reversible unitary evolution?

For many years these questions remained purely theoretical, but recent experimental progress in the field of quantum optics and atomic physics finally allowed to directly probe the emergence of classical behavior in almost-perfectly controlled isolated quantum environment. In particular, ultracold atomic gases became the modern tool of choice to study macroscopic quantum effects.

This thesis addresses exciting physics of cold atoms in one spacial dimension, as this regime allows to study the whole spectrum of thermalization and out-of-equilibrium phenomena, from the integrable free limit to the complete ergodicity of quantum chaos.

The first chapter is devoted to a process of cooling of a one-dimensional Bose-Einstein quasicondensate. Using analytical model of the Luttinger liquid, I describe a novel mechanism of cooling in an integrable system and show that it doesn't require thermalization. The latter fact is highly counter-intuitive and displays some of the most interesting features of integrable models. In addition, presented theory agrees well with experimental results.

But what if we perturb an integrable system? Will the chaos set in immediately or is there an intermediate semi-integrable phase? This question is addressed in detail in the second chapter, where I present a numerical study of relaxation of ultracold atoms in a one-dimensional optical lattice. I explore the whole spectrum of quantum thermalization, addressing equilibration, initial state independence, entanglement, eigenstate thermalization, emergent generalized Gibbs ensemble and its deformation, and kinetic Boltzmann equation.

Appendices C–E contain additional work in progress on a squeezed Generalized Gibbs ensemble, limitations of truncated Wigner approximation, and ergodic eigenstate thermalization.

I hope that presented study will inspire new breakthroughs in the fascinating interdisciplinary area of non-equilibrium quantum physics with cold atoms.

Contribution. During my post-graduate studies I have been working on several research projects; three of them have been already published, and include numerical and analytical studies of emergent thermalization after a quench in a degenerate 1D Bose gas [1], the dynamics of coupled 1D quasicondensates at finite temperatures [2], and application of the Metropolis-Hastings algorithm to thermal state sampling of a 1D BEC [3]. These three works are attached to the thesis in a special section after the list of references. The thesis incorporates some of the published results, but also includes original research of the author.

Research on cooling of a 1D BEC, reported in Chapter 1, has been done at the Institute of Atomic and Subatomic physics of the Vienna University of Technology in the closest collaboration with Igor E. Mazets, Bernhard Rauer, Tim Langen and Wolfgang Rohringer. My main contribution to the project was analytical description of the cooling quench in terms of the Luttinger liquid model in/out of the trap, explanation of the quasistationary dissipative cooling and preparation of numerical simulations. I greatly benefited from discussions with Jörg Schmiedmayer.

The work on thermalization in a 1D Bose-Hubbard chain, described in the second part, was done mostly independently after the problem was suggested to me by Anatoli Polkovnikov during my secondment stay at Boston University. Shainen Davidson contributed at the early stages of the project with truncated-Wigner and DMRG numerical simulations. While in Boston, my understanding of the rich field of non-equilibrium phenomena grew extensively in discussions with Anatoli, Shainen, and Luca D'Alessio.

Table of Contents

Chapter 1

Cooling of one-dimensional Bose-Einstein quasicondensate

1.1   Introduction

Physicists working in the field of one-dimensional atomic gases know how well the gas can be cooled by the so called 'evaporative cooling' technique, when the trap is being opened from above to let the high-energy particles to escape, reducing in such a way the mean energy per particle. But theoretical understanding of this phenomenon had never been complete, taking into account the fact that a degenerate bosonic gas in 1D represents an integrable quantum system with a high degree of accuracy, meaning that thermalization of the remaining atoms is highly suppressed.

This chapter resolves this long-standing controversy by introducing a new mechanism—*dissipative cooling*—responsible for cooling 1D degenerate gas without any need of thermalization.

Section 1.2 begins with a minimal review of Bose-Einstein condensation (BEC) in the amount necessary to understand the following material. Then I introduce one of the central notions of the theory—the Wigner function—in Section 1.3.

The derivation of the cooling mechanism is based on the Luttinger liquid description and Petrov's generalization, which are presented in Sections 1.4 and 1.5. Discussion on the phenomenon of prethermalization follows in Section 1.6, which will appear to be closely related to the cooling mechanism.

Section 1.10 is devoted to a specific type of a thought experiment, when a density of 1D BEC is quenched down, leaving the phase intact. I show that such a quench leads to temperature decrease and derive scaling laws for the temperature in case of both harmonically trapped and untrapped degenerate gases. In the end I discuss the emergence of a Generalized Gibbs ensemble.

Section 1.11 contains the main results of the chapter. Firstly I explain the conventional evaporative cooling and the reasons why it cannot be applied to 1D quasicondensate. Then I present the atomic loss mechanism and show

how it is connected to the previously considered thought experiment of quench cooling. Finally I show that there is indeed cooling without thermalization by presenting the power-law scaling of temperature, and compare the theory with experimental results.

An impatient reader may skip directly to the conclusions on page 54, where the cooling mechanism is summarized in a few words, as well as the outlook to future studies.

1.2 Bose-Einstein condensates

Bose-Einstein condensation is a phenomenon known for about a century since the works of Bose and Einstein, and brought into the spotlight of modern physics in 1995, when the first Bose-Einstein condensates (BEC) of neutral atoms were experimentally realized [4, 5]. This is a well-established area of research, so I present only the shortest introduction necessary to understand the reported original research. More information on BEC basics can be found in many books and reviews, e.g. [6, 7, 8].

Non-interacting bosons. Basic understanding of condensation phenomena can be gained by considering non-interacting particles.

Bose-Einstein distribution tells us that the number of non-interacting bosons n_i occupying a one-particle state with energy ϵ_i at thermal equilibrium is given by

$$n_i = \frac{1}{e^{(\epsilon_i - \mu)/k_b T} - 1},$$

where μ is the chemical potential, entering the equation as the Lagrange multiplier to ensure the constant total number of particles $N = \sum n_i$.

For a classical gas μ is much less than zero, but as temperature drops, μ increases to the point when it becomes equal to the energy of the lowest lying level $\epsilon_0 = \mu$, which formally leads to divergence of n_0. In fact, this signifies the onset of Bose-Einstein condensation, i.e. macroscopic occupation of a single quantum state ($n_0 \gg n_i$). This lowest-lying single-particle state from now on will be called the *Bose-Einstein condensate*. In fact, μ quantifies how much the system's energy increases when there is another particle added to the condensate. For non-interacting gas it is obviously ϵ_0.

Knowing the density of states $g(\epsilon)$, the number of particles in the excited states is given by

$$N_e = \int_{\epsilon_0}^{\infty} d\epsilon \, g(\epsilon) \, n(\epsilon, \mu, T), \tag{1.1}$$

and the critical temperature T_c of the Bose-Einstein condensation can be calculated from the fact that it is the marginal temperature at which all the particles can still be accommodated in the excited levels $N = N_e(T_c, \mu = 0)$.

For an experimetally relevant case of a 3D condensate in an isotrpoic harmonic trap of angular frequency ω, the density of states $g(\epsilon) \propto \epsilon^2$, and the critical temperature can be calculated as

$$kT_c^{3D} = \frac{\hbar \omega N^{1/3}}{\zeta(3)^{1/3}},$$

where ζ is the Riemann zeta-function [6].

A non-interacting gas can be confined in one dimension in a highly anisotropic trap where the longitudinal trapping frequecy ω is much smaller than the radial one ω_r (for instance, in modern experimental realizations on atomchips, $\omega \sim 2\pi \cdot 10\,\text{Hz}$, $\omega \sim 2\pi \cdot 2000\,\text{Hz}$). Then if the temperature $k_B T$ is small compared to the radial trapping frequency $\hbar\omega_r$, particles occupy only the lowest-energy state of the radial potential, 'freezing' any movement in this direction ($50\,\text{nK}$ corresponds to $\approx 1000\,\text{Hz}$). Energy levels of the longitudinal trap can still be considerably occupied.

Considering the density of states in 1D, which is $g(\epsilon) \propto 1/\sqrt{\epsilon}$ in the case of a box, and $g(\epsilon) = \text{const}$ in a harmonic trap, one can perform integration in (1.1) and easily convince oneself that N_e diverges, meaning that there are always particles in the excited states and that there can be no real condensation in 1D at any finite temperature in thermodynamic limit. Though taking the discreteness of the energy levels into account (which stems from the finite size of the cloud), one can still get macroscopic population of the longitudinal ground state below a critical temperature $T_c^{1D} = \frac{\hbar\omega}{k_B}\frac{N}{\log N}$ [9].

Interacting bosons in 1D.   Non-interacting theory is not sufficient to describe modern experiments, so one has to take into account atomic interactions.

Intaratomic interaction potential is short-range, and we can effectively approximate it as hard-core, where particles interact only locally. Then the first-quantized Hamiltonian for an interacting bosonic gas in 1D reads

$$\hat{H} = \sum_{i=1}^{N}\left(-\frac{\hbar^2}{2m}\frac{\partial^2}{\partial z_i^2} + V(z_i)\right) + \sum_{i<j} g\,\delta(r_i - r_j), \qquad (1.2)$$

where the summation is over all partice locations z_i, m is the mass of one particle, V is the external potential, $g = 2\omega_r a_s$ is the interaction constant [10], and a_s is the scattering length.

In case of a 1D homogeneous system with repulsive interactions $g > 0$, this Hamiltonian is exactly solvable by Bethe ansatz [11, 12] and exhibits several different physical regimes [13].

These regimes can be characterized with two parameters, the first of them being the Lieb-Liniger parameter

$$\gamma = \frac{mg}{\hbar^2 \rho_0},$$

where ρ_0 is the linear density. It measures the typical interaction to kinetic energy ratio. The second one is the degeneracy temperature

$$T_d = \frac{\hbar^2 \rho_0^2}{2m k_B},$$

which is the temperature at which the thermal de Broglie wavelength $\lambda_{dB} = \sqrt{\frac{2\pi\hbar^2}{mk_B T}}$ becomes equal to the average interparticle distance.

At $\gamma > 1$ and $T < T_d\gamma^2$, the gas is in the strongly interacting Tonks-Girardeau regime [14, 15]. There strong repulsion dominates and the particles cannot be found at the same spot, resembling a gas of fermions (more on this in Section 2.3).
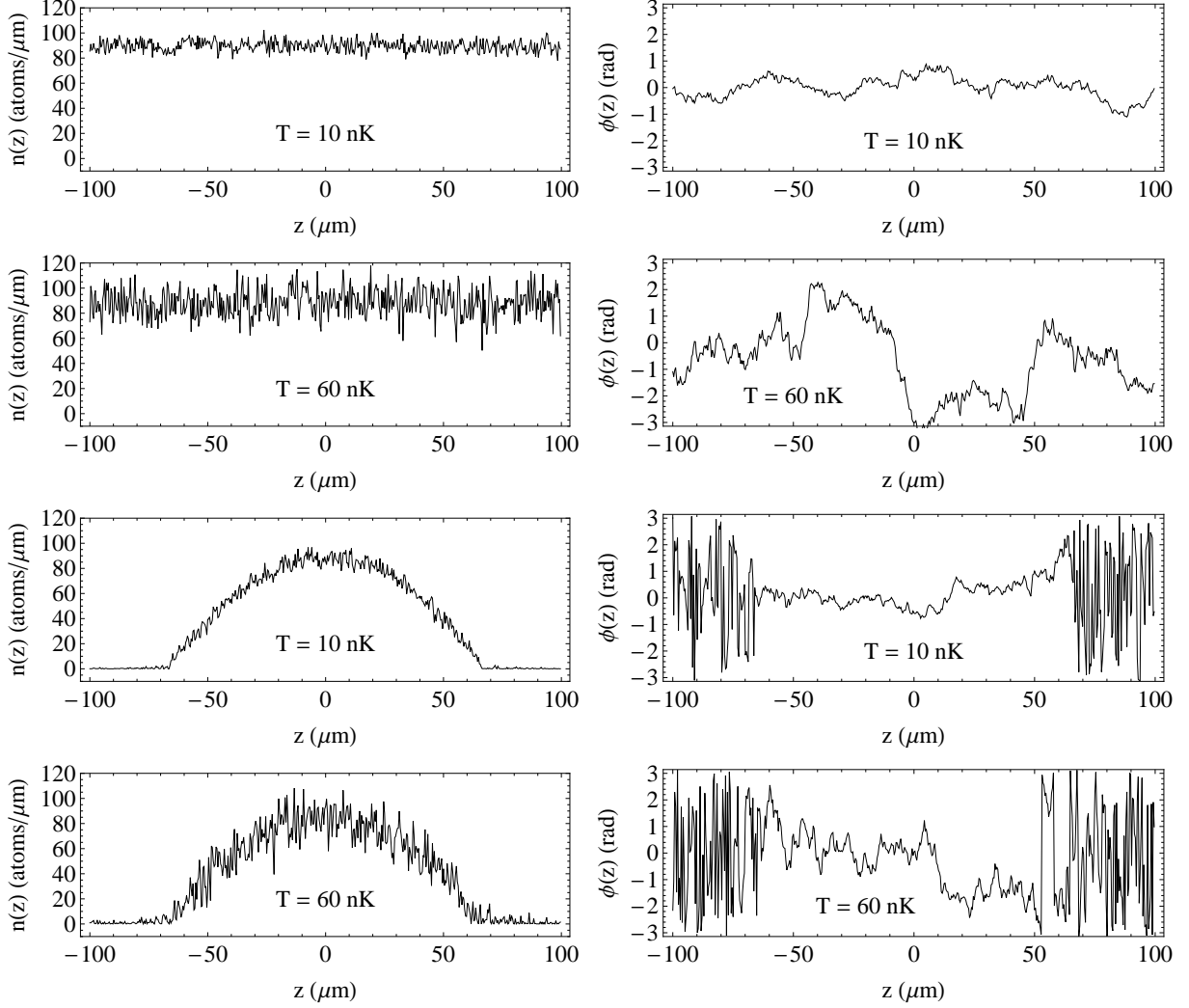
Figure 1.1: Example density (left) and phase profiles (right) for untrapped (top four panels) and harmonically trapped (bottom four panels) ^{87}Ru bosonic gas with the parameters usual for experiments on an atomchip. The quasicondensate regime is evident from large phase fluctuations. Density fluctuations are considerable only on scales smaller than the healing length $\xi \sim 1\,\mu$m, but over larger distances the cloud appears smooth. Intense phase fluctuations at the edge of some figures are due to the fact that there are no atoms there. Profiles acquired through numerical simulations and taken from our published research [3].

At $\gamma < 1$ and $T < T_d\sqrt{\gamma}$ the gas is in the so called *quasicondensate* regime, first predicted by Popov in 1972 [16] and experimentally realized in 2001 [17], where the density fluctuations are suppressed on the length scales larger than the so called healing length $\xi = \sqrt{\hbar^2/mg\rho_0}$. As this is the regime considered in this chapter, the example density and phase profiles of the quasicondensate are presented in Figure 1.1, where $\gamma \sim 0.01$ and $T_d \sim 1000\,\mathrm{nK}$. I consider only the regime where the fluctuations are predominantly thermal $T > T_d\gamma$. 1D quasicondensate will be abbreviated simply as 1D BEC in the following.

Regime of $T > T_d\sqrt{\gamma}$ is not considered here as the gas loses coherence and is characterized by large fluctuations both in phase and density.

The discussion above can be generalized to a trapped inhomogeneous gas as long as the density profile varies sufficiently smoothly. In this so called *local density approximation*, one can treat the gas locally as being untrapped and having γ and T_d given by the local density.

Gross-Pitaevskii equation. Ground state of a quasicondesate can be described by a celebrated Gross-Pitaevskii equation (GPE), which is recovered in the Hartree-Fock approximation by representing the full many-body wavefunction as a product of single-particle functions

$$\Psi(z_1, z_2, \ldots) = \psi(z_1) \cdot \psi(z_2) \cdot \ldots$$

(here I present the 1D case for simplicity, but GPE is valid in any dimension).

One-particle wavefunction is found variationally as the one minimizing the expectation value of the Hamiltonian (1.2) under the normalization condition $\int dz \, |\psi(z)|^2 = N$ and is given by [18, 19]

$$\mu\psi(z) = \left(-\frac{\hbar^2}{2m}\nabla^2 + V(z) + g\rho(z) \right) \psi(z),$$

where the local density $\rho(z) = |\psi(z)|^2$.

Obviously, such a state is stationary and evolves with time as

$$\psi(z, t) = \psi(z, 0)e^{-i\mu t/\hbar}.$$

Gross-Pitaevskii equation can be generalized to a time-dependent variant to study the dynamics and the collective modes of the quasicondensate, when it reads

$$i\hbar\frac{d\psi(z)}{dt} = \left(-\frac{\hbar^2}{2m}\nabla^2 + V(z) + g\rho(z) \right) \psi(z).$$

It is interesting to note that in 1D this non-linear partial differential equation is exactly solvable by the inverse scattering method [20], supproting non-decaying solitonic solutions as well as complete set of local integrals of motion, and was considered in detail in one of the autor's publications [1]. Classical and quantum integrability will be one of the central notions of this thesis and there are special sections devoted to it.

Elementary excitations of the quasicondensate were found by Bogoliubov by representing the wavefunction in terms of stationary and fluctuating parts

$$\psi(z, t) = \psi_0(z, t) + \delta\psi(z, t) = \sqrt{\rho(z)}e^{-i\mu t} + \delta\psi(z, t).$$

Substituting it into GPE and linearizing it to the first order in $\delta\psi$, we can convince ourselves that the latter is satisfied by a trial elementary fluctuation

$$\delta\psi = e^{-i\mu t}[u(z)e^{-i\omega t} - v^*(z)e^{i\omega t}].$$

In the homogeneous system u and v are simply counterpropagating plane waves with momentum q, and the spectrum of elementary excitation is given by

$$\hbar\omega = \epsilon_q = \sqrt{\frac{\hbar^2 q^2}{2m}\left(\frac{\hbar^2 q^2}{2m} + 2g\rho_0\right)}.$$

Note that this dispersion relation is phonon-like at small q: $\epsilon_q = c|q|$, where $c = \sqrt{ng/m}$ is the speed of sound, and particle-like at large q: $\epsilon_q = \hbar^2 q^2/2m$. The crossover happens around the inverse healing length $q \sim \xi^{-1}$. Somehow this dispersion relation can be called anti-relativistic, as for normal relativistic particles the regimes of linear and quadratic dispersion correspond to the opposite limits of q.

Knowing the dispersion relation we see that the quasicondensate satisfies the Landau superfluidity criterion, and an object moving in the quasicondensate at the speed lower than c will move without friction and will not produce excitations.

In Sections 1.4 and 1.5 another formalism to study the elementary excitations of the quasicondensate is addressed in detail, which however is equivalent to Bogoliubov's at length scales larger than ξ.

1D to 3D crossover.   Real experiments are performed with 3D traps, so it is an important question at which parameter regime the gas is really one-dimensional.

Earlier I mentioned that the thermal energy must be smaller than the transverse level spacing, $k_B T < \hbar\omega_r$, but in the interacting condensate the strength of the interaction is characterized by the chemical potential, which must be also small $\mu = g\rho_0 < \hbar\omega_r$.

In such a case the transversal dynamics is frozen out, and the system's wavefunction can be factorized into longitudinal and radial parts $\psi(z,r) = \psi_z(z) \cdot \psi_r(r)$. Radial part can be efficiently described by a variational Gaussian ansatz [13, 21].

In usual experiments with atomchips in a harmonic trap, length scales of variations in local density and external potential are large comparing to phase coherence length, allowing to employ the Thomas-Fermi approximation by neglecting the kinetic energy term in the Gross-Pitaevskii equation [6]. At zero temperature it leads to an inverse parabolic longitudinal density profile.

The condition for the chemical potential naturally limits the maximal densities allowed in 1D experiments, which are about 100 atoms/μm in ^{87}Ru . Though it was theoretically and experimentally proven that quasicondensate picture is still valid in this high-density 1D–3D crossover regime if the chemical potential is corrected as $\mu = \hbar\omega_r(\sqrt{1 + 4\rho_0 a_s} - 1)$ [22, 17, 23].

Temperature measurements.   Temperature is the central topic of this thesis, so it is important to understand the experimentally available tools to measure it.

The most widely used thermometer for 1D BEC is the so called *density ripple* method, when the trap is abruptly switched off, and the gas is allowed to expand freely (the so called *time-of-flight* measurement). The fluctuating phase in the longitudinal direction will lead to appearance of matter interference fringes— the density ripples [24, 25]. Time-of-flight density-density correlation function was proven to map to the initial thermal phase correlation function, given for an untrapped gas by [26, 27]

$$\Re\langle \psi^*(z)\,\psi(z')\rangle = \rho_0\,e^{-|z-z'|/\lambda},$$

where $\lambda = 2\hbar^2\rho_0/mk_BT$ is the thermal coherence length, and the density fluctuations are neglected. Such exponentially decaying correlation function is characteristic to thermal occupation of the quasipartice modes.

1.3   Wigner functions

In the next sections I'll show that a quasicondensate can be represented in terms of quantum harmonic oscillators, and here I introduce the Wigner function as one of the most powerful tools to study (and visualize) harmonic oscillator states.

The Wigner function was introduced in 1932 by Eugene Wigner as a quasiprobability distribution for studying the quantum corrections to classical statistical mechanics [28]. Later in 1949 José Moyal rediscovered the Wigner function and realized that it could be used as a quantum moment-generating functional [29], establishing a whole new way of formulating quantum mechanics—the so called phase-space representation (which nowadays is being used along the more familiar second-quantized and path integral formalisms [30]).

Basically, the Wigner function is a classical real-valued function, completely determined by a density matrix, and classically representing a statistical ensemble given by the latter. For instance, one-particle density matrix in momentum representation $\rho(p,p')$ is mirrored by a W-function

$$W(x,p) = \frac{1}{\pi\hbar} \int \rho(p+q, p-q)e^{-2ixq/\hbar}\,dq.$$

Non-classical features of dynamics are represented by negative values of the W-function, which is clearly not allowed for a proper probability distribution. However, those regions were proven to be small, not extending $\sim \hbar$ area in the phase space (so a straightforward semiclassical approximation would imply smoothening W-function over such an area).

Physical significance of the Wigner function lies in the fact that marginal probabilities are given by 'shadows' of the W-function on the appropriate axis, e.g. probability to find a particle on the line interval $[a,b]$ is

$$P[a \leqslant x \leqslant b] = \int_a^b \int_{-\infty}^{+\infty} W(x,p)\,dp\,dx.$$

Secondly, for a particular case of a free bosonic field (a harmonic oscillator), the averages of symmetrically ordered products of the field operators are given by moments of the W-function in the coherent state basis (which is nothing else
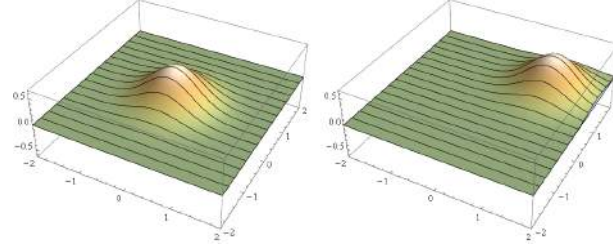
Figure 1.2: Wigner functions of coherent states of a harmonic oscillator.
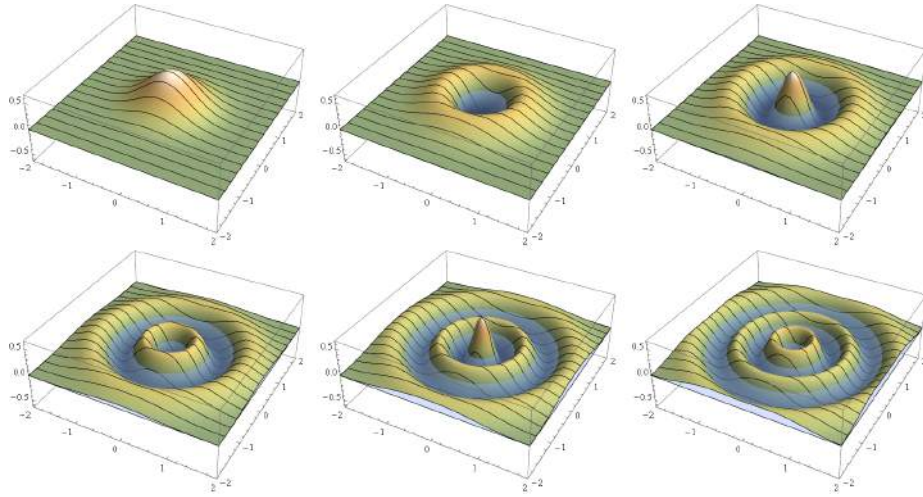
Figure 1.3: Wigner functions of Fock states of a harmonic oscillator containing 0 to 5 bosons (left to right then top to bottom). Sea level represents zero, so landscapes going underwater correspond to highly non-classical states with negative quasiprobability distribution.
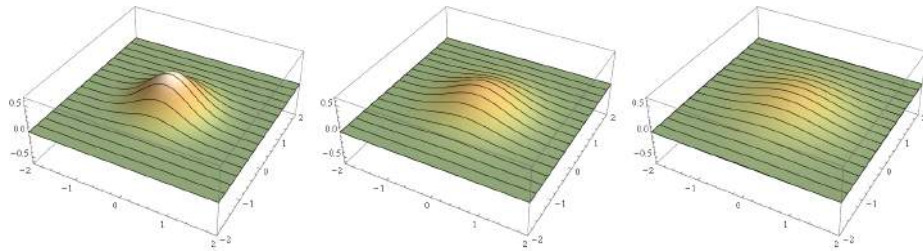
Figure 1.4: Wigner functions of thermal states of a harmonic oscillator at $\sigma = 1/2$, $5/8$ and $3/4$ (left to right), with the corresponding temperatures $k_B T = \hbar\omega / 2 \operatorname{arctanh}\left(1/4\sigma^2\right)$. Note that the vacuum state is a Fock state, a thermal state and a coherent state at the same time.

than a complex rotation of the coordinates: $a = \sqrt{m\omega/2\hbar}\,[x + ip/m\omega]$, $a^* = \sqrt{m\omega/2\hbar}\,[x - ip/m\omega]$), for example

$$\langle \{\hat{a}^\dagger \hat{a}\}_{sym} \rangle = \langle \frac{1}{2}(\hat{a}^\dagger \hat{a} + \hat{a}\hat{a}^\dagger) \rangle = \iint da\, da^*\, aa^*\, W(a, a^*).$$

This formalism is particularly well suited for studies of classical to quantum correspondence and developing semiclassical approximations [31, 32].

As will be shown later, a 1D cold bosonic gas can be formulated in terms of a free bosonic theory, so the free modes can be readily represented by Wigner functions. In this chapter I will mostly consider thermal Wigner functions, which for one mode are given by a Gaussian distribution

$$W(a, a^*) = \frac{1}{2\pi\sigma^2} e^{-\frac{|a|^2}{2\sigma^2}},$$

where the width σ is given by the temperature T

$$\frac{1}{\sigma^2} = 4 \tanh \frac{\hbar\omega}{2k_B T}.$$

At zero temperature $\sigma = 1/2$, which corresponds to a vacuum state having non-zero variance in x and p quadratures in accordance to the Haisenberg uncertainty relation. Note that thermal states are classical in the sense that their W-functions are everywhere positive and represent well-defined probability distributions. Non-classical states, such as Fock states, have $W < 0$ in some parts of the phase space, but we will not encounter them in this chapter. A gallery of common W-functions is presented in Figures 1.2–1.4.

1.4   Tomonaga-Luttinger liquid

Tomonaga-Luttinger liquid (or simply *Luttinger liquid*, abbreviated as LL) is a theoretical model initially developed by Tomonaga [33] and Luttinger [34] to describe interacting electrons in a one-dimensional conductor. Later it was realized by Haldane that the same mechanism can be applied to interacting bosons in 1D [35].

The model.   In the current section I will briefly describe the formalism as applied to bosons following the notation of Cazalilla [36].

First of all let's consider a 1D BEC in a box of length L with periodic boundary conditions, defined by field operators $\hat{\Psi}(z)$ and $\hat{\Psi}^\dagger(z)$, which annihilate or create a particle at position z, and obey standard bosonic commutation relations

$$[\hat{\Psi}(z), \hat{\Psi}^\dagger(z')] = \delta(z - z').$$

The dynamics of a 1D quantum gas interacting via two-body potential $v(z - z')$ is governed by the Hamiltonian

$$\hat{H} = \frac{\hbar^2}{2m} \int_0^L dz\, \partial_z \hat{\Psi}^\dagger(z)\, \partial_z \hat{\Psi}(z) + \frac{1}{2} \int_0^L dz\, dz'\, v(z - z')\hat{\rho}(z)\hat{\rho}(z'), \quad (1.3)$$

where m is the atomic mass and $\hat{\rho}(z) = \hat{\Psi}^\dagger(z)\hat{\Psi}(z)$ is the local density operator.

Phase-density representation of the field operators is defined as follows

$$\hat{\Psi}^\dagger(z) = \sqrt{\hat{\rho}(z)}e^{-i\hat{\phi}(z)} = \sqrt{\rho_0 + \hat{\Pi}(z)}e^{-i\hat{\phi}(z)},$$

where ρ_0 is the mean density, $\hat{\Pi}(z)$ is the local density fluctuation operator and $\hat{\phi}(z)$ is the local phase operator.

It can be proven that phase and density operators are again canonically conjugated if we take their 'slow' parts, meaning that we neglect fluctuations on the scales shorter than the condensate healing length ξ (see [36, Appendix A] for derivation and additional discussion in [26, 37])

$$[\hat{\Pi}(z), \hat{\phi}(z')] = i\delta(z - z').$$

Assuming completely local interaction between particles $v(z - z') = g\,\delta(z - z')$, where g is the interaction strength, we can derive the low-energy effective Hamiltonian in the phase-density representation by leaving only the slowly varying terms in (1.3)

$$\hat{H}_{\text{eff}} = \frac{\hbar c}{2} \int_0^L dz \left[\frac{K}{\pi}(\partial_z \hat{\phi}(z))^2 + \frac{\pi}{K}(\hat{\Pi}(z))^2 \right], \qquad (1.4)$$

where $c = \sqrt{\rho_0 g/m}$ is the speed of sound, and $K = \hbar\pi\sqrt{\rho_0/mg}$ is a dimensionless parameter related to the strength of quantum fluctuations and describing the physical regime of the gas: Tonks-Girardeau (hard-core) gas for $K = 1$, repulsive interactions for $K > 1$ and non-interacting gas for $K = +\infty$. For purely local interaction K cannot decrease below one [27]. For usual experiments with weakly interacting ^{87}Ru atoms $K \sim 50$ [38, 24, 25].

Let's introduce the so-called counting field $\hat{\Theta}(z)$, which changes by π every time z surpasses the location of another particle

$$\frac{1}{\pi}\partial_z \hat{\Theta}(z) = \rho_0 + \hat{\Pi}(z).$$

Then in his pioneering work Tomonaga showed that the counting field $\hat{\Theta}(z)$ and phase field $\hat{\phi}(z)$ can be cast in terms of emergent bosons $[\hat{b}_q, \bar{b}_{q'}] = \delta_{q,q'}$ [33]

$$\hat{\Theta}(z) = \theta_0 + \frac{\pi z}{L}N + \frac{1}{2}\sum_{q\neq 0}\left|\frac{2\pi K}{qL}\right|^{1/2} e^{-a|q|/2}[e^{iqz}\hat{b}_q + e^{-iqz}\hat{b}_q^\dagger],$$

$$\hat{\phi}(z) = \phi_0 + \frac{\pi z}{L}J + \frac{1}{2}\sum_{q\neq 0}\left|\frac{2\pi}{qLK}\right|^{1/2} e^{-a|q|/2}\text{sign}\,q\,[e^{iqz}\hat{b}_q + e^{-iqz}\hat{b}_q^\dagger], \quad (1.5)$$

where N is the total number of particles in the gas, J is the total momentum, θ_0 and ϕ_0 are arbitrary (non-physical) initial phases, $q = (\ldots, -2, -1, 1, 2, \ldots) \cdot \frac{2\pi}{L}$ is the wave number, and a is the high-frequency cutoff.

Taking into account that the total momentum $J = 0$, neglecting the high-frequency cutoff a (which is justified by a natural 'cutoff' due to the exponentially small Bose-Einstein thermal occupation number of the high-lying modes

$\langle b_q^\dagger b_q \rangle$), and taking into account that $\pi\Pi(z) = \nabla\theta(z) = \nabla(\Theta(z) - \pi\rho_0 x)$, we get

$$\pi\hat{\Pi}(z) = \frac{1}{2}\sum_{q\neq 0}\left|\frac{2\pi K}{qL}\right|^{1/2} iq[e^{iqz}\hat{b}_q - e^{-iqz}\hat{b}_q^\dagger],$$

$$\hat{\phi}(z) = \frac{1}{2}\sum_{q\neq 0}\left|\frac{2\pi}{qLK}\right|^{1/2} \text{sign}\, q\, [e^{iqz}\hat{b}_q + e^{-iqz}\hat{b}_q^\dagger]. \tag{1.6}$$

Fourier transforming[1] the fields $f(z) = \frac{1}{\sqrt{L}}\sum e^{iqz}f_q$, we get their momentum components[2]

$$\pi\hat{\Pi}_q = \frac{1}{2}\left|\frac{2\pi K}{q}\right|^{1/2} iq(\hat{b}_q + \hat{b}_{-q}^\dagger),$$

$$\hat{\phi}_q = \frac{1}{2}\left|\frac{2\pi}{qK}\right|^{1/2} \text{sign}\, q\, (\hat{b}_q - \hat{b}_{-q}^\dagger). \tag{1.7}$$

Substituting (1.6) into the Hamiltonian (1.4) casts the latter into a collection of uncoupled harmonic oscillators

$$\hat{H}_{eff} = \sum_{q\neq 0}\hbar\, c|q|\, \bar{b}_q\hat{b}_q + \hat{H}_0, \tag{1.8}$$

where $\hat{H}_0$ is the constant contribution of the macroscopically occupied $q = 0$ mode.

So we see that the Luttinger liquid model describes uncoupled phonon-like excitations. This result is in full agreement with Bogoliubov theory as long as we are limited to length scales larger than the condensate healing length ξ. The only type of low-energy excitations are collective modes and not the individual particle-like ones, so the Fermi liquid theory breaks down in 1D.

Emergent Tomonaga bosons evolve freely under this Hamiltonian

$$\hat{b}_q(t) = e^{-ic|q|t}\hat{b}_q, \quad \bar{b}_q(t) = e^{ic|q|t}\bar{b}_q, \tag{1.9}$$

so dephasing is the only type of relaxation possible. An important application of this dephasing is the phenomenon of *prethermalization* of 1D BEC, which is the topic of Section 1.6. Later we will see that the same dephasing plays its role in cooling of 1D gas.

Temperature regimes of the Luttinger liquid.   Quantum Bose-Einstein statistics has two distinct classical limits: the Rayleigh-Jeans limit, when there is a lot of bosons in each mode $\langle n_q \rangle \gg 1$, and the quantum noise can be neglected and the field can be represented in terms of classical waves; and the Boltzmann limit, where $\langle n_q \rangle \ll 1$, and the system can be approximated by a classical gas of particles. The occupation numbers and mode energies are shown in Figure 1.5.

---

[1]Note that in Matlab the Fourier transform must be implemented as `ffourier = dx/sqrt(L) * fft(f)`, where `dx` is the distance between the grid points.

[2]According to tradition I call q the 'momentum' though it has dimension of inverse length, so a more precise term would be the 'wave number'. It should not lead to any confusion as the correct physical momentum can always be recovered by $p = \hbar q$.
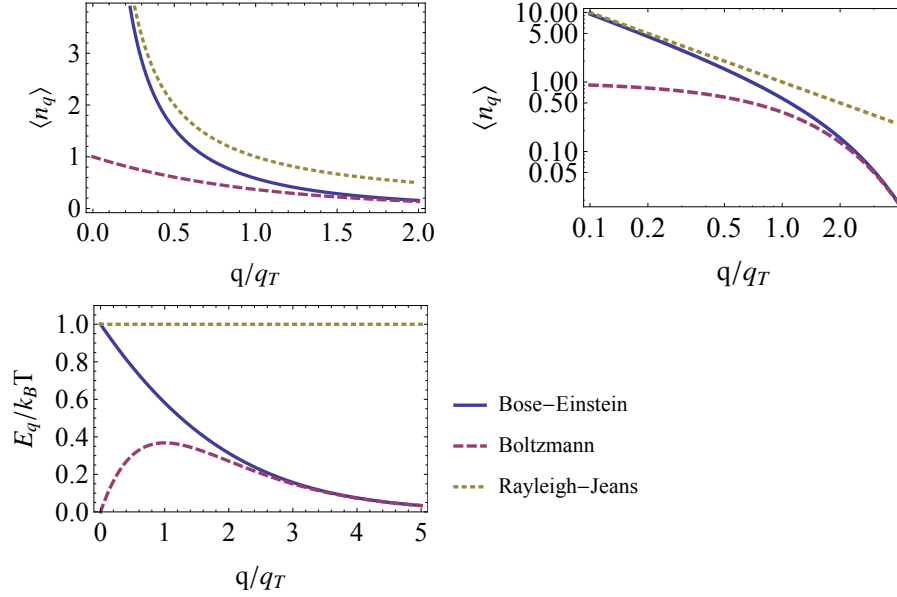
Figure 1.5: Comparison between Bose-Einstein $\langle n_q \rangle = (\exp(\epsilon_q/k_bT)-1)^{-1}$, Boltzmann $\langle n_q \rangle = \exp(-\epsilon_q/k_bT)$ and Rayleigh-Jeans $\langle n_q \rangle = k_bT/\epsilon_q$ distributions, where $\epsilon_q = \hbar c |q|$ is the energy of the mode. Top: mode occupation number as a function of momentum in linear and log-log scales. Bottom: total energy of one mode $E_q = \epsilon_q \langle n_q \rangle$ in units of k_BT as a function of momentum. Momentum is measured in units of thermal momentum $q_T = k_BT/\hbar c$; it is called thermal because a phonon with momentum q_T will have exactly k_BT of energy. Note that the Rayleigh-Jeans distribution describes the classical equipartition (every mode holds the same energy).

Depending on which length scales of the 1D BEC are experimentally achievable, we can probe different limits of the Bose-Einstein distribution. Modern experiments, measuring density correlation in time of flight [25], are currently limited to $\Delta z_{\text{optical}} \approx 1\mu m$ optical resolution. An average healing length, giving the applicability criterion of the LL formalism, in those experiments $\xi \approx 0.3\mu m$, meaning that we are probing only modes well described by the Luttinger theory.

The temperature regime we are able to probe is governed by the quantity q_{optical}/q_T, where $q_{\text{optical}} = 1/\Delta z_{\text{optical}}$ is experimentally achievable momentum and $q_T = k_BT/\hbar c$ is the thermal momentum. Taking an experimental value of the sound speed to be $c = 2600\mu m/s$, we can plot $q_{\text{optical}} = 1/\Delta z_{\text{optical}}$ vs temperature (Figure 1.6). Comparing it to the Figure 1.5 we immediately see that for all experimetally achievable temperatures of $T > 10$ nK we are always deeply in the Rayleigh-Jeans regime.

This observation will be of crucial importance later when I'll be comparing the cooling theory with experimental data.

1.5   Harmonically trapped 1D BEC

In modern experiments cold 1D bosonic gases are usually confined in magnetic/optical traps. For low-energy modes the central region of the cloud, where
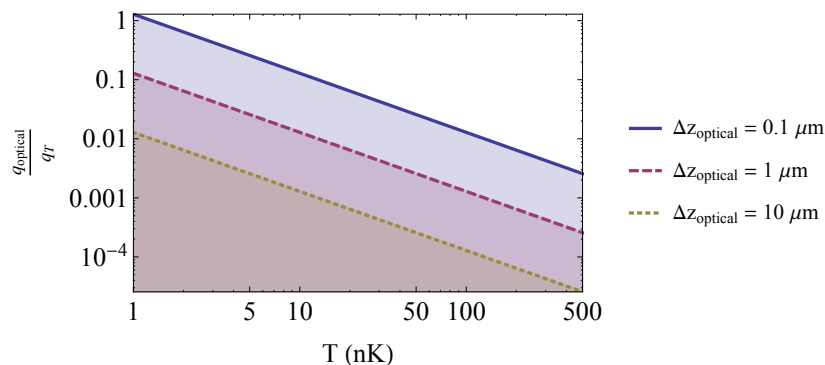
Figure 1.6: Shaded area: achievable momentum range in modern experimens with cold ^{87}Rb gases [24, 25, 39], limited by three different optical resolutions of the apparatus, as a function of temperature in nK for $c = 2600\,\mu m/s$. Comparing it to Figure 1.5, we see that for all experimentally achievable temperatures of $T > 10$ nK, and the optical resolution of 1 μm (middle line), we are always deeply in the Rayleigh-Jeans regime. Though the future technology may lead to increase of the optical resolution, allowing to measure the full Bose-Einstein statistics (top line). Here I imply measurements only in the very center of the cloud, where the local density approximation holds and the homogeneous Luttinger theory is applicable.

its density is almost constant, can be well approximated by the Luttinger theory from the previous section. But in the case of measurements on the cloud as a whole, its inhomogeneous density profile should be taken into account.

So here I review the theory for an experimentally relevant case of a harmonically confined degenerate 1D gas following the work of Petrov, Shlyapnikov and Walraven [40].

As usual, let's introduce the local density $\rho(z)$, central peak density $\rho_0 = \rho(0)$, scattering length a_s, transversal harmonic trap angular frequency ω_r, 1D interaction strength $g = \hbar\omega_r a_s$, longitudinal trapping frequency ω, atomic mass m and global chemical potential $\mu = g\rho_0$. (see Section 1.2 for a review).

Then using the Thomas-Fermi approximation the density profile of the condensate becomes

$$\rho(z) = \rho_0(1 - z^2/R_{TF}^2),$$

where $R_{TF} = \sqrt{2\mu/m\omega^2}$ is the Thomas-Fermi radius.

The phase and density fluctuation operators are given by

$$\hat{\rho}(z) = \rho(z)^{1/2} \sum_{j=1}^{\infty} i f_j^-(z)\hat{b}_j + h.c.,$$

$$\hat{\phi}(z) = [4\rho(z)]^{-1/2} \sum_{j=1}^{\infty} f_j^+(z)\hat{b}_j + h.c., \tag{1.10}$$

where $[\hat{b}_j, \bar{b}_k] = \delta_{jk}$ are the bosonic annihilation/creation operators for quasi-

particles in modes $\{j, k\}$, $f_j^{\pm}(x)$ being the auxiliary functions

$$f_j^{\pm}(x) = \left(\frac{j + 1/2}{R_{TF}}\right)^{1/2} \left[\frac{2\mu}{\epsilon_j}(1 - x^2)\right]^{\pm 1/2} P_j(x), \qquad (1.11)$$

$$x = z/R_{TF},$$

and $P_j(x)$ —the Legendre polynomials.

The spectrum of the quasiparticles is given by

$$\epsilon_j = \hbar\omega\sqrt{j(j+1)/2} = \hbar c\sqrt{j(j+1)}/R, \qquad (1.12)$$

where $c = \sqrt{g\rho_0/m}$ is the speed of sound in the central (homogeneous) region of the cloud, and R is the instantaneous radius (in the non-equilibrium case it can differ from the Thomas-Fermi radius R_{TF}).

Substituting the TF profile into (1.10) and (1.11), we get

$$\hat{\rho}(z) = \rho_0^{1/2} \sum_{j=1}^{\infty} i\left(\frac{j + 1/2}{R_{TF}}\right)^{1/2} \left[\frac{2\mu}{\epsilon_j}\right]^{-1/2} P_j(x)(\hat{b}_j - \hat{b}_j^{\dagger}),$$

$$\hat{\phi}(z) = (4\rho_0)^{-1/2} \sum_{j=1}^{\infty} \left(\frac{j + 1/2}{R_{TF}}\right)^{1/2} \left[\frac{2\mu}{\epsilon_j}\right]^{1/2} P_j(x)(\hat{b}_j + \hat{b}_j^{\dagger}).$$

Decomposing the fluctuations into normal modes and using orthogonality relations for Legendre polynomials, we arrive at

$$\hat{\rho}_j = \int n(x) P_j(x) dx = \rho_0^{1/2} \frac{2i}{2j + 1} \left(\frac{j + 1/2}{R_{TF}}\right)^{1/2} \left[\frac{2\mu}{\epsilon_j}\right]^{-1/2} (\hat{b}_j - \hat{b}_j^{\dagger}),$$

$$\hat{\phi}_j = \int \phi(x) P_j(x) dx = (4\rho_0)^{-1/2} \frac{2}{2j + 1} \left(\frac{j + 1/2}{R_{TF}}\right)^{1/2} \left[\frac{2\mu}{\epsilon_j}\right]^{1/2} (\hat{b}_j + \hat{b}_j^{\dagger}).(1.13)$$

So we see that fluctuations on top of a parabolic Thomas-Fermi profile can be bosonized the very similar way as the fluctuations on a homogenous profile (1.7); the resulting noninteracting Petrov bosons $\hat{b}_j$ are completely analogous to Tomonaga bosons $\hat{b}_q$ (1.9), so discussion from the previous section applies to them fully, including dephasing, prethermalizaton and temperature regimes.

Slight differences between Petrov and Tomonaga bosons include the structure of the spectrum and the fact that momentum $q \in (-\infty, 0) \cup (0, +\infty)$, but mode number $j \in (0, +\infty)$.

1.6 Prethermalization

Prethermalization is a concept first introduced in 2004 by Berges, Borsányi and Wetterich [41] to describe a very interesting and somewhat counter-intuitive out-of-equilibrium phenomenon, when in spite of being far from thermal equilibrium, the system rapidly establishes some properties of a thermal state. Those properties include the equation of state (a constant ratio of pressure over density) and equipartition between kinetic and potential energy, allowing to introduce 'kinetic temperature', proportional to the average kinetic energy per mode. It is crucial that prethermalization establishes on time scales much shorter than

those needed for full thermalization, and in the prethermalized state the mode occupation numbers are far from being populated according to the Bose-Einstein or Fermi-Dirac statistics.

In the original work [41] prethermalization was formulated in the context of high-energy physics and colliding heavy nuclei. Using the analytical technique of two-particle irreducible effective action approach to path integration, the authors were able to show that prethermalizaton timescale is independent of the interaction strength or scattering properties, but is described by 'dephasing' in the basis of non-interacting particles [42].

Applications. Since then the prethermalization description has been applied to many different out-of-equilibrium phenomena outside the high-energy physics, especially in connection with dephasing in (nearly-)integrable models and establishment of the Generalized Gibbs ensemble (GGE). Some notable results in this field include prethermalization in an integrable Lieb-Liniger model [43, 44], Bose-Hubbard and Fermi-Hubbard models [45, 46, 47], as well as in other Hubbard-type lattice models [48], a noisy Ising chain [49], other non-integrable quantum spin chains [50], a weakly non-integrable interacting Peierls insulator [51, 52], and many others. So prethermalizaion opened a new rapidly developing sub-field in the area of out-of-equilibrium physics.

However later the term 'prethermalization' became somewhat fuzzy and currently is often used just as a synonym to 'GGE'. In the current thesis I will use the term 'prethermalization' in its original sense as a more strict notion than GGE. For prethermalization I require the establishment of some sort of global thermal properties with one well-defined temperature, which might be different from the final temperature of the fully thermalized state though.

Prethermalization with cold gases. In the field of cold atomic gases probably the most prominent result on prethermalization was achieved in the laboratories of Schmiedmayer's group, where a pretermalized state was experimentally realized as a result of a sudden splitting of a 1D quasi-BEC [38].

The experimentally realized cigar-shaped 1D quasi-BEC is described in terms of its long-wavelength dynamics in the central region, where the density may be considered almost constant and it can be well approximated with the Luttinger liquid theory. The sudden coherent splitting of the quasi-BEC along its longitudinal z-axis creates two 1D clouds (called *left* and *right*) with almost the same phase and Gaussian noise in density: if we pick a length element Δz of the original condensate containing N atoms, then the splitting can be thought of as atoms randomly jumping to the corresponding Δz element either in the left or in the right cloud. So the probability of the right cloud having M atoms will be, according to the binomial distribution

$$\Pr\left(M;N\right) = \frac{N!}{M!(N-M)!} \cdot 0.5^N,$$

which gives the Gaussian distribution for large enough N.

Labelling the local density operators of the left and the right condensate as $\hat{n}_L(z)$ and $\hat{n}_R(z)$, and phase operators respectively as $\hat{\phi}_L(z)$ and $\hat{\phi}_R(z)$, we can introduce the symmetric and antisymmetric operators of the total L+R system

as

$$\hat{n}^{\pm}(z) = \frac{1}{2}(\hat{n}_L(z) \pm \hat{n}_R(r)), \quad \hat{\phi}^{\pm}(z) = \hat{\phi}_L(z) \pm \hat{\phi}_R(r).$$

Taking into account the fact that the density fluctuations are uncorrelated beyond some small unobservable length scale ξ_s, but exhibit Gaussian noise locally, we get

$$\langle \hat{n}^-(z)\hat{n}^-(z')\rangle = \frac{\rho}{2}\delta(z - z'), \tag{1.14}$$

where ρ is the local density of the BEC before splitting.

Introducing phase and density operators in momentum space $\hat{n}_k^{\pm}, \hat{\phi}_k^{\pm}$ as the Fourier transform of $\hat{n}^{\pm}(z)$ and $\hat{\phi}^{\pm}(z)$, we get

$$\langle \hat{n}_k^- \hat{n}_{k'}^- \rangle = \frac{\rho}{2}\delta_{k,-k'}.$$

This initial state (after splitting) represents a highly out-of-equilibrium (squeezed) state with large fluctuations in average densities $\langle \hat{n}_k^- \hat{n}_{-k}^- \rangle = \rho/2$ and small fluctuations in $\phi_{\pm k}^-$. The density and phase fluctuations in Luttinger formalism can be understood as the conventional quadratures of a harmonic oscillator, so as this initial state evolves, the energy oscillates between them. Oscillation frequency is different for different k, and after a short initial 'dephasing' time, the relative phases of all the oscillators k may be considered random.

Note that the initial state after the splitting has the same energy in each mode $E_k \propto \langle \hat{n}_k^- \hat{n}_{-k}^- \rangle = \rho/2$ according to (1.4), and this energy cannot be redistributed among the different modes as they are uncoupled. The 'classical' temperature in the Rayleigh-Jeans limit can be defined in terms of equipartition: each degree of freedom has to have the same mean energy, a quantity proportional to this mean energy being called the temperature.

So we immediately see that after the splitting, the modes k of the antisymmetric combination of the left and the right clouds are uncorrelated and have the same energy E_k, allowing to define a 'prethermalized' Rayleigh-Jeans temperature $T \propto E_k \propto \rho/2$, which depends on the initial density only, and not on the interaction strength or the initial temperature of the quasicondensate before splitting.

This formalism describes prethermalization in its original sense: we do not get just a steady state, but a steady state that has thermal properties in spite the system being far from equilibrium. Experiments fully confirmed the predictions of the theory [38]. Note that the resulting 'squeezed GGE' is generally different from a conventional GGE, see Figure 1.7 and additional discussion in Appendix C.

More details on the formalism can be found in [43, 53]. A similar mechanism of prethermalization will be developed in the next sections as it will appear to be crucially important to our research concerning cooling of 1D BEC.

Prethermalization and classical chaos. Additionally I would like to note that prethermalization can be understood in terms of completely classical models of non-linear physics [54, 55]. The basic idea is simple: the evolution of a finite-dimensional integrable classical system can be always formulated in terms of the action-angle variables, where the actions, being integrals of motion, stay constant, but phases monotonously increase in time. A sudden change in the Hamiltonian will generally turn on the evolution of the actions to their thermal
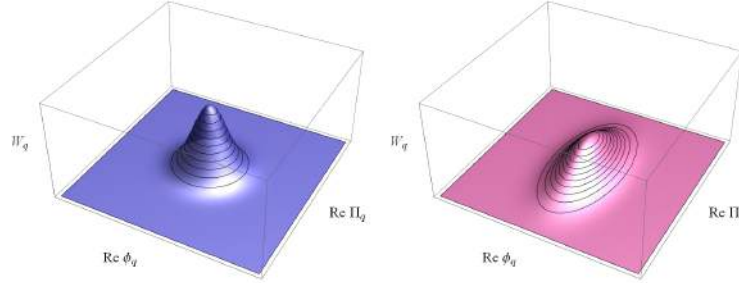
Figure 1.7: Prethemalization. Left: before splitting, each Luttinger mode of the antisymmetric quasicondensate $\hat{\psi}_a = \hat{\psi}_r - \hat{\psi}_l$ is in the vacuum state. Right: after the splitting, the phase quadrature stays almost untouched, but the density quadrature becomes streched because of the Gaussian noise (atoms 'don't know' whether to go to the left or to the right cloud). Note that the Wigner functions are normalized, and the number of bosons per mode is proportional to the width of the distribution.

equilibrium values (assuming the perturbation is sufficiently strong that KAM theorem conditions are not satisfied), giving rise to the thermalization time scale. But in many cases this evolution of the actions is much slower than the winding speed of the angles (the phases), so for one period of phase evolution an appropriate action can be assumed constant. That means that the possible initial alignment of the phases will be almost suddenly disrupted, the actions will appear dephased on a time scale much shorter than the thermalization time scale.

In some special cases prethermalization can be proved to be stemming from this dephasing. For instance, when the unperturbed modes can be approximated by harmonic oscillators, the phases describe the ratios of kinetic to potential energies. Then in the dephased regime we have to take average of all the different phases (as they evolve with different uncorrelated frequencies and their angles become effectively random) and can immediately prove the equipartition between kinetic and potential energies, even if the actions are far from being at their equilibrium values.

1.7 Evaporative cooling

Evaporative cooling is usually the last step to prepare atoms at the lowest temperatures possible. Its main idea can be grasped from looking at a cooling cup of coffee: only the hottest atoms can escape the cup, meaning that the mean energy per remaining atom decreases, and the coffee cools down.

In the case of quantum gases such mechanism was proposed by Hess [56], a comprehensible review can be found in [57, 58]. Schematically this process is represented in Figure 1.8.

In practice one can separately address the high-energy atoms with radio-frequency field (rf-field), which couples the state of trapped atoms to the un-trapped on even anti-trapped state. If this rf-field is detuned in such a way as to
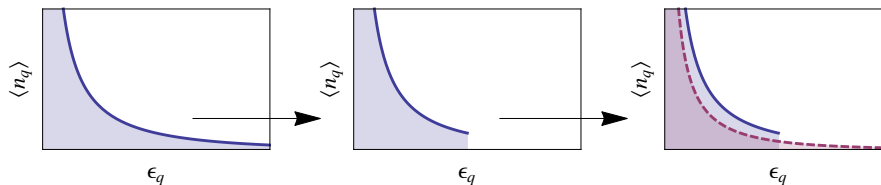
Figure 1.8: Scheme of the conventional 2D and 3D evaporative cooling. Initial Bose-Einstein distribution of mode occupation numbers $\langle n_q \rangle = (\exp[\beta \epsilon_q] - 1)^{-1}$ with energy ϵ_q (left) is deformed by removing high-energy atoms (middle). Then the remaining atoms rethermalize to a BE-distribution at a lower temperature (right, dashed line).

be resonant only with the high-energy atoms (say, having energies higher than some ϵ_t), then only they will be outcoupled and expelled off the trap, which leads to cooling. Low-energy atoms are off-resonant and remain in the trap.

A crucial part of evaporative cooling is rethermalization of remaining atoms (see Figure 1.8, right), when atoms collide and some of them are promoted to energies higher than ϵ_t to be able to escape the trap again. But as the temperature of the gas drops, the number of such promoted atoms drops exponentially $\sim \exp(-\epsilon_t/k_B T)$ [59], so eventually the cooling rate is counterbalanced by always-present heating mechanisms, such as shaking of the trap or collisions with the background gas.

By the moment the experimental technique of evaporative cooling is implemented in almost all setups dealing with cold atoms, including cooling of spin-polarized atomic hydrogen [60], ^{87}Ru atoms on atomchips [61, 62, 24, 63], cooling into double-wells [64, 65, 66, 67] and optical lattices [68, 69], and many others.

Analytical results concentrate mostly on Boltzmann equation approach [70] and include emergent scaling laws in the course of adiabatically trap lowering [71], as well as path integral effective action approaches for rapid cooling [72, 73]. It is conjectured that after rapid cooling Kibble-Zurek phenomena should be observable [74, 75].

Numerical simulations of evaporative cooling include stochastic GPE approaches [37], Monte-Carlo [76, 77] and real-time quantum-dynamical simulations [78].

1.8 Limitations on thermalization in 1D

In spite of all before mentioned successes of the evaporative cooling model, it is not sufficient to explain the cooling of a bosonic gas deeply in 1D regime. The reason being that cold gases in 1D represent a realization of an integrable system to a high degree of accuracy.

1.8.1 Lack of thermalization in free systems.

As we saw in Sections 1.4 and 1.5, 1D gas below degeneracy temperature in Bogoliubov approximation can be cast into a form of a collection of non-interacting harmonic oscillators, realizing the simplest quantum integrable system—a free system. It is obvious that the occupation number of different harmonic modes

stay constant during evolution, meaning that such a system will remember its initial state much better than conventional classically chaotic 3D systems, where the only conserved quantities are energy, momentum and particle number.

And as quasiparticles cannot travel between energy levels, the energy of the system cannot be effectively redistributed to lead to thermalization. In such a way we see that the most essential ingredient of evaporative cooling is missing.

Lack of thermalization in integrable systems is not a novelty, and it has been addressed in a great detail in a series of publications. Some of the most influential studies on the subject were performed by M. Rigol et. al. considering mostly different variants of quenches of one-dimensional hard-core bosons on a lattice, which can be mapped to an integrable free system of spinless fermions by Jordan-Wigner transformation (more on that in Section 2.3). Respectively, numerical experiments showed that indeed an equilibrium state of such a system after a quench retains a lot of information about the initial state and can be described in terms of the generalized Gibbs ensemble [79], which is one of the central topics of Chapter 2.

A beautiful experiment named "the quantum Newton's craddle" confirmed the predictions of the theory. In the experiment a 1D quasicondensate of ultra-cold bosons close to hardcore Tonks-Girardeau regime was split into counter-propagating two clouds, which were made to collide with each other [80]. There was no evidence of redistribution of momenta on long timescales, meaning no thermalization, in full agreement with the theory.

1.8.2 Lack of thermalization in Bethe-ansatz-integrable systems.

The works referenced in the previous paragraph concern the simplest type of integrable models, namely those which are mappable to free systems (such as our model of Tomonaga/Petrov bosons from Section 1.10), but the full description of locally-interacting bosons in 1D is given by the Lieb-Liniger theory, which is integrable via Bethe ansatz and cannot be mapped to a free system, in this sense showing another type of quantum integrability.

For such a system, a description in terms of conserved quasimomenta (rapidities) is possible [81, 82]. But those rapidities are neither local in position space nor constructed with few second-quantized field operators (e.g. in contrast to Jordan-Wigner fermions), and applicability of Generalized Gibbs description for such systems is still an open question [83, 84].

There are studies explicitly addressing lack of thermalization in Lieb-Liniger gas, such as preservation of memory of the initial state in course of relaxation after a quench [44],

Our studies on the classical counterpart of this system, namely the Gross-Pitaevskii equation (integrable via Zakharov-Shabat construction [20]), showed that it doesn't thermalize to a classical thermal equilibrium, but retains some of the information about the initial state [1], confirming the consensus that integrable models don't thermalize completely. Additionally, we saw that provided we started close to a (classical) thermal equilibrium, after relaxation the long-wavelength modes will end up close to equilibrium as well, so for those modes some sort of emergent thermalization can be formulated.

Obviously, the long-wavelength and short-time phenomena of Lieb-Liniger model can be described in terms of Luttinger liquid, in this sense connecting

those two types of integrability classes [85, 36, 86].

Additional studies of the lack of thermalization include quenches in XXZ model [87]

1.8.3 Integrability breaking

Lieb-Liniger model still doesn't describe all the physics of 1D cold bosonic field. Various physical effects limit the applicability of the model and render the system essentially non-integrable. Coupling to an external bath can obviously lead to thermalization [88], but here I'll discuss mechanisms inherent to isolated systems.

One of the proposed integrability breaking mechanisms includes excitations of radial modes due to two-body collisions. Rate of populating radially excited modes can be estimated using Fermi's golden rule and is proportional to the Boltzmann factor for the fraction of atoms in the radial ground state fast enough to scatter out [89]

$$\Gamma_{2b} \propto \exp\left(-\frac{2\hbar\omega_r}{k_B T}\right).$$

In the case of a degenerate gas in 1D, considered in this thesis, $k_B T \approx \frac{1}{2}\hbar\omega_r$, which renders this mechanism of integrability breaking completely irrelevant.

Three-body collision rate is independent of temperature but scales as local density squared, which is way too small to support effective thermalization in the case of experimentally relevant dilute gas. For example, for $n_{1D} = 50\,\text{atoms}/\mu\text{m}$ the thermalization time is estimated to be $\tau_{th} \sim 1\,\text{s}$ [90, 89, 91, 92]. The time scales of 1D cooling are usually ten–hundred times shorter, so in the following we stick to the essential physics of the Lieb-Liniger model.

In addition, I'd like to note that integrability breaking is a novel and rapidly growing subfield of non-equilibrium physics and thorough studies had been performed for many different models, including spinless fermion models, where a prethermalization plateau for few-body observables was reported [51, 93], as well as emergence of Wigner-Dyson level statistics [94]; Ising-like spin chains [95]; and even for only two zero-range-interacting atoms, where the onset of quantum chaos had been found to be responsible for thermalization [96].

The whole Chapter 2 of this thesis is devoted to the problem of thermalization of bosonic gas in 1D optical lattices in the presence of integrability breaking.

1.8.4 Emergence of temperature in 1D BEC

So we have seen that in Bogoliubov approximation to the Lieb-Liniger model the ultracold atomic gas does not thermalize. But what if we go beyond Bogoliubov approximation? What type of relaxation should we expect in a Lieb-Liniger model and its classical analog, the Gross-Pitaevskii equation? Is there any possibility of an emergent temperature for some degrees of freedom despite the integrability of the model?

These are the questions we addressed numerically in one of our previous publications, and the current section builds upon its results [1].

Numerical approach. We start with the Gross-Pitaevskii equation

$$i\hbar\frac{\partial}{\partial t}\Psi(x,t) = -\frac{\hbar^2}{2m}\frac{\partial^2}{\partial x^2}\Psi(x,t) + g|\Psi(x,t)|^2\Psi(x,t),$$

where $\Psi(x,t)$ is a classical complex field representing a quasicondensate of atoms with mass m and g is the effective coupling constant in one dimension (we assume $g > 0$). The interaction strength is characterized by the Lieb-Liniger parameter [11] $\gamma = mg/(\hbar^2\bar{n}) \equiv (\bar{n}\xi)^{-2}$, where ξ is the quasicondensate healing length and $\bar{n} \equiv \langle|\Psi(x,t)|^2\rangle$ is the mean 1D number density (weak interaction limit corresponds to $\gamma \ll 1$). We assume periodic boundary conditions for $\Psi(x,t)$, with the period L being long enough to ensure the loss of correlations over the half period: $\langle\Psi^*(x,t)\Psi(x+L/2,t)\rangle \ll \bar{n}$. The angle brackets denote here averaging over the ensemble of realizations.

For each realization the initial conditions are prepared in a manner similar to the truncated Wigner approach [97, 98] but taking into account thermal fluctuations only (cf. Ref. [99]). We express the macroscopic order parameters in terms of the phase ϕ and density δn fluctuations: $\Psi = (\bar{n} + \delta n)^{1/2}e^{i\phi}$. The initial (at $t = 0$) fluctuations are expanded into plane waves as

$$\delta n(x,0) = 2\sqrt{\bar{n}/L}\sum_{k\neq 0}\beta_k\sqrt{\eta_k/\epsilon_k}\cos(kx+\varpi_k),$$

$$\phi(x,0) = (1/\sqrt{\bar{n}L})\sum_{k\neq 0}\beta_k\sqrt{\epsilon_k/\eta_k}\sin(kx+\varpi_k),$$

where $\epsilon_k = \sqrt{\eta_k(\eta_k + 2g\bar{n})}$ is the energy of the elementary (Bogoliubov) excitation with the momentum $\hbar k$ and $\eta_k = (\hbar k)^2/(2m)$. The real numbers β_k and ϖ_k have the meaning of the scaled amplitude and the offset of the thermally excited elementary wave with the momentum $\hbar k$ at $t = 0$. The values of ϖ_k are taken as (pseudo)random numbers uniformly distributed between 0 and 2π. Each ensemble of realizations is also characterized by a distribution of the β_k values with $\langle\beta_k^2\rangle$ being equal to the main number $\mathcal{N}_0(k)$ of elementary excitation quanta (quasiparticles) in the given mode[1]. In equilibrium at the temperature T the populations of the bosonic quasiparticle modes are given by $\mathcal{N}_{\rm BE}(k,T) = \{\exp[\epsilon_k/(k_{\rm B}T)] - 1\}^{-1}$. For our particular numerical experiments we have taken the classical distribution instead $\mathcal{N}_0(k) = \mathcal{N}_0(-k)$ (equipartition), which is justified for the low momenta, where there is much more than one boson per degree of freedom and so the mode occupation numbers can be approximated by continuous variables.

We found that for a range of initial conditions when the Bogoliubov modes are occupied in a momentum band around $k = 0$ the system develops an effective classical temperature of the low-energy modes. To see it, let's consider the equilibrated mode energies E_k, which are given by

$$E_k = \left\langle \frac{m}{2}\bar{n}|v_k|^2 + \left(\frac{\hbar^2 k^2}{8m\bar{n}} + \frac{g}{2}\right)|\delta n_k|^2 \right\rangle,$$

where δn_k and v_k are the Fourier transforms of the density $\delta n(x,t)$ and velocity $v(x,t) = \frac{\hbar}{m}\frac{\partial\phi}{\partial x}$ fluctuations. Results of the numerical experiment show

---

[1]In our simulations we neglect the fluctuations of β_k and always choose $\beta_k = \sqrt{\mathcal{N}_0(k)}$.
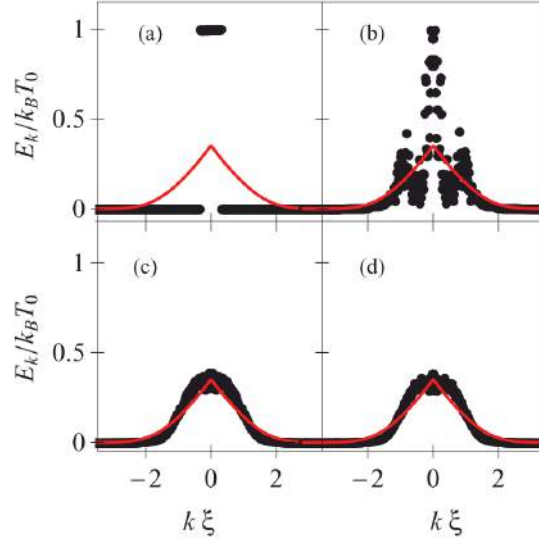
Figure 1.9: An example of an initial state that leads to an emergent temperature of the low energy Bogoliubov modes in classical fields approximation. Dots: mean energies per mode E_k in units of the initial temperature $k_B T_0$ as a function of the wave number k in units of the inversed healing length ξ^{-1} for different times: (a) at $t = 0$ only the modes in a narrow momentum band $|k| < k_0, k_0 \xi = 0.33$ are initialized in thermal states at classical temperature T_0 (equipartition). (b) Complicated evolution at $\tau = g\bar{n}t/\hbar = 50$. (c,d) The steady state at $\tau \sim 3000$ and ~ 6000, where the modes near $k = 0$ hold almost constant energy, which corresponds to classical equipartition at $T_{eq} \approx 0.35 T_0$. The Lieb-Liniger parameter $\gamma = 0.005$, the unit of the reduced time τ is about 0.1 ms in case of weakly interacting 1D gas of ^{87}Ru atoms. Red solid line represents the Bose-Einstein distribution at T_{eq} for reference. The data are averaged over 200 realizations. Units on axes are dimensionless. The figure is taken from our published article [1].

that interaction between Bogoliubov modes lead to the establishment of almost-constant population of the low-lying modes in the stationary state, supporting the claim of the classical equipartion of energy and so the emergence of temperature $k_B T \sim E_k = \epsilon_k \mathcal{N}_k(t)$, where $k \approx 0$ (Figure 1.9, lower panels).

Elementary excitations at different momenta are found to be uncorrelated for all propagation times, i.e., $\langle \delta n_{k'} \delta n_k^* \rangle = \langle |\delta n_k|^2 \rangle \delta_{k\,k'}$ and $\langle v_{k'} v_k^* \rangle = \langle |v_k|^2 \rangle \delta_{k\,k'}$, as expected for a thermal state.

I note that not all the initial conditions lead to the emergence of temperature. A particular counterexample is presented in Figure 1.10.

Integrability of the Gross-Pitaevskii equation as a measure of numerical accuracy. It is well-known that the GPE is integrable by the inverse scattering method [20]. Respectively, there is an isospectral linear operator (Lax operator) associated with the GPE,

$$\hat{L} = \begin{pmatrix} i\partial/\partial\bar{x} & q \\ q^* & -i\partial/\partial\bar{x} \end{pmatrix},$$
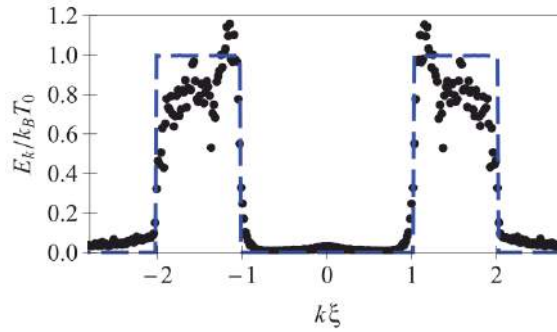
Figure 1.10: An example of an initial state (dashed line, physically representing particle-like excitations propagating in opposite directions) that does not relax to a thermal equilibrium. The equilibrated state at $\tau \sim 20\,000$ is presented with dots. The units and parameters of the simulations are explained in the previous figure. The figure is taken from our published article [1].

where $\bar{x} = x/\xi$ and $q = \bar{n}^{-1/2}\Psi(x,t)$. Its isospectrality during time evolution can be used as a convenient measure of numerical stability (Figure 1.11, left).

In addition, GPE possesses a full set of local integrals of motion, defined recursively

$$I_n = \int_0^L f_n(x)dx,$$

$$f_n = q^* \frac{1}{dx} \frac{1}{q^*} f_{n-1} + \sum_{j+k=n-1} f_j f_k, \qquad f_0 = -|q|^2.$$

First three integrals are proportional to the total particle number I_0, total momentum I_1 and energy I_2. Higher-order integrals of motion don't have a simple physical meaning. A numerical accuracy measure based on the conservation of the integrals of motion is presented in Figure 1.11, bottom.

An independent measure of numerical accuracy is the so called fidelity, defined as $\mathcal{F} = \left|1 - (\bar{n}L)^{-1} \int_0^L dx\, \Psi^*(x,0)\Psi_{\text{fb}}(x,t,-t)\right|$, where $\Psi_{\text{fb}}(x,t,-t)$ is the numerical solution of the GPE with the initial condition $\Psi(x,0)$ first propagated forward in time (up to time t) and then propagated backward over the same time interval. This measure is presented in Figure 1.11, right.

1.8.5 Discussion

In the current section I've showed that when the interaction between the Bogoliubov modes is taken into account, some particular initial conditions exhibit thermalization in the sense of classical equipartition of the low-energy modes, and any observable will show thermal character on long length scales (e.g. the correlation functions on distances $\Delta x \gg \xi$).

Nevertheless, the main topic of this chapter deals with the dissipative cooling of 1D BEC, where the system already starts in a thermal state, which corresponds to the classical equipartition for the low-energy Bogoliubov modes (as long as their occupation number is $\gg 1$). Even if there were some few
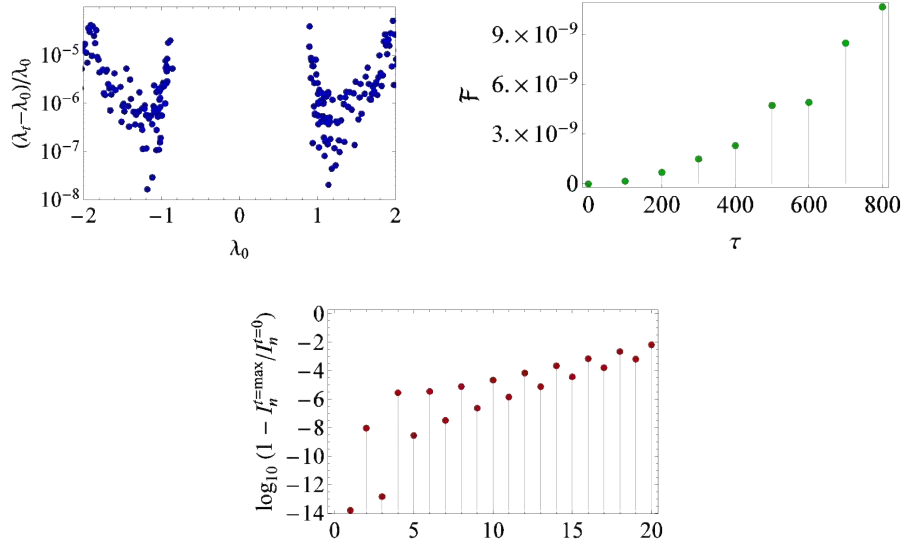
Figure 1.11: Integrability of GPE as a measure of numerical accuracy. **Left.** Lax operator eigenvalue in the steady state λ_t relative error to its value in the initial state λ_0. Isospectrality of the Lax operator assures that $\lambda_t = \lambda_0$ at all times, and a small error is due to numerical algorithm. Lax operator eigenvalues are non-local conserved quantities of classical integrable non-linear equations analogous to the rapidities of the Bethe-ansatz solvable quantum models. **Right.** Fidelity (one minus the Loschmidt echo) as a function of the reduced time τ. $\mathcal{F} = 0$ corresponds to perfect numerical accuracy. **Bottom.** Relative error of the n-th integral of motion (in logarithmic scale) relative to its value in the initial state as a function of the integral number n. I_0, I_1, I_2 are proportional to the total atom number, momentum and energy respectively; higher I_n do not have simple physical meanting. The apparent decrease of accuracy is due to the recurrence relations for the value of the integrals: to compute $(n + 1)$-th integral one have to know the value of the n-th, meaning accumulation of numerical error. In this sense isospectrality of the Lax operator is a better numerical test for convergence of the algorithm. The units and parameters of the simulations are explained in the Figure 1.9.

highly occupied B-modes on top of a thermal background, perturbative calculations show that their decay rate scale with the momentum as $\Gamma_{LL} \propto k^{3/2}$ [100], meaning that this decay is highly suppressed at small momenta and large wavelengths (which are the only ones observed with current experimental technology). For the experiments discussed later in this thesis, lifetime of the modes with wavelength larger that the healing length is estimated to be of the order of 100–300 ms [101], which is still 5–20 times larger than any other relevant time scale, including the cooling time.

So the conclusion is that if we consider the cooling of 1D degenerate gas, not only all the integrability breaking mechanisms are irrelevant (as they enter the game at longer times), but also the interaction of Bogoliubov modes can be safely ignored as long as we stay close to thermal equilibrium, validating the applicability of the Luttinger model.

1.9 Toy models for quantum dissipation

1.9.1 Modified Leggett-Caldeira model

Before we turn to dissipative cooling of 1D BEC, let's consider first a couple of toy models to gain insight.

Perhaps the simplest quantum toy system, where dissipation arises as a consequence of unitary dynamics is the Leggett-Caldeira model [102]. Thorough description of the model can be found in almost any textbook on quantum open systems, e.g. [103].

In this section I introduce the model with a slight modification in the coupling term. The model amounts to having one single quantum harmonic oscillator[1] with the frequency ω and creation/annihilation operators $a^\dagger$ and a, coupled to a bath of harmonic oscillators with frequencies ω_s and field operators $b^\dagger$ and b. But the interaction term involves 'hopping' terms from and into the bath $H_{int} = \sum_s g_s(a^\dagger b_s + b_s^\dagger a)$. Then the Hamiltonian of the model reads

$$H = \omega a^\dagger a + \sum_s g_s(a^\dagger b_s + b_s^\dagger a) + \sum_s \omega_s b_s^\dagger b_s.$$

The model is quadratic, so it allows for an exact solution, and conserves the number of bosonic particles. Physically it may be thought of as a ground level of a trapping potential having energy ω, filled with *non-interacting* bosonic atoms (the number of particles is given by $n = \langle a^\dagger a \rangle$), weakly coupled to the continuum of modes by the real hopping coefficients g_s. For instance, if the bath parameter s represents momentum, and the dispersion relation of the bath is quadratic $\omega_s \propto s^2$, then the Hamiltonian may represent free non-interacting atoms with momenta s escaping from or being trapped into a harmonic trap.

This model is not directly applicable to the 1D BEC, as the Hamiltonian of the latter is not quadratic (interactions are important), but in the next section we will see how the latter could be reduced to a similar system.

If we consider a standard Leggett-Caldeira model (LC), then the system and the bath would be coupled through their x coordinates,

$$H_{int}^{\text{LC}} \propto \sum_s xx_s \propto \sum_s (\omega\omega_s)^{-1/2} \cdot (a^\dagger + a)(b_s^\dagger + b_s) = \sum_s (\omega\omega_s)^{-1/2} \cdot (a^\dagger b_s^\dagger + ab_s^\dagger + a^\dagger b_s + ab_s),$$

which doesn't conserve particle number. I've made use of the standard harmonic oscillator field quadratures

$$x = \sqrt{\hbar/2m\omega}\,(a + a^\dagger), \qquad p = i\sqrt{m\omega\hbar/2}\,(a^\dagger - a),$$

where $m = m_s = \hbar = 1$.

In our modified Leggett-Caldeira model (MLC) the coupling is given by

$$H_{int}^{\text{MLC}} \propto \sum_s (ab_s^\dagger + a^\dagger b_s) \propto \sum_s (\omega\omega_s)^{1/2} xx_s + (\omega\omega_s)^{-1/2} pp_s.$$

So our modification amounts to an additional coupling through the momentum quadrature in comparison to the standard LC model.

---

[1]In the current section I will omit the hats over the operators and set $\hbar = 1$ where it doesn't lead to confusion

If the Hamiltonian is time-independent and the bath modes ω_s are in thermal equilibrium (including the case of $T = 0$, when the bath is initially empty), they can be integrated out exactly using the standard second quantized formalism or the Matsubara technique. Nevertheless, let's solve the system in Keldysh formalism for a possibility to potentially introduce explicit time-dependence. In this section I closely follow and generalize the solution of the Caldeira-Leggett model presented in [104] to the case of complex fields.

The Keldysh action for our system is given by $S = S_0 + S_{bath} + S_{int}$. The first term

$$S_0 = \iint dt \, dt' \, \bar{\phi}^{\mathsf{T}}(t) \, G^{-1}(t, t') \, \phi(t')$$

is the action for a free bosonic field given by the two-component vector

$$\bar{\phi}^{\mathsf{T}} = \left(\begin{array}{cc} \bar{\phi}_{cl} & \bar{\phi}_q \end{array} \right), \qquad \phi = \left(\begin{array}{c} \phi_{cl} \\ \phi_q \end{array} \right),$$

the bar ($^-$) denotes the complex conjugate, and ($^{\mathsf{T}}$) denotes matrix transpose, and ϕ are fields given by the coherent states of $\hat{a}|\phi\rangle = \phi|\phi\rangle$. The Green's function for a free field is given by its causality structure

$$G^{-1} = \left(\begin{array}{cc} 0 & G_A^{-1} \\ G_R^{-1} & G_K^{-1} \end{array} \right), \tag{1.16}$$

with the retarded and advanced components

$$G_{R(A)}^{-1}(\epsilon) = \epsilon - \omega \pm i0, \tag{1.17}$$

$$G_{R(A)}^{-1}(t, t') = \delta(t - t')(i\partial_t' - \omega_0 \pm i0).$$

The Keldysh contrubution G_K^{-1} for a free field is only a regularization and plays no role in continuum notation.

The bath contribution is given by the sum of actions of harmonic oscillators, each of them being completely equivalent to S_0 save the different frequency $\omega \to \omega_s$:

$$S_{bath} = \sum_s \iint dt \, dt' \, \bar{\varphi}_s^{\mathsf{T}}(t) \, G_s^{-1}(t, t') \, \varphi_s(t').$$

The interaction Hamiltonian $H_{int} = \sum_s g_s(a^\dagger b_s + b_s^\dagger a)$ translates into the action coupling ϕ and φ fields

$$S_{int} = \sum_s g_s \int dt \, [(\bar{\phi}_+ \varphi_{+,s} + \phi_+ \bar{\varphi}_{+,s}) - (\bar{\phi}_- \varphi_{-,s} + \phi_- \bar{\varphi}_{-,s})] =$$

$$= \sum_s g_s \int dt \, [\bar{\phi}_{cl} \varphi_{q,s} + \bar{\phi}_q \varphi_{cl,s} + \phi_{cl} \bar{\varphi}_{q,s} + \phi_q \bar{\varphi}_{cl,s}]$$

The interaction is local in time so I have omitted the $\int dt' \, \delta(t - t')$ terms for brevity.

Gaussian integration for φ_s fields can be performed according to

$$Z(\bar{J}, J) = \int \prod_{j=cl,q} d[\bar{\varphi}_j, \varphi_j] \exp \left[-\sum_{i,j=cl,q} \bar{\varphi}_i A_{ij} \varphi_j + \sum_{j=cl,q} (\bar{\varphi}_j J_j + \bar{J}_j \varphi_j) \right] \tag{1.18}$$

$$= \frac{1}{\det A} \exp \left[\sum_{i,j=cl,q} \bar{J}_i (A^{-1})_{ij} J_j \right],$$

where we notice that $J_1 = \phi_q$, $J_2 = \phi_{cl}$ and $A_{ij} = (-G_s^{-1})_{ij}$.

Integrating out the bath degrees of freedom leaves us with the dissipative action for ϕ fields

$$
S_{diss} = -\iint dt\, dt' \begin{pmatrix} \bar{\phi}_q & \bar{\phi}_{cl} \end{pmatrix}_t \left[\sum_s g_s^2 \begin{pmatrix} G_{K,s} & G_{R,s} \\ G_{A,s} & 0 \end{pmatrix}_{t,t'} \right] \begin{pmatrix} \phi_q \\ \phi_{cl} \end{pmatrix}_{t'} =
$$

$$
= -\iint dt\, dt' \begin{pmatrix} \bar{\phi}_{cl} & \bar{\phi}_q \end{pmatrix}_t \left[\sum_s g_s^2 \begin{pmatrix} 0 & G_{A,s} \\ G_{R,s} & G_{K,s} \end{pmatrix}_{t,t'} \right] \begin{pmatrix} \phi_{cl} \\ \phi_q \end{pmatrix}_{t'} =
$$

$$
= \iint dt\, dt'\, \bar{\phi}(t)\, D^{-1}(t,t')\, \phi(t').
$$

The inverse dissipative Green's function has the same causality structure as (1.17):

$$
D^{-1} = \begin{pmatrix} 0 & D_A^{-1} \\ D_R^{-1} & D_K^{-1} \end{pmatrix} = -\sum_s g_s^2 \begin{pmatrix} 0 & G_{A,s} \\ G_{R,s} & G_{K,s} \end{pmatrix}.
$$

Retarded and advanced components of the inverse dissipative Green's function $(D^{-1})_{R/A}$ are given by the respective components of G_s:

$$
D_{R/A}^{-1}(\epsilon) = -\sum_s g_s^2 G_{R/A,s} = -\sum_s \frac{g_s^2}{\epsilon - \omega_s \pm i0} = -\int \frac{d\omega}{\pi} \frac{J(\omega)}{\epsilon - \omega_s \pm i0},
$$

where $J(\omega) = \pi \sum_s g_s^2 \delta(\omega - \omega_s)$ is the spectral density of the bath.

Let's assume a constant coupling with the bath modes $g_s^2 = \gamma$, and the continuum of the latter, allowing to write the spectral density as $J(\omega) = \gamma$, then

$$
D_{R/A}^{-1}(\epsilon) = -\gamma \int \frac{d\omega}{\pi} \frac{1}{\epsilon - \omega_s \pm i0} =
$$

$$
= -\gamma \int \frac{d\omega}{\pi} \left(\frac{1}{\omega - \epsilon} \mp i\pi\delta(\omega - \epsilon) \right) = C \pm i\gamma,
$$

where C is an infinite real constant used to renormalize the potential ('Lamb's shift'). Other choices of the spectral density will lead to a different type of (possibly non-Markovian) dissipation and noise kernels, but won't change the picture qualitatively.

Due to the fact that the loss process is quasistationary and the bath is infinite, the latter can be always assumed to be at thermal equilibrium, which leads to the fluctuation-dissipation theorem for the Keldysh component of the bath Green's function

$$
G_{K,s}(\epsilon) = (G_{R,s}(\epsilon) - G_{A,s}(\epsilon)) \coth \frac{\epsilon}{2T}.
$$

This translates into the same expression for the inverse dissipative Green's function

$$
D_K^{-1}(\epsilon) = (D_R^{-1}(\epsilon) - D_A^{-1}(\epsilon)) \coth \frac{\epsilon}{2T} = 2i\gamma \coth \frac{\epsilon}{2T}.
$$

We are interested in the case where the bath is initially empty, so $T = 0$ and

$$
D_K^{-1}(\epsilon) = 2i\gamma.
$$

In time domain all the components of D^{-1} are local:

$$D_{R/A}^{-1}(t, t') = \pm i\gamma \, \delta(t - t'),$$
$$D_K^{-1}(t, t') = 2i\gamma \, \delta(t - t').$$

Finally substituting the found D into the full action $S = S_0 + S_{diss}$ in time representation and noting that the action is completely time-local, we get

$$S = \int dt \, (\, \bar{\phi}_{cl} \quad \bar{\phi}_q \,) \begin{pmatrix} 0 & i\partial_t - \omega - i\gamma \\ i\partial_t - \omega + i\gamma & 2i\gamma \end{pmatrix} \begin{pmatrix} \phi_{cl} \\ \phi_q \end{pmatrix}. \quad (1.19)$$

If only linear terms in $\phi_q, \bar{\phi}_q$ are kept in the action, the standard saddle-point approximation leads to

$$(i\partial_t - \omega + i\gamma)\phi_{cl}(t) = 0, \quad\quad\quad\quad (1.20)$$
$$(-i\partial_t - \omega - i\gamma)\bar{\phi}_{cl}(t) = 0,$$

leading to the exponential decay of the fields

$$\phi_{cl}(t) = \phi_{cl}(0)e^{-i\omega t - \gamma t}$$
$$\bar{\phi}_{cl}(t) = \bar{\phi}_{cl}(0)e^{i\omega t - \gamma t}.$$

This amounts to the classical approximation, where there is no noise in the fields (the variance is zero); for example, a classical x coordinate of a harmonic oscillator would evolve as $x(t) \propto \bar{\phi}_{cl}(t) + \phi_{cl}(t) \propto e^{-\gamma t} \cos \omega t$, exhibiting damping (friction).

The resulting dissipative action is quadratic again, meaning that it is possible to integrate it exactly and gain access to all the correlation functions of the fields ϕ, including their variance at equal times (fluctuations). But this would imply knowing the initial density matrix of the system.

To keep the discussion as general as possible we can postpone the introduction of the initial density matrix, but instead introduce fluctuations into the classical fields (1.20) by the Hubbard-Stratonovich transformation on the $q - q$ term in the iS, where S is given by (1.19):

$$\exp\left[-2\gamma \int dt |\phi_q|^2\right] = \int D[\xi(t), \bar{\xi}(t)] \exp\left[-\int dt \left(\frac{1}{2\gamma}|\xi(t)|^2 + i\bar{\xi}(t)\phi_q(t) + i\xi(t)\bar{\phi}_q(t)\right)\right].$$

Any observable $O[\bar{\phi}_{cl}, \phi_{cl}]$ of a classical coordinate can be represented as

$$\langle O[\bar{\phi}_{cl}, \phi_{cl}]\rangle = \int D[\forall \phi] O[\bar{\phi}_{cl}, \phi_{cl}] e^{iS[\forall \phi]} =$$

$$= \int D[\xi(t), \bar{\xi}(t)] e^{-\frac{1}{2\gamma} \int dt |\xi(t)|^2} \int D[\bar{\phi}_{cl}, \phi_{cl}] O[\bar{\phi}_{cl}, \phi_{cl}] \times$$

$$\times \int D[\bar{\phi}_q, \phi_q] e^{\bar{\phi}_q[(-\partial_t - i\omega - \gamma)\phi_{cl} - i\xi] + \phi_q[(\partial_t - i\omega + \gamma)\bar{\phi}_{cl} - i\bar{\xi}]}.$$

where $\forall \phi = \{\bar{\phi}_{cl}, \phi_{cl}, \bar{\phi}_q, \phi_q\}$. Integrating over the quantum fields in the last integral gives us the functional delta-function leading to the equation of motion of the classical fields

$$(\partial_t + i\omega + \gamma)\phi_{cl}(t) + i\xi(t) = 0, \quad\quad\quad\quad (1.21)$$
$$(\partial_t - i\omega + \gamma)\bar{\phi}_{cl}(t) - i\bar{\xi}(t) = 0,$$

where the complex terms $\xi, \bar{\xi}$ must be integrated over all possible paths in time with the Gaussian weight $e^{-\frac{1}{2\gamma}\int dt |\xi(t)|^2}$. Gaussian statistics implies that $\xi, \bar{\xi}$ can be represented by correlated complex white noise sources with

$$\langle \bar{\xi}(t)\xi(t')\rangle = 2\gamma\delta(t-t'),$$

and so can be constructed as combinations of two independent real white noise sources η, ζ having the same correlator:

$$\xi(t) = \frac{\eta(t)+i\zeta(t)}{\sqrt{2}}, \qquad \bar{\xi}(t) = \frac{\eta(t)-i\zeta(t)}{\sqrt{2}}.$$

These considerations make (1.21) the Langevin equation, which solution is given by

$$\phi_{cl}(t) = \phi_{cl}(0)e^{(-i\omega-\gamma)t} - i\int_0^t dt'\, \xi(t')\, e^{(-i\omega-\gamma)(t-t')},$$

$$\bar{\phi}_{cl}(t) = \bar{\phi}_{cl}(0)e^{(i\omega-\gamma)t} + i\int_0^t dt'\, \bar{\xi}(t')\, e^{(i\omega-\gamma)(t-t')},$$

$$\langle \bar{\phi}_{cl}(t)\phi_{cl}(t)\rangle = \langle \bar{\phi}_{cl}(0)\phi_{cl}(0)\rangle e^{-2\gamma t} + (1 - e^{-2\gamma t}),$$

$$n(t) = n_0 e^{-2\gamma t},$$

where the last expression is recovered from the classical fields correlator in the Keldysh formalism $\langle \bar{\phi}_{cl}(t)\phi_{cl}(t)\rangle = 2n(t) + 1$.

This result allows us to estimate the validity of purely classical approximation (1.20), when the quantum noise is neglected and the fields correlator is approximated as $\langle \bar{\phi}_{cl}(t)\phi_{cl}(t)\rangle \approx 2n(t)$

$$2n_0\, e^{-2\gamma t} \gg 1 - e^{-2\gamma t},$$

$$2n_0 \gg e^{2\gamma t} - 1,$$

$$\log(2n_0 + 1) \gg 2\gamma t,$$

which means that the initial particle number must be much larger than zero and the observation time must be $t \ll \log(2n_0 + 1)/2\gamma$.

Discussion.   When we couple a harmonic system to a thermal bath, the runaway of energy quanta is inevitably followed by an induced noise due to the fluctuation-dissipation relation. In case of the zero temperature bath the noise is still there, but has not thermal, but quantum character.

In this section I showed the validity of classical approximation for one specific realization of the bath spectral density, which lead to Markovianity of the loss process and subsequent simplification of calculations. Nevertheless, qualitatively the result shouldn't change even for a non-Markovian dissipation kernel, as the fluctuation-dissipation relation is universal.

The result is that the classical approximation completely neglecting the quantum noise is appropriate as long as the initial mode occupation number is big and the time of evolution is short enough $t \ll \log(2n_0 + 1)/2\gamma$, where n_0 is the initial mode occupation number.

Current analysis is not directly applicable to a Bose-Einstein condensate, as the dynamics of the latter is given by a self-interacting (non-quadratic) Hamiltonian. But in the next section I will show at which conditions it can be approximated by a harmonic system by utilizing the Bogoliubov theory.

1.9.2 Dissipative Bose-Hubbard dimer

In this section I consider another toy model which will lead us closer to description of the full Bose-Einstein condensate. Let's introduce a Bose-Hubbard dimer (a double well or a bosonic Josephson junction) given by the Hamiltonian H_0, following the approach of [105].

$$H_0 = -J(a^\dagger b + b^\dagger a) + \frac{U}{2}[(a^\dagger a)^2 + (b^\dagger b)^2],$$

where J is the Josephson hopping parameter, U is the self-interaction energy, and the fields operators a and b destroy a particle in the left and right well respectively. I introduce the full Bose-Hubbard Hamiltonian with more than two sites later in Section 2.3.

To add dissipation I introduce coupling to two different harmonic baths (their harmonicity ensures that particles in the baths are non-interacting), where the coupling and the bath Hamiltonians are given by

$$H_{int} = \sum_s g_s(a^\dagger a_s + a_s^\dagger a) + h_s(b^\dagger b_s + b_s^\dagger b),$$

$$H_{bath} = \sum_s \omega_s a_s^\dagger a_s + \varpi_s b_s^\dagger b_s,$$

with g_s and h_s being the coupling coefficients, field operators a_s and b_s destroy a boson in one or the other baths, and the harmonic frequencies of the bath modes are given by ω_s and ϖ_s.

Physically this system again can be viewed as bosonic particles confined in the two ground states of the double-well potential, but this time the particles are *hard-core interacting*, meaning that it costs energy to put more than one particle in each of the wells. Finite hopping energy J implies that the particles can move between the wells. If we again assume that s is the momentum and $\omega, \varpi \propto s^2$, the coupling Hamiltonian will describe free particles tunneling in and out from the double-well.

The Bogoliubov approximation amounts to introducing the symmetric and antisymmetric field operators

$$c_0 = \frac{a+b}{\sqrt{2}}, \qquad c = \frac{a-b}{\sqrt{2}},$$

and considering the occupation of the symmetric (low-energy) mode to be of the order of the total particle number N. When $N = \text{const}$, it is legitimate to replace the operator c_0 by a real number $\sqrt{N - c^\dagger c} \approx \sqrt{N} - c^\dagger c/2\sqrt{N}$, where only terms up to the second order in c are kept, as due to the spontaneous symmetry breaking c_0 acquires a time-independent phase, which is non-observable and thus can be safely put equal to zero. In time-dependent setting this type of Bogoliubov transformation is questionable. Nevertheless, I'll stick to this definition as we are only interested in the quasistationary regime, when at short times the total particle number can be assumed constant (more on this later).

Then the appropriate parts of the Hamiltonian (up to the second order in

the field operator c) become

$$H_0 = \frac{1}{8}UN^2 - NJ + \left(\frac{1}{2}UN + 2J\right)c^\dagger c + \frac{1}{4}UN(cc + c^\dagger c^\dagger),$$

$$H_{int} = \sum_s g_s \left[(\sqrt{N} - \frac{c^\dagger c}{2\sqrt{N}})(a_s + a_s^\dagger) + a_s c^\dagger + a_s^\dagger c\right] + h_s \left[(\sqrt{N} - \frac{c^\dagger c}{2\sqrt{N}})(b_s + b_s^\dagger) - b_s c^\dagger - b_s^\dagger c\right],$$

$$H_{bath} = \sum_s \omega_s a_s^\dagger a_s + \varpi_s b_s^\dagger b_s.$$

Another simplification can be achieved by considering the two baths completely identical

$$h_s = g_s, \qquad \varpi_s = \omega_s.$$

This allows us to introduce the symmetric and antisymmetric bath field operators

$$d_s = \frac{a_s + b_s}{\sqrt{2}}, \qquad c_s = \frac{a_s - b_s}{\sqrt{2}},$$

and the interaction and bath Hamiltonians become

$$H_{int} = \sum_s g_s \left[(\sqrt{N} - \frac{c^\dagger c}{2\sqrt{N}})d_s + c^\dagger c_s + H.c.\right],$$

$$H_{bath} = \sum_s \omega_s (d_s^\dagger d_s + c_s^\dagger c_s).$$

Interaction Hamiltonian can be simplified further taking into account that after tracing out the bath, terms $c^\dagger c$ would produce quartic terms in the dissipative action $\sim \bar{\phi}\bar{\phi}\phi\phi$, which are not allowed in the Bogoliubov approximation, and the fact that after that the symmetric modes of the bath d_s become coupled to a classical field, so their occupation numbers don't change and their contribution amounts to a constant shift in energy and so can be safely ignored (of course, as long as we are following the Bogoliubov approximation). So

$$H_{int} = \sum_s g_s \left[\sqrt{N}d_s + c^\dagger c_s + H.c.\right] = \sum_s g_s \left[c^\dagger c_s + H.c.\right],$$

$$H_{bath} = \sum_s \omega_s c_s^\dagger c_s.$$

Next I perform the standard Bogoliubov rotation on the fields of the system to diagonalize H_0

$$c = u(t)\gamma - v(t)\gamma^\dagger, \qquad c^\dagger = \bar{u}(t)\gamma^\dagger - \bar{v}(t)\gamma,$$
$$u(t) = \cosh\chi(t), \qquad v(t) = \sinh\chi(t),$$
$$|u(t)|^2 - |v(t)|^2 = 1,$$
$$\tanh 2\chi(t) = \frac{U}{U + 4J/N(t)}.$$

Note that the total number of particles is time-dependent, making our Bogoliubov rotation coefficients time-dependent as well.

In the Bogoliubov basis the Hamiltonian becomes

$$H_0 = \frac{1}{4}UN(N-1) - J(N+1) + \omega(t)\left(\gamma^\dagger\gamma + \frac{1}{2}\right),$$

$$H_{int} = \sum_s g_s[(\bar{u}(t)\gamma^\dagger - \bar{v}(t)\gamma)c_s + H.c.],$$

$$H_{bath} = \sum_s \omega_s c_s^\dagger c_s.$$

Time-dependence of the Bogoliubov rotation coefficients (as well as the frequency of the B-mode ω) will lead to complicated non-Markovian dissipation dynamics. A reasonable first approximation would be to imply that the number of particles N decays so slowly that for short times

$$N, \omega, u, v = \text{const}.$$

I will show that in this quasistationary regime we still recover simple exponential decay of B-mode occupation number in case of Markovian baths.

Introducing the coherent fields

$$\hat{c}_s|\varphi\rangle = \varphi|\varphi\rangle, \qquad \hat{\gamma}|\phi\rangle = \phi|\phi\rangle,$$

we see that despite a complicated interaction term, the Hamiltonian is still quadratic in the operators of the bath, meaning that it's possible to integrate them out exactly. Performing the Gaussian integral (1.18) where A is given by the standard causality structure of the free field (1.16), $\varphi_1 = \varphi_{cl}$, $\varphi_2 = \varphi_q$, and J is given by H_{int}

$$J_1 = u\phi_q - v\bar{\phi}_q, \qquad J_2 = u\phi_{cl} - v\bar{\phi}_{cl}.$$

After integration the dissipative action $D = \bar{J}_i(A^{-1})_{ij}J_j$ will have a similar causality structure as the model from the previous secttion save to additional anomalous correlators

$$D = -\int dt\ (\ \bar{\phi}_{cl}\ \ \bar{\phi}_q\ )\left[\sum_s g_s^2\left(\begin{array}{cc} 0 & |u|^2 G_{A,s} + |v|^2 G_{R,s} \\ |u|^2 G_{R,s} + |v|^2 G_{A,s} & D_K \end{array}\right)\right]\left(\begin{array}{c} \phi_{cl} \\ \phi_q \end{array}\right) -$$

$$-\sum_s g_s^2(G_{R,s} + G_{A,s})(v\bar{u}\,\bar{\phi}_{cl}\bar{\phi}_q + \bar{v}u\,\phi_{cl}\phi_q)$$

Again I took advantage of time-locality of the free field Green's function, which left us with only one time integration. The Keldysh component D_K can be found from the fluctuation-dissipation theorem due to thermality of the bath. Assuming the very same Markovian heat bath as in the previous section, we come to

$$D_R^{-1}(\epsilon) = -\sum_s g_s^2(|u|^2 G_{R,s} + |v|^2 G_{A,s}) = -\sum_s g_s^2\left(\frac{|u|^2}{\epsilon - \omega_s + i0} + \frac{|v|^2}{\epsilon - \omega_s - i0}\right) =$$

$$= -\gamma\int\frac{d\omega}{\pi}\frac{|u|^2}{\epsilon - \omega + i0} + \frac{|v|^2}{\epsilon - \omega - i0} =$$

$$= -\gamma\int\frac{d\omega}{\pi}\left(\frac{|u|^2 + |v|^2}{\omega - \epsilon} - i\pi|u|^2\delta(\omega - \epsilon) + i\pi|v|^2\delta(\omega - \epsilon)\right) =$$

$$= C + i(|u|^2 - |v|^2)\gamma = C + i\gamma.$$

Discussion. As we see the dissipative action in quasistationary approximation resulted in an imaginary constant being added to the energy of the Bogoliubov mode, implying that its occupation number decays exponentially absolutely the same way as for the model of the previous section. The discussion on quantum noise fully applies here as well, meaning that one can approximate the Bogoliubov mode with a classical noiseless field as long as its occupation $\gg 1$. This result is again achieved by postulating a particular effective spectral density of the bath, but the applicability criterion of the classical description should hold due to the universal character of the fluctuation-dissipation theorem, applied to the systems coupled to an equilibrium bath.

Based on this validity criterion we develop a somewhat simpler picture of dissipation of classical matter waves, valid when the loss of atoms is slower than any other relevant time scale. As it will demonstrated later, the classical picture is enough to describe actual experiments with weakly interacting 1D BEC.

On the other hand, when the decay of the condensate mode is not quasistationary, u and v coefficients acquire time dependence and we can expect larger particle number fluctuation in the B-mode. An extreme case would be to outcouple a finite number of atoms instantaneously ($\gamma_N \to \infty$), which is similar to a coherent splitting of a BEC leading to prethermalization [38]. It was proven that such coherent splitting results in fluctuations of the local density of the order of the local density itself. Solution of the full quantum problem and its relation to the instantaneous splitting is a promising direction of future studies.

1.10 Dissipative quench for classical matter waves

1.10.1 Introduction

A quantum quench is an abrupt change of some parameter in the Hamiltonian or in the boundary conditions. Studies of quenches in Luttinger liquid model (LL) have a long and fruitful history. Quenches in LL are especially easy to deal with analytically, as LL represents one of the simplest and purest integrable models—a free system, and arbitrary perturbations to LL Hamiltonian can lead to a whole family of interesting nearly-integrable models. And what is maybe even more important, in recent years it became possible to experimentally realize a bosonic Luttinger model with cold atom setups.

Some of the most recent advancements in the field of LL-quenches include studies of dynamics following a sudden switch-on of interactions [106], an interaction quench with simultaneous switching on of commensurate periodic potential [107], emergent power-laws in the prethermalized regime [108], universal 'rephasing' dynamics [109], quench from Luttinger liquid to Mott insulator [110] and many more. A special case of prethermalziation, described in the previous section, results from a specific type of quench in Luttinger liquid as well [111, 38, 43].

Based on the validity criteria of the classical approximation developed in the previous section, I consider a classical limit of the Luttinger liquid (hydrodynamic regime of 1D cold atomic cloud). In this approximation we neglect non-commutativity of LL field operators and substitute them by complex matter-wave amplitudes.

In this section I report on a specific type of thought experiment, namely a

dissipative density quench, when the cloud density is decreased abruptly, but the phase stays almost unaffected. Such a density quench to my knowledge has never been extensively studied before. The main result of this section will be an apparent *decrease of temperature* after a dissipative density quench, so it can be called a 'quench cooling'.

This type of quench cannot be realized on existing setups used previously to demonstrate prethermalization [38]. In those experiments a 1D ultracold cloud was coherently split along the longitudinal direction, then the two resulting clouds were recombined in time-of-flight measurement to reveal the dynamics of the relative (antisymmetric) phase. But such coherent splitting introduces large density fluctuations in each cloud (1.14), which doesn't lead to temperature decrease [112]. This is due to the shot noise, an intrinsically quantum effect, that cannot be taken into account in the classical matter-wave approximation.

The gedankenexperiment of dissipative quench will be important in understanding cooling of 1D BEC and the mechanism of the dissipative cooling, presented in the next section.

1.10.2 Periodic boundary conditions

To see how such a decrease of temperature is possible, let's consider a sudden density quench in the classical counterpart of the Luttinger liquid Hamiltonian

$$H_{eff} = \sum_{q \neq 0} \hbar \, c|q| \, \bar{b}_q b_q + H_0,$$

where $\bar{b}$ and b are complex numbers representing the amplitude A and phase θ of the corresponding matter waves through the relations $b = Ae^{i\theta}, \bar{b} = Ae^{-i\theta}$, and the bar signifies the complex conjugate. The classical Hamiltonian can be derived from the quantum one (1.8) by the substitution $\hat{b}^\dagger \to \bar{b}, \hat{b} \to b$, meaning that we are neglecting the non-commutativity of the field operators, and have classical waves instead of bosons. Such an approximation is valid as long as the mode occupation numbers $\langle \hat{b}^\dagger \hat{b}_q \rangle \gg 1$, see the discussion in Section 1.9. I'm always considering only the low-energy modes of the 1D BEC where the Luttinger description is sufficient, see Section 1.4 for discussion.

The classical phase and density fluctuations in momentum space read

$$\pi \Pi_q = \frac{1}{2} \left| \frac{2\pi K}{q} \right|^{1/2} iq(b_q + \bar{b}_{-q}),$$

$$\phi_q = \frac{1}{2} \left| \frac{2\pi}{qK} \right|^{1/2} \text{sign}\, q \; (b_q - \bar{b}_{-q}). \tag{1.22}$$

So the state of our classical matter-wave system can be unambiguously defined by a classical probability distribution on Π_q and ϕ_q for all q. Note that this probability distribution is nothing else than the Wigner function in those cases when it's strictly positive (e.g. for thermal states which I'll be considering shortly, see Section 1.3 for details on Wigner functions).

The dissipative density quench happens when the density of the condensate (zeroth mode ρ_0 of the Luttinger liquid Hamiltonian suddenly changes γ times, $\rho_0' = \gamma \rho_0$, and the density fluctuations change α times, $\Pi_q' = \alpha \Pi_q$ ($\forall q \neq 0$). For all experimentally relevant situations the mean density is believed to be

quenched at the same degree as the fluctuations, but it is instructive to carry out the calculations separating these two contributions and letting $\alpha = \gamma$ in the final result.

So after the quench the old and the new variables (1.22) are transformed as

$$\Pi'_q = \alpha \Pi_q, \quad \phi'_q = \phi_q,$$
$$K' = \sqrt{\gamma} K, \quad c' = \sqrt{\gamma} c,$$

as both Luttinger parameter K and the speed of sound c scale as $\sqrt{\rho_0}$.

Decomposing density and phase fluctuation in both the old $\{\bar{b}, b\}$ and the new $\{\bar{\mathfrak{b}}, \mathfrak{b}\}$ basis of Tomonaga waves and taking into account that the basis itself changes due to the changes in the Luttinger parameter and the speed of sound, we get

$$\alpha \frac{1}{2} \left| \frac{2\pi K}{q} \right|^{1/2} iq(b_q + \bar{b}_{-q}) = \frac{1}{2} \left| \frac{2\pi K'}{q} \right|^{1/2} iq(\mathfrak{b}_q + \bar{\mathfrak{b}}_{-q}),$$
$$\frac{1}{2} \left| \frac{2\pi}{qK} \right|^{1/2} \operatorname{sign} q \, (\hat{b}_q - \bar{b}_{-q}) = \frac{1}{2} \left| \frac{2\pi}{qK'} \right|^{1/2} \operatorname{sign} q \, (\mathfrak{b}_q - \bar{\mathfrak{b}}_{-q}),$$

and simplifying

$$\alpha K^{1/2}(b_q + \bar{b}_{-q}) = K'^{1/2}(\mathfrak{b}_q + \bar{\mathfrak{b}}_{-q}),$$
$$K^{-1/2}(b_q - b^\dagger_{-q}) = K'^{-1/2}(\mathfrak{b}_q - \bar{\mathfrak{b}}_{-q}),$$

we get

$$\alpha(b_q + \bar{b}_{-q}) = \gamma^{1/4}(\mathfrak{b}_q + \bar{\mathfrak{b}}_{-q}),$$
$$(b_q - \bar{b}_{-q}) = \gamma^{-1/4}(\mathfrak{b}_q - \bar{\mathfrak{b}}_{-q}).$$

Introducing auxiliary variables

$$A = \frac{1}{2}(\alpha \gamma^{-1/4} + \gamma^{1/4}), \quad B = \frac{1}{2}(\alpha \gamma^{-1/4} - \gamma^{1/4}),$$

we arrive at

$$\mathfrak{b}_q = A b_q + B \bar{b}_{-q}, \qquad \bar{\mathfrak{b}}_q = B b_{-q} + A \bar{b}_q.$$

Note that it is a unitary Bogoliubov transformation only in the case $\alpha = 0$, which correspond to a conventional quantum quench of K and c. We are interested in the case $\alpha \neq 0$, which renders the transformation non-unitary, being the reason why it's called the 'dissipative quench'.

So this particular model cannot be translated back into quantum operator language because after the substitution $\mathfrak{b} \to \hat{\mathfrak{b}}$ the new field operators will not obey the canonical commutation relation $[\hat{\mathfrak{b}}, \hat{\mathfrak{b}}^\dagger] \neq 1$. The physical reason is that we are explicitly neglecting the phase fluctuations: a real quench reducing the variance in the density quadrature will inevitably increase variance in the conjugate phase quadrature due to the Heisenberg uncertainty principle, which in the second quantized formalism expresses itself through the canonical commutation relations. Nevertheless, when the mode occupation number is much

larger than one, it it legitimate to neglect the induced phase noise and say that the phase of the matter wave stays constant.

Now we proceed with the calculation of the mode occupation numbers after the quench:

$$\bar{\mathfrak{b}}_q \mathfrak{b}_q = (Bb_{-q} + A\bar{b}_q)(Ab_q + B\bar{b}_{-q}) =$$
$$= ABb_{-q}b_q + A^2\bar{b}_q b_q + B^2 b_{-q}\bar{b}_{-q} + AB\bar{b}_q\bar{b}_{-q}.$$

Averages in a thermal state read

$$\langle \bar{\mathfrak{b}}_q \mathfrak{b}_q \rangle = (A^2 + B^2)\langle \bar{b}_q b_q \rangle, \tag{1.23}$$

where it was taken into account that $b, \bar{b}$ are complex numbers that commute, the anomalous averages $\langle \bar{b}_q \bar{b}_p \rangle = \langle b_q b_p \rangle = 0$ if $q \neq p \neq 0$, different modes are uncorrelated in the initial state $\langle \bar{b}_q b_{-q} \rangle = 0$, and in the absence of currents $\langle \bar{b}_{-q} b_{-q} \rangle = \langle \bar{b}_q b_q \rangle$.

It is important to note from (1.23) that different q modes do not mix, in the sense that the relative occupation of two modes n_q/n_p stays constant across the quench.

Initial quasiparticle occupation numbers are given by the Bose-Einstein distribution

$$\langle \bar{b}_q b_q \rangle = n_q = (e^{\beta\epsilon_q} - 1)^{-1} \approx \frac{1}{\beta\epsilon_q},$$

where $\epsilon_q = c|q|$ is the energy of the quasiparticle, and the last term is equal to the classical equipartition in the regime of validity of classical fields approximation $(n_q \gg 1)$.

After the quench the occupation numbers become

$$n_q' = (A^2 + B^2)n_q = \frac{\alpha^2 + \gamma}{2\sqrt{\gamma}}n_q.$$

The thermal properties are dependent on the length scale we are observing, and all the low-energy modes, with occupation numbers $n(q), n'(q) \gg 1$ will have a well-defined and equal temperature β' (classical wave limit). We can see it by noticing that the mode energies after the quench become

$$\epsilon_q' = \frac{c'}{c}\epsilon_q = \sqrt{\gamma}\epsilon_q,$$

$$\beta' = \frac{\epsilon}{\epsilon'}\frac{2\sqrt{\gamma}\beta}{\alpha^2 + \gamma} = \frac{2\beta}{\alpha^2 + \gamma},$$
$$T' = T \cdot \frac{\alpha^2 + \gamma}{2},$$
$$\lambda' = \lambda\frac{2\gamma}{\alpha^2 + \gamma},$$

where $\lambda = 2\hbar^2\rho_0\beta/m$ is the thermal coherence length.

So both the quench of the condensate mode and the quench of the density fluctuations have their influence on the final temperature. In the experimentally

relevant case the mean density is quenched at the same rate as the density fluctuations, so $\gamma = \alpha$ and we get (see Figure 1.17)

$$
\boxed{
\begin{aligned}
n_q' &= \frac{1}{2}\sqrt{\alpha}(\alpha + 1)n_q, \\
T' &= T \cdot \frac{\alpha(\alpha + 1)}{2}, \\
\lambda' &= \lambda \cdot \frac{2}{\alpha + 1}.
\end{aligned}
}
\tag{1.24}
$$

1.10.3 Harmonic trap

Density quench. Quenching density α times, we can repeat the calculations of the previous subsection, taking into account resolution of the density and phase fluctuations into Petrov modes before $\{b_j, \bar{b}_j\}$ and after the quench $\{\mathfrak{b}_j, \bar{\mathfrak{b}}_j\}$ (1.13)

$$
\alpha \rho_0^{1/2}\left(\frac{1}{R}\right)^{1/2}\left[\frac{\mu}{\epsilon_j}\right]^{-1/2}(b_j - \bar{b}_j) = \rho_0^{1/2}\left(\frac{1}{R}\right)^{1/2}\left[\frac{\mu}{\epsilon_j}\right]^{-1/2}(\mathfrak{b}_j - \bar{\mathfrak{b}}_j),
$$

$$
(\rho_0)^{-1/2}\left(\frac{j+1/2}{R}\right)^{1/2}\left[\frac{\mu}{\epsilon_j}\right]^{1/2}(b_j + \bar{b}_j) = (\rho_0)^{-1/2}\left(\frac{j+1/2}{R}\right)^{1/2}\left[\frac{\mu}{\epsilon_j}\right]^{1/2}(\mathfrak{b}_j + \bar{\mathfrak{b}}_j).
$$

We simplify further considerations taking $\alpha = \gamma$ from the beginning, meaning that all j modes are quenched at the same rate, including $j = 0$ mode.

Then noticing that $\rho_0 \propto \alpha, \mu \propto \alpha, \epsilon_j \propto c \propto \sqrt{\alpha}$ and keeping the radius constant (because right after splitting the radius does not change) we get

$$
b_j - \bar{b}_j = \alpha^{-3/4}(\mathfrak{b}_j - \bar{\mathfrak{b}}_j),
$$

$$
b_j + \bar{b}_j = \alpha^{-1/4}(\mathfrak{b}_j + \bar{\mathfrak{b}}_j),
$$

which after trivial manipulations reduces precisely to the untrapped case of the previous subsection.

Though immediately after splitting the cloud will start to breathe, with its temperature adiabatically varying as a function of radius

$$
\frac{T(t)}{T(0)} = \left(\frac{R(t)}{R(0)}\right)^{-3/2}.
\tag{1.25}
$$

Theory and experiment in adiabatic breathing are presented in [63], but its physical idea is straightforward: if the dynamics of the condensate is slow comparing to the inverse energy scale between longitudinal energy levels $t \sim 1/\omega$, then we can assume that number of Petrov bosons stays constant during such evolution $\langle n_j \rangle = const$.

In the classical wave limit temperature is given by equipartition, meaning that the total energy of each mode is proportional to the temperature

$$
k_B T(t) = \hbar\omega\sqrt{j(j+1)}\langle n_q \rangle = \hbar c(t)\sqrt{j(j+1)}\langle n_q \rangle / R(t),
$$

so $T(t) \propto c(t)/R(t)$, where $c(t) \propto \sqrt{\rho_0(t)}$ is the instantaneous speed of sound in the center of the cloud. Finally we notice that given the constant total number

of particles N, central density scales as $\rho_0(t) \propto 1/R(t)$, assuming self-similar shape change of the cloud during breathing. Combining all the scaling laws we recover (1.25) as $T(t) \propto c(t)/R(t) \propto \sqrt{\rho_0(t)}/R(t) \propto R(t)^{-3/2}$.

Sudden density and radius quench. A trapped condensate is somewhat a more complicated object than a plain Luttinger liquid as it has its radius R as an additional degree of freedom. In this paragraph I develop a theory for a double quench, when the density $\rho \to \rho'$ and radius $R \to R'$ are quenched at $t = 0$ at different rates.

I am unaware of any experimental setup able to perform such a double quench, but this gedankenexperiment is more than another exercise in algebra as it will prove to be crucial in understanding the next section describing the dissipative cooling in trapped geometry.

So let's set the ratio of the final to the initial radius $\zeta = R'/R$, radius being

$$R = \sqrt{2\mu/m\omega_e^2} = \sqrt{2\rho_0 g/m\omega_e^2},$$
$$\omega_e = R^{-1} \cdot (2\rho_0 g/m)^{1/2},$$

where ω_e is the effective trap frequency (the frequency at which the condensate with central density ρ_0 and radius R would be in equilibrium).

Again equating density and phase fluctuations before and after the quench, but now taking into account both density and radius change we get

$$\alpha(\rho_0)^{1/2} \left(\frac{1}{R}\right)^{1/2} \left[\frac{\mu}{\epsilon_j}\right]^{-1/2} (b_j - \bar{b}_j) = (\rho_0')^{1/2} \left(\frac{1}{R'}\right)^{1/2} \left[\frac{\mu'}{\epsilon_j'}\right]^{-1/2} (\mathfrak{b}_j - \bar{\mathfrak{b}}_j),$$

$$(\rho_0)^{-1/2} \left(\frac{j+1/2}{R}\right)^{1/2} \left[\frac{\mu}{\epsilon_j}\right]^{1/2} (b_j + \bar{b}_j) = (\rho_0')^{-1/2} \left(\frac{j+1/2}{R'}\right)^{1/2} \left[\frac{\mu'}{\epsilon_j'}\right]^{1/2} (\mathfrak{b}_j + \bar{\mathfrak{b}}_j).$$

Substituting the scaling relations $R \propto \zeta, \rho_0 \propto \mu \propto \alpha, \epsilon_j \propto \omega_e \propto \zeta^{-1}\alpha^{1/2}$ we arrive at the relationship between the old and the new Petrov waves

$$b_j - \bar{b}_j = \alpha^{-1}\alpha^{1/2}\zeta^{-1/2} \left[\frac{\alpha}{\zeta^{-1}\alpha^{1/2}}\right]^{-1/2} (\mathfrak{b}_j - \bar{\mathfrak{b}}_j),$$

$$b_j + \bar{b}_j = (\alpha)^{-1/2}\zeta^{-1/2} \left[\frac{\alpha}{\zeta^{-1}\alpha^{1/2}}\right]^{1/2} (\mathfrak{b}_j + \bar{\mathfrak{b}}_j),$$

which simplifies to

$$b_j - \bar{b}_j = \alpha^{-3/4}\zeta^{-1}(\mathfrak{b}_j - \bar{\mathfrak{b}}_j),$$
$$b_j + \bar{b}_j = \alpha^{-1/4}(\mathfrak{b}_j + \bar{\mathfrak{b}}_j).$$

Repeating the calculations of the previous subsection we get (see Figure 1.12)

$$\langle \mathfrak{b}_j^\dagger \mathfrak{b}_j \rangle = \frac{1}{2}\sqrt{\alpha}(\alpha\zeta^2 + 1)n_j,$$

$$T' = T \cdot \frac{1}{2}\alpha\zeta^{-1}(\alpha\zeta^2 + 1),$$

where it was taken into account that $T \propto \epsilon_j n_j \propto \omega_e n_j \propto \zeta^{-1}\alpha^{1/2}n_j$, and $\lambda_T \propto \rho_0/T \propto \alpha/n_j$.
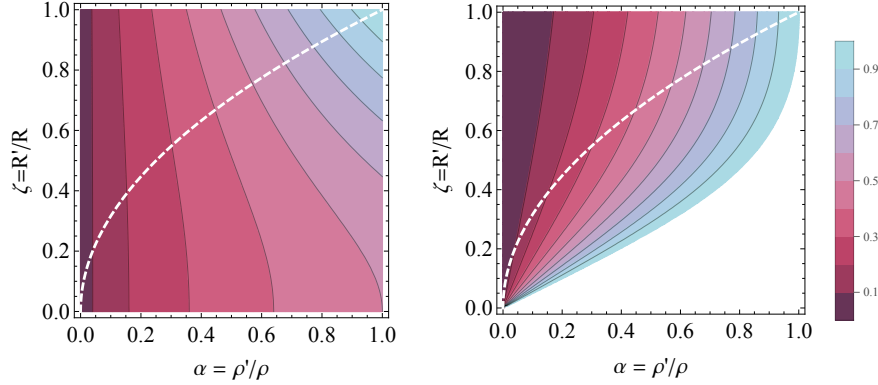
Figure 1.12: Harmonic trap: Quasiparticle occupation numbers n'_j/n_j (left) and temperature T'/T (right) as functions of the density and radius quenching parameters. Dashed line represents the manifold of stationary states $\zeta = \sqrt{\alpha}$ (a sudden quench along the dashed line will not excite cloud breathing, though it will affect the temperature). Note that for non-equilibrium quenches the temperature can be increased to arbitrary value (lower white region in the right figure), but equilibrium quenches lead only to decrease in temperature (cooling).

Quench to equilibrium. Let's consider a specific type of quench to equilibrium: when central density is quenched α times, but the final radius is quenched to the equilibrium Tomas-Fermi radius at the new central density. We know that in equilibrium $R_{TF} \propto \rho_0^{1/2}$, so $\zeta = \alpha^{1/2}$. As a final result for the equilibrium quench we get

$$b_j - \bar{b}_j = \alpha^{-5/4}(\mathfrak{b}_j - \bar{\mathfrak{b}}_j),$$
$$b_j + \bar{b}_j = \alpha^{-1/4}(\mathfrak{b}_j + \bar{\mathfrak{b}}_j).$$

$$\boxed{\begin{aligned} \langle \bar{\mathfrak{b}}_j \mathfrak{b}_j \rangle &= \frac{1}{2}\sqrt{\alpha}(\alpha^2 + 1)n_j, \\ T' &= T \cdot \frac{1}{2}\sqrt{\alpha}(\alpha^2 + 1). \end{aligned}} \tag{1.26}$$

I will use this result in the next section in derivation of the dissipative cooling.

1.10.4 Discussion

By this thought experiment I've shown that after a dissipative density quench on long scales the system looks thermal with a well-defined temperature β'.

Even more, for a density quench the temperature of the harmonically trapped gas behaves exactly as if the gas was untrapped, so I'll discuss only the case of periodic boundary conditions and conventional Luttinger liquid in the following.

An intuitive understanding can be gained from Figures 1.13 and 1.14. A density quench prepares squeezed thermal states of momentum modes, which are all initially in phase. During the free evolution according to Hamiltonian
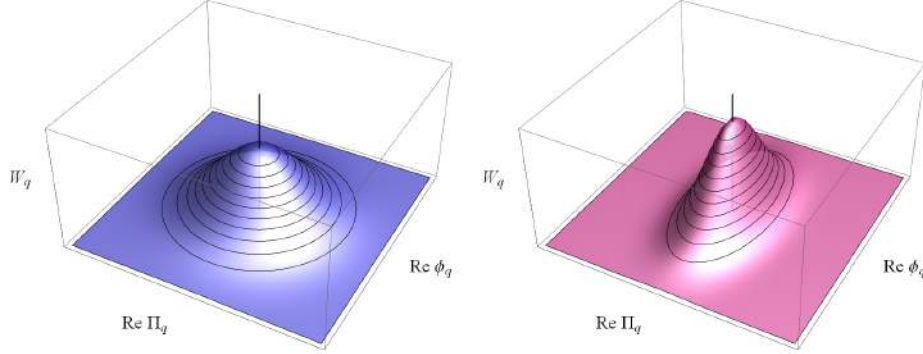
Figure 1.13: Quench cooling. Wigner functions of one Luttinger mode $q \neq 0$, in terms of the real parts of the density Π_q and phase ϕ_q fluctuations. Initially the mode is in thermal Gaussian state (left). In our thought experiment, after a sudden dissipative density quench, the mode ends up being squeezed in density quadrature (right), keeping the phase quadrature intact. Free evolution under Hamiltonian (1.8) corresponds to the rotation of the Wigner function around $\Pi = \phi = 0$ axis (vertical line). Average number of bosons in a mode in the classical picture corresponds to the squared modulus of the wave amplitude, and is proportional to the average variance of the Wigner function—so after the quench occupation number decreases. Each mode q rotates with its own angular velocity $\omega_q = c\,|q|$, and different modes quickly become dephased.

(1.4), shape of the Wigner function doesn't change, but it rotates as a rigid body, so fluctuations in density and phase quadratures oscillate periodically.

As explained in detail in [43], the two-point correlation function

$$g_1(z, z') = \frac{\langle \hat{\Psi}^{\dagger}(z)\hat{\Psi}(z') \rangle}{\langle \hat{\Psi}^{\dagger}(z) \rangle \langle \hat{\Psi}(z') \rangle} \approx \mathrm{Re}\, \langle e^{i[\phi(z') - \phi(z)]} \rangle$$

will have exponential character in the long time limit (when all the modes have lost their initial coherence)

$$g_1(z, z') = \exp(-(z - z')/\lambda'),$$

with a well-defined thermal coherence length $\lambda' \propto 1/T'$, which is indistinguishable from a thermal equilibrium.

A resulting after-quench ensemble cannot be fully described with a conventional GGE with a partition function Z_{GGE} though, where the latter is given by a free theory with mode-dependent temperature

$$Z_{GGE} = \int [db^*][db]e^{-\sum_q \beta_q \epsilon_q b_q^* b_q},$$

because the modes after the quench are not in Gaussian states, but squeezed (Figure 1.13, right). We can call the resulting state a squeezed-GGE, and Wick's
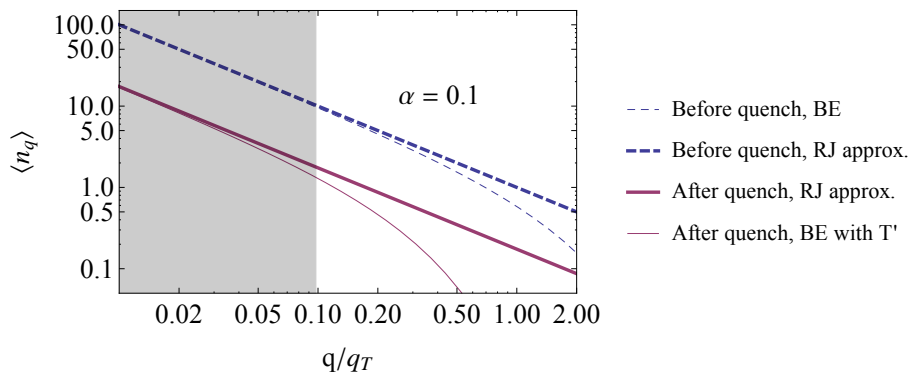
Figure 1.14: An example of mode occupation number as a function of momentum (in units of thermal momentum $q_T = k_B T/\hbar c$ at initial temperature T) for density quenched ten times ($\alpha = 0.1$). Initial BE distrtibution (thin dashed) at temperature T is transformed into a squeezed-GGE distribution with apparent temperature T', which in the classical fields approximation is nothing else than the Rayleigh-Jeans distribution (thick solid line). Thin solid line represents how a real BE distribution would look like at T'. Periodic boundary conditions implied. Shaded region represents the low momenta at which temperature is being measured in real experimental setups. In this region resulting GGE is almost indistinguishable from the respective Bose-Einstein distribution, meaning that experimentally a well-defined temperature T' of the gas will be measured.

theorem has to be modified accordingly [113]. See Appendix C for additional discussion.

Prethermalization time scale can be straightforwardly calculated from (1.5) and (1.6), taking into account the free evolution of after-quench waves $\mathfrak{b}_q(t) = e^{-ic'|q|t} \mathfrak{b}_q$, but a simple estimate can be done noticing that for $g_1(\Delta z)$ to have established prethermalized value on a lenght scale Δz, a wave with momentum $q = 1/\Delta z$ must have performed a nearly full rotation, so

$$2\pi \sim c'|q|t = c't/\Delta z \quad \Rightarrow \quad t \sim 2\pi\Delta z/c'.$$

In usual experiments $c \sim 2500 \ \mu m/s$, length scales are limited by the optical resolution and the size of the condensate, so $\Delta z \sim 1 \div 50 \ \mu m$, from which follows that prethermalization time scale $t \sim 3 \div 150 \ ms$.

Note that prethermalization time scale is proportional to the length scale, meaning that just after the quench perturbations in the cloud propagate ballistically with a finite speed, forming a causal cone of correlations. For conventional prethermalization in antisymmetric degree of freedom after splitting the condensate this propagation speed was found to be equal to the speed of sound, which was confirmed experimentally [114]. The light cone emergence after the density quench considered in the current section is a scheduled direction of future research.

1.11 Dissipative cooling

1.11.1 Introduction

In this section I report on a novel model of cooling of 1D BEC. The model is largely based on the gedankenexperiment from the previous section and can be thought of as a sequence of infinitesimal dissipative density quenches followed by a long equilibration time. This mechanism was independently confirmed by hydrodynamic calculations (Appendix B), numerical simulations with Gross-Pitaevskii equations, and, most importantly, with experiment (see the Results section below).

A notable previous attempt to understand cooling in 1D is made by Witkowska et al. in a numerical work [75]. Their model is based on the loss of atoms at the wings of the potential only; in contrary, our model uses analytical Luttinger theory and considers the outcoupling of atoms in the bulk of the cloud.

It is remarkable that the experimental sequence for 1D cooling is absolutely identical to the one used in 2D and 3D, where the cooling mechanism is well understood and known under the name of *evaporative cooling*. So for long time it was thought that the evaporative cooling should also work in 1D the very same way.

Our results show that this 'common lore' is wrong, and instead of conventional evaporation, a completely new mechanism is responsible for decrease of temperature, which we call the *dissipative cooling*.

1.11.2 Atom loss mechanism

Let's consider a real experimental setup used to cool degenerate ^{87}Ru atoms to ultracold temperatures of $10 - 100$ nK. Such procedure is routinely implemented in the labs of J. Schmiedmayer's group [65, 39, 38, 66, 24], and in the current thesis I present the theory behind its applicability.

Our level scheme consists of three hyperfine levels of the ^{87}Ru ground state in inhomogeneous magnetic field (Figure 1.15). The trapped $m_F = 2$ state is coupled with the untrapped $m_F = 0$ state by a radio-frequency electromagnetic field (rf-field), inducing the two-photon transitions. The two-photon process can be characterized by frequency $\omega_{2\mathrm{p}} = 2\omega_{1\mathrm{p}}$, which is sum of frequencies of two microwave photons.

To create a true one-dimensional quantum gas, the magnetic trap for $m_F = 2$ state is harmonic with high trapping frequency ω_r in radial x, y directions and low frequency ω in longitudinal z direction. In usual experiments $\omega_r \gtrsim 100\omega$, which creates a long cigar-shaped trapping potential. Gravity acts along the x direction.

The atomic resonance frequency $\nu_{20} = \nu^* + \mu$ can be represented as a sum of two terms. The first term ν^* is the frequency distance between the ground state of the parabolic potential for the $m_F = 2$ state (which is located for $\rho = \sqrt{x^2 + y^2} = 0$) and the value of the potential for the $m_F = 0$ state at the same point $\rho = 0$. If there were no gravitation, the potential for $m_F = 0$ would be flat, but due to the presence of gravitation it is $U_{m_F=0} = -mgx$. The second term μ is the positive chemical potential due to the atomic interactions.

The condition $\nu_{20} > \omega_{2\mathrm{p}}$ corresponds to the positive released kinetic energy. The two-photon effective Rabi frequency Ω_{eff} is, in the perturbative regime, the
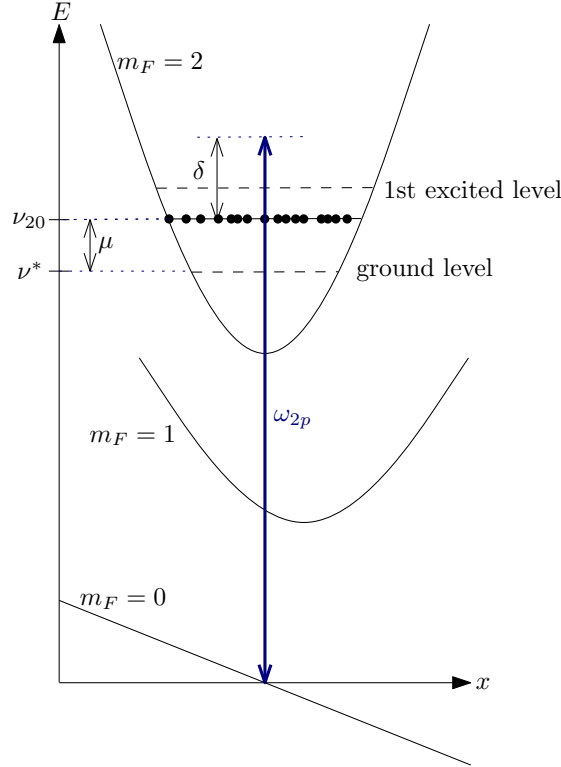
Figure 1.15: Scheme of the coupling of two hyperfine levels of the ^{87}Ru ground state (not to scale, only x direction is shown). Inhomogeneous magnetic field creates harmonic trapping potentials for $m_F = 2$ and $m_F = 1$ states, $m_F = 0$ remaining untrapped but tilted due to gravity (note that minima of $m_F = 2$ and $m_F = 1$ states are shifted due to gravity as well). Atoms trapped in $m_F = 2$ state are represented as dots and have energy higher than the ground level of the harmonic trap due to interactions (positive chemical potential). Both temperature and chemical potential are smaller than the distance between the energy levels $\omega_r \sim 2\pi \cdot 2000$ Hz, so the occupation of the excited states in the radial direction can be neglected. The atoms are coupled to the $m_F = 0$ state with two-photon transition with effective frequency ω_{2p}, where they fall off the trapping region due to gravity and repulsion from the remaining atoms. Negative detuning δ corresponds to released kinetic energy. The experimental procedure includes gradual decrease of detuning δ, which in case of 2D and 3D gases leads to evaporative cooling. In our case of 1D gas the mechanism behind cooling is different despite the fact that the experimental setup is completely the same.

product of two Rabi frequencies for the transitions $m_F = 2 \leftrightarrow m_F = 1$ and $m_F = 1 \leftrightarrow m_F = 0$ divided by the single-photon detuning from the transition between the (interacting) ground state of $m_F = 2$ atoms and the (empty) $m_F = 1$ ground state [115].

This two-photon outcoupling leads to a loss term Γ in the Gross-Pitaevskii equation

$$i\hbar\partial_t\Psi = -\frac{\hbar^2}{2m}\partial_z^2\Psi + g|\Psi|^2\Psi - i\hbar\Gamma\,\Psi,$$

where the sought-for relaxation rate is [116]

$$\Gamma = |\Omega_{\text{eff}}|^2\,\text{Re}\int_0^\infty dt\,\exp[-i(\omega_{2p} - \nu_{20})t - \eta t]\int dx\int dy\,\psi_2^*(x,y)\bar{\psi}(x,y,t),$$

where, regularization is introduced via $\eta \to 0+$. The ground-state radial wavefunction of an interacting gas is given by a Gaussian ansatz [26, 22]

$$\psi_2(x,y) = \frac{1}{\sqrt{\pi}\sigma}\exp\left(-\frac{x^2+y^2}{2\sigma^2}\right),$$

where the width of the wave function $\sigma^2 = \dfrac{\hbar}{m\omega_r}\sqrt{1 + 2n_{1D}a_s}$, and n_{1D} is the local 1D density in longitudinal direction. If we put this wave packet into the potential for the untrapped state at $m_F = 0$ and follow its time evolution, we obtain, $\bar{\psi}(x,y)$:

$$i\hbar\partial_t\bar{\psi} = -\frac{\hbar^2}{2m}(\partial_x^2 + \partial_y^2)\bar{\psi} - mgx\bar{\psi},$$

$$\bar{\psi}(x,y,0) = \psi_2(x,y).$$

The Fourier transform $\int\frac{dk_x}{\sqrt{2\pi}}\int\frac{dk_y}{\sqrt{2\pi}}\ldots$ yields conservation of the scalar product

$$\int dx\int dy\,\psi_2^*(x,y)\bar{\psi}(x,y,t) = \int dk_x\int dk_y\,\psi_{2\,k_xk_y}^*\bar{\psi}_{k_xk_y}(t).$$

If we take $\hbar\omega_r$ and $\sqrt{\hbar/(m\omega_r)}$ as the units of energy and length, then

$$i\left(\partial_t + \tilde{g}\partial_{k_x}\right)\bar{\psi}_{k_xk_y} = -\frac{k_x^2 + k_y^2}{2}\bar{\psi}_{k_xk_y}.$$

In these units $\tilde{g} = g/(\omega_r\sqrt{\hbar\omega_r/m})$ and $\sigma^2 = \sqrt{1 + 2n_{1D}a_s}$. The solution is

$$\bar{\psi}_{k_xk_y}(t) = \frac{A(t)\sigma}{\sqrt{\pi}}\exp\left\{-\frac{\sigma^2 + it}{2}[(k_x - \kappa(t))^2 + k_y^2]\right\},$$

where, since $\frac{d}{dt}[(\sigma^2 + it)\kappa(t)] - \tilde{g}(\sigma^2 + it) = 0$,

$$\kappa(t) = \frac{\tilde{g}(\sigma^2 t + it^2/2)}{\sigma^2 + it} = \frac{\tilde{g}t}{2}\left(\frac{\sigma^2}{\sigma^2 + it} + 1\right),$$

$$\frac{1}{A}\frac{dA}{dt} = -\frac{i}{2}\kappa^2(t).$$

The scalar product of ψ_2 and $\bar{\psi}$ is to be taken numerically (in k-space), and then the time Fourier is to be performed.

The equations for $\Gamma[n_{1D}(z,t)]$ can be efficiently solved numerically, see Figure 1.16. Two main conclusions are drawn from the numerical solution:

1. Local density fluctuation plays almost no role, and an effective approximation is considering the loss rate only as a function of the mean density (or chemical potential)

$$\Gamma[n_{1\mathrm{D}}(z,t)] = \Gamma[\bar{n}_{1\mathrm{D}}(t)].$$

2. Gravity is an important player in the dissipation process, and its role can be visualized as the atoms first being driven to the state $m_F = 0$ with rf-field and then falling freely from the trap (compare with the toy model of Section 1.9). Interactions would also 'push' the $m_F = 0$ atoms from the trap, but their contribution in dissipation is much smaller.

1.11.3   Results for quasistationary density variation

As we've seen from the previous section, atom loss can be characterized with a parameter Γ dependent only on the chemical potential (mean density). Such loss leads to continuous squeezing in the density quadrature of Luttinger/Petrov modes (cf. Section 1.10 for a sudden finite squeezing). In different words, in the classical fields approximation a quasistationary (with the rate smaller than quasiparticle energy level splitting $\Gamma > c\,dq$, $dq = \frac{2\pi}{L}$) atom loss can be represented as a series of infinitesimal dissipative density quenches, followed by long periods of equilibration.

This amounts to a power-law approximation to the formulas (1.24) and (1.26) around $\alpha = 1$, where $\alpha = \rho'/\rho$ is the ratio between final and initial central densities. In the case of periodic boundary conditions the power law becomes

$$\boxed{\begin{aligned}
&n_q'/n_q = \alpha, \\
&T'/T = \alpha^{3/2} = (N'/N)^{3/2}, \\
&\lambda'/\lambda = \alpha^{-1/2},
\end{aligned}}$$

and in the case of a harmonic trap

$$\boxed{n_j'/n_j = T'/T = \alpha^{3/2} = N'/N.}$$

Note that the temperature scales with the central density the same way both in untrapped and trapped cases, but in the trap temperature is proportional to the total particle number because $N \propto \rho^{3/2}$. The thermal coherence length and Luttinger/Petrov mode occupation numbers scale differently depending on the confinement geometry.

These scaling laws are compared with the results for density quench in Figures 1.17 and 1.18, and summarize the main findings of the present chapter.

This result has been independently confirmed with hydrodynamic-type calculations (Appendix B), numerical simulations (Figure 1.19) and experiments done in J. Schmiedmayer's group (Figures 1.20 and 1.21).

Intuitive understanding of the cooling process can be gained from Figure 1.22.
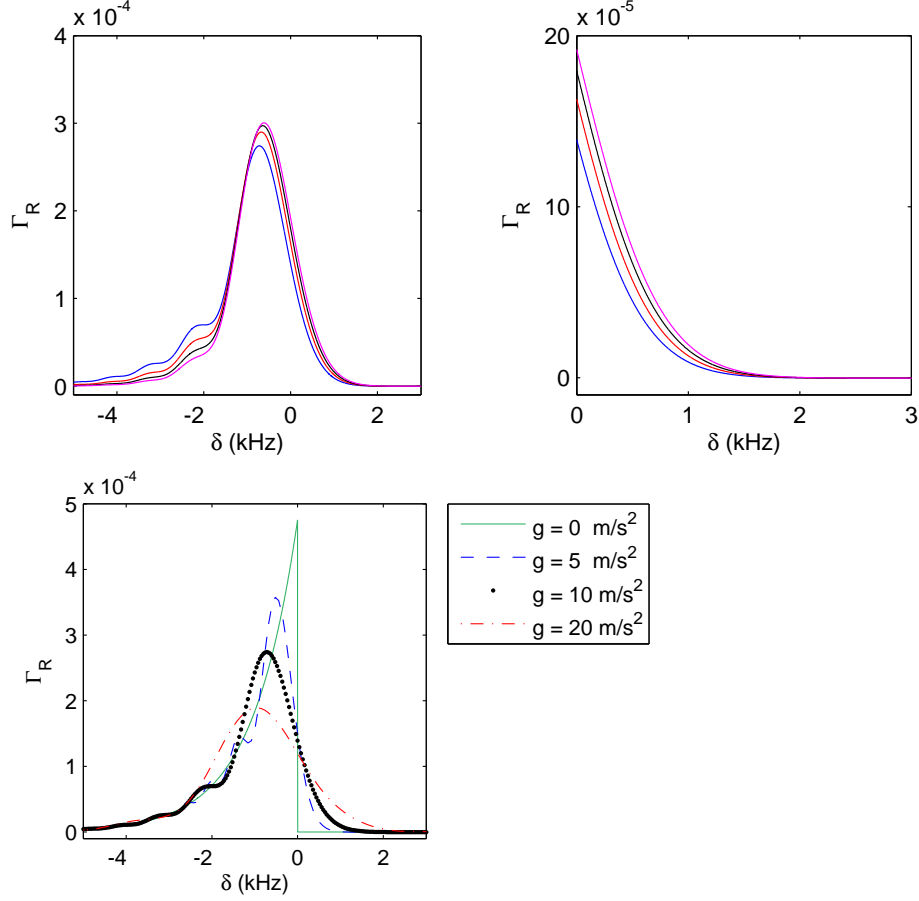
Figure 1.16: **Top row:** Dissipation rate scaled to the effective Rabi frequency $\Gamma_R = \Gamma/\Omega^2$ as a function of rf-field detuning from the resonance $\delta = \omega_{2p} - \nu_{20}$. Conventional evaporative cooling procedure implies decreasing δ from above, so physically interesting region of $\delta > 0$ is depicted to the right. Different lines correspond to densities of $n_{1D} = 0, 50, 100, 150\,\mu\mathrm{m}^{-1}$, from bottom to top. Important conclusion is that Γ_R is almost independent of the density, meaning that in the cooling mechanism it is legitimate to neglect the density fluctuations. **Bottom:** Different dissipation rates as a function of the gravity field (repulsive interactions are neglected). Sharp cutoff at $g = 0$ can be explained by the fact that at $\delta > 0 \Rightarrow \omega_{2p} > \nu_{20}$, the transition is completely prohibited as in the absense of gravity the kinetic energy, that the atom acquire after the transition, is $E_k = \nu_{20} - \omega_{2p} = -\delta$, and it cannot be negative. Numerical calculations were performed by Bernhard Rauer.

Figure 1.17: Periodic boundary conditions: Quasiparticle occupation numbers, temperature and thermal coherence length as a function of the density quenching parameter α for sudden (solid line) and quasistationary (dashed line) regimes.

Fast cooling. If the quasicondensate is long enough, the evolution rate of low-energy modes can be quite slow. In this case the picture of infinites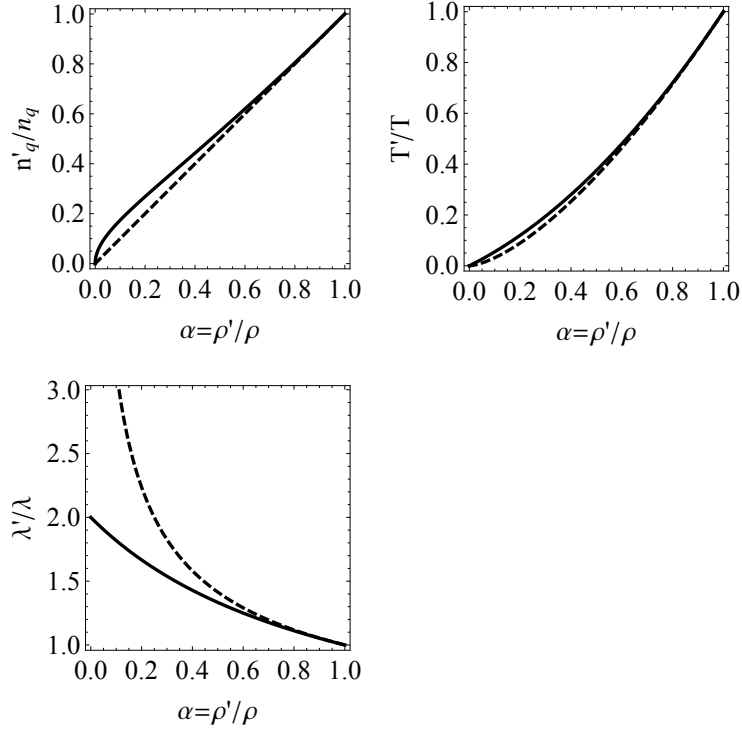imal density quenches followed by long equilibration times breaks down, and the cooling cannot be considered quasistationary any more.

Let's estimate the relevant length scales for Luttinger liquid using dimensional considerations. Wigner function of a mode with energy $\epsilon_q = c\,|q|$ will make one revolution in $t_\epsilon = 2\pi/c\,|q|$, which must be smaller than the relevant time scale associated with dissipation $t_\Gamma = 1/\Gamma$ for the dissipative cooling mechanism to be applicable: $t_\epsilon \lesssim t_\Gamma$, which leads to $q \gtrsim \Gamma/2\pi c$.

For usual cooling experiments $\Gamma \sim 14\,\mathrm{s}^{-1}$, $c \sim 0.2\,\mathrm{cm/s}$ which corresponds to the momentum $q \gtrsim 11\,\mathrm{cm}^{-1}$ and the corresponding length scale $l = 1/q \lesssim 900\,\mu\mathrm{m}$, which is much larger than usual condensate length of about $50\,\mu\mathrm{m}$.

So for usual experimental conditions the cooling can be considered slow enough for described mechanism to work. Even if there are deviations for the long-wavelength modes, they are irrelevant as the temperature for BEC is measured on the length scales much smaller.

1.12 Summary and Outlook

In this chapter I presented theory behind cooling of 1D BEC. Despite the fact that the experimental procedure being essentially the same as one employed for
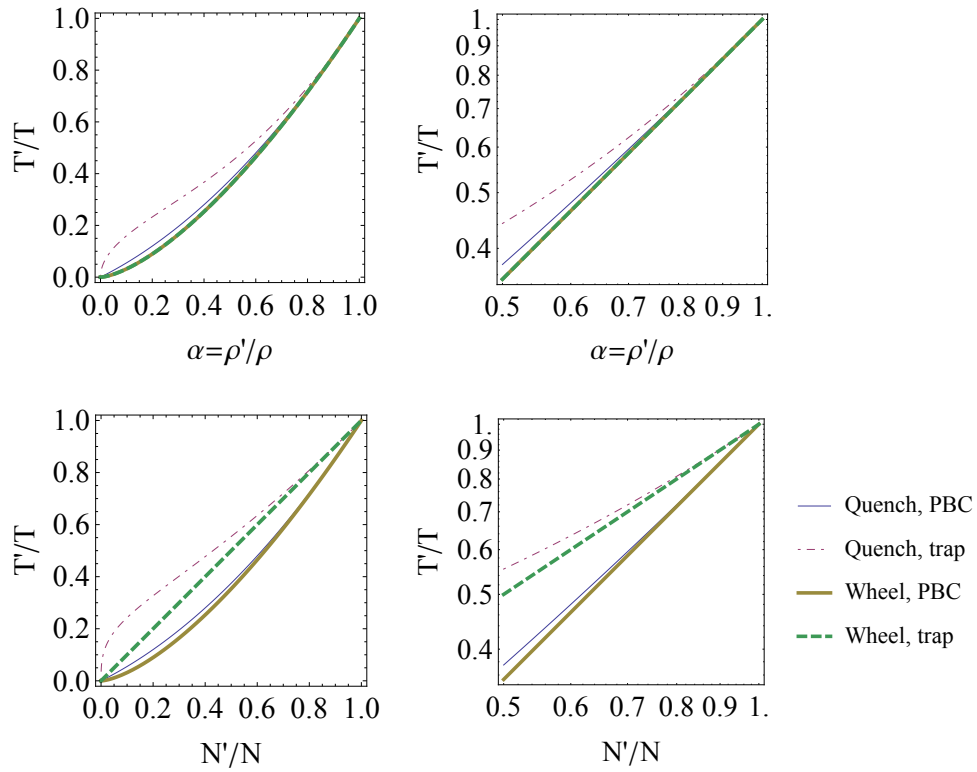
Figure 1.18: Top: final temperature T' to initial temperature T as a function of the central density quenching parameter α (top) and as a function of total final particle number to initial particle number (bottom) in linear (left) and double-logarithmic (right) scales for periodic boundary conditions (PBC) and harmonic trap in Tomas-Fermi approximation (trap), as well as for a sudden density/radius quench (quench) and slow quasistationary density/radius variation (wheel). Note that 'Wheel, PBC' and 'Wheel, trap' give the same results for temperature drop as a function of central density (top panels). Dashed line on the bottom panels is the theoretical prediction to be directly compared with experiment (see Figures 1.20 and 1.21).
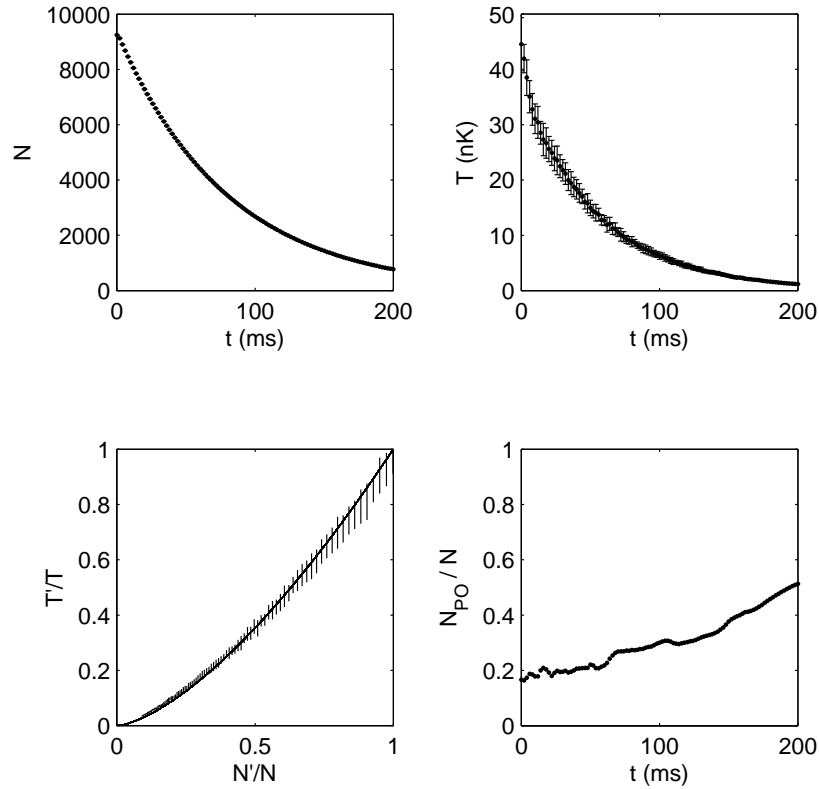
Figure 1.19: Numerical results for slow cooling of untrapped gas. **Top row:** Particle number (left) and temperature (right) as a function of time with error bars. **Bottom left:** Reduced temperature as a function of reduced density with error bars. Solid line is the analytical Luttinger liquid prediction $T \propto N^{3/2}$. **Bottom right:** Penrose-Onsager mode occupation relative to the total number of particles as a function of time. Steady growth signifies phase space density increase, as well as decrease in entropy per particle. Simulations were performed with 1D Gross-Pitaevskii equation and initial condition picked from a thermal ensemble given by the truncated Wigner approximation. Error bars on temperature are due to the finite size of the ensemble. Parameters of the simulation were typical to actual experiments.
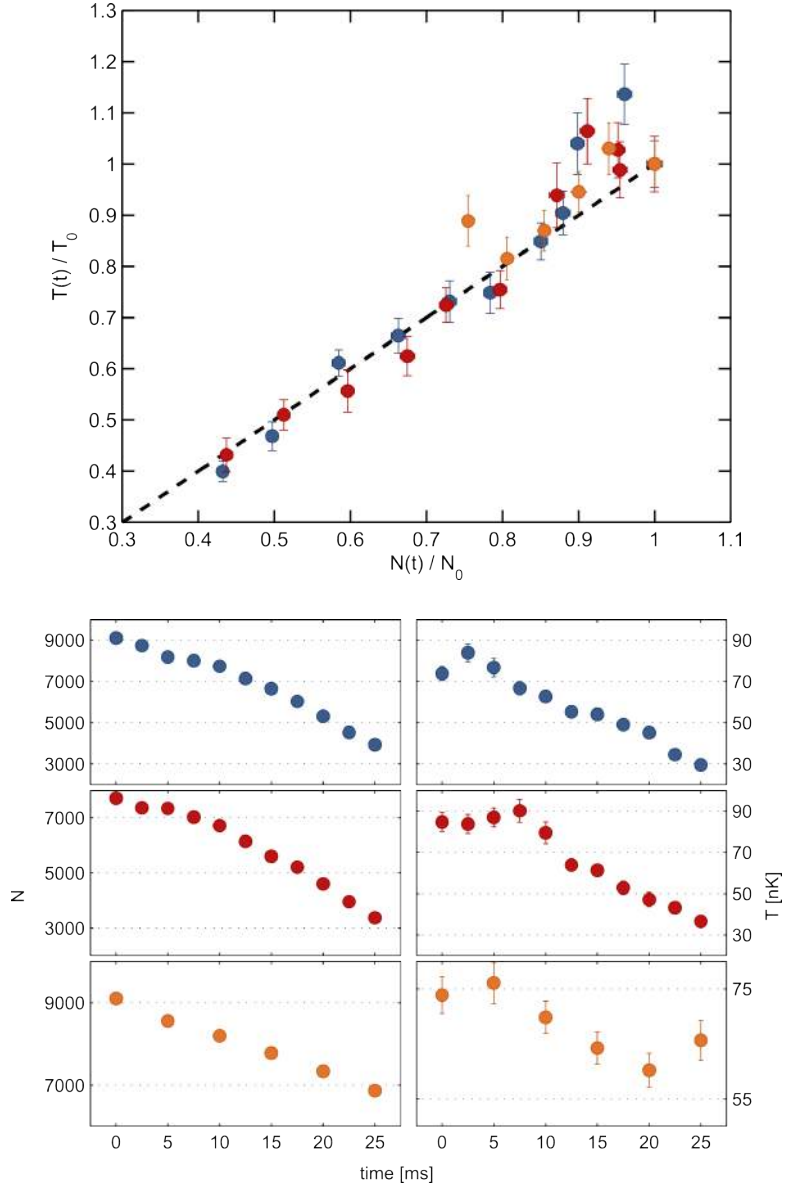
Figure 1.20: Preliminary results of a 1D cooling experiment performed on an atom-chip in the group of J. Schmiedmayer [117, manuscript in preparation]. Top panel: temperature measured with density ripple technique [25] as a function of total atom number. Dashed line shows the $T \propto N$ scaling law derived in this chapter. Colored dots correspond to different measurements, which are presented in detail in six lower panels: total number of atoms vs time (left) and temperature vs time (right). Figures prepared by B. Rauer.

Figure 1.21: Preliminary results of a 1D cooling experiment performed on an atomchip in the group of J. Schmiedmayer [117, manuscript in preparation]. Temperature as a function of total atom number. Shaded region represents the true 1D region of the quasicondensate ($k_B T < \hbar\omega_r$, $\mu < \hbar\omega_r$). Dashed line shows the $T \propto N$ scaling law derived in this chapter. The measurement scheme differs from the one utilized in the previous figure by the fact that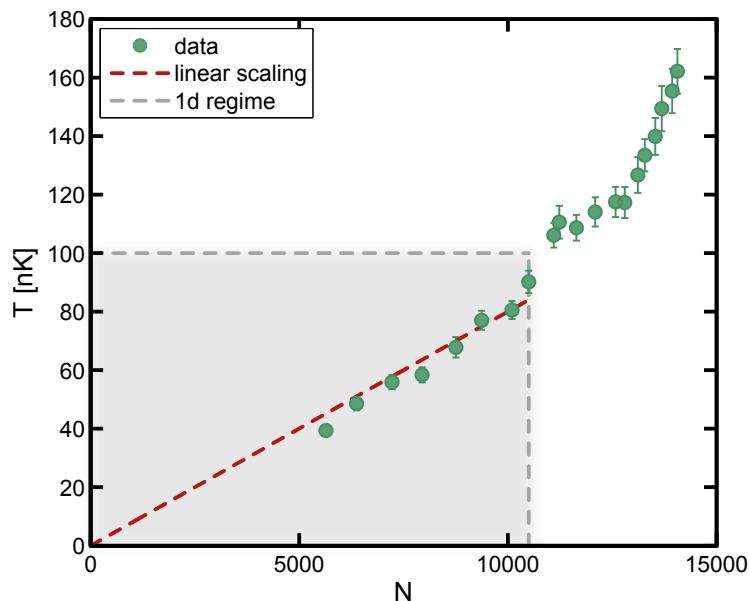 all the data points were taken at constant time, but with different outcoupling rates Γ. Figure prepared by B. Rauer.

evaporative cooling of 2D and 3D, here the mechanism is different.

Due to almost perfect integrability of 1D degenerate bosinic gas, thermalization is highly suppressed, so conventional evaporative cooling is rendered inefficient.

Our proposed explanation—the dissipative cooling—implies out-tunneling of the atoms out of a rf-dressed potential. This out-tunneling is insensitive to velocity of the atoms in longitudinal direction of a long cigar-shaped trap, leading to quasistationary density decrease. It is also a coherent process, retaining the phase of the quasicondensate intact, so in the mean-field description (which is valid at low temperatures of 10–100 nK present in the experiment) this amounts to an addition of a loss term to the Gross-Pitaevskii equation.

Elementary excitations of the system are phonons at long length scales, which incorporate density Π and phase ϕ fluctuations of the cloud as field quadratures (analogous to x and p coordinates of a conventional harmonic oscillator). Free evolution of the phonons can be represented as rotation of the Wigner function in Π–ϕ space, and when combined with the constant loss of density (which amounts to squeezing of the Wigner function in Π quadrature), leads to loss in quasiparticle occupation numbers.

Cartoon picture of the process is creating pottery on a classical potter's wheel (Figure 1.22): we can imagine a piece of clay in form of a Gaussian, representing initial thermal state of a quasiparticle more, is being rotated (free evolution) and squeezed from two sides by potter's hands (density loss). This

results in a 'sharper' Gaussian, as the volume of the clay is conserved the same way as the normalization of the Wigner function. But occupation number of the mode is proportional to the width (standard deviation) of the Gaussian, which decreases, meaning that we are loosing quasiparticles from each mode.

Dissipation in our open quantum system is due to a coupling to a bath at zero temperature, and in the case of quasistationary atom loss the fluctuations in the modes are purely quantum (given by the fluctuation-dissipation relation of the zero-temperature bath), and can be neglected as long as the occupation number of the modes is $\gg 1$. It is always the case for low-momenta modes $k \ll \xi^{-1}$ at experimentally realizable temperatures of 10–100 nK and supports the classical fields approximation taken in the derivation.

For long-wavelength modes the classical equipartition shall hold, meaning that temperature is proportional to the average energy of a mode

$$\forall q : \quad T(t) \propto E_q(t).$$

In the case of untrapped gas

$$T(t) \propto E_q(t) = \hbar c(t) \, |q| \, n_q(t).$$

It is important that the relative occupation number of the modes is preserved during our cooling,

$$\frac{n_q(t)}{n_p(t)} = \frac{n_q(0)}{n_p(0)},$$

where $q \neq p$ are some arbitrary mode numbers.

So it follows that if the initial state had a well-defined classical temperature, and $E_q(0) = E_p(0)$, it will also have one after the cooling as $E_q(t) = E_p(t)$ (see Figure 1.14).

So our mechanism amounts to a process of cooling without any need of thermalization.

Our cooling mechanism cannot be called adiabatic in a strict sense, because the modes' energy is composed of two time-dependent terms, one of them being adiabatic change in the energy levels (due to changing sound velocity proportional to the square root of mean density $c(t) \propto \sqrt{\bar{\rho}(t)}$), but another one—change of quasiparticle occupation numbers $n_q(t)$.

Numerical simulations show increase of the relative population of the Penrose-Onsager mode, defined as the largest eigenvalue of a one-body density matrix, which correspond to decrease of Boltzmann entropy (the entropy of the normalized one-body reduced density matrix, $S_B = -\text{tr} \, \rho_1 \log \rho_1$), see Figure 1.19, bottom right. On the other hand, the Gibbs entropy of the full normalized many-body density matrix $S_G = -\text{tr} \, \rho \log \rho$ in Bogoliubov approximation stays constant, due to the fact that the relative occupation of the Bogoliubov modes doesn't change. This discrepancy is no surprise as by performing the partial trace to get the one-body density matrix we are neglecting a lot of information about many-particle correlations, so $S_B > S_G$ for an interacting system, and S_B can decrease as long as it stays larger than S_G with no violation of the second law of thermodynamics. Relationship between Boltzmann and Gibbs entropies is discussed in detail in [118].

Being able to construct a simple Luttinger liquid model of 1D cooling, we are in principle able to calculate all the relevant correlation functions. In the current thesis I presented power laws for temperature scaling, which were already confirmed in experiment (Figures 1.20 and Figure 1.21).

The same discussion applies to a trapped condensate in Thomas-Fermi approximation and leads to the very same power law dependence of the temperature on the central peak density.

Outlook.   Presented results open a wide field of future study.

The current study was concentrated on the slow quasistationary decay, but in the case of fast decay I anticipate production of phonons, which would counterbalance the temperature drop. Currently we are investigating at which conditions the resulting state may be considered thermal. In particular, other studies showed emergence of true thermal states by slow variation of parameters of the Hamiltonian in free systems [119, 120].

A direction of future study is to develop a fully quantum theory of losses in 1D BEC, which should incorporate quasistationary dissipative cooling and the sudden splitting of the condensate (e.g. in prethermalization experiments) as limiting cases.

Experimental study on the topic will continue by measuring the higher-order correlation functions. (Generalized) Gibbs ensemble implies decoupling of correlators through Wick's theorem, so probing higher-order moments will provide important information on the regimes of the model's applicability and possible future refinements. Another experimental study could concern with fast cooling, where the model predicts appearance of non-classical squeezed thermal states.

One can note that Bogoliubov-Luttinger modes are not completely independent, but interact at long time scales [100, 101]. Future studies will elucidate how this process affects the cooling mechanism.

I hope that presented results will lead to even better experimental techniques to cool and manipulate bosonic gases, opening new horizons in exploring the fascinating area of non-equilibrium many-body quantum physics.
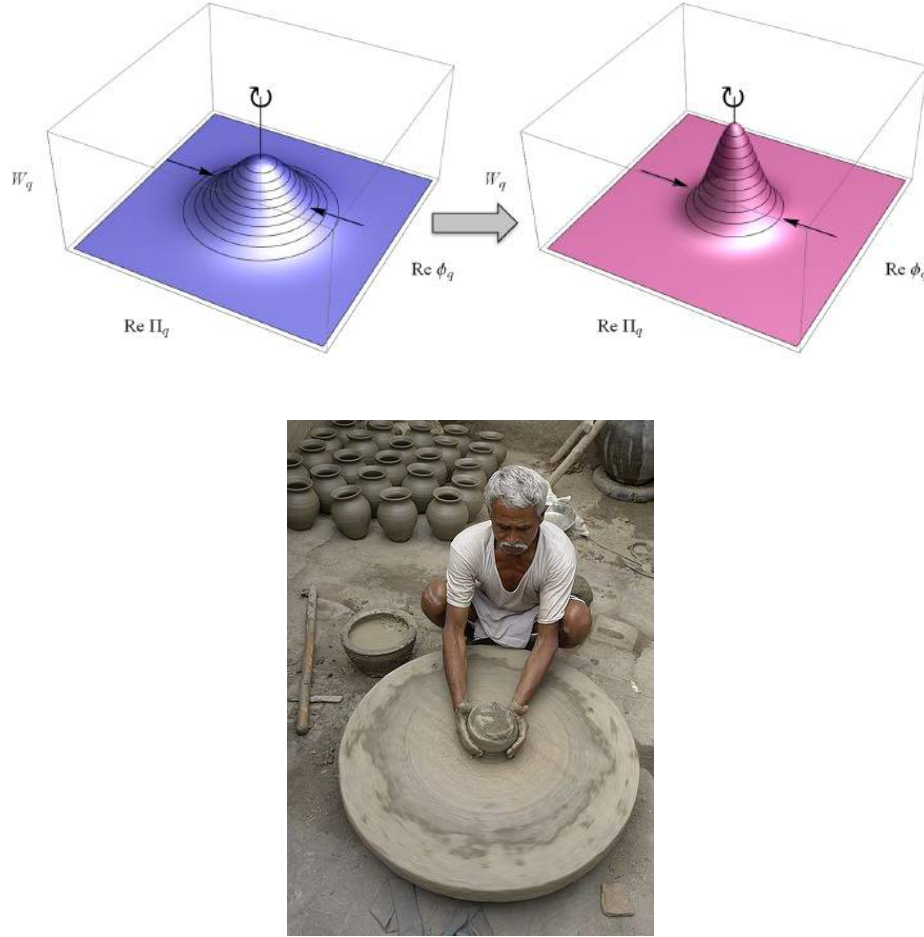
Figure 1.22: **Top.** Dissipative cooling in 1D—the quantum potter's wheel. Wigner functions of one specific Luttinger/Petrov mode q as functions of density Π and phase ϕ field quadratures during time evolution (from left to right). Quasistationary squeezing in the density quadrature is represented with arrows. The free evolution is rotation around the symmetry axis. The analogy with a classical potter's wheel is apparent from the picture: the free evolution of the Wigner function corresponds to the rotation of the piece of clay on a potter's wheel, and the squeezing in the density quadrature due to atom loss corresponds to potter's hands squeezing the clay blank. Normalization of the Wigner function corresponds to the constant volume of the clay. Compare this with Figure 1.13, where the density quench is instantaneous. Number of bosons per mode is proportional to the width (standard deviation) of the Gaussian, so it's apparent that this number decreases, which leads to decrease of temperature in the low-momenta modes as described in detail in Section 1.10. **Bottom.** Classical potter's wheel: Indian potter shaping a not-so-Gaussian piece of clay. [Image by Wikipedia user Yann licensed under GNU FDL]

Chapter 2

Thermalization at the breakdown of integrability

2.1 Introduction

Out-of-equilibrium phenomena. Since the inception of quantum mechanics researchers have been challenged by the complexity of quantum many-body interacting systems. During the last century most of them could be prepared only near thermal equilibrium, as there were no effective techniques of reducing environmentally induced decoherence and thermalization.

But in recent decades, experimental advancements in atomic phycics, quantum optics and nanoscience finally allowed to study many-body systems in isolation. This had huge consequences, opening whole new branches of science such as the quantum non-equilibrium physics, which is the field the author had been working in.

There are many ways to drive the system out of equilibrium, such as application of external time-dependent fields or coupling the system to a non-thermal reservoir. The main topic of this chapter will be another very common approach in studies of non-equilibrium phenomena—the so called *quantum quench*. It happens when a system, initially prepared in an eigenstate (e.g. the ground state) of some Hamiltonian H_0, is evolving under action of *another* Hamiltonian H. This change in Hamiltonian is sudden in the sense that the time scale of the manipulation is be smaller than the inverse energy level spacing of H_0. The opposite to a quench would be the *adiabatic* regime, when the Hamiltonian changes so slowly that there are no transitions between energy levels. Note that for gapless Hamiltonians there may be no such a slow adiabatic regime in thermodynamic limit [121].

In a nutshell, the dynamics after a quench can be often imagined as a relaxation of a great number of quasiparticles (ground state of H_0 corresponds to an excited state of H). Incoherent quasiparticles from points $2x$ apart move with the group velocity $v = dE/dk$ and meet after the time $t = x/v$, destroying local correlations at the meeting point, which is viewed as thermalization. Sure, dispersion relation and scattering events make this picture much more complicated [122].

On the other hand, in an important case of conformal field theories (CFT),
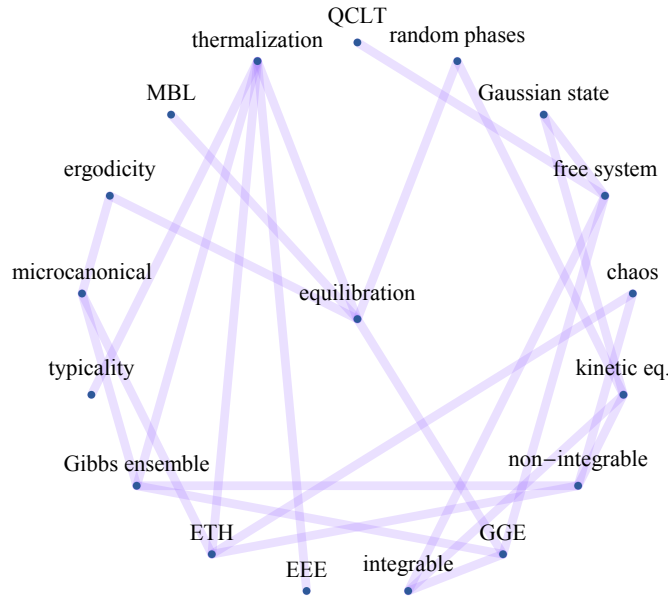
Figure 2.1: Notions of non-equilibrium physics, addressed in this chapter. Acronyms are explained in the text and summarized in Appendix A.

such as Luttinger liquid, discussed in the previous chapter, quasiparticles are non-dispersing non-interacting phonons, which leads to a clean light-cone spreading of correlations after a quench. Such behavior was experimentally confirmed with cold 1D gas [114].

There exist few overviews of non-equilibrium phenomena as the field itself is very novel. Quenches are addressed in detail in [123], and applications to cold gases in [124].

Motivation of the study. The study reported in this chapter is devoted to understanding how the laws of statistical physics emerge from the many-body quantum mechanics. In particular, I will address one of the most fundamental questions of non-equilibrium physics: whether an isolated system can thermalize, serving as its own bath.

I will present the results of equilibration and thermalization in a mesoscopic quantum system after a quench. Motivation for the study is the rich physics of the model, exhibiting both integrable and non-integrable regime. Usually people say that non-integrable systems thermalize and integrable—not. I will show that there exists a whole spectrum of different levels of thermalization at integrability crossover.

The size of the system under study is limited by exact diagonalization method, so no strong conclusions about the thermodynamic limit can be drawn. Nevertheless, I will show that even a small system can possess definite features, characteristic to macroscopic statistical description. Some recent results on small systems demonstrate application of thermodynamics even to a single quantum harmonic oscillator [125].

Even more, thermalization of mesoscopic systems is interesting by its own in

the context of modern advancements in nanotechnology and quantum computing. Mid-level many-body systems represent an ideal bridge between the areas of quantum information and quantum foundations, tensor networks, thermodynamics, and statistical mechanics.

Structure of the chapter. I will study a particular mesoscopic quantum system, which can be experimentally realized with cold bosonic atoms in optical lattices (Section 2.2).

Section 2.3 introduces the Bose-Hubbard model. I argue about the particularly interesting features of the model in 1D, namely that it exhibits two integrable limits as well as a chaotic regime. I discuss the exact diagonalization, which is the numerical method used in this study, in comparison with the other widely used numerical approaches.

Section 2.4 proceeds with a brief summary of the most important concepts of non-equilibrium physics, which will later appear to be helpful in understanding thermalization.

After the scene has been set up, I turn to the dynamics after a quantum quench in Section 2.5. This particular quench had been already experimentally realized, studied analytically (in the limiting cases of $U = 0$ and ∞) and numerically, using DMRG in positon space [126, 127, 128]. The theory showed excellent agreement with the experiment.

I extend the existing studies to the intermediate non-integrable regime and perform calculations with momentum (Fourier) modes, which are interesting due to the fact that this formulation might be able to open a way to kinetic description and wave turbulence phenomena [129].

In the same section I address the interesting properties of the initial state, explicitly calculate the full and reduced density matrix of the steady state and evolution of the entanglement entropy.

As our system has both integrable and non-integrable regimes, quantum integrability is discussed in detail in Section 2.6. I present the spectrum of our Hamiltonian, which has clear signatures of quantum chaos.

If we want to claim that a quantum system thermalizes, then we would expect that it somehow forgets its initial state. This question is addressed in Section 2.7, where I apply a measure known as the *entanglement in the eigenbasis* to quantify the 'forgetfulness'.

Section 2.8 is devoted to the cornerstone of modern thermalization description—the *eigenstate thermalization hypothesis*, which assures the thermality of expectation values after equilibration. I demonstrate how it can be used to measure degree of integrability.

Generalized Gibbs ensemble, which is a straightforward generalization of a conventional thermal ensemble, is discussed in Section 2.9. I show that the equilibrated state after a quench can be described in terms of a deformed GGE at integrability crossover.
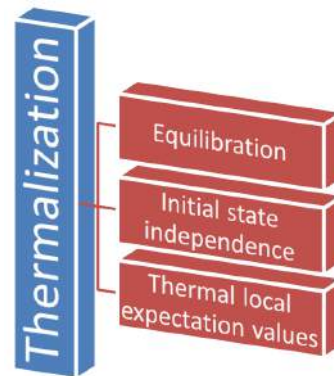
The last observation allows for applications of kinetic description, which is the topic of Section 2.10. There I show that quantum Boltzmann equation is indeed able to describe small deviations from thermal and generalized thermal states.

The chapter is concluded with summary and outlook in Section 2.11.

An additional goal of the study was to check the applicability of semiclassical approximation schemes. Results on the limitations of the truncated Wigner approximation (TWA) are summarized in Appendix D.

2.2   Optical lattices

Optical lattice is a spatial pattern of varying electric field intensity produced by interference of counter-propagating laser beams. It effects in a spatially periodic potential able to trap neutral atoms by Stark shift, with the resulting arrangement of atoms resembling a crystal lattice, hence the name.

Principle of operation.   To get a qualitative understanding of the mechanism let's follow the example given in [6] and consider two counterpropagating linearly-polarized laser beams, creating electric field of the form

$$\vec{E}(z,t) = \vec{E}(z)e^{-i\omega t} + \vec{E}^*(z)e^{i\omega t},$$

$$\vec{E}(z) = E_0(\hat{e}_x e^{iqz} + \hat{e}_y e^{-iqz}).$$

Polarization state of the electric field oscillates in the direction of z axis between being linearly and circularly polarized, polarization vector given by

$$\vec{e} = \frac{1}{\sqrt{2}}(\hat{e}_x + \hat{e}_y e^{-2iqz}).$$

Now let's imagine that the lasers are tuned to the $^2S_{1/2} \leftrightarrow \, ^2P_{3/2}$ transition in an alkali atom. Intensities of the two circularly polarized components of the electric field change in space, leading to a position-dependent shift in the energy levels, so two ground states $g^\pm$ feel the potential

$$V^\pm = V_0(-2 \pm \sin 2qz),$$

where V_0 is the magnitude of the potential, dependent on the detuning δ, Rabi frequency Ω_R and the inverse lifetime of the excited level Γ_e as

$$V_0 = -\frac{2}{3}\frac{\hbar\Omega_R^2\delta}{\delta^2 + \Gamma_e^2/4}.$$

This picture can be generalized to more complicated laser arrangements to create position-dependent potentials in 1D, 2D and 3D geometries.

Applications.   Area of application of optical lattices is tremendous, growing larger and larger every year.

First of all, optical lattices provide an unprecedented level of control over experimental parameters thus becoming an ultimate quantum simulator for various condensed matter systems [130].

The systems being successfully simulated include a chain of interacting Ising spins at the phase transition point [131], self-trapping in an array of 1D BEC [132], geometrically frustrated systems with large degeneracy of low-energy states [133], quantum criticality [134], and many others.

A sub-field of its own includes simulation of quantum magnetism, which results from spin-orbit coupling [135]. Some recent results on this frontier include simulations of a frustrated classical spin system by creating strong effective magnetic field [136], vortices formation due to a synthetic magnetic field [137, 138], unique Hofstadter-Harper Hamiltonian exhibiting a fractal structure and describing electrons in a magnetic field [139, 140], and others.

Optical lattices allow to build a quantum system from the bottom, with control of positioning single atoms. Those atoms can act as qubits allowing realization of quantum gates for prospects of quantum computers [141, 142, 143].

An interesting result is an observation of negative absolute temperatures in an inverted optical lattice, which is possible due to the fact that the system's Hamiltonian is bounded from above [144].

A novel tool in studying atoms in optical lattices is so called *quantum gas microscope*, which is able to detect single atoms for precise control over quantum simulations or read-out of potential qubits [69, 145].

In addition, optical lattices can be used to cool atoms below the Doppler limit, which states that the minimal temperature achievable via laser cooling is limited by the recoil energy of an atom at rest, absorbing one photon $T_{Doppler} = (\hbar q)^2 / 2mk_B$, where $\hbar q$ is the momentum of the photon. This is achieved by so called *Sisyphus cooling*, when atoms loose kinetic energy when they climb up the potential hill just to be driven to the low-energy state by the optical pumping, giving away their energy to the light field [146, 147].

2.3 Bose-Hubbard model

2.3.1 Introduction

Interacting bosons in optical lattices can be approximately described by a Bose-Hubbard (BH) model, first introduced by Gersch and Knollman in 1963 [148]. The model is a close kin to Hubbard model, used in condensed matter theory to describe interacting fermions on a lattice [149]. Name 'Bose' doesn't refer to the inventor of the model though, but is accounting for the fact that here the particles are bosons.

The Hamiltonian of the model (implying periodic boundary conditions) is given by

$$\hat{H} = -J \sum_{\langle ij \rangle} (\hat{a}_i^\dagger \hat{a}_j + \hat{a}_j^\dagger \hat{a}_i) + \frac{U}{2} \sum_{i=1}^{M} \hat{n}_i (\hat{n}_i - 1), \qquad (2.1)$$

where $\hat{a}_i$ is the bosonic annihilation operator and $\hat{n}_i = \hat{a}_i^\dagger \hat{a}_i$ is the number operator on site i, J is the hopping parameter, quantifying the tendency of particles to move to a neighboring site, U is the on-site self-interaction parameter, $U > 0$ makes it more energetically costly for several particles to occupy one site, which corresponds to repulsive interactions, M is the total number of sites, and $\langle ij \rangle$ stands for summation over the nearest neighbors only (short-range interactions). In this study I'm not interested in the equilibrium properties of the

model in the grand-canonical ensemble, so I omit the chemical potential term $H_\mu = -\mu \sum_i \hat{n}_i$, which in any case amounts just to a constant shift in energy due to total particle number conservation.

BH model is notable by its phase diagram: at zero temperature it can be either in superfluid phase at large J/U, where particles can flow freely between the sites or in a Mott insulating phase at small J/U, characterized by integer bosonic on-site occupation numbers and existence of an energy gap [150]. In superfluid phase long-wavelength modes don't 'feel' the lattice and exhibit universality of the Luttinger liquid model, described in Section 1.4.

2.3.2 One-dimensional case

Fourier-transforming the field operators by

$$\hat{b}_q = \frac{1}{\sqrt{M}} \sum_{j=1}^{M} e^{2\pi i j q / M} \hat{a}_j,$$

we arrive at the representation of the Hamiltonian (2.1) in momentum space

$$\hat{H} = -2J \sum_{q=0}^{M-1} \cos(2\pi q/M)\hat{b}_q^\dagger \hat{b}_q + + \frac{U}{2M} \sum_{q_{1,2,3,4}=0}^{M-1} \hat{b}_{q_1}^\dagger \hat{b}_{q_2}^\dagger \hat{b}_{q_3} \hat{b}_{q_4} \delta_{q_1+q_2,q_3+q_4}, \quad (2.2)$$

where the interaction becomes completely non-local in terms of new bosons $\hat{b}$, the delta-function assuring the conservation of momentum.

One-dimensional BH model is of particular interest as it is integrable in two limiting cases: $U = 0$, where it describes a free system (quadratic Hamiltonian) with cosine dispersion law, and $U = \infty$, hard-core bosons, which can be cast into a form of non-interacting fermions.

integrable	non-integrable	integrable
$U = 0$		$U = \infty$

More on what exactly is quantum integrability is written in Sections 1.8 and 2.6, but for now I'll note that a free system with quadratic Hamiltonian represents the simplest possible integrable model (as different quasiparticle occupation numbers are conserved, so the Hilbert space can be split into many non-coupled symmetry sectors). In the intermediate regime $0 < U < \infty$ there is no mapping to a free model and BH chain is non-integrable.

2.3.3 Hard-core bosons

An important case of infinitely-strong repulsive on-site interaction is realized in the hard-core regime of BH model. Then because of the infinite energy barrier there cannot be more than one boson per site, which reminds of Pauli exclusion principle $\{\hat{a}_i, \hat{a}_i^\dagger\} = 1$. Though on different sites bosons commute $[\hat{a}_i, \hat{a}_j^\dagger] = 0$, so they themselves cannot be thought of as fermions.

But there exists a highly non-local many-body unitary transformation, which allows to cast the Hamiltonian into a free form for new true fermionic field operators $\hat{c}_i$

$$\hat{H} = -J \sum_{\langle ij \rangle} (\hat{c}_i^\dagger \hat{c}_j + \hat{c}_j^\dagger \hat{c}_i),$$

or in the momentum space

$$\hat{H} = -2J \sum_{q=0}^{M} \cos(2\pi q/M)\, \hat{c}_q^\dagger \hat{c}_q. \tag{2.3}$$

This Jordan-Wigner transformation, which was initially developed to map spin operators into fermions to solve 1D XY model by Jordan and Wigner in 1928 [151], and in the case of fermionization of bosons reads as [152, 79, 153]

$$\hat{a}_j^\dagger = \hat{c}_j^\dagger \prod_{\ell=1}^{j-1} e^{i\pi \hat{c}_\ell^\dagger \hat{c}_\ell}.$$

The product part represents a 'string' operator which contains the sum of the occupation numbers of fermions to the left of site j and ensures the right anticommutation relation $\{\hat{c}_i, \hat{c}_j^\dagger\} = 1$.

The main advantage of this model is its Hilbert space being orders of magnitude smaller than that of the system of soft-core bosons, meaning that efficient techniques of exact diagonalization can be used to study longer chains, allowing conclusions on thermodynamic limit. That's why hard-core bosons have been fruitfully exploited in many studies of peculiarities of quantum thermalization (more on that in the next sections).

Bethe Ansatz studies showed that presented hard-core description can be generalized to low-enegrgy soft-core bosons, which can be formulated as a pair of entangled fermionic quasiparticles and a fermionic collective excitation [154]. At $U \to \infty$ the pairs break and give raise to a free fermionic gas in accordance to Jordan-Wigner transformation

In this thesis I don't concentrate on hard-core bosons, but explore the BH-chain in the full range of interaction strength to uncover the effects of integrability breaking on different aspects of thermalization.

2.3.4 Applications

So far most of the studies on the BH-model concentrated on two topics: either studies of equilibrium properties and the phase transition or its application in the context of equilibration and thermalization.

Some recent advancements of the former topic include experimental observation of superfluid to Mott insulator phase transition, realized in optical lattices [155]; description of a ordered spin-liquid state on a kagome lattice [156]; studies of spin-orbit coupling [157]; calculations of non-equilibrium steady states, maintained by coupling BH chain to a heat bath [158]; new analytical approaches in studies of thermodynamics of the model in terms of diagrammatic expansion in hopping parameter [159], and many others.

Studies of the second topic are of direct relevance to my thesis and will be considered in detail in the next sections in the context of specific aspects of thermalization.

2.3.5 Numerical simulations

Nowadays there exist a plethora of numerical methods of studying condensed matter systems, all of them having their positive and negative traits. But gen-

erally speaking, they all can be separated in three classes only: variational, stochastic and exact.

Variational methods. These are based on an initial ansatz of a specific trial wavefunction for a many-body system. One of the most famous algorithms of this type are based on an ansatz called *tensor networks* or *matrix product states*, where exact diagonalization steps are followed by truncation of the Hilbert space, which leaves only relevant states and prevents the exponential growth of the latter [160].

Variational methods are especially efficient at low temperatures and 1D geometry, and have been successfully applied to studies of the Kondo problem [161], the fractional charge and fractional statistics [162, 163] and even to relativistic models, allowing investigation of the holographic principle and AdS/CFT correspondence [164]. Of course, there are many studies of the Bose-Hubbard model itself [165, 127].

Some variations of the algorithms include those able to explicitly deal with the thermodynamic limit [166, 167].

Drawback of these methods usually lies in the fact that they are applicable to finite times only because of entanglement growth. Also they are not so well suited for studies of highly excited systems, as entropy area laws don't usually hold there [168].

Stochastic methods. Also called quantum Monte Carlo methods, they aim at calculating physical quantities by averaging over some stochastic ensembles. The main advantage is that methods' precision is dependent on the size of such ensemble, and not the size of the Hilbert space, hypothetically allowing studies of systems of arbitrary size [169].

For bosonic systems such as BH model, a particularly fruitful approach is the path integral Monte Carlo, which exploits the fact that n-dimensional quantum system can be mapped to a $(n + 1)$-dimensional classical system, and quantum fluctuations of the former correspond to thermal fluctuations of the latter [170, 171, 172].

Strong advantages of stochastic methods lie in the feature that they can be applied to 2D and 3D systems, giving especially good results for near-thermal equilibrium simulations, and that they can be efficiently run on a parallel computer. Drawbacks include sometimes slow convergence of the observables (especially at phase transitions), difficulties in analytical continuation to the real-time case (in contrast to the imaginary time thermodynamic case[1]), infamous sign problem for fermions, and requirement of a lot of computational power.

Numerical simulations in Chapter 1 were done using a specific stochastic method, namely the truncated Wigner approximation (TWA) [37, 32]. I tried to use it for the present study of thermalization in a BH-chain and found that it is not able to describe the system. More on the limitations of TWA in Appendix D.

Exact diagonalization. Variational and stochastic methods lead to experimentally relevant predictions, but they don't reveal the 'inner gears' of quantum mechanics, respectively exact eigenstates and eigenenergies. And because this

---

[1]An interesting recent paper suggests using AdS/CFT correspondence instead of performing analytical continuation to study dynamics [173].
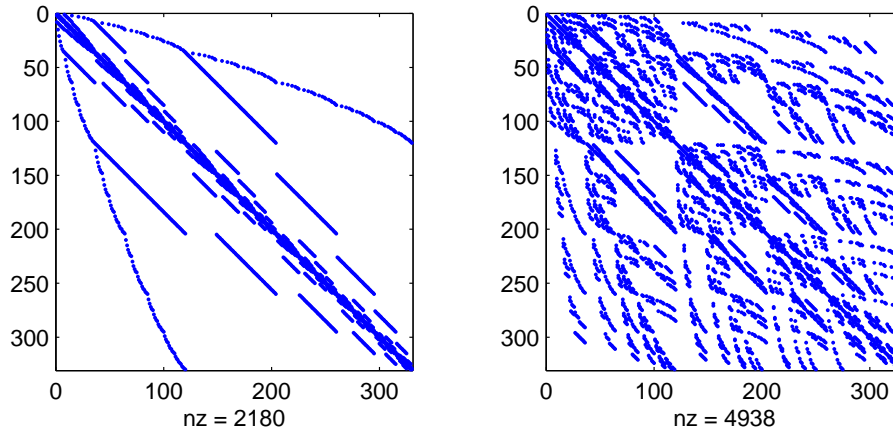
Figure 2.2: Example structures of 1D Bose-Hubbard Hamiltonians for a chain of 8 sites and 4 particles in position space, left (2.1); and in momentum space, right (2.2). On axes are exact many-body eigenstates $|i\rangle$, and non-zero elements of H_{ij} are marked with dots; 'nz' stands for the number of non-zero elements. In position space only few eigenstates are coupled by the Hamiltonian, which reflects the locality of the hopping term in real space.

study is not aimed at getting an agreement with some specific experiment, but to shed light on how exactly the process of thermalization is happening in a many-body system, I've chosen to use exact diagonalization.

The obvious positive side of it is that we have access to all possible physics and are able to calculate all the quantities, including spectrum of the Hamiltonian, reduced density matrices in any basis, equilibrium states after $t \to \infty$, entanglement entropies etc.

A considerable drawback of the method is its applicability to small chains only as the dimension of the Hilbert space grows exponentially with the system size. And because I consider soft-core bosons, the system sizes are still much smaller than those in the simulations of hard-core bosons, so I abandon the hope to make conclusions of thermodynamic limit. Still small systems are of interest of its own as they can be realized in experiments with optical lattices. And I claim there are some universal features of non-equilibrium dynamics, so even studies on small system can lead to important insights. This is going to be the topic of the next sections.

Hamiltonians were constructed following the procedure of [174], and the particle conservation was explicitly taken into account. Example of the structure of the Hamiltonian is shown in Figure 2.2. All results of this chapter were obtained on a desktop computer.

2.4   Thermalization glossary

Before diving into physics of thermalization I'll provide a set of definitions that will play a major role in the following. Some of key notions such are Eigenstate Thermalization hypothesis of Generalized Gibbs ensemble are not in the glossary

as there are whole sections dedicated to them.

Free system. A system with quadratic Hamiltonian in second-quantized field operators. For example, (2.1) and (2.2) correspond to free systems if $U = 0$. A free system is the simplest quantum integrable system (more on that in Section 2.6). A free bosonic system can be represented as a set on uncoupled harmonic oscillators. Luttinger liquid from Chapter 1 is a paradigmatic example of a free system.

Microcanonical state. Describes completely isolated system with the density matrix diagonal in the eigenstate basis $\rho = \frac{1}{Z}\delta(\hat{H} - E)$, meaning that the eigenstates sufficiently close in energy to E contribute with the same weight [175].

Gaussian state. Density matrix $\hat{\rho}$ of the system holds all the statistical information about the ensemble. Quantum characteristic function is a representation of the density matrix defined as

$$\chi(\vec{\lambda}, \vec{\lambda}^*) = \text{tr}\left[\hat{\rho} \cdot \exp\left(\sum_i \lambda_i \hat{a}_i^\dagger - \lambda_i^* \hat{a}_i\right)\right],$$

where $\vec{\lambda}$, $\vec{\lambda}^*$ are complex vectors and $\hat{a}_i$ are quantum field annihilation operators in some basis [31, 176]. For example, the set of $\hat{a}_i$ may correspond to annihilation operators on site i in (2.1).

By definition, a Gaussian state is a state for which the characteristic function is Gaussian in all the variables. Important consequence is that the characteristic function factorizes

$$\chi(\vec{\lambda}, \vec{\lambda}^*) = \prod_i \chi(\lambda_i, \lambda_i^*),$$

which corresponds to a product state in a specific basis (a classical state where different parts of the system are not entangled with each other).

In the Gaussian state Wick theorem applies, allowing to express higher order correlation functions in terms of the lower-order correlators. In this regard Gaussian states are very convenient for calculations.

An important example of a Gaussian state is a thermal state of a free system (even a vacuum is a Gaussian state as it is a thermal state at zero temperature). The same logic applies to a generalized thermal state of a free system, namely the Generalized Gibbs ensemble. I note that a thermal state of a non-free (interacting) system is in general non-Gaussian.

Wigner function of a Gaussian state is also a Gaussian (Section 1.3).

Equilibration. A tendency of the system to relax to a steady state, which is the starting observation for applying statistical methods and the expression of the second law of thermodynamics.

Weak equilibration. The time average of an observable converges to a specific value as $t \to \infty$. This allows for fluctuations around a time-averaged state [177].

Strong equilibration. At almost all times the local observables are equal to the observables in time-averaged (equilibrated) state. It is conjectured that all systems exhibiting weak equilibration also exhibit strong equilibration in thermodynamic limit [178].

Equilibrated state. The time averaged state with the density matrix given by

$$\hat{\varsigma} = \overline{(\hat{\rho}_t)} = \lim_{\tau \to \infty} \frac{1}{\tau} \int_0^\tau \hat{\rho}_t dt.$$

For system without degenerate eigenstates it is given by a diagonal state, namely the state given by a density matrix, which has only diagonal values in its eigenrepresentation

$$\lim_{\tau \to \infty} \frac{1}{\tau} \int_0^\tau dt \, \hat{\rho}(t) = \lim_{\tau \to \infty} \frac{1}{\tau} \int_0^\tau dt \sum_{k\ell} e^{i(\epsilon_k - \epsilon_\ell)t} \langle k | \hat{\rho}_0 | \ell \rangle = \sum_k \langle k | \hat{\rho}_0 | k \rangle,$$

where $|k\rangle$ and ϵ_k are exact eigenstate and the corresponding eigenenergy.

In case of a degenerate spectrum the equilibrated state retains more information about the initial state as the equilibrated density matrix has coherence terms between degenerate eigenstates. But this case can be reduced to a diagonal matrix by splitting the Hilbert space into non-coupled symmetry sectors, each of which contains no degenerate eigenstates. So in the following I will use terms 'diagonal' and 'equilibrated' states interchangeably.

Thermalization. A more narrow notion than equilibration (thermal state must be equilibrated, but equilibrated state can be non-thermal), meaning that observables of equilibrated system (even starting from a pure state) can be predicted by usual statistical ensembles, i.e. observables computed with density matrix an equilibrated system are close to observables computed with a micro-canonical density matrix at the same energy.

I note that a small subsystem of a large microcanonical ensemble can be always formulated in terms of a canonical (or grand canonical) ensemble, as long as the interactions along the subsystem boundary are sufficiently weak (e.g. short-range). Classical case can be found in any textbook on statistical physics [175, 179]. An explicit derivation in quantum case can be found in [180].

Typicality. A randomly picked pure state will almost always locally appear fully thermalized (subsystems having maximal possible entanglement entropy with their complement). It was proven by the geometry of the Hilbert space by invoking Levy's lemma, that states that for multidimensional spheres a smooth function evaluated at a random spot will be exponentially close to its mean value [181].

Typicality has to be distinguished from ETH (to be defined later in Section 2.8): in ETH we are considering one eigenstate which locally looks thermal; typicality claims that a random state, being a superposition of arbitrary many eigenstates, will in general look thermal.

In classical physics typicality has a very simple intuitive understanding: if we pick a random state of, say, a gas in a box, that with overwhelming probability we will pick a state of largest entropy, which is thermal by definition [118].

Typicality is a statistical concept and doesn't deal with time evolution. Some criticism of the notion is based on the fact that in physics we never deal with random states: we usually prepare a system in a very controlled specific state (say, a ground state) and then follow its time evolution. Nevertheless, typicality argument was recently shown to be fruitful in numerical simulations where it is sometimes easier to pick a random pure state and evolve it in time rather than to diagonalize the Hamiltonian [182].

There are ways to extend typicality to dynamical processes, e.g. it was shown that for almost any interacting system in a pure state, a subsystem of it will spend overwhelmingly large time near its equilibrated value during evolution [178].

There are two more notions which are defined a bit different from the actual typicality in original sense:

Weak typicality: the diagonal ensemble has a thermal structure, meaning that observables calculated using weakly equilibrated state are indistinguishable from observables calculated on a corresponding microcanonical thermal state [183].

Strong typicality: the reduced density matrix of the system is thermal, implying that at each point in time the system looks locally thermal (no need of time averaging) [183].

Quantum central limit theorem (QCLT). States that when the entanglement of the initial state of a 1D system is weak enough (e.g. if the initial state is a product state or if the correlators $\left\langle a_i^\dagger a_j \right\rangle$ decay algebraically with $|i - j|$), the system will relax to a Gaussian state after evolution given by a free (quadratic) Hamiltonian [184].

2.5 Dynamics after a quench

This section begins the main part of the chapter devoted to studies of relaxation and thermalization of a quantum many-body system after a quench to a highly non-equilibrium state. In this section I address the first aspect of thermalization: equilibration to a steady state.

I have already discussed a specific type of quench in a continuous quantum system in Section 1.10 of the previous chapter, but now I'm introducing a quench in a discrete analogue of it, namely a quench in a one-dimensional Bose-Hubbard chain.

2.5.1 Setup

My setup is inspired by an actual experiment performed in I. Bloch's group [126]. In a nutshell the experiment looked like this: initially a one-dimensional optical lattice was initialized with a density wave state with every other site occupied with one atom in a Fock state

$$\left| \psi_0 \right\rangle = \left| \ldots 010101 \ldots \right\rangle = \hat{a}_1^\dagger \hat{a}_3^\dagger \hat{a}_5^\dagger \ldots \hat{a}_M^\dagger \left| 0 \right\rangle.$$

I will call this initial state a *Néel state* by analogy with a ground state of an antiferromagnet $\left| \ldots \uparrow\downarrow\uparrow\downarrow\uparrow\downarrow \ldots \right\rangle$ [185]. Initially there is no tunneling,
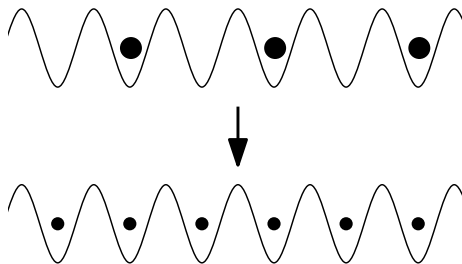
Figure 2.3: Scheme of the system under study in the current chapter. Initially every second site in 1D optical lattice (Bose-Hubbard chain in Mott-insulating regime) is occupied with one boson in Fock state (Néel state). At $t = 0$ the tunneling rate is quenched from $J = 0$ to $J = 1$. Atoms start to tunnel between the wells, and eventually an equilibrium state is reached with $1/2$ of a particle per site on average (in thermodynamic limit). I study the dynamics and the steady state as a function of the on-site self-interaction $U \in [0, \infty]$. The setup is inspired by the experiments performed in I. Bloch's group [165, 126].

corresponding to $J = 0$ in the BH Hamiltonian (2.1). At $t = 0$ the parameters J, U are quenched to a finite values and the system starts to evolve, Figure 2.3.

The experiment showed relaxation of the charge-density with the final state even and odd site occupation numbers being $1/2$ on average. Numerical DMRG simulations agreed very well with experimental data, confirming the full relaxation of the system in position space [127].

When implying periodic boundary conditions, this result is anticipated because of the translation invariance of the Hamiltonian (2.1). On the other hand, relaxation in momentum space under Hamiltonian (2.2) is far from being trivial and will be the main topic of this chapter.

In the following I will put $J = 1$, so the only free parameter being U. Real value of J can be always recovered by rescaling of time.

2.5.2 Initial State

I've already discussed the initial state in position space, but now let's turn to the system's description in momentum space, namely to the reduced one-mode states with momentum k, given by the density matrices ρ_0^k (in the following I will omit hats over operators where it cannot lead to confusion)

$$\rho_0^k = \operatorname{tr}_{\ell \neq k}(\rho_0), \tag{2.4}$$

where the trace is performed over all modes that are not k.

For example, if our system is given by the Hamiltonian in momentum space (2.2) and has four bosons, then ρ_0^k for mode k is a 5×5 matrix with rows and columns corresponding to $n = 0 - 4$ bosons. Its diagonal elements give probabilities of finding n bosons in mode k (so $\operatorname{tr} \rho_0^k = 1$), and off-diagonal elements represent coherences due to superpositions of different occupation numbers.

Note that it is not the same as the one-body density matrix ρ_0^1 given by

$$\langle k | \rho_0^1 | \ell \rangle = \operatorname{tr}(\rho_0 \, b_k^\dagger b_\ell), \qquad k, \ell \in [0, M-1].$$

The latter can give expectation values of all one-body operators $\langle O_1 \rangle = \text{tr}\,(O_1 \rho_0^1)$, but has no information about higher order moments.

On the other hand, the one-mode density matrix ρ_0^k gives all the information about correlators of all orders, but only for one mode k.

It is possible to show that

> The initial reduced one-mode states are Gaussian and correspond to locally infinite temperature (i.e. $\langle \hat{n}_k \rangle = 1/2$ for all k regardless of energy).

This statement amounts to the fact that if we would perform any measurement on one mode only in an initial state, we couldn't distinguish it from a thermal state at $T = \infty$, cf. Figure 2.9. Of course, the system as a whole is not thermal as there are correlations between different modes that are neglected performing the trace in (2.4).

Proof.   1. Assume that our system is non-interacting.

2. Then quantum central limit theorem holds as in [184], and the final state after dephasing is a product state of Gaussian states on each site.

3. Fourier transformation of uncorrelated chain of Gaussian states gives us again a set of uncorrelated Gaussian modes.

4. The modes are non-interacting, meaning that their expectation values of all one-mode (and many-body) correlation function stay constant in time, e.g. $\langle \hat{n}_k \rangle = \text{const}$, $\langle \hat{n}_k^2 \rangle = \text{const}$, etc. This also implies that all one-mode Wigner functions retain their shape from the very initial state (of course, the relative phases between the modes will change during evolution—that's the dephasing).

5. That means that the reduced one-mode density matrix of the initial state is Gaussian (the system looks locally Gaussian in the momentum space; though the initial state is not the product state of Gaussians as different modes are correlated in the beginning).

6. The initial state is independent of interaction, so the initial state looks the same for any interaction strength: the reduced density matrix gives the same Gaussian state for each mode. A local measurement in momentum space (tracing out all the modes except one k-mode, by this forgetting all the correlations between different modes k_1, k_2 etc.) will show a Gaussian state with the same shape for any k, so a momentum-local observer would conclude that the initial state is an infinite temperature state.

$\square$

Finally I note that if we define 'bath' as all degrees of freedom we are tracing out, then it was showed that physically cutting off the 'bath' and letting the system thermalize will lead to the same outcome [183].

2.5.3   Equilibration

Recurrence times for quantum many-body systems, which happen when the initial state is perfectly restored due to realignment of all the eigenstates, is
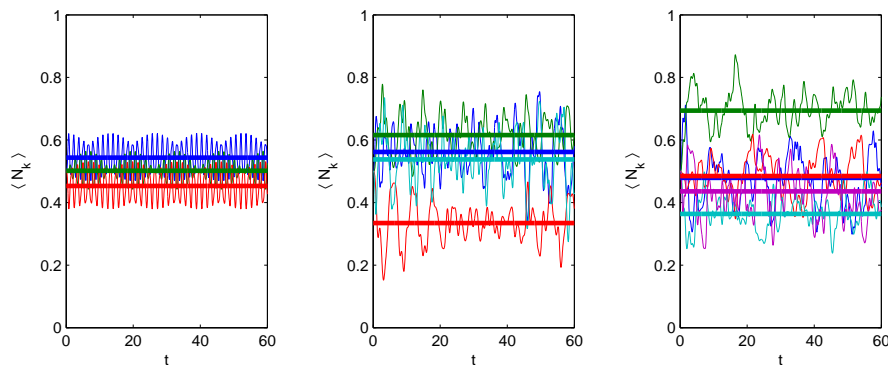
Figure 2.4: Weak equilibration in mesoscopic system: mode occupation numbers (thin zigzag lines) for $M = 4, 6, 8$, $J = U = 1$ are fluctuating around equilibrium values $\bar{n}_k = \text{tr}\,(\varsigma\,\hat{n}_k)$, thick horizontal lines, where ς is the diagonal (equilibrated) state. Different colors correspond to different modes k. Note that $\forall k : n_k|_{t=0} = 1/2$ as described in Section 2.5.2.

generally exponentially large in the number of particles, so it must have no relevance even to modest-sized quantum systems.

Neglecting the revivals, a quantum system is expected to equilibrate in a weak or strong sense. Considering relaxation after a quench, our mesoscopic Bose-Hubbard chain clearly equilibrates in the weak sense, Figure 2.4, so in the following sections I'll be considering the properties of the system in the equilibrated state ς.

An important question is whether different modes are correlated in the equilibrated state. This can be checked using correlator $C_{kl} = \text{tr}\,\varsigma\,\bar{b}_k b_l$. For a non-interacting system the modes must be uncorrelated due to the QCLT. On the other hand, for hard-core bosons the modes must be highly correlated as a lot of modes contribute to a single fermionic quasiparticle.

It was checked numerically that for small U the modes are almost uncorrelated, which supports the random phase approximation hypothesis; more on that in Section 2.10.

It is interesting to look at the entanglement entropies in mode basis, as the initial one-mode states are highly entangled with the other modes in the 'bath', but this entanglement decreases as the system evolves, leading to disentanglement and apparent *reverse thermalization*, Figure 2.5. Of course, in the complimentary site basis we started from a product state, meaning that initially there was no entanglement, and it developed as the system evolved. In some sense thermalization correspond to 'equilibration' of entanglement in both bases.

There is a close analogy with the process of decoherence from quantum foundational studies, and applying this insight to condensed matter systems is an interesting direction of future study [186].
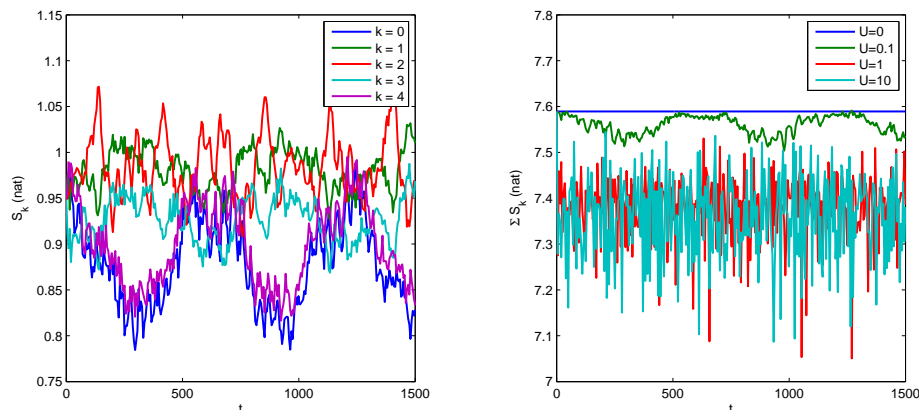
Figure 2.5: One-mode entanglement entropies $S_k = -\text{tr}\,(\rho^k \log \rho^k)$ for $M = 8$, $U = 0.1$ (left) and total one-mode entropy $\sum_k S_k$ for different interaction strengths (right). We see that the total entropy in the mode basis is larger initially than during the evolution, which correspond to some kind of *reverse thermalization* in modes basis.

2.6 Quantum Integrability

Classical integrability is a well-defined and thoroughly studied concept [54, 55], but its quantum counterpart is still far from being fully understood.

Caux and Mossel introduce a chain of integrability classes considering how the number of integrals of motion scales with the system size in appropriate basis [189]. For example, Luttinger liquid is linear integrable in sites basis as it can be cast into a free theory by Fourier transformation.

Many algebraic-Bethe-ansatz integrable models also fall into the linear integrability class, including Heisenberg chains (and Tonks-Girardeau hardcore bosonic gas in a 1D optical lattice, as it is mappable to the Heisenberg XXZ magnet), t-J and Hubbard models, restricted Bose-Hubbard with up to two bosons per site, and few others.

Some long-range interacting systems such as Haldane-Shastry model [190] have quasi-polynomial density character such as $O(N^{\log N}) \sim O(e^{\log^2 N})$, in this sense possessing a weaker form of integrability than Heisenberg spin chains. Its energy level statistics is neither Poissonian nor Wigner-type.

Quantum counterparts of classical chaotic systems, which possess Wigner-type energy level statistics, should fall into exponential integrability class with numbers of integrals of motion scaling as $O(e^N)$ (e.g. they can be projectors on the exact eigenstates), so such systems can be called quantum non-integrable.

Sticking to this classification we see that our Bose-Hubbard chain is linearly quantum integrable in sites basis in non-interacting and hardcore-interacting limits, as in both cases it is mappable to a free system. How to classify the system in the intermediate regime $0 < U < \infty$ is not completely clear.

It is conjectured that in thermodynamic limit even the infinitely small integrability breaking term leads to emergence of chaos, in this way denying existence of a quantum KAM theorem [94].

The spectrum of the BH-model is thoroughly studied and is known to exhibit
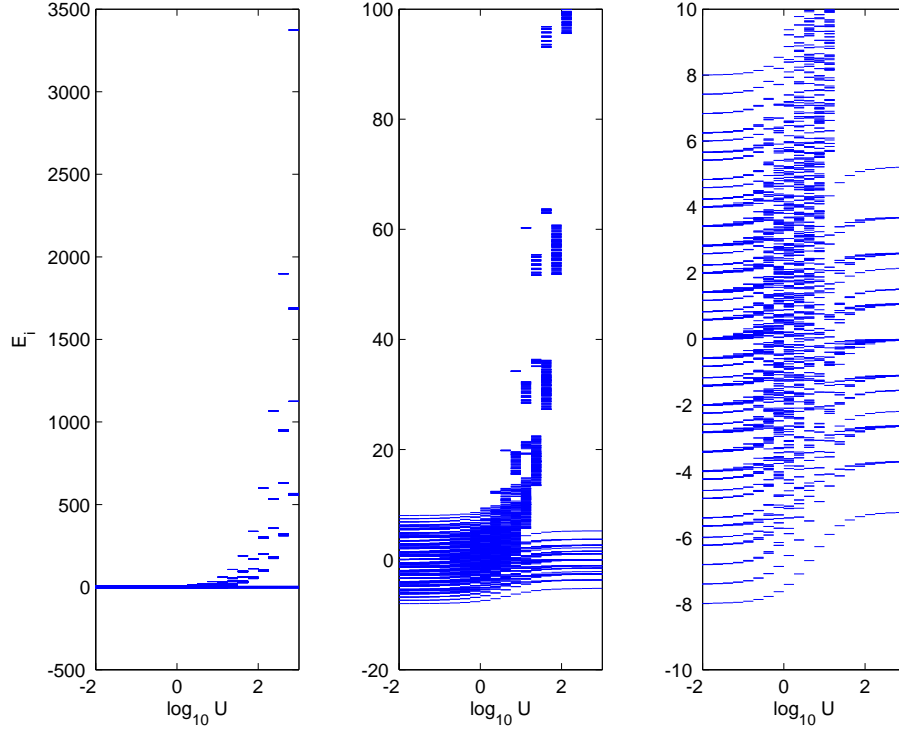
Figure 2.6: Integrability crossover from the spectrum perspective for a system of $N = 4$ bosons on $M = 8$ lattice sites. Line segments represent energies E_i of the exact many-body eigenstates as a function of interaction strength U. Three panels differ in the energy scale only. At small U we observe continuous phononic spectrum of non-interacting oscillators (its apparent discreteness stems from the finite size of the system), which evolve into tight clusters of eigenstates, characterized by 1–4 particles sitting on the same site. Note that the energy of those states with more than one particle per site goes to infinity with $U \to \infty$, so in the end we are left with only one cluster of eigenstates—the fermionic spectrum of the hard-core gas (right panel). Note the uniqueness of the many-body ground state and chaotic region at $0.1 < U < 10$, where the eigenenergies are proved to obey Wigner-Dyson statistics—a well-known criterion for quantum non-integrability [187, 188].

regular statistics in both integrable limits and the Wigner-Dyson statistics in between [187, 188], in this way stating its non-integrability. The spectrum for a particular symmetry sector $M = 8$, $N = 4$ is shown in Figure 2.6.

One can see from the figure how exactly Poisson-type spectrum of integrable system at $U = 0$ transforms into a chaotic region, and then the latter dissipates due to the fact that eigenstates having more than one boson per site acquire infinite energies and disappear from the spectrum. Finally at $U \to \infty$ one recovers again a Poisson-type spectrum of four noninteracting fermions, governed by the Hamiltonian (2.3).

In the next following sections I develop new measures of integrability as functions of interaction strength, which are based on eigenstate thermalization and 'forgetfulness' of the initial state.

2.7 Initial State Independence

The Second aspect of thermalization is initial state independence, namely the statement that the properties of a small subsystem in a thermalized state should not depend on this subsystem's initial state and on the initial state of the 'bath', but rather only on some aggregate properties like energy density.

It is generally believed that integrable systems retain the information about the initial state better (as there are many integrals of motion that separate the phase space into non-connected parts, only one of which is left for the system to explore). On the other hand, non-integrable systems should be more forgetful, as for them the whole microcanonical shell is open to explore.

Many-body localization (MBL). First of all, in the recent years it has been shown that a simple classification of quantum many-body systems into integrable vs non-integrable is not sufficient due to a discovery of a new—many-body localized—phase.

Anderson localization is a well-known concept of one-particle physics, which exhibits itself in the absence of transport in disordered potential [191]. However, for a long time it was believed that introduction of inter-particle interaction will break the localization and restore transport, until it was proven that in some cases localization can still persist [192], opening a whole new branch of non-equilibrium physics.

It is interesting that despite the system being localized and exhibiting no transport, the entanglement still grows logarithmically in time [193], in contrast to a conventional non-integrable system with diffusive transport, where it grows linearly [194]. Sure, there is no contradiction as entanglement is not an observable and doesn't carry information.

Novel research suggests that MBL phase is closer to integrable systems, where integrals of motion may be constructed from tight clusters of eigenstates, which are localized in real space [195]. It is not yet clear if a GGE can be constructed in this case.

So in the following when talking about initial state dependence in non-integrable systems, I will exclude MBL states from this category.

Effective entanglement in the eigenbasis (EEE). It is known that sometimes many-body nonintegrable systems don't relax and preserve memory of the initial
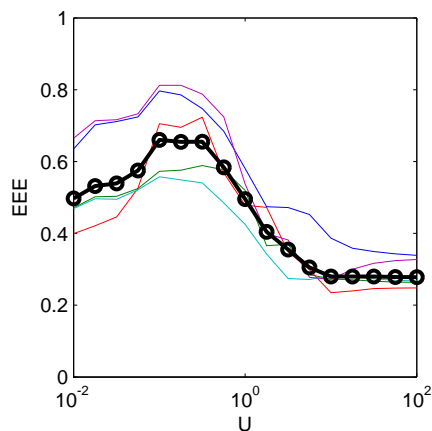
Figure 2.7: Results for a 1D Bose-Hubbard chain with 4 bosons on 8 sites: effective entanglement in the eigenbasis (EEE)—the measure of how much the relevant energy eigenstates resemble locally the initial state. Small EEE means that two systems, prepared initially in distinguishable states, will remain distinguishable after quantum evolution; large EEE means that the system will effectively forget its initial condition after equilibration [196]. Different modes k are represented with different colors, black line being the average. The shape of the curve suggests that the system forgets its initial state better in the chaotic regime $U \sim 1$, meaning that EEE can be used as a measure of quantum integrability. I note that the Hamiltonian does not contain any disorder.

state, and Gogolin, Müller and Eisert developed a measure of such memory preservation [196]. This measure is effective entanglement in the eigenbasis $R(\rho)$ defined for a non-degenerate Hamiltonian as

$$R(\rho) = \sum_j \left| \langle j | \rho | j \rangle \right|^2 \cdot \mathcal{D}(\rho_k, \mathrm{tr}_B \, |j\rangle\langle j|),$$

where $|j\rangle$ are the eigenstates, ρ_k is a reduced density matrix of some subsystem, partial trace is performed over the 'bath' (complement of k), and $\mathcal{D}(x, y) = ||x - y||_1$ is a trace distance between two density matrices.

Physical understanding of this measure can be gained from the fact that $\mathcal{D}(\rho_k, \mathrm{tr}_B \, |j\rangle\langle j|)$ shows how much an eigenstate $|j\rangle$ resembles the state ρ *locally*, locality in this context doesn't necessary indicate real space locality, but is manifest in an arbitrary splitting of the system into subsystem ρ_k and the bath B. And second observation is that the term $\left| \langle j | \rho | j \rangle \right|^2$ weights the eigenstates by their overlap with the initial state, including only the relevant ones in the sum.

Let's perform the trace over the bath on our time-averaged state, with resulting reduced density matrix $\varsigma_k = \mathrm{tr}_B \, \varsigma$ enough to calculate all the observables in subsystem k. Then a theorem proved in [196] states that the systems well distinguishable locally in the beginning (say, we are starting from different initial states) will remain distinguishable during time evolution (meaning that there is some memory of the initial state) if EEE is small.

$$\mathcal{D}[\varsigma_k, \varsigma'_k] \geqslant \mathcal{D}[(\rho_0)_k, (\rho'_0)_k] - R(\rho_0) - R(\rho'_0).$$

That suggests using EEE as a measure of how much information the system forgets during time evolution. Naive expectation would be that a non-integrable system loses information about the initial state quickly, meaning that EEE can serve as a measure of integrability. And indeed, calculations with 1D Bose-Hubbard model suggest that it's precisely the case, see Figure 2.7.

Conclusion is that EEE can serve as another quantum integrability measure in addition to those known before (e.g. Poisson to Wigner-Dyson statistics crossover). Here I note that there was no frustration in the Hamiltonian, meaning that MBL effects cannot be present.

2.8 Eigenstate Thermalization Hypothesis

Our third aspect of thermalization is the fact that we may call a system thermalized if measurements in the steady state give us the very same results as a conventional thermal ensemble (e.g. microcanonical) would predict. In modern quantum mechanics this conjecture is known under the name of Eigenstate thermalization hypothesis (ETH).

Definition. ETH is a conjecture stating that a general non-integrable system prepared in an eigenstate looks thermal (in the sense of microcanonical ensemble) for some set of observables. Equivalent to say is that those observables are smooth functions of energy. ETH implies that apparent thermalization is just dephasing of the eigenstates, but non-equilibrium states don't look thermal because of finely-adjusted phases.

Following the discussion in [197], we start with an arbitrary initial state $|\psi_0\rangle$ evolving as

$$|\psi_t\rangle = e^{-i\hat{H}t}|\psi_0\rangle = \sum_i C_i e^{-i\epsilon_i t}|i\rangle,$$

where $C_i = \langle i|\psi_0\rangle$ and ϵ_i is the energy of the eigenstate $|i\rangle$. Then an expectation value of some observable $\hat{O}$ will be

$$\langle\hat{O}(t)\rangle = \langle\psi_0|\hat{O}|\psi_0\rangle = \sum_{ij} C_i^* C_j e^{i(\epsilon_i - \epsilon_j)t} O_{ij},$$

where $O_{ij} = \langle i|\hat{O}|j\rangle$.

If the observable relax, it must only be to the time-averaged value

$$\langle\hat{O}\rangle = \sum_i |C_i|^2 O_{ii},$$

where the spectrum is taken not to have degenerate energy gaps for the sake of simplicity. This non-degeneracy condition is not essential and can be lifted. The ensemble on the right-hand side is called the diagonal ensemble.

Statement that the diagonal ensemble predictions agree with those of the microcanonical one can be formulated as

$$\sum_i |C_i|^2 O_{ii} = \langle\hat{O}\rangle_{E_0} = \mathcal{N} \sum_j O_{jj} \cdot \theta(|E_0 - \epsilon_j| < \Delta E),$$

where $\left\langle \cdot \right\rangle_{E_0}$ stands for a microcanonical ensemble average centered at the energy E_0 with the width of ΔE, θ is the Heaviside step function, and $\mathcal{N}$ is a normalization factor.

Eigenstate Thermalization hypothesis conjectures that this universality is due to the fact that the observable looks thermal in each eigenstate

$$\boxed{\langle i|\hat{O}|i\rangle = \left\langle \hat{O} \right\rangle_{E_0}.}$$

We see that the left-hand side contains properties of exact eigenstates, but the right-hand side—nothing but energy. So the most simple statement for ETH could be formulated as:

"Eigenstates close in energy are similar in all relevant aspects."

An open question is which aspects should we consider relevant. Usually relevant observables are measurable ones, which can be represented as sums over few-body field operators in second quantized formalism. For example, relevant operators in this case would be local density $\hat{n}(z) = \bar{b}(z)\hat{b}(z)$ or mode occupation numbers $\hat{n}_q = \bar{b}_q\hat{b}_q = \frac{1}{L}\sum e^{iq(z-z')}\bar{b}(z)\hat{b}(z')$. This leading role of locality stems from the fact that physical interactions are local in position space. Obviously, one can always explicitly construct non-local observables, which never thermalize, e.g. projectors on eigenstates, but there is no physical procedure to measure them. In Appendix E I formulate a conjecture which addresses ETH without explicitly appealing to locality.

In the following I will accept the locality condition, which implies that if ETH holds, then for all local few-body observables the diagonal state is close to the microcanonical state.

History and recent developments. ETH, believed to bridge the gap between the statistical description of a classically chaotic system and quantum mechanics, has a long history. One of the predecessors of ETH was *Berry's conjecture*, which states that for a gas of hard spheres the exact many-body eigenstates are superpositions of plane waves with random phases and amplitudes, but fixed momenta (eigenstates are infinitely sharp in energy) [198, 199, 200].

Later Srednicki proved Berry's conjecture [201], and coined the term ETH as a generalization of it for systems other than hard-sphere gases. Similar ideas have been independently formulated by Perez [202] and Deutsch [203].

One can even trace the roots of ETH to the heroic times of establishment of the quantum theory in the first half of the 20th century, as it was proven that one assumption of *quantum ergodic theorem* by von Neumann [204] is equivalent to ETH [205]. Recently quantum ergodic hypothesis was revived under the name of *normal typicality* [206].

In the new century ETH was brought into spotlight of modern non-equilibrium theory by the seminal paper of Rigol, Dunjko and Olshanii [197], where a clear distinction between integrable and non-integrable systems (being in this case 1D and 2D hard-core bosonic gases) was numerically demonstrated, which declares itself in the absence/presence of thermal eigenstates, in full agreement with ETH.

Since then it became a widespread belief that ETH can serve as an ultimate litmus test of quantum (non-)integrability. In the following I show that this conjecture can be applied even to small systems.

Shortly after many more studies on ETH started to appear. Detailed analysis of onset of quantum chaos in a system of hard-core bosons, when the non-integrability is caused by next-nearest-neighbor hopping, showed that in a quantum chaotic system states close in energy seem statistically similar, linking quantum chaos and ETH. Localized eigenstates, on the other hand, were shown not to obey ETH, which opens new interesting connections between ETH and many-body localization phenomena [207].

ETH was also generalized to integrable systems, where it was shown that majority of states close in the values of all the conserved charges are similar in all relevant observables, thus assuming that the diagonal ensemble can be efficiently approximated by a generalized microcanonical one [208].

Note that observables can have thermal values even in absence of ETH. For example, due to the finite number $N \gg 1$ of eigenstates contributing to an initial state, averaging can bring expectation values close to their microcanonical values even in the integrable case when ETH doesn't hold. This idea was noted in the seminal paper by Peres [202], and recently has been applied under the name of Eigenstate Randomization Hypothesis [209].

Finally I'd like to note that there is an alternative way of addressing the thermal expectation values of the operators besides ETH, namely the application of Mazur's inequality [210, 189, 211], which states that if we take an arbitrary observable with zero mean A_t, then the long-time average of correlations will be

$$\overline{\langle A_0 A_t \rangle} \geqslant \sum_{i=1}^{N} \frac{|\langle A \cdot Q_i \rangle|^2}{\langle Q_i^2 \rangle},$$

where N is the number of properly normalized integrals of motion Q_i. Note that right-hand side corresponds to overlap of the observable with all the integrals of motion, and if it is finite, then there is quasiperiodic behavior of correlators and the current observable is integrable. It remains an interesting question how this approach is linked with ETH.

ETH and integrability breakdown. I studied the applicability of ETH at integrability breakdown with the same 1D Bose-Hubbard chain, as a function of on-site interaction U, see Figure 2.8. As we are interested in the properties of the Hamiltonian, the dynamical evolution is irrelevant.

Implying that physical observables should be represented with few field operators in position basis, I turned to momentum occupation numbers

$$\hat{n}_k = \bar{b}_k \hat{b}_k = \frac{1}{L} \sum e^{ik(z-z')} \bar{b}(z) \hat{b}(z').$$

Eigenstate expectation values $\bar{n}_k = \langle \epsilon_i | \hat{n}_k | \epsilon_i \rangle$ follow the similar pattern independent of k (the figure shows a typical example for $k = 2$), but strongly dependent on U.

In the free boson limit $U = 0$ expectation values of $\bar{n}_q$ (EEV) fluclutate wildly between the eigenstates close in energy, as expected for an integrable system where ETH does not hold (green stars on the figure). This behavior can be easily understood noting that the exact eigenstates for an ensemble of uncoupled harmonic oscillators are multiply degenerate and result in integer boson occupation numbers.
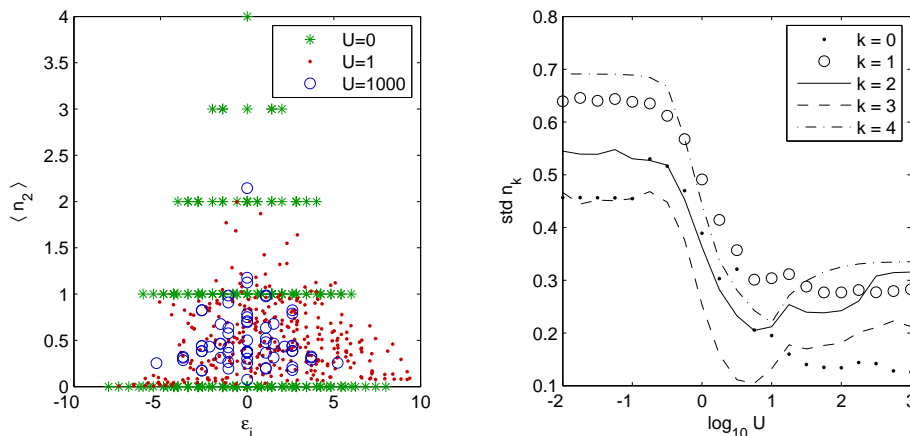
Figure 2.8: Results for eigenstate thermalization hypothesis applicability to 1D Bose-Hubbard chain. **Left:** Eigenstate expectation values (EEV) of the occupation of the 2nd momentum mode $\langle n_2 \rangle = \langle \epsilon_i | \hat{n}_2 | \epsilon_i \rangle$ for non-interacting bosons $U = 0$, soft-core $U = 1$ and almost-hardore ones $U = 1000$. **Right:** Eigenstate non-thermality $Q_0 = \mathrm{std}\,\bar{n}_k$ (for a microcanonical window $\Delta E = 2$ centered at zero, it was checked that the overall behavior doesn't depend on ΔE much) as a measure of breakdown of the eigenstate thermalization: the closer Q is to zero, the closer are predictions of the diagonal ensemble and the microcanonical ensemble, and the better ETH holds. For some observables the microcanonical prediction fits better at the chaotic region $U \sim 1$ (a dip in the functions), which hints to applicability of ETH even for mesoscopic systems and shows that ETH can serve as a measure of quantum integrability.

As U grows and integrability fades, the fluctuations in EEV go down, meaning that eigenstates close in energy become more similar to each other with respect to $\bar{n}_q$.

To quantify ETH applicability I introduce *eigenstate non-thermality*, which is given by a standard deviation of $\bar{n}_q$ in a small microcanonical window around energy E

$$Q_E = \mathrm{std}\left\{ \langle i | \hat{n}_q | i \rangle : \ |E - \epsilon_i| < \Delta E. \right\}$$

The closer Q_E is to zero, the closer are prediction of the diagonal ensemble and the microcanonical ensemble, and the better ETH holds.

Q_E is dependent on energy, meaning that this measure takes into account the initial state. Our usual pick is the Néel state, which has zero energy, so in Figure 2.8 I consider Q_0.

Right panel of Figure 2.8 shows an interesting feature: we know that Bose-Hubbard chain is integrable in both limits $U = 0$ and $U = \infty$, and for high-energy modes Q_0 exhibits a dip in the chaotic region $U \sim 1$, meaning that ETH holds better there, and values of $\langle n_k \rangle$ computed with diagonal ensemble would agree better with microcanonical prediction.

The conclusion is that ETH is still applicable to small mesoscopic systems and can be used as a measure of integrability.

2.9 Generalized Gibbs Ensemble

In the previous sections we discussed the equilibration of a quantum many-body system after a quench in the non-integrable regime, where it is supposed to thermalize in microcanonical sense in accordance with ETH (the conventional thermal partition function $Z = \text{tr}\exp(-\beta\hat{H})$ can always be recovered if the density of states grows fast enough [180]). But is there any analogous steady state after eqilibration in the integrable regime?

Definition. A popular conjecture is that indeed there is a statistical ensemble able to describe the steady state in thermodynamic limit, which is known under the name of the generalized Gibbs ensemble (GGE) and is given by the partition function

$$Z = \text{tr}\exp\left(-\sum_{i=1}^{N}\beta_i\hat{I}_i\right),$$

where $\{\hat{I}_i\}$ is a set of conserved quantities (the Hamiltonian being one of them), and β_i are generalized temperatures.

This claim is not as trivial as it might look from the first sight. Stating that the system equilibrates to a GGE (meaning it spends most of the time near GGE) is essentially equivalent to claiming the generalized ergodic hypothesis, meaning that during evolution the system uniformly explores the whole generalized microcanonical shell ν_I of the phase space, given by $\{\hat{I}_i\}$.

If we consider the whole phase space (and not only the shell ν_I), then GGE can be viewed as the high-probability region that maximizes the full Gibbs-von Neumann entropy $S = -\text{tr}\,\hat{\rho}\log\hat{\rho}$, and ergodicity implies that at almost all times we'll find the system inside that region just because it's overwhelmingly large. In thermodynamic limit this region collapses to the shell ν_I, and we recover the equivalence of ensembles [208]. The same discussion applied to Gibbs ensemble can be found in [118].

An important observation was made by Caux and Mossel in [189] which can help to pick the relevant I_i, at least for finite systems. Normally a system after a quantum quench is not in an eigenstate, but in a superposition of eigenstates around some central energy with finite spread. If some integral $\hat{I}_i$ varies slowly in that region, it will have large β_i, and is important for our statistical description (e.g. energy obviously satisfies that); on the other hand if $\hat{I}_i$ has large variance, then $\beta_i \to 0$, and it can be omitted from the GGE.

In most studies $\hat{I}_i$ are assumed to be local in real space (due to the locality of interaction), but there is no rigorous proof why should they be. There is neither a consensus on what number N of integrals of motion one should consider.

One easy choice would be to pick the projectors on the eigenstates as conserved charges $\hat{I}_i = |i\rangle\langle i|$, where β_i can be recovered from self-consistency condition; but this choice is unphysical as there is no procedure of measuring highly non-local many-body operators such as projectors. Even more, their number must be equal to the dimensionality of the Hilbert space, which grows at least exponentially with system size[1].

---

[1] It has been proven that most of the states in the Hilbert space cannot be reached anyway with any experimental procedure [212]

The general consensus in the community seems to be that GGE is a well defined and fruitful notion for all systems that can be cast into a free form, such as Luttinger liquid, non-interacting or hard-core bosons on a 1D lattice, etc. Hamiltonian of free models has a quadratic form

$$\hat{H} = \sum_i \epsilon_i \bar{b}_i \hat{b}_i,$$

where $\hat{b}_i$ is a bosonic/fermionic field operator. In this case the partition function of the GGE can be readily recovered as

$$Z = \text{tr} \exp\left(-\sum_{i=1}^{N} \beta_i \epsilon_i \bar{b}_i \hat{b}_i\right).$$

An important property of such a free GGE, shared with conventional thermal state, is the fact that correlations factorize due to Wick's theorem (e.g. $\langle \bar{b}_i \bar{b}_i \hat{b}_i \hat{b}_i \rangle = 2 \langle \bar{b}_i \hat{b}_i \rangle^2$ for bosons), which leads to a great simplification of analytic description [103, 213]. But one can easily imagine initial states where Wick's theorem doesn't apply (see Appendix C).

History and recent developments. The new wave of GGE studies came with the seminal paper by Rigol, Dunjko, Yurovsky and Olshanii, where it was numerically observed that the state of a 1D hard-core bosonic gas after relaxation can be very well described with a GGE [79]. After that many more studies on hard-core bosons followed, as this system can be solved efficiently with exact diagonalization.

When a system is weakly non-integrable, it is widely accepted that it establishes a prethermalized plateau, where it stays for a long time before the final relaxation to the thermal state. At the plateau the system may be described with a deformed GGE (e.g. by calculating perturbative corrections to a free system in powers of interaction parameter). There are many results supporting this claim, including studies of nearly-integrable Hubbard model [48], perturbed Falicov-Kimball model [214], weakly non-integrable interacting Peierls insulator [51].

It is still an open question how to apply GGE to other types of integrable models beyond free ones, e.g. those integrable with Bethe Ansatz. The Lieb-Liniger model of one-dimensional locally interacting bosons has always been a paradigmatic quantum integrable system, so it is a natural candidate for construction of a GGE. Although using thermodynamic Bethe Ansatz it is possible to explicitly address the local conserved quantities [83, 81], recently the applicability of the GGE was put under question as it was shown that the Lieb-Liniger gas develops divergent integrals of motion after a quench [215]. It was conjectured that such behavior is endemic to other integrable continuum models with contact interactions. Nevertheless, in long time limit the system end up in a steady state far away from a thermal one.

Another method was proposed to cure this, namely, the 'quench action' approach, where a steady state of 1D Bose gas is found by a variational method as a saddle-point of a particularly constructed action, which can be viewed as some type of a generalized Hamiltonian. [216, 217].
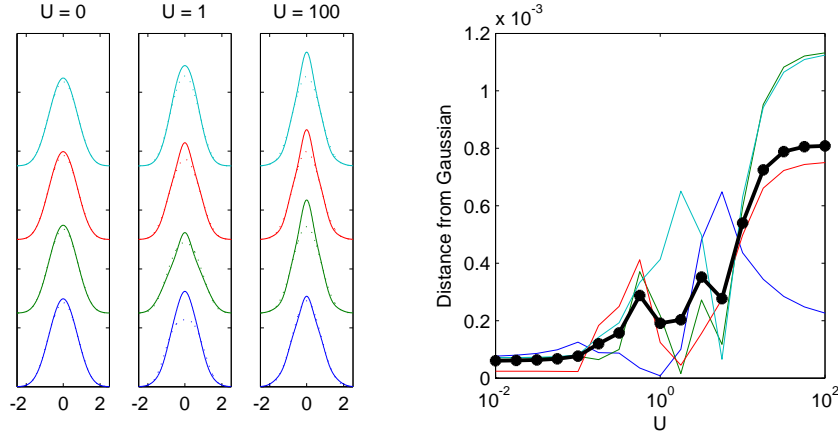
Figure 2.9: **Left:** Wigner functions $W_n(x, p = 0)$ of the first four modes in the equilibrated state (solid) and microcanonical state (dots). At $U = 0$ the modes are Gaussians due to the quantum central limit theorem (Section 2.5.2), which corresponds to a true free GGE in thermodynamic limit. **Right:** Distance from the Gaussian $\mathcal{G} = \int dx \, [W_n(x) - G_n(x)]^2$, where G_n is the Gaussian best fit to W_n. At small interaction strengths W_n are well approximated by a Gaussian, indicating a deformed GGE. Different colors correspond to different modes, black curve is the average. Significance of the measure $\mathcal{G}$ is elucidated in the next section devoted to the kinetic approach.

Emergent GGE at the breakdown of integrability. So in the limiting cases $U = 0$ and $U \rightarrow \infty$ the Bose-Hubbard chain is integrable, and then its equilibrated state in thermodynamic limit should be describable by a GGE. On the other hand, in the intermediate soft-core regime it is non-integrable, so the question is how exactly the applicabilty of GGE breaks down at the integrability crossover.

To address this question in the case of the familiar Néel state to superfluid quench I looked at the shape of the Wigner functions of the one-mode reduced density matrices.

GGE in a free system would correspond to a Gaussian density matrix in momentum mode representation. Arbitrary slices of a Gaussian are Gaussian again, so a measure of gaussianity of one-mode reduced states can serve a test for deviation from a GGE. Results are presented in Figures 2.9 and 2.10.

At $U = 0$ the system is describable by a true free GGE in thermodynamic limit as the modes are Gaussian due to the quantum central limit theorem (Section 2.5.2), and there is no correlation between the modes in the time-evolved state, because in the Heisenberg picture field operators evolve with different frequencies $\bar{b}_q(t) = e^{i\epsilon_q t}\bar{b}_q(0)$ and quickly dephase from the initial highly-correlated state.

On the other hand, at $U \rightarrow \infty$ the modes are in non-Gaussian states and are highly correlated even in the time-averaged state due to Jordan-Wigner mechanism. We know that it still corresponds to a GGE in the basis of emergent free fermions. It illustrates the simple fact that it is possible to have a GGE in one basis (emergent Fermions) and none in another basis (normal modes).

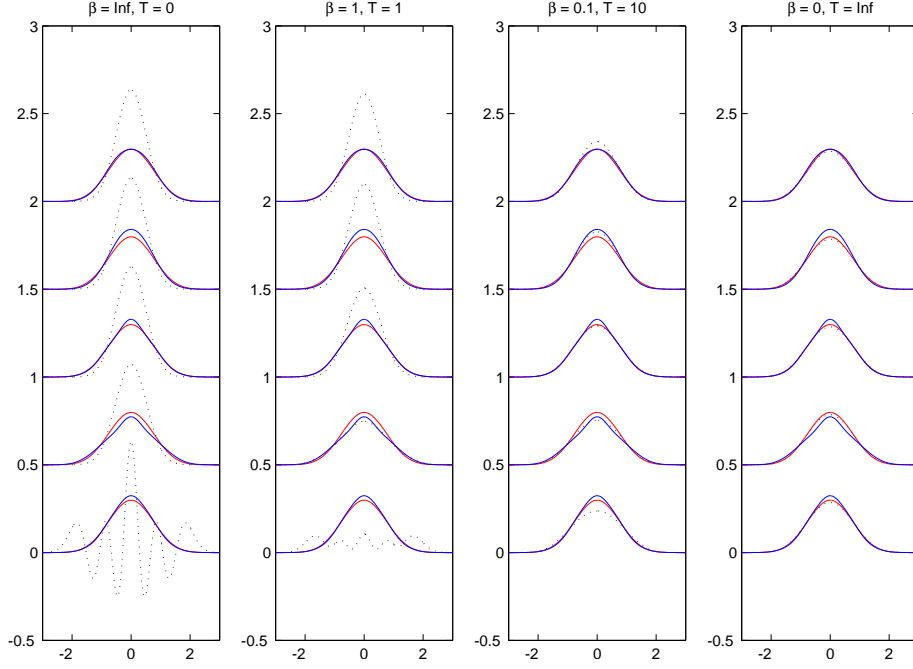At the intermediate regime the modes are in deformed Gaussian states. A

Figure 2.10: BH-chain with moderate interaction strength: $U = 1, J = 1, M = 8, N = 4$. Comparison between the Wigner function of the thermal state (dots), initial state (red) and steady state (blue line). Temperature increases from left to right. Mode numbers increase from bottom to top. Left-most figure: at zero temperature in thermal equilibrium the lowest-lying mode is filled with almost four bosons in a Fock state ('condensate'), other modes are in an almost-vacuum state ('almost' because of the interaction-induced depletion of the condensate). Right-most figure: the initial state is almost indistinguishable locally (in momentum space) from the infinite-temperature thermal state. The steady state is also Gaussian with good accuracy (meaning deformed-GGE), but doesn't correspond to a conventional thermal ensemble (e.g. compare blue lines with dots on the third figure).

straightforward route of analytically quantifying the deformation of the GGE would be to construct the partition function from the full BH Hamiltonian (2.2), and then to use standard diagrammatic techniques for perturbation over the small parameter U [218, 219].

Another possibility would be to consider the integrals of motion of the nearby integrable models such as nonlinear Schrödinger equation and Ablowitz-Ladik lattice [220]. It has been shown that in some cases nearby integrable modes constraint the dynamics of quantum chaotic system [48]. Note the problem's similarity with the scarring phenomena of in the context of classical chaos [201].

Maybe the most important question considering the emergent GGE could be: "Who cares? Maybe there is some deformed GGE, but what benefits does this description provide?" I turn to this question in the next section devoted to the kinetic theory.

2.10 Kinetic theory

Kinetic theory describes evolution of a classical/quantum system driven out of equilibrium. This approach was pioneered by Boltzmann in 1872 when he derived his famous equation

$$\hat{L}[f] = \hat{C}[f],$$

where $\hat{L} = \frac{d}{dt} = \frac{\partial}{\partial t} + \frac{\vec{p}}{m} \cdot \nabla + \vec{F} \cdot \frac{\partial}{\partial \vec{p}}$ is the Liouville operator describing the evolution of a phase space volume, $f(\vec{r}, \vec{p}, t)$ is the one-particle probability density function, and $\hat{C}$ is the collision operator.

The key insight of Boltzmann was the molecular chaos hypothesis or *Stosszahlansatz*, stating that one can neglect correlations between particles, which leads to a great simplification of the collision term and renders they dynamics Markovian (time-local and memory-less). For example, in the case of two-body collisions in a nearly ideal classical gas the collision term becomes

$$\hat{C}[f] = \iiint \omega \left[f_2 f_3 - f f_1 \right] d\Gamma_1 \, d\Gamma_2 \, d\Gamma_3,$$

where $d\Gamma_i$ are phase space elements, $\omega = \omega(\Gamma, \Gamma_1; \Gamma_2, \Gamma_3)$ is a function describing effectiveness of collision which drives two particles from the phase space elements Γ and Γ_1 into Γ_2 and Γ_3. The term in square brackets has an intuitive meaning of the 'income term' $f_2 f_3$, given by the occupancies of phase space elements where the particles can come from, and the 'outflow term' $f f_1$, given by the occupancies of the parts of the phase space from where the particles are drained [221].

In this section I'll show how to apply the Boltzmann kinetic equation to dynamics of a quantum Bose-Hubbard chain driven out of equilibrium by a quench.

Recent developments and applications. Kinetic approach is historically the first method of studying systems out of equilibrium, and it has a strong record of successful applications. In the context of condensed matter, it has been used to describe evaporative cooling and condensation of a bosonic gas in a trap [59, 70, 222], decay of quasiparticles in 1D BEC [92], equilibration after a quench in multidimensional Hubbard model [223, 48, 47], thermalization in the BH model with next-neighbor-hopping terms [46], and many other setups.

In this study I derive quantum Boltzmann equation in the second quantized formalism, but there exist more advanced approaches to kinetic theory. One of them is the Keldysh formalism of path integration [224]. For instance, in such a way kinetic equation was formulated and numerically solved for a Luttinger liquid with periodic potential approximated by a sine-Gordon model [107, 108].

Another one is the two-particle irreducible effective action approach, which accounts for off-shell scattering and the situation when there is no quasiparticles with well-defined dispersion relation. In such a way new results had been achieved for quantum turbulence and emergence of Kolmogorov-like scaling laws in BEC far away from equilibrium [225, 226, 227]

Application to a quenched Bose-Hubbard chain. Let's apply kinetic theory to the equilibrated state after the familiar quench from Néels state to superfluid

in 1D Bose-Hubbard chain. BH Hamiltonian in momentum space reads

$$\hat{H} = \sum_{q=0}^{M-1} \epsilon_q \hat{b}_q^\dagger \hat{b}_q + u \sum_{q_{1,2,3,4}=0}^{M-1} \hat{b}_{q_1}^\dagger \hat{b}_{q_2}^\dagger \hat{b}_{q_3} \hat{b}_{q_4} \delta_{q_1+q_2, q_3+q_4},$$

where for brevity $\epsilon_q = -2J\cos(2\pi q/M)$, $u = U/2M$.

The Heisenberg equation of motion for q-mode occupation number $\hat{n}_q = \hat{b}_q^\dagger \hat{b}_q$ is

$$\frac{d\hat{n}_q}{dt} = -i[\hat{n}_q, \hat{H}]. \tag{2.5}$$

The equilibrium condition for a stationary state is

$$\frac{dn_q}{dt} = \frac{d\langle \hat{n}_q \rangle}{dt} = 0,$$

which should be satisfied in the time averaged state no matter which statistical ensemble describes it.

To get some constraints on the possible values of n_q in this stationary state, I separate the fast and the slow dynamics. It is known that a general near-integrable system can be reformulated in terms of action-angle variables [55, 54]. Angles dephase fast, leading to prethermalized states. But the actions (being the integrals of motion) are conserved only for strictly integrable systems, and they diffuse in case of any integrability breaking, leading to proper thermalization (on a much longer time scale compared to the dephasing though). So dephasing can be considered the 'fast' part of dynamics. To average out those fast oscillations of the angles I perform an integration of (2.5) over a small time window (small in the sense that actions are changed only a little, but the angles are completely dephased)

$$n_q(t) = -i \int [n_q(t'), H] dt'$$

Assuming that in this time window the interaction between the modes is negligible and the field operators are governed by free evolution only

$$\bar{b}_q(t) = \bar{b}_q(t_0) e^{i\epsilon_k(t-t_0)}, \qquad \hat{b}_q(t) = \hat{b}_q(t_0) e^{-i\epsilon_k(t-t_0)},$$

we get

$$\hat{n}_q(t) = -4u^2 \int \sum_{mnrt} (-\bar{b}_{q+t-r} \bar{b}_{m+n-q} \bar{b}_r \hat{b}_m \hat{b}_t \hat{b}_n - \bar{b}_q \bar{b}_{m+n-q+t-r} \bar{b}_r \hat{b}_m \hat{b}_t \hat{b}_n +$$

$$+ \bar{b}_q \bar{b}_{m+n-q} \bar{b}_r \hat{b}_{m-t+r} \hat{b}_t \hat{b}_n + \bar{b}_q \bar{b}_{m+n-q} \bar{b}_{r+t-m} \hat{b}_r \hat{b}_t \hat{b}_n + H.c.) \cdot e^{it'(\epsilon_m + \epsilon_n - \epsilon_q - \epsilon_{m+n-q})} dt'.$$

Integration over the small time window gives the delta function over the energy

$$\hat{n}_q(t) = -8\pi u^2 \sum_{mnrt} (-\bar{b}_{q+t-r} \bar{b}_{m+n-q} \bar{b}_r \hat{b}_m \hat{b}_t \hat{b}_n - \bar{b}_q \bar{b}_{m+n-q+t-r} \bar{b}_r \hat{b}_m \hat{b}_t \hat{b}_n +$$

$$+ \bar{b}_q \bar{b}_{m+n-q} \bar{b}_r \hat{b}_{m-t+r} \hat{b}_t \hat{b}_n + \bar{b}_q \bar{b}_{m+n-q} \bar{b}_{r+t-m} \hat{b}_r \hat{b}_t \hat{b}_n + H.c.) \cdot \delta_{\epsilon_m + \epsilon_n}^{\epsilon_q + \epsilon_{m+n-q}}.$$

The results of the previous section state that at $U \to 0$ the system is described by a Gaussian GGE, so we can substitute this result back into (2.5) and
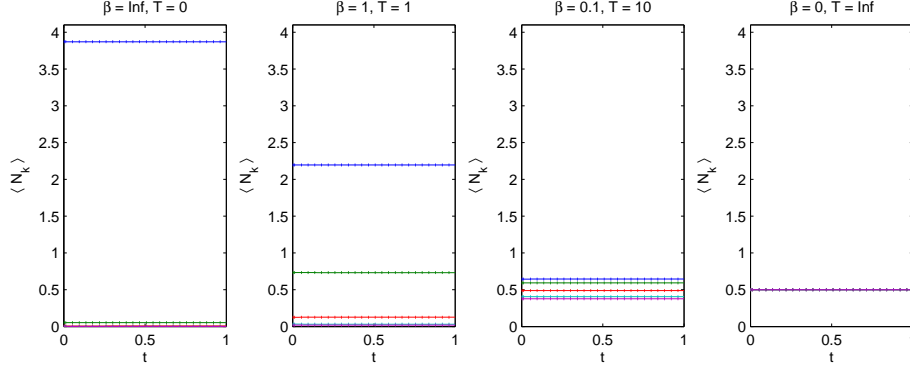
Figure 2.11: Kinetic description of the thermal state for a BH-chain with moderate non-linearity $U = 1, J = 1, M = 8, N = 4$ and different temperatures. Dots: thermal state prediction for mode occupation numbers n_q, solid lines: n_q evolution in time due to kinetic equations, initial condition being the thermal state. Different colors represent different modes q. There is almost no deviation as the thermal state is an equilibrium state and $dn_q/dt = 0$.

perform the averaging $n_q(t) = \langle \hat{n}_q(t) \rangle$ by utilizing Wick's theorem to factorize higher order correlators. Noticing that lowest-order correlators are given by $\langle \bar{b}_q \hat{b}_p \rangle = n_q \delta_{qp}$, $\langle \hat{b}_p \bar{b}_q \rangle = (n_q - 1)\delta_{qp}$, we arrive at the final result

$$\frac{dn_q}{dt} = \frac{\pi}{2} \sum_{q_1, q_2, q_3} T^2 \cdot F_{q123} \cdot \delta(q + q_1 - q_2 - q_3) \cdot \delta(\epsilon_q + \epsilon_1 - \epsilon_2 - \epsilon_3), \quad (2.6)$$

where $T = 8u$ and

$$F_{q123} = n_2 n_3 (n_1 + n_q + 1) - n_1 n_q (n_2 + n_3 + 1),$$

which gives us the well known quantum four-wave kinetic equation for weak turbulence [129]. Note that F_{q123} describes the usual for the Boltzmann's approach particle inflow minus outflow for the mode q into all other modes given by the energy and momentum conservation (cf. Fermi's golden rule), and the ones are due to bosonic amplification.

Note that three-wave term of the form $F_{q12} = n_1 n_2 - n_q(n_1 + n_2 + 1)$ is absent due to particle conservation. There is no assumption about the thermodynamic limit, so kinetic approach should work even for small systems.

Kinetic description for the modes is possible if (1) the one-mode reduced states are close to Gaussian (Wick's theorem), which usually implies weak non-linearity and near-equilibrium initial state, and (2) the initial phases of the modes are uncorrelated (random phase approximation) [129].

The initial momentum modes, though being Gaussian, are not uncorrelated, which breaks down the random phase approximation and renders the kinetic description of the short-time evolution impossible.

Even more, if we neglect correlations, then the initial condition in momentum space is nothing else than a state of infinite temperature, which is a steady state solution for kinetic equations (as any other thermal state), so kinetic equations would never predict any evolution at all.
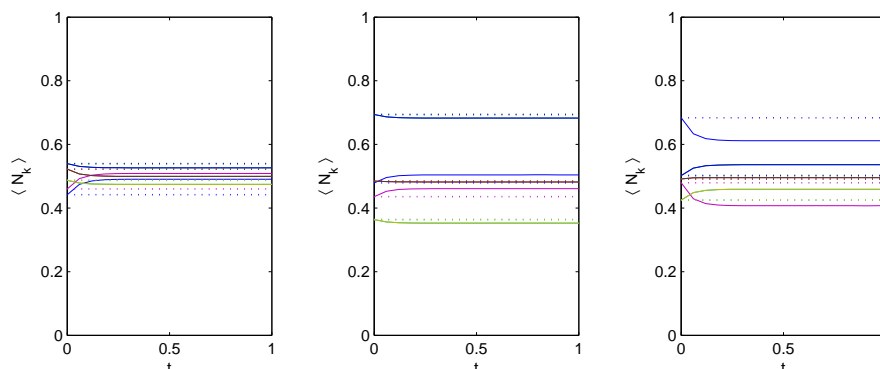
Figure 2.12: Quantum kinetic equation prediction for mode occupation numbers (thin lines) for a Bose-Hubbard chain for $M = 8, N = 4, J = 1, U = 0.1, 1, 10$ (from left to right) compared with the steady state solutions $\mathrm{tr}\,(\hat{\varsigma}\,\bar{b}_q\hat{b}_q)$, dotted lines. Different colors represent different modes q. Initial condition for kinetic equations are taken to be the steady state solutions, so if kinetic equations were a good description of the system, then solid lines and dots would coincide. With moderate nonlinearity (middle) we indeed see a good agreement. Deviations from the kinetic theory are evident for strong nonlinearity (right) due to non-Gaussianity of the modes.

True thermal equilibrium is a steady state, so dn_q/dt must be zero and kinetic equation should not lead to any deviation. It is indeed the case with high accuracy for all interaction strengths U, an example for $U = 1$ is presented in Figure 2.11.

Another question is whether kinetic description is applicable to the diagonal (equilibrated) state. To test it numerically I used the diagonal state as the initial condition for the kinetic equation (2.6), Figure 2.12. Surprisingly, at moderate non-linearities $U \approx 1$ the kinetic equations show very small deviation from the diagonal states. I attribute it to the fact that the diagonal state is close to the Generalized Gibbs ensemble (each mode having different temperature and different modes being non-correlated). At strong nonlinearities kinetic approach perform poorly as the two assumptions it's based are obviously violated.

The conclusion is that kinetic description is applicable not only to studies of small deviations from conventional thermal state, but also from GGE in case of an integrable or near-integrable system, even for systems of modest size. An interesting observation is that kinetic description works even for moderately strong nonlinearity $U = 1$, when the system is deeply in the chaotic regime. I attribute it to the fact that in this regime the stationary state is still described by an approximate GGE with almost-Gaussian one-mode reduced density matrices.

2.11 Summary and outlook

This chapter was devoted to studies of thermalization in a mesoscopic quantum system driven far from equilibrium by a quantum quench. The explicit example was a small 1D Bose-Hubbard chain quenched from a Néel state $|\psi_0\rangle = |\dots 10101\dots\rangle$ to superfluid, the setup being inspired by an experiment realized in I. Bloch's group, in which bosons were relaxed from a product state in a 1D

optical lattice [126, 165].

I showed that the initial Néel state in momentum space looks like being at infinite temperature, and the momentum modes are strongly entangled. On the other hand, the initial state in position space is a product state with zero entanglement. In this regard the thermalization process can be thought of as redistribution of entanglement entropy between complimentary bases, stating the conservation of quantum information, which in turn is deeply rooted in linearity of quantum mechanics [228].

An interesting finding of the present work is that the methods of quantum statistical mechanics can be applied to mesoscopic systems, and hints of thermodynamic behavior can be acquired even from a system as small as four particles.

As expected, a quantum many-body system equilibrates to its diagonal state. But in the case of a mesoscopic system this is a weak equilibration, meaning that one needs to average out the fluctuations to recover the diagonal state.

The system is of a particular conceptual interest, as it is quantum linearly integrable (in the sense of [189]) in the two limiting cases of non-interacting and hard-core bosons, but quantum chaotic in between, allowing to study all the spectrum of integrability breaking.

As the behavior of integrable and non-integrable systems is believed to be drastically different (e.g. the integrable systems generally don't relax to conventional Gibbsian thermal states), it is interesting to quantify the integrability in a system which can undergo a smooth transition between the tho regimes. In this study I demonstrated the application of some new measures of integrability in addition to the well-known measures of quantum chaos (such as the onset of Wigner-Dyson statistics in the distribution of the energy level0.

I showed that the non-integrable phase is characterized by increased effective entanglement in the eigenbasis, In a nutshell, this very anticipated result shows that a non-integrable system retains less memory about its initial state. I note that the Hamiltonian didn't include any noise, ruling out possible many-body localization effects.

Eigenstate thermalization hypothesis (ETH) is the modern backbone of quantum thermalization, believed to hold if observable expectation values in the equilibrated state are close to thermal prediction. I demonstrated that even for a small system ETH holds better in the non-integrable regime, meaning that the eigenstates of a chaotic system are indeed more thermal.

Equilibrated states of general non-integrable systems are well-known to be simple Gibbsian thermal states, characterized by few intensive parameters such as temperature and chemical potential, but the situation around integrable and near-integrable systems remains far from being completely understood. Addressing the last question, I showed that for a 1D Bose-Hubbard chain after a quench there exists a region of integrability breaking where the momentum modes are close to being in a Gaussian state, supporting the claim that close-to-integrable systems relax to a deformed generalized Gibbs ensemble (GGE).

Surprisingly enough, this region is not limited to small integrability breaking, but extends far into the chaotic region.

A reasonable question is why such an emergent GGE should be of any interest. I tried to answer to this question in the last part of the chapter, where I derived the kinetic Boltzmann equation for mode occupation numbers. Initial one-mode states are highly correlated, so no surprise that kinetic description

was not able to predict the short-time evolution after the quench. But the non-trivial result that the equilibrated state is close to a Gaussian ensemble even in the chaotic regime allowed to successfully apply the kinetic equation to the equilibrated state itself.

I additionally note that kinetic description's applicability is based on random phase approximation and Gaussianity of the states, so it should be applicable not only to situations near thermal equilibrium, but also for studying small deviations from a proper GGE in case when the non-linerarity of the Hamiltonian is weak enough.

Finally, this study helped to shed light on the limitations of the truncated Wigner approach, which are reported in Appendix D.

Outlook. Present study opens a lot of interesting questions both on the behavior of mesoscopic systems and on the onset of thermalization at integrability breakdown.

First of all, the presented study can be straightforwardly generalized to larger system sizes to be run on a supercomputer or a computational cluster. This would allow for a careful finite-scaling analysis to elucidate onset of ETH and breakdown of GGE at the integrability crossover. Another route to the thermodynamic limit would be to employ quantum Monte-Carlo and tensor network algorithms.

An important question to address in the further studies would be which number of intensive parameters is enough to characterize a given nearly-integrable experimental system, statistical equilibrium of which is given by a deformed GGE.

Analytical ways of quantifying GGE deformation could include a standard perturbative diagrammatic expansion in the small interaction parameter, if we start from a non-interacting free Gaussian ensemble of the modes. But presumably the quest for quasi-conserved quantities should not stop at effectively free models such as free or hard-core bosons, but might be continued by exploring the nearby integrable models such as Lieb-Liniger model, Gross-Pitaevskii equation with the Zakharov-Shabat construction [20], or the integrable Ablowitz-Ladik lattice [229].

The breakdown of GGE can be additionally addressed with the method suggested by Caux and Mossel, which would show itself in the gradual decrease of all the generalized temperatures to zero, leaving only the real temperature in the final completely chaotic state at $U \sim 1$ [189].

There are results stating that a many-body quantum system after a quench undergoes a regime of quantum turbulence, characterized by a Kolmogorov-like cascade of energy and particle number during the equilibration time, see e.g. [226]. The numerical simulations done by the author with classical number of particles $N \gg 1$ and truncated Wigner approach indeed showed an emergence of a cascade (to be published elsewhere). In the future it would be interesting to approach this beyond quasiclassical approximation. If the system holds nontrivial integrals of motion, should they exhibit cascades as well?

Another prospective research direction would be trying to describe the thermalization of an isolated system from the point of view of the quantum information theory, where decoherence is a well-established way of deriving the classical from the quantum [186, 230, 231].

The research reported in this chapter lies at the interface between thermodynamics, statistical mechanics, quantum foundations and quantum information theory, dynamical systems, and non-equilibrium quantum field theory, and I hope that the results presented here will inspire new breakthroughs in this rapidly growing interdisciplinary area of physics.

Conclusion

In this thesis I addressed many fundamental questions of non-equilibrium physics, as applied to ultracold atomic gases[1].

In the first Chapter I showed how a one-dimensional Bose-Einstein quasi-condensate could be effectively cooled using experimental 'evaporative cooling' technique, despite the fact that the 1D BEC represented an almost perfect integrable system. The answer was that 'evaporative cooling' proceeded completely differently in 1D: the gradual loss of quasiparticles on long length scales led to an establishment of apparent classical equipartition and a single well-defined temperature, as a result of a process that could be called prethermalization. Experiments on atomchip were able to probe those long length scales and showed a good agreement with theoretically predicted power-law temperature decrease.

The second chapter was devoted to the process of integrability breaking in a mesoscopic quantum system of several bosonic atoms in a one-dimensional optical lattice (the Bose-Hubbard model). I showed that notions of thermodynamics and statistical mechanics were applicable even to small systems, which might appear relevant to future applications in nanoscale devices. I developed novel measures of integrability breaking (in addition to the well-known ones such as the onset of the Wigner-Dyson statistics), based on the eigenstate thermalization and entanglement in the eigenbasis. Further results included emergence of a deformed generalized Gibbs ensemble and applicability of kinetic Boltzmann approach in the regime of integrability crossover.

To conclude, I hope that my study was able to shed some light on the fundamental question of how thermodynamics and statistical description emerged from purely unitary quantum many-body dynamics. In the following years, I anticipate many more theoretical and experimental advancements to come in this interdisciplinary area of non-equilibrium physics, and I am happy that I was able to make a humble contribution to its foundations.

---

[1]Much more detailed summary, discussion, conclusions and outlook are to be found in Sections 1.12 and 2.11

Appendix A

Acronyms

1D	One-dimensional
BE	Bose-Einstein
BEC	Bose-Einstein condensate
BH	Bose-Hubbard model
CFT	Conformal field theory
DMRG	Density matrix renormalization group
EEE	Effective entanglement in the eigenbasis
EEV	Eigenstate expectation values
ETH	Eigenstate thermalization hypothesis
GGE	Generalized Gibbs ensemble
GPE	Gross-Pitaevskii equation
LC	Leggett-Caldeira model
LL	Tomonaga-Luttinger liquid
KAM	Kolmogorov-Arnold-Moser theorem
MBL	Many-body localization
PBC	Periodic boundary conditions
QCLT	Quantum central limit theorem
RJ	Rayleigh-Jeans approximation
rf-field	Radio-frequency field
RWA	Rotating wave approximation
TF	Thomas-Fermi
TWA	Truncated Wigner approximation

Appendix B

Hydrodynamic derivation of the scaling law $T \propto N$

Here I formulate hydrodynamic derivation of the scaling law presented in Section 1.11.3 for cooling of trapped 1D BEC, which uses Thomas-Fermi and adiabatic approximations. This calculation was done by Dr. I. E. Mazets.

Gross-Pitaevskii equation for our trapped degenerate cloud with dissipation γ reads

$$i\hbar\dot{\psi} = -i\hbar\gamma(t)\psi - \frac{\hbar^2}{2m}\partial_{zz}\psi + \frac{m\omega z^2}{2}\psi + g|\psi|^2\psi, \qquad (B.1)$$

where $g = 2\hbar\omega_r a_s$.

Implying phase-density approximation the order parameter of the gas is represented with density n and phase ϕ fields

$$\psi = e^{i\phi}\sqrt{n}. \qquad (B.2)$$

Local velocity of atoms is given by

$$v = \frac{\hbar}{m}\partial_z\psi = b(t)z + \delta v, \qquad (B.3)$$

and includes fluctuations δv and stationary flow of the atoms due to cloud breathing, where $b(t)$ is the scaling parameter defined through the instantaneous radius of the cloud

$$b(t) = \frac{R(t)}{R(0)}$$

Density includes parabolic time-dependent profile $\bar{n}$ and density fluctuations δn, 'freezed in' the profile.

$$n = \bar{n} + \delta n, \qquad (B.4)$$

$$\bar{n} = \frac{3N(t)}{4R(t)}\left(1 - \frac{z^2}{R^2(t)}\right)\theta(R(t) - |z|),$$

where $\theta(x)$ is the Heaviside function.

Substituting (B.3) and (B.4) into (B.2), the result into (B.1), and neglecting phase and density fluctuations we get the evolution equation for the scaling parameter

$$\ddot{b} + \omega^2 b - \omega^2\left(\frac{R_{TF0}}{R(0)}\right)^3\frac{e^{-2\int\gamma\,dt}}{b^2} = 0,$$

where R_{TF0} is the Thomas-Fermi radius corresponding to the initial particle number $N(0)$ (for the sake of generality we assume that initially the cloud radius can be different from that of the equilibrium Thomas-Fermi, $R(0) \neq R_{TF0}$)

$$R_{TF0} = \sqrt[3]{\frac{3N(0)\hbar\omega_r a_s}{m\omega^2}}.$$

Taking into account that particle number decays exponentially with time

$$N(t) = N(0)e^{-2\int \gamma\, dt},$$

and the initial density in the centre of the cloud $n_c(0)$ is given by

$$n_c(0) = \frac{3N(0)}{4R(0)},$$

we can linearize (B.1) with respect to density and velocity fluctuations. Then substituting $\bar{n}$ and v from (B.4) and (B.3) we arrive at

$$\frac{\partial}{\partial t}\delta n + \frac{\dot{b}}{b}\delta n + \frac{\dot{b}}{b}z\frac{\partial}{\partial z}\delta n = -\frac{n_c(0)}{b}\frac{\partial}{\partial z}\left[\left(1 - \frac{z^2}{b^2 R^2(0)}\right)\delta v\right]e^{-2\int \gamma\, dt} - 2\gamma(t)\delta n,$$

$$\frac{\partial}{\partial t}\delta v + \frac{\dot{b}}{b}\delta v + \frac{\dot{b}}{b}z\frac{\partial}{\partial z}\delta v = -\frac{g}{m}\frac{\partial}{\partial z}\delta n. \tag{B.5}$$

Let's introduce rescaled time-dependent reference frame with spatial coordinate ζ 'frozen in' the breathing oscillation of the cloud and $\tau = t$ as we are in non-relativistic limit

$$\zeta = \frac{z}{bR(0)},$$

$$z = b(\tau)R(0)\zeta,$$

$$\frac{\partial}{\partial t} = \frac{\partial}{\partial \tau} - \frac{1}{b(\tau)}\frac{db(\tau)}{d\tau}\zeta, \frac{\partial}{\partial z}$$

$$\frac{\partial}{\partial z} = \frac{1}{b(\tau)R(0)}\frac{\partial}{\partial \zeta},$$

Decomposing phase and density fluctuations into Petrov modes (which is legitimate in the case of Thomas-Fermi parabolic profile, see Section 1.5) we get

$$\delta n = \sum_{\ell=1}^{\infty}\frac{\nu_\ell}{b}P_\ell(\zeta), \qquad \delta v = \sum_{\ell=1}^{\infty}\frac{\chi_\ell}{b}\frac{\partial}{\partial \zeta}P_\ell(\zeta), \tag{B.6}$$

where $P_\ell(\zeta)$ are Legendre polynomials, defined the standard way as solutions to the following Sturm-Liouville problem

$$\frac{\partial}{\partial \zeta}(1 - \zeta^2)\frac{\partial P_\ell(\zeta)}{\partial \zeta} = -\ell(\ell + 1)P_\ell(\zeta).$$

After substituting (B.6) into (B.5) we arrive at

$$\frac{\partial}{\partial \tau}\nu_\ell = \frac{n_c(0)}{b^2(\tau)R(0)}\ell(\ell + 1)e^{-2\int \gamma\, d\tau}\chi_\ell - 2\gamma\nu_\ell, \tag{B.7}$$

To simplify derivation we introduce auxiliary variable ρ_ℓ to absorb the exponential factor

$$\frac{\partial}{\partial \tau}\chi_\ell = -\frac{g}{mb(\tau)R(0)}\nu_\ell,$$

$$\nu_\ell = e^{-2\int \gamma \, d\tau}\rho_\ell,$$

$$\frac{\partial}{\partial \tau}\rho_\ell = \frac{n_c(0)}{b^2(\tau)R(0)}\ell(\ell+1)\chi_\ell,$$

$$\frac{\partial}{\partial \tau}\chi_\ell = -\frac{ge^{-2\int \gamma \, d\tau}}{mb(\tau)R(0)}\rho_\ell,$$

and combining it with (B.7) we get

$$\frac{\partial}{\partial \tau}\left[b^2(\tau)\frac{\partial\rho_\ell}{\partial\tau}\right] = -\frac{\omega^2}{2}\ell(\ell+1)\left[\frac{R_{TF0}}{R(0)}\right]^3\frac{e^{-2\int \gamma \, d\tau}}{b(\tau)}\rho_\ell.$$

Let's define the efficient mode frequency at the initial time $\omega_\ell(0)$ as

$$\omega_\ell^2(0) = \frac{\omega^2}{2}\ell(\ell+1)\left[\frac{R_{TF0}}{R(0)}\right]^3.$$

Note that $\omega_\ell(0)$ reduces to standard definition (1.12) in the case we start from an equilibrium Thomas-Fermi profile $R_{TF0} = R(0)$.

Then we introduce action A_ℓ and angle η_ℓ variables in a procedure similar to transformation from Cartesian to polar coordinates (the difference being explicit time-dependence)

$$\chi_\ell = -\frac{g}{mR(0)\omega_\ell(0)}\sqrt{b}e^{-2\int \gamma \, d\tau}A_\ell \sin\eta_\ell,$$

$$\rho_\ell = A_\ell \cos\eta_\ell.$$

After some algebra we arrive at

$$\dot{A}_\ell \cos\eta_\ell - A_\ell\dot{\eta}_\ell \sin\eta_\ell = -\frac{\omega_\ell(0)}{b^{3/2}}e^{-\int \gamma \, d\tau}A_\ell \sin\eta_\ell,$$

$$\dot{A}_\ell \sin\eta_\ell - A_\ell\dot{\eta}_\ell \cos\eta_\ell + \frac{1}{2}\frac{\dot{b}}{b}A_\ell \sin\eta_\ell - \gamma A_\ell \sin\eta_\ell = \frac{\omega_\ell(0)}{b^{3/2}}e^{-\int \gamma \, d\tau}A_\ell \cos\eta_\ell,$$

$$\frac{\dot{A}_\ell}{A_\ell} = -\frac{1}{2}\frac{\dot{b}}{b}\sin^2\eta_\ell + \gamma\sin^2\eta_\ell, \tag{B.8}$$

$$\dot{\eta}_\ell = \omega_\ell(\tau) - \frac{1}{2}\frac{\dot{b}}{b}\sin\eta_\ell \cos\eta_\ell + \gamma\sin\eta_\ell \cos\eta_\ell. \tag{B.9}$$

So now we have evolution equation for action-angle variables. Integrating (B.9) and (B.8) from 0 to some final time t_f taken to much larger than one period of revolution $T_\ell = 2\pi/\omega_\ell$, sine- and cosine-like contributions average out to zero, so

$$\eta_\ell = \int \omega_\ell d\tau,$$

and sine- and cosine-squared terms average to $1/2$, so we get

$$A_\ell(\tau) = b^{-1/4} A_\ell(0) e^{\frac{1}{2} \int \gamma \, d\tau}$$

In the classical wave limit (classical equipartion, see Section 1.4) temperature is proportional to the total energy of the system $T \propto E$, and the energy stored in fluctuation is given by, cf. (1.4)

$$E = \int_{-R}^{R} dz \left[\frac{\hbar^2}{2m} \bar{n} \delta v^2 + \frac{g}{2} \delta n^2 \right] = \sum_{\ell > 0} E_\ell,$$

which is calculated substituting resulting A_ℓ and η_ℓ into δn and δv. The result for temperature scaling is

$$\frac{T(t)}{T(0)} = \frac{E(t)}{E(0)} = \frac{N(\tau)}{N(0)} \frac{\omega_\ell(t)}{\omega_\ell(0)} = b^{-3/2} e^{-3 \int \gamma \, dt} = b^{-3/2}(t) N^{3/2}(t).$$

Finally we note that in adiabatic regime $b(t) \propto N^{1/3}(t)$, so

$$T(t) \propto N(t),$$

which confirms our result from Section 1.11.3.

Appendix C

Squeezed GGE

It has become a common lore that a steady equilibrated state, produced after relaxation after a quantum quench in an integrable system, can be described by a Generalized Gibbs ensemble. Here I show that at least for free systems it is not the case by providing an explicit example of a relaxed integrable system, which has observables that cannot be described by GGE.

This claim can be intuitively understood taking into account a very special nature of the free systems, namely that different quasiparticles don't interact, so they remain in the states they were intially. For example, if we initialize the Luttinger liquid with bosons in Fock states in each mode, this ensemble will not be described by GGE, because for Fock states correlations don't factorize according to Wick's theorem.

As an instance, let's consider a prethermalized state discussed in detail in Section 1.6. As we know after prethermalization Luttinger modes end up in Gaussian squeezed states, see Figure 1.7 on page 24 and [43, Figure 6 on page 21]. Then those squeezed states rotate as rigid bodies with different frequencies, leading to dephasing.

The question is whether this squeezed dephased ensemble is equivalent to a conventional GGE. My answer is no.

Proof. Let's consider an ensemble of Luttinger modes in squeezed states, meaning that their Wigner function are given by

$$W_q(\mathfrak{x}, \mathfrak{y}) = \frac{1}{2\pi\sigma_{q\mathfrak{x}}\sigma_{q\mathfrak{y}}} e^{-\frac{\mathfrak{x}^2}{2\sigma_{q\mathfrak{x}}^2} - \frac{\mathfrak{y}^2}{2\sigma_{q\mathfrak{y}}^2}},$$

where q is the mode number, $\mathfrak{x}, \mathfrak{y}$ are the field quadratures (e.g. appropriately scaled Π_q and ϕ_q), and $\sigma_{q\mathfrak{x}} \neq \sigma_{q\mathfrak{y}}$ are the initial widths of the Gaussian in both quadratures.

Note that for a conventional GGE $\sigma_{q\mathfrak{x}} = \sigma_{q\mathfrak{y}} = \sigma_q$, so the Wigner function is rotationally symmetric.

Free evolution under Luttinger Hamiltonian is nothing but rigid rotation of the modes:

$$\begin{pmatrix} \mathfrak{x} \\ \mathfrak{y} \end{pmatrix} = \begin{pmatrix} \cos\theta & -\sin\theta \\ \sin\theta & \cos\theta \end{pmatrix} \begin{pmatrix} \mathfrak{x}_0 \\ \mathfrak{y}_0 \end{pmatrix},$$

where $\theta = \omega_q t$. So the Wigner function becomes

$$W_q(\mathfrak{x}, \mathfrak{y}, t) = \frac{1}{2\pi\sigma_{q\mathfrak{x}}\sigma_{q\mathfrak{y}}} e^{-\frac{(\mathfrak{x}\cos\theta - \mathfrak{y}\sin\theta)^2}{2\sigma_{q\mathfrak{x}}^2} - \frac{(\mathfrak{y}\cos\theta + \mathfrak{x}\sin\theta)^2}{2\sigma_{q\mathfrak{y}}^2}}.$$

Employing phase space representation, the expectation value of an observable is given by [32]

$$\langle \hat{O} \rangle = \int O_W \cdot W(\mathfrak{x}, \mathfrak{y}, t)\, d\mathfrak{x}\, d\mathfrak{y},$$

where O_W is Weyl symbol for operator $\hat{O}$ and I utilize the Schrödigner picture with stationary operators and evolving quantum states.

After some algebra it is straightforward to get the expressions for average occupation number per mode $N_q = \langle \hat{N} \rangle$ and its variance $\Delta_q = \langle \hat{N}^2 \rangle - \langle \hat{N} \rangle^2$, both for squeezed and conventional GGE (note they are not time-dependent).

Squeezed GGE	Conventional GGE
$\tilde{N}_q = \sigma_{\mathfrak{x}q}^2 + \sigma_{\mathfrak{y}q}^2 - 1/2$	$N_q = 2\sigma_q^2 - 1/2$
$\tilde{\Delta}_q = 2\sigma_{\mathfrak{x}q}^4 + 2\sigma_{\mathfrak{y}q}^4 - 1/4$	$\Delta_q = 4\sigma_q^4 - 1/4$

So it's always possible to find a GGE with $\sigma_q^2 = (\sigma_{\mathfrak{x}q}^2 + \sigma_{\mathfrak{y}q}^2)/2$, which will give the same predictions for the mode occupation numbers $\tilde{N}_q = N_q$. But the variances will in general be different:

$$\tilde{\Delta}_q - \Delta_q = (\sigma_{\mathfrak{x}q}^2 - \sigma_{\mathfrak{y}q}^2)^2 \geqslant 0,$$

meaning that the variance of quasiparticle occupation number of the squeezed GGE is always larger than the variance of a conventional GGE constructed in such a way that to match mean occupations $\tilde{N}_q = N_q$. $\qquad\square$

If we are interested in some observables in real space, say interference contrast, given by $\langle \cos[\phi(z) - \phi(z')] \rangle$, where $\phi(z)$ is the phase of the antisymmetric condensate, then

$$\hat{\phi}(z) \propto \frac{1}{\sqrt{L}} \sum e^{iqz} \hat{\phi}_q \propto \frac{1}{\sqrt{L}} \sum e^{iqz} (\bar{b}_q + \hat{b}_{-q}) \cdot f(q),$$

where $\hat{b}_q$ are the annihilation operators of the Luttinger modes, and $\hat{N}_q = \bar{b}_q \hat{b}_q$, we see that fluctuations of operators in real space will decay to zero in thermodynamic limit, the similar way as the equivalence between conventional thermal ensembles is proven in statistical mechanics [175].

The conclusion is that in general for a free system after a quench

$$Z \neq \sum_q e^{-\beta_q \epsilon_q \bar{b}_q \hat{b}_q}.$$

Speaking about GGE, it's necessary to specify the observables of interest, as there can be some (like variances of the mode occupation numbers) that will not agree with GGE predictions. In real space though GGE can provide the full description, but only in thermodynamic limit. For finite size systems real-space observables will have larger fluctuations than those predicted by GGE,

and the discrepancy can be straightforwardly calculated given the structure of the steady state.

The fact that GGE still applies in the thermodynamic limit must be attributed to the fact that initially we have Gaussian noise in the modes of anti-symmetric condensate, meaning we start with Gaussian states initially, and then no matter how do Gaussian states are squeezed or rotated, they remain Gaussian, and transforming back to the real space we get measurements according to GGE due to the central limit theorem. One can speculate that this might be generalized to Unruh thermal radiation thought as Bogoliubov transformation of the vacuum (a Gaussian state) [232].

When applied to discussion on prethermalization, I propose to substitute the statement

> "Prethermalized system is in a steady state which is fully described by a GGE, and predicts thermal expectation values for some observables."

with a new one

> "Prethermalized system is in steady state which is fully described by a squeezed GGE, which looks like a GGE and a thermal ensemble for some observables."

Finally I note that presented derivation in no way conflicts with results of Imambekov, Kitagawa and others on prethermalization [43, 233, 25, 61, 24].

Appendix D

Limitaitions of the truncated Wigner approximation

Truncated Wigner approximation (TWA) is a semiclassical approximation scheme, where the quantum averages are approximated with an average over an ensemble of the classical field equation solutions with initial conditions sampled from the Wigner function of the initial quantum state [32].

TWA has a long record of successful applications in numerical simulations of Bose-Einstein condensates [37, 234, 99]. In particular, numerical simulations for cooling of 1D BEC from the Chapter 1 were performed with TWA. The approximation is believed to hold when the initial quantum state has a positive Wigner function, which is the case for thermal, coherent states, and possibly for Fock states with a large number of particles [98, 235].

On the other hand, when applied to the studies of Néel state (where the atoms are in Fock states initially) to superfluid quench in a Bose-Hubbard chain from Chapter 2, TWA failed to reproduce the experimental results of [126].

Let's see why Fock states are so special and whether there exist semiclassical ways to appoximate them.

Fock-1 state. The Wigner function for the Fock-1 state reads [31]

$$W_1(a, a^*) = -\frac{2}{\pi} e^{-2|a|^2} L_1(4|a|^2) = \frac{2}{\pi} e^{-2|a|^2}(4|a|^2 - 1),$$

where $L_n(x)$ is the Laguerre polynomial.

Exploiting the rotational symmetry we can represent the W-function in the polar coordinates and integrate out the phase

$$W_1(\rho) = 4\rho e^{-2\rho^2}(4\rho^2 - 1)$$

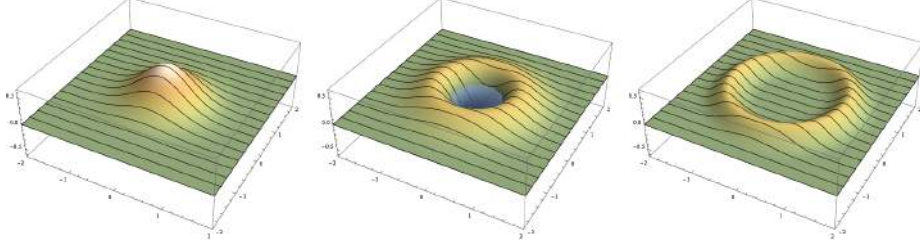$$\int_0^{+\infty} W_1(\rho) d\rho = 1.$$

Figure D.1: Wigner functions of the Fock-0 (vacuum), Fock-1 and Ring-1 states (from left to right). Sea level represents zero, so W-function for Fock-1 state is not a proper probability distribution as it becomes negative in some regions.

For instance, moments can be calculated using Wick symbol [32, 30]

$$\langle \hat{N} \rangle = \int_0^{+\infty} \hat{N}_W W_1(\rho) d\rho = \int_0^{+\infty} (\rho^2 - \frac{1}{2}) W_1(\rho) d\rho = 1$$

$$\langle \hat{N}^2 \rangle = \int_0^{+\infty} (\hat{N}^2)_W W_1(\rho) d\rho = \int_0^{+\infty} (\rho^4 - \rho^2) W_1(\rho) d\rho = 1$$

To study dynamics, it's convenient to work in Heisenberg representation, where the state vector (Wigner function is stationary), but the operators evolve according to Heisenberg's equation. For instance, time-dependent number operator can be calculated as

$$\langle \hat{N}(t) \rangle = \int_0^{+\infty} \hat{N}(t)_W W(\rho, t = 0) d\rho = \int_0^{+\infty} (\rho(t)^2 - \frac{1}{2}) W(\rho, t = 0) d\rho$$

where $\rho(t) = |a(t)|^2$ is acquired by solving classical equations of motion for the field operators (GPE), with initial conditions picked from $W(\rho, t = 0)$.

But the W-function of Fock-1 state has negative values, so it's not a well-defined probability distribution (Figure D.1). How can one circumvent this problem?

The initial thought was to split the W-function into (positive) exponential part and (negative) polynomial part, constructing the new observable from the old one times the polynomial part and then averaging this new observable with the weight of the exponential part of the W-function (sampling the random initial conditions only from the exponential part):

$$\langle \hat{N}_t \rangle = \int (\hat{N}_t)_W W(x_0, p_0) dx_0 \, dp_0 =$$

$$= \int (x_t^2 + p_t^2 - \frac{1}{2}) W(x_0, p_0) dx_0 \, dp_0 =$$

$$= \int \left[\frac{2}{\pi} (x_t^2 + p_t^2 - \frac{1}{2})(4(x_0^2 + p_0^2) - 1) \right] e^{-2(x_0^2 + p_0^2)} dx_0 \, dp_0 =$$

$$\int \tilde{N}_t e^{-2(x_0^2 + p_0^2)} dx_0 \, dp_0,$$

where x and p are the field quadratures (real), $\rho^2 = x^2 + p^2$.

But this approach failed because if we sample the initial conditions, say, for the first site (which is supposed to be in Fock-1 state) from the Gaussian distribution $e^{-2(x_0^2 + p_0^2)}$—it effectively represents only the vacuum state. So the initial conditions for the equation of motion are all vacuum (e.g. the second site, which is coupled to the first, has no clue that the first site is in Fock-1 state, besause it sees only the Gaussian distribution in the initial state of the first site).

So the only solution seems to be using the 'ring states', introduced first by A. Polkovnikov under the name of the 'best Gaussian approximation' [236].

Best Gaussian approximation (a ring state). The ring state $R_n(\rho)$, approximating the Fock-n state $W_n(\rho)$, is defined to have the W-function

$$R_n(\rho) = \frac{1}{\sqrt{2\pi}\sigma} \exp \frac{(\rho - \bar{\rho})^2}{2\sigma^2}$$

with σ and $\bar{\rho}$ such that the occupation number and variance are the same for $R_n(\rho)$ and $W_n(\rho)$ (the higher moments will unavoidably differ).

$$\langle \hat{N}_n \rangle = \int \hat{N}_W W_n(x, p) dx\, dp = \int \hat{N}_W R_n(x, p) dx\, dp = n$$
$$\langle \hat{N}^2 \rangle = \int \hat{N}_W^2 W_n(x, p) dx\, dp = \int \hat{N}_W^2 R_n(x, p) dx\, dp = n^2$$

For Ring-1 state (approximating Fock-1) the parameters were numerically found to be $\sigma = 0.20, \bar{\rho} = 1.208$, Figure D.1.

However, TWA with ring states failed to predict the correct steady state solution for a Bose-Hubbard chain (see e.g. Figure D.2).

Discussion. The 1D Bose-Hubbard chain initially in a Néel state (see Chapter 2), solved with TWA without quantum corrections, shows classical thermalization to the Boltzmann ensemble and even some hints of turbulent scaling laws during equilibration (to be published elsewhere). But the initial state must be interpreted just as an ensemble of classical systems with close initial conditions. Most importantly, even if U is large, the quantum system relaxes to a state $\forall i n_i = 1/2$, but the TWA results show self-trapping (e.g. $n_i = 0.1$ for even sites, which are initially unoccupied, and $n_i = 0.9$ for odd sites, which are initially occupied with one particle). This shows that TWA fails to account for the discreteness of particles and may be used only if the sites are occupied initially with many particles (high wave amplitudes—in the quantum case there is self-trapping as well, see e.g. experiments with Josephson junctions [237, 132]). But it's impossible to experimentally prepare optical lattice with high imbalance between neighboring sites, which in this case makes TWA description irrelevant.
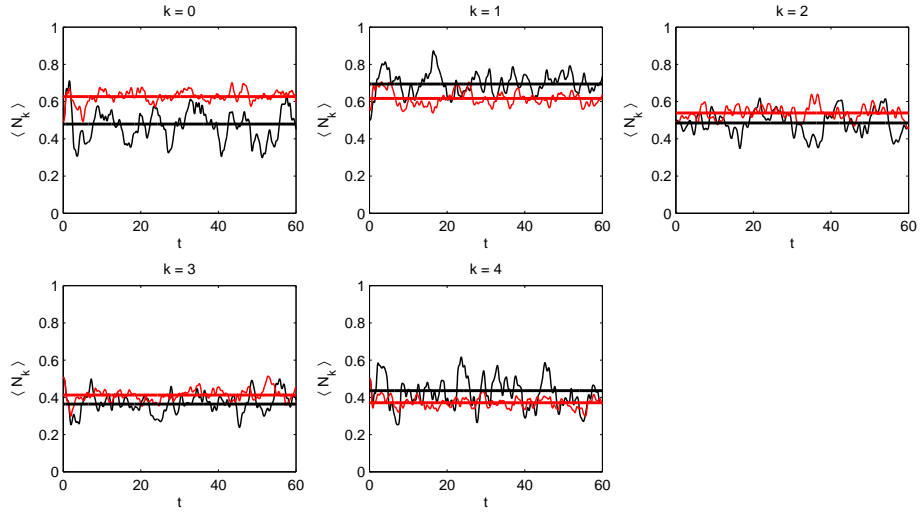
Figure D.2: The 1D Bose-Hubbard chain initially in a Néel state, quenched to a superfluid (see Chapter 2). Mode occupation number evolution ($k = 0 \ldots N$), calculated by TWA ring-state simulations (red), in comparison with exact diagonalization (black) for a chain with $M = 8, N = M/2, J = 1, U = 1$. Black horizontal line represents the quantum diagonal steady-state ς prediction, and horizontal red line—TWA long-time average. It seems that TWA fails to predict the correct steady state. Note that TWA predicts larger occupation for low-lying modes, which must correspond to a state closer to a classical thermal equilibrium at lower temperatures.

Appendix E

Ergodic eigenstate thermalization theorem

Summary. Eigenstate thermalization hypothesis was formulated in Section 2.8, and usually reads:

> In a quantum non-integrable system, eigenstates close in energy are close in all other local observables.

In this appendix I explore the locality criterion and argue that it stems from a more general concept of *ergodic eigenstates* (to be defined later).

Statement. Let $\{|K\rangle, |L\rangle \ldots\}$ be the exact many-body eigenstates of an interacting system (further called simply 'eigenstates').

ETH claims that eigenstates close in energy are close in observables, which reads

$$\langle K|\hat{n}|K\rangle \approx \langle L|\hat{n}|L\rangle \qquad if \qquad \epsilon_K \approx \epsilon_L,$$

where $\hat{n}$ is some observable and $\epsilon_K \equiv \langle K|\hat{H}|K\rangle$ are the energies of the eigenstates, so that a system prepared in the eigenstate $|K\rangle$ can be well described by a microcanonical ensemble around the energy ϵ_K.

A reasonable question would be for which observables does ETH hold. Obviously, it won't hold for projectors on eigenstates $|K\rangle\langle K|$ in the role of the observables.

Let's define an arbitrary complete many-body basis $\{|k\rangle, |\ell\rangle \ldots\}$ (later referenced as the 'preferred basis'). Then each eigenstate can be decomposed into the basis states

$$|K\rangle = \sum_m |m\rangle\langle m|K\rangle = \sum_m C_{m,K}|m\rangle.$$

An example of a preferred basis may be the eigenbasis of the corresponding non-interacting system.

Following [238] we define the *energy shell* in the preferred basis with respect to the eigenstate $|K\rangle$ as the range in energies between the basis state $|a\rangle$ with the lowest energy ϵ_a and the basis state $|z\rangle$, with the highest energy ϵ_z with the condition that states ϵ_a and ϵ_z contribute to the eigenstate $|K\rangle$, i.e. $C_{a,K} \neq 0$ and $C_{z,K} \neq 0$:

$$Energy\ shell = [\epsilon_a, \epsilon_z].$$

Then the eigenstate $|K\rangle$ is called *ergodic* in the working basis if it fills the energy shell densely,

$$\forall m,\ \epsilon_a \le \epsilon_m \le \epsilon_z : C_{m,K} \ne 0.$$

Note that this notion of ergodicity is defined in the Hilbert space, and is different from the conventional ergodicity, defined on the phase space, as there is no one-to-one continuous correspondence between vectors in Hilbert space and regions in phase space (e.g. states close in phase space may be orthogonal in Hilbert space [202]).

> I claim that if there exists a preferred basis where the eigenstates are *ergodic*, then the observables diagonal in this basis will exhibit ETH.

I stress that I do not explicitly appeal to 'locality' of operators to justify ETH.

Proof. Let's have an observable X diagonal in the preferred basis, i.e. $\langle k|X|m\rangle = x_m \delta_{km}$. Then the observable in the exact eigenstate is

$$\langle K|X|K\rangle = \sum_m \langle K|m\rangle x_m \langle m|K\rangle = \sum_m |C_{m,K}|^2 x_m.$$

Ergodicity implies that there is a lot of preferred basis states $\{|m\rangle\}$ with energies close to the exact eigenstate energy $E_m \approx E_K$, and non-zero $C_{m,K}$, so following the approach of [180], I define the microcanonical distribution function

$$F_{m,K} = |C_{m,K}|^2 = F(E_m - E_K).$$

Then it is easy to see that if F is smooth enough (as it should be in an ergodic state), then X average in an eigenstate K is dependent *only* on the energy E_K,

$$\langle K|X|K\rangle = \frac{\sum_m x_m F(E_m - E_K)}{\sum_m F(E_m - E_K)} = X(E_K),$$

proving the ETH. □

Discussion. So what is a preferred basis and at what condition the eigenstates are ergodic in it? There is no single definite answer.

A general belief, confirmed with numerical simulations, states that for quantum chaotic (non-integrable) systems, the eigenfunctions are ergodic with respect to a local basis[1] [238], which immediately shows that ETH should hold for local observables.

The first to–do for future study would be to find an explicit example of a non-local basis, where eigenstates are ergodic, and show that indeed ETH is satisfied there.

---

[1] E.g. the vectors of the local basis may be defined with respect to the Fock states on single sites of a Bose-Hubbard chain, like $|2100\rangle = \hat{a}_1^\dagger \hat{a}_1^\dagger \hat{a}_2^\dagger |0\rangle$.

Bibliography

[1] P. Grišins and I. Mazets. Thermalization in a one-dimensional integrable system. *Phys. Rev. A* **84** 053635 1 [2011]

[2] P. Grišins and I. E. Mazets. Coherence and Josephson oscillations between two tunnel-coupled one-dimensional atomic quasicondensates at finite temperature. *Phys. Rev. A* **87** 013629 1 [2013]

[3] P. Grišins and I. E. Mazets. Metropolis-Hastings thermal state sampling for numerical simulations of Bose-Einstein condensates. *Comput. Phys. Commun.* **185** 7 1926 [2014]

[4] K. Davis, M. Mewes, and M. Andrews. Bose-Einstein condensation in a gas of sodium atoms. *Phys. Rev. Lett.* **75** November [1995]

[5] M. Anderson, J. Ensher, M. Matthews, Wieman, and Cornell. Observation of Bose-Einstein condensation in a dilute atomic vapor. *Science* [1995]

[6] C. J. Pethick and H. Smith. *Bose-Einstein Condensation in Dilute Gases.* Cambridge University Press [2001]. ISBN 0511018703

[7] Y. Castin. Bose-Einstein condensates in atomic gases : simple theoretical results. *Small* October [2000]

[8] A. J. Leggett. Bose-Einstein condensation in the alkali gases: Some fundamental concepts. *Rev. Mod. Phys.* **73** 2 307 [2001]

[9] N. van Druten and W. Ketterle. Two-Step Condensation of the Ideal Bose Gas in Highly Anisotropic Traps. *Phys. Rev. Lett.* **79** 4 549 [1997]

[10] M. Olshanii. Atomic Scattering in the Presence of an External Confinement and a Gas of Impenetrable Bosons. *Phys. Rev. Lett.* **81** 5 938 [1998]

[11] E. H. Lieb and W. Liniger. Exact analysis of an interacting Bose gas. I. The general solution and the ground state. *Phys. Rev.* **130** 4 1605 [1963]

[12] E. H. Lieb. Exact analysis of an interacting Bose gas. II. The excitation spectrum. *Phys. Rev.* **1291** 1953 [1963]

[13] I. Bouchoule, N. V. Druten, and C. Westbrook. Atom chips and one-dimensional Bose gases. *arXiv Prepr.* pp. 1–34 [2009]

[14] M. Girardeau. Relationship between Systems of Impenetrable Bosons and Fermions in One Dimension. *J. Math. Phys.* **1** 6 516 [1960]

[15] T. Kinoshita, T. Wenger, and D. Weiss. Observation of a one-dimensional Tonks-Girardeau gas. *Science* **305** August 1125 [2004]

[16] V. N. Popov. On the theory of the superfluidity of two-and one-dimensional Bose systems. *Theor. Math. Phys.* **11** 3 565 [1972]

[17] S. Dettmer, D. Hellweg, P. Ryytty, J. Arlt, W. Ertmer, K. Sengstock, D. Petrov, G. Shlyapnikov, H. Kreutzmann, L. Santos, and M. Lewenstein. Observation of Phase Fluctuations in Elongated Bose-Einstein Condensates. *Phys. Rev. Lett.* **87** 16 160406 [2001]

[18] E. Gross. Structure of a quantized vortex in boson systems. *Nuovo Cim. Ser. 10* [1961]

[19] L. P. Pitaevskii. Vortex lines in an imperfect Bose gas. *Sov. Phys. JETP-USSR* **13** 2 451 [1961]

[20] V. Zakharov and A. Shabat. Interaction between solitons in a stable medium. *Sov. Phys. JETP* **37** 5 823 [1973]

[21] E. Lieb, R. Seiringer, and J. Yngvason. One-Dimensional Basons in Three-Dimensional Traps. *Stab. Matter From Atoms to ...* pp. 1–5 [2005]

[22] F. Gerbier. Quasi-1D Bose-Einstein condensates in the dimensional crossover regime. *Europhys. Lett.* **66** 6 771 [2004]

[23] D. Petrov, G. Shlyapnikov, and J. Walraven. Phase-Fluctuating 3D Bose-Einstein Condensates in Elongated Traps. *Phys. Rev. Lett.* **87** 5 050404 [2001]

[24] S. Manz, R. Bücker, D. I. T. Betz, C. Koller, S. Hofferberth, I. E. Mazets, A. Imambekov, E. Demler, a. Perrin, J. Schmiedmayer, and T. Schumm. Two-point density correlations of quasicondensates in free expansion. *Phys. Rev. A* **81** 3 1 [2010]

[25] A. Imambekov, I. E. Mazets, D. S. Petrov, V. Gritsev, S. Manz, S. Hofferberth, T. Schumm, E. Demler, and J. Schmiedmayer. Density ripples in expanding low-dimensional gases as a probe of correlations. *Phys. Rev. A* **80** 3 033604 [2009]

[26] C. Mora and Y. Castin. Extension of Bogoliubov theory to quasicondensates. *Phys. Rev. A* **67** 5 053615 [2003]

[27] T. Giamarchi. *Quantum physics in one dimension.* Clarendon Oxford University Press, Oxford New York [2004]. ISBN 0198525001

[28] E. Wigner. On the quantum correction for thermodynamic equilibrium. *Phys. Rev.* [1932]

[29] J. E. Moyal. Quantum mechanics as a statistical theory. *Math. Proc. Cambridge Philos. Soc.* **45** 01 99 [1949]

[30] C. Zachos, D. Fairlie, and T. Curtright. *Quantum Mechanics in Phase Space: An Overview With Selected Papers.* World Scientific [2005]

[31] C. Gardiner and P. Zoller. *Quantum noise : a handbook of Markovian and non-Markovian quantum stochastic methods with applications to quantum optics.* Springer, New York [2004]. ISBN 3540223010

[32] A. Polkovnikov. Phase space representation of quantum dynamics. *Ann. Phys.* **325** 8 1790 [2010]

[33] S. Tomonaga. Remarks on Bloch's method of sound waves applied to many-fermion problems. *Prog. Theor. Phys.* **5** 4 544 [1950]

[34] J. M. Luttinger. An Exactly Soluble Model of a Many-Fermion System. *J. Math. Phys.* **4** 1154 [1963]

[35] F. D. M. Haldane. Effective Harmonic-Fluid Approach to Low-Energy Properties of One-Dimensional Quantum Fluids. *Phys. Rev. Lett.* **47** 25 2 [1981]

[36] M. Cazalilla. Bosonizing one-dimensional cold atomic gases. *J. Phys. B* **37** 7 S1 [2004]

[37] P. Blakie, A. Bradley, M. Davis, R. Ballagh, and C. Gardiner. Dynamics and statistical mechanics of ultra-cold Bose gases using c-field techniques. *Adv. Phys.* **57** 5 363 [2008]

[38] M. Gring, M. Kuhnert, T. Langen, T. Kitagawa, B. Rauer, M. Schreitl, I. E. Mazets, D. A. Smith, E. Demler, and J. Schmiedmayer. Relaxation and Prethermalization in an Isolated Quantum System. *Science* **337** 6100 1318 [2012]

[39] A. Perrin, R. Bücker, S. Manz, D. I. T. Betz, C. Koller, T. Plisson, T. Schumm, and J. Schmiedmayer. Hanbury Brown and Twiss correlations across the BoseâĂŞEinstein condensation threshold. *Nat. Phys.* **8** 3 195 [2012]

[40] D. S. Petrov, G. V. Shlyapnikov, and J. T. M. Walraven. Regimes of quantum degeneracy in trapped 1D gases. *Phys. Rev. Lett.* **85** 18 4 [2000]

[41] J. Berges, S. Borsányi, and C. Wetterich. Prethermalization. *Phys. Rev. Lett.* **93** 14 14 [2004]

[42] F. Cooper, S. Habib, Y. Kluger, and E. Mottola. Nonequilibrium dynamics of symmetry breaking in $\lambda\Phi4$ theory. *Phys. Rev. D* **55** 10 6471 [1997]

[43] T. Kitagawa, A. Imambekov, J. Schmiedmayer, and E. Demler. The dynamics and prethermalization of one-dimensional quantum systems probed through the full distributions of quantum noise. *New J. Phys.* **13** 7 073018 [2011]

[44] D. Iyer, H. Guan, and N. Andrei. An exact formalism for the quench dynamics of integrable models. *arXiv Prepr.* p. 20 [2013]

[45] F. Queisser, K. V. Krutitsky, P. Navez, and R. Schützhold. Equilibration and prethermalization in the Bose-Hubbard and Fermi-Hubbard models. *Phys. Rev. A* **89** 3 033616 [2014]

[46] M. Fürst, C. Mendl, and H. Spohn. Dynamics of the Bose-Hubbard Chain for Weak Interactions. *arXiv Prepr. arXiv1312.6737* p. 16 [2013]

[47] M. Stark and M. Kollar. Kinetic description of thermalization dynamics in weakly interacting quantum systems. *arXiv Prepr. arXiv1308.1610* 4 [2013]

[48] M. Kollar, F. Wolf, and M. Eckstein. Generalized Gibbs ensemble prediction of prethermalization plateaus and their relation to nonthermal steady states in integrable systems. *Phys. Rev. B* **84** 054304 1 [2011]

[49] J. Marino and A. Silva. Relaxation, prethermalization, and diffusion in a noisy quantum Ising chain. *Phys. Rev. B* **86** 6 060408 [2012]

[50] M. Marcuzzi, J. Marino, A. Gambassi, and A. Silva. Prethermalization in a Nonintegrable Quantum Spin Chain after a Quench. *Phys. Rev. Lett.* **111** 19 197203 [2013]

[51] F. H. L. Essler, S. Kehrein, S. R. Manmana, and N. J. Robinson. Quench Dynamics in a Model with Tuneable Integrability Breaking. *arXiv Prepr. arXiv 1311.4557* p. 22 [2013]

[52] F. H. L. Essler, S. Kehrein, S. R. Manmana, and N. J. Robinson. Quench Dynamics in a Model with Tuneable Integrability Breaking. *arXiv:1311.4557* p. 22 [2013]

[53] T. Langen, M. Gring, and M. Kuhnert. Prethermalization in one-dimensional Bose gases: description by a stochastic Ornstein-Uhlenbeck process. *arXiv Prepr. arXiv . . .* pp. 1–10 [2012]

[54] Zaslavskii. *Stochasticity of Dynamical Systems.* Nauka, Moscow [1984]

[55] Zaslavskii and Sagdeev. *Introduction to nonlinear physics.* Nauka, M. [1988]

[56] H. Hess. Evaporative cooling of magnetically trapped and compressed spin-polarized hydrogen. *Phys. Rev. B* **34** 5 [1986]

[57] E. Surkov, J. T. M. Walraven, and G. V. Shlyapnikov. Collisionless motion and evaporative cooling of atoms in magnetic traps. *Phys. Rev. A* **53** 5 3403 [1996]

[58] W. Ketterle and N. J. V. Druten. Evaporative Cooling of Trapped Atoms. In B. Bederson and H. Walther, eds., *Adv. At. Mol. Opt. Phys.*, vol. 37 of *Advances In Atomic, Molecular, and Optical Physics*, pp. 181–236. Academic Press [1996]

[59] O. Luiten, M. W. Reynolds, and J. T. M. Walraven. Kinetic theory of the evaporative cooling of a trapped gas. *Phys. Rev. A* **53** 1 381 [1996]

[60] P. Pinkse, A. Mosk, and M. Weidemüller. One-dimensional evaporative cooling of magnetically trapped atomic hydrogen. *Phys. Rev. A* **57** 6 4747 [1998]

[61] S. Hofferberth, I. Lesanovsky, T. Schumm, A. Imambekov, V. Gritsev, E. Demler, and J. Schmiedmayer. Probing quantum and thermal noise in an interacting many-body system. *Nat. Phys.* **4** 6 489 [2008]

[62] L. LeBlanc, A. Bardon, and J. McKeever. Dynamics of a tunable superfluid junction. *Phys. Rev. Lett.* pp. 1–7 [2011]

[63] W. Rohringer, D. Fischer, and F. Steiner. Scaling of phonons and shortcuts to adiabaticity in a one-dimensional quantum system. *arXiv Prepr. arXiv . . .* pp. 1–9 [2013]

[64] R. Gati, B. Hemmerling, J. Fölling, M. Albiez, and M. K. Oberthaler. Noise Thermometry with Two Weakly Coupled Bose-Einstein Condensates. *Phys. Rev. Lett.* **96** 13 130404 [2006]

[65] T. Berrada, S. V. Frank, R. Bücker, T. Schumm, J.-F. Schaff, and J. Schmiedmayer. Integrated Mach-Zehnder interferometer for Bose-Einstein condensates. *Nat. Commun.* **4** 2077 [2013]

[66] D. I. T. Betz, S. Manz, R. Bücker, T. Berrada, C. Koller, G. Kazakov, I. E. Mazets, H.-P. Stimming, a. Perrin, T. Schumm, and J. Schmiedmayer. Two-Point Phase Correlations of a One-Dimensional Bosonic Josephson Junction. *Phys. Rev. Lett.* **106** 2 1 [2011]

[67] R. Gati. Bose-Einstein Condensates in a Single Double Well Potential. *Sci. York* [2007]

[68] O. Morsch and M. K. Oberthaler. Dynamics of Bose-Einstein condensates in optical lattices. *Rev. Mod. Phys.* **78** 1 179 [2006]

[69] W. S. Bakr, J. I. Gillen, A. Peng, S. Fölling, and M. Greiner. A quantum gas microscope for detecting single atoms in a Hubbard-regime optical lattice. *Nature* **462** 7269 74 [2009]

[70] D. Jaksch, C. Gardiner, and P. Zoller. Quantum kinetic theory. II. Simulation of the quantum Boltzmann master equation. *Phys. Rev. A* **56** 1 575 [1997]

[71] K. O'Hara, M. Gehm, S. Granade, and J. Thomas. Scaling laws for evaporative cooling in time-dependent optical traps. *Phys. Rev. A* **64** 5 051403 [2001]

[72] B. Nowak, S. Erne, M. Karl, and J. Schole. Non-thermal fixed points: universality, topology, & turbulence in Bose gases. *arXiv Prepr. arXiv . . .* August [2013]

[73] M. Schmidt, S. Erne, B. Nowak, D. Sexty, and T. Gasenzer. Non-thermal fixed points and solitons in a one-dimensional Bose gas. *New J. Phys.* **14** 7 075005 [2012]

[74] W. Zurek. Causality in Condensates: Gray Solitons as Relics of BEC Formation. *Phys. Rev. Lett.* **102** 10 4 [2009]

[75] E. Witkowska, P. Deuar, M. Gajda, and K. Rzazewski. Solitons as the Early Stage of Quasicondensate Formation during Evaporative Cooling. *Phys. Rev. Lett.* **106** 13 1 [2011]

[76] H. Wu and C. Foot. Direct simulation of evaporative cooling. *J. Phys. B At. Mol. . . .* **321** [1996]

[77] B. Jackson and E. Zaremba. Modeling Bose-Einstein condensed gases at finite temperatures with N-body simulations. *Phys. Rev. A* **66** 3 1 [2002]

[78] P. Drummond and J. Corney. Quantum dynamics of evaporatively cooled Bose-Einstein condensates. *Phys. Rev. A* **60** 4 R2661 [1999]

[79] M. Rigol, V. Dunjko, V. Yurovsky, and M. Olshanii. Relaxation in a Completely Integrable Many-Body Quantum System: An Ab Initio Study of the Dynamics of the Highly Excited States of 1D Lattice Hard-Core Bosons. *Phys. Rev. Lett.* **98** 5 1 [2007]

[80] T. Kinoshita, T. Wenger, and D. S. Weiss. A quantum Newton's cradle. *Nature* **440** 7086 900 [2006]

[81] J. Mossel and J.-S. Caux. Generalized TBA and generalized Gibbs. *J. Phys. A* **45** 25 255001 [2012]

[82] J.-S. Caux. Correlation functions of integrable models: A description of the ABACUS algorithm. *J. Math. Phys.* pp. 1–30 [2009]

[83] J.-S. Caux and R. M. Konik. Constructing the Generalized Gibbs Ensemble after a Quantum Quench. *Phys. Rev. Lett.* **109** 17 175301 [2012]

[84] B. Davies and V. Korepin. Higher conservation laws for the quantum non-linear Schrödinger equation. *Physica A* pp. 1–23 [1990]

[85] J. Sirker. the Luttinger Liquid and Integrable Models. *Int. J. Mod. Phys. B* **26** 22 1244009 [2012]

[86] A. Del Maestro and I. Affleck. Interacting bosons in one dimension and the applicability of Luttinger-liquid theory as revealed by path-integral quantum Monte Carlo calculations. *Phys. Rev. B* **82** 6 1 [2010]

[87] B. Pozsgay. The dynamical free energy and the Loschmidt echo for a class of quantum quenches in the Heisenberg spin chain. *J. Stat. Mech.* **2013** 10 P10028 [2013]

[88] P. Reimann. Canonical thermalization. *New J. Phys.* **12** 5 055027 [2010]

[89] I. E. Mazets and J. Schmiedmayer. Thermalization in a quasi-one-dimensional ultracold bosonic gas. *New J. Phys.* **12** 5 055023 [2010]

[90] P. Navez and A. Lazarides. Quantum stochastic description of collisions in a canonical Bose gas. *arXiv Prepr. arXiv1112.3557* 1 1 [2011]

[91] I. E. Mazets, T. Schumm, and J. Schmiedmayer. Breakdown of Integrability in a Quasi-1D Ultracold Bosonic Gas. *Phys. Rev. Lett.* **100** 21 2 [2008]

[92] I. E. Mazets. Dynamics and kinetics of quasiparticle decay in a nearly-one-dimensional degenerate Bose gas. *Phys. Rev. A* **83** 4 043625 [2011]

[93] N. Sedlmayr, J. Ren, F. Gebhard, and J. Sirker. Closed and Open System Dynamics in a Fermionic Chain with a Microscopically Specified Bath: Relaxation and Thermalization. *Phys. Rev. Lett.* **110** 10 100406 [2013]

[94] L. F. Santos and M. Rigol. Fluctuations in the delocalization level of eigenstates and thermalization. *Physica Scripta* [2012]

[95] C. Ates, J. Garrahan, and I. Lesanovsky. Thermalization of a Strongly Interacting Closed Spin System: From Coherent Many-Body Dynamics to a Fokker-Planck Equation. *Phys. Rev. Lett.* [2012]

[96] V. Yurovsky and M. Olshanii. Memory of the Initial Conditions in an Incompletely Chaotic Quantum System: Universal Predictions with Application to Cold Atoms. *Phys. Rev. Lett.* **106** 2 1 [2011]

[97] M. Steel, M. Olsen, L. Plimak, P. Drummond, S. Tan, M. Collett, D. Walls, and R. Graham. Dynamical quantum noise in trapped Bose-Einstein condensates. *Phys. Rev. A* **58** 6 4824 [1998]

[98] A. Sinatra, C. Lobo, and Y. Castin. The truncated Wigner method for Bose-condensed gases: limits of validity and applications. . . . *Phys. B At. Mol.* . . . **3599** [2002]

[99] H.-P. Stimming, N. Mauser, J. Schmiedmayer, and I. E. Mazets. Dephasing in coherently split quasicondensates. *Phys. Rev. A* **83** 2 1 [2011]

[100] A. F. Andreev. The hydrodynamics of two- and one-dimensional liquids. *Sov. Phys. JETP* **78** 2064 [1980]

[101] I. E. Mazets. Relaxation of phonons in a one-dimensional integrable bosonic system. In *44th Winter Colloq. Phys. Quantum Electron.* Snowbird, Utah, USA [2014]

[102] A. Caldeira and A. Leggett. Influence of dissipation on quantum tunneling in macroscopic systems. *Phys. Rev. Lett.* 4 4 [1981]

[103] A. Altland and B. D. Simmons. *Condensed Matter Field Theory*. Cambridge University Press, New York [2006]. ISBN 0521845084

[104] A. Kamenev. *Field theory of non-equilibrium systems*. Cambridge University Press, Cambridge New York [2011]. ISBN 978-0521760829

[105] G.-S. Paraoanu, S. Kohler, F. Sols, and a. J. Leggett. The Josephson plasmon as a Bogoliubov quasiparticle. *J. Phys. B* **34** 23 4689 [2001]

[106] M. Cazalilla. Effect of Suddenly Turning on Interactions in the Luttinger Model. *Phys. Rev. Lett.* **97** 15 156403 [2006]

[107] M. Tavora and A. Mitra. Quench dynamics of one-dimensional bosons in a commensurate periodic potential: A quantum kinetic equation approach. *Phys. Rev. B* pp. 30–34 [2013]

[108] A. Mitra. Correlation functions in the prethermalized regime after a quantum quench of a spin chain. *Phys. Rev. B* **205109** 1 [2013]

[109] E. D. Torre, E. Demler, and A. Polkovnikov. Universal Rephasing Dynamics after a Quantum Quench via Sudden Coupling of Two Initially Independent Condensates. *Phys. Rev. Lett.* **110** 090404 [2013]

[110] M. S. Foster, E. Yuzbashyan, and B. L. Altshuler. Quantum Quench in One Dimension: Coherent Inhomogeneity Amplification and 'Supersolitons'. *Phys. Rev. Lett.* **105** 13 135701 [2010]

[111] M. Gring. *Prethermalization in an Isolated Many Body System.* Ph.D. thesis, TU Wien [2012]

[112] T. Langen. *Non-equilibrium dynamics of one-dimensional Bose gases.* Ph.D. thesis, TU Wien [2013]

[113] A. Vaglica, C. Leonardi, and G. Vetri. Generalized Wick's Theorem for a Boson Field in the Squeezed Vacuum. *J. Mod. Opt.* **37** 9 1487 [1990]

[114] T. Langen, R. Geiger, and M. Kuhnert. Local emergence of thermal correlations in an isolated quantum many-body system. *Nat. Phys.* pp. 1–4 [2013]

[115] S. Stenholm. *Foundations of Laser Spectroscopy.* Dover, Mineola NY [2005]

[116] E. N. Economou. *Green's functions in quantum physics.* Springer, New York [2006]. ISBN 9783540288381

[117] B. Rauer, P. Grišins, I. E. Mazets, W. Rohringer, T. Schweigler, M. Kuhnert, M. Gring, R. Geiger, T. Langen, and J. Schmiedmayer. 'Evaporative' cooling of one-dimensional Bose gas. *Manuscr. Prep.* [2014]

[118] E. Jaynes. Gibbs vs Boltzmann entropies. *Am. J. Phys.* [1965]

[119] C. Barceló, S. Liberati, and M. Visser. Probing semiclassical analog gravity in Bose-Einstein condensates with widely tunable interactions. *Phys. Rev. A* **68** 5 053613 [2003]

[120] P. Fedichev and U. Fischer. 'Cosmological' quasiparticle production in harmonically trapped superfluid gases. *Phys. Rev. A* **69** 3 033602 [2004]

[121] A. Polkovnikov and V. Gritsev. Breakdown of the adiabatic limit in low-dimensional gapless systems. *Nat. Phys.* **4** 6 477 [2008]

[122] P. Calabrese and J. Cardy. Quantum quenches in extended systems. *J. Stat. Mech.* **2007** 06 P06008 [2007]

[123] A. Polkovnikov, K. Sengupta, A. Silva, and M. Vengalattore. Colloquium: Nonequilibrium dynamics of closed interacting quantum systems. *Rev. Mod. Phys.* **83** 3 863 [2011]

[124] I. Bloch, J. Dalibard, and W. Zwerger. Many-body physics with ultracold gases. *Rev. Mod. Phys.* **80** September [2008]

[125] J. Dunkel and S. Hilbert. Consistent thermostatistics forbids negative absolute temperatures. *Nat. Phys.* **10** 12 1 [2013]

[126] S. Trotzky, Y. Chen, A. Flesch, and I. Bloch. Probing the relaxation towards equilibrium in an isolated strongly correlated one-dimensional Bose gas. *Nat. Phys.* **8** 325 [2012]

[127] M. Cramer, A. Flesch, I. McCulloch, U. Schollwöck, and J. Eisert. Exploring Local Quantum Many-Body Relaxation by Atoms in Optical Superlattices. *Phys. Rev. Lett.* **101** 6 063001 [2008]

[128] M. Cramer, C. Dawson, J. Eisert, and T. Osborne. Exact Relaxation in a Class of Nonequilibrium Quantum Lattice Systems. *Phys. Rev. Lett.* **100** 3 030602 [2008]

[129] V. Zakharov, V. L'vov, and G. Falkovich. *Kolmogorov Spectra of Turbulence.* Springer-Verlag, Berlin Heidelberg [1992]

[130] I. Bloch, J. Dalibard, and S. Nascimbène. Quantum simulations with ultracold quantum gases. *Nat. Phys.* **8** 4 267 [2012]

[131] J. Simon, W. S. Bakr, R. Ma, M. E. Tai, P. M. Preiss, and M. Greiner. Quantum simulation of antiferromagnetic spin chains in an optical lattice. *Nature* **472** 7343 307 [2011]

[132] A. Reinhard, J.-F. Riou, L. a. Zundel, D. S. Weiss, S. Li, A. M. Rey, and R. Hipolito. Self-Trapping in an Array of Coupled 1D Bose Gases. *Phys. Rev. Lett.* **110** 3 033001 [2013]

[133] G.-B. Jo, J. Guzman, C. K. Thomas, P. Hosur, A. Vishwanath, and D. M. Stamper-Kurn. Ultracold Atoms in a Tunable Optical Kagome Lattice. *Phys. Rev. Lett.* **108** 4 045305 [2012]

[134] X. Zhang, C.-L. Hung, S.-K. Tung, and C. Chin. Observation of quantum criticality with ultracold atoms in optical lattices. *Science* **335** 6072 1070 [2012]

[135] J. Dalibard, F. Gerbier, G. Juzeliåńnas, and P. Öhberg. Colloquium: Artificial gauge potentials for neutral atoms. *Rev. Mod. Phys.* **83** 4 1523 [2011]

[136] M. Aidelsburger, M. Atala, S. Nascimbène, S. Trotzky, Y.-a. Chen, and I. Bloch. Experimental Realization of Strong Effective Magnetic Fields in an Optical Lattice. *Phys. Rev. Lett.* **107** 25 255301 [2011]

[137] D. Greif, T. Uehlinger, G. Jotzu, L. Tarruell, and T. Esslinger. Short-range quantum magnetism of ultracold fermions in an optical lattice. *Science* p. 10 [2012]

[138] Y.-J. Lin, R. L. Compton, K. Jiménez-García, J. V. Porto, and I. B. Spielman. Synthetic magnetic fields for ultracold neutral atoms. *Nature* **462** 7273 628 [2009]

[139] M. Aidelsburger, M. Atala, M. Lohse, J. T. Barreiro, B. Paredes, and I. Bloch. Realization of the Hofstadter Hamiltonian with Ultracold Atoms in Optical Lattices. *Phys. Rev. Lett.* **111** 18 185301 [2013]

[140] H. Miyake, G. a. Siviloglou, C. J. Kennedy, W. C. Burton, and W. Ketterle. Realizing the Harper Hamiltonian with Laser-Assisted Tunneling in Optical Lattices. *Phys. Rev. Lett.* **111** 18 185302 [2013]

[141] P.-I. Schneider and A. Saenz. Quantum computation with ultracold atoms in a driven optical lattice. *Phys. Rev. A* **85** 5 050304 [2012]

[142] I. H. Deutsch, G. K. Brennen, and P. S. Jessen. Quantum Computing with Neutral Atoms in an Optical Lattice. *Fortschritte der Phys.* **48** 9-11 925 [2000]

[143] T. D. Ladd, F. Jelezko, R. Laflamme, Y. Nakamura, C. Monroe, and J. L. O'Brien. Quantum computers. *Nature* **464** 7285 45 [2010]

[144] S. Braun, J. Ronzheimer, M. Schreiber, S. S. Hodgman, T. Rom, I. Bloch, and U. Schneider. Negative absolute temperature for motional degrees of freedom. *Science* [2013]

[145] J. F. Sherson, C. Weitenberg, M. Endres, M. Cheneau, I. Bloch, and S. Kuhr. Single-Atom Resolved Fluorescence Imaging of an Atomic Mott Insulator. *Nature* **467** 7311 68 [2010]

[146] J. Dalibard and C. Cohen-Tannoudji. Dressed-atom approach to atomic motion in laser light: the dipole force revisited. *J. Opt. Soc. Am. B* **2** 11 1707 [1985]

[147] H. Metcalf. *Laser cooling and trapping.* Springer, New York [1999]. ISBN 9780387987286

[148] H. Gersch and G. Knollman. Quantum Cell Model for Bosons. *Phys. Rev.* **948** [1963]

[149] J. Hubbard. Electron correlations in narrow energy bands. *Proc. R. Soc. London. Ser. A. Math. Phys. Sci.* **276** 1365 238 [1963]

[150] M. Capello, F. Becca, M. Fabrizio, and S. Sorella. Superfluid to Mott-Insulator Transition in Bose-Hubbard Models. *Phys. Rev. Lett.* **99** 5 056402 [2007]

[151] P. Jordan and E. P. Wigner. About the Pauli exclusion principle. *Zeitschrift fur Phys.* **47** 631 [1928]

[152] M. Rigol. Finite-temperature properties of hard-core bosons confined on one-dimensional optical lattices. *Phys. Rev. A* **72** 6 1 [2005]

[153] P. Coleman. Simple examples of second quantization: Jordan Wigner Transformation [2004]

[154] A. Neto, H. Lin, Y. Chen, and J. Carmelo. Pseudoparticle-operator description of an interacting bosonic gas. *Phys. Rev. B* **50** [1994]

[155] M. Greiner, O. Mandel, T. Esslinger, T. Hänsch, and I. Bloch. Quantum phase transition from a superfluid to a Mott insulator in a gas of ultracold atoms. *Nature* pp. 39–44 [2002]

[156] S. V. Isakov, M. B. Hastings, and R. G. Melko. Topological entanglement entropy of a Bose-Hubbard spin liquid. *Nat. Phys.* **7** 10 772 [2011]

[157] W. S. Cole, S. Zhang, A. Paramekanti, and N. Trivedi. Bose-Hubbard Models with Synthetic Spin-Orbit Coupling: Mott Insulators, Spin Textures, and Superfluidity. *Phys. Rev. Lett.* **109** 8 085302 [2012]

[158] I. Pižorn. One-dimensional Bose-Hubbard model far from equilibrium. *Phys. Rev. A* **88** 4 043635 [2013]

[159] M. Ohliger and A. Pelster. Green's Function Approach to the Bose-Hubbard Model. *World J. Condens. Matter Phys.* **1** 2 1 [2013]

[160] U. Schollwöck. The density-matrix renormalization group. *Rev. Mod. Phys.* **77** April [2005]

[161] K. Wilson. The renormalization group: Critical phenomena and the Kondo problem. *Rev. Mod. Phys.* **47** 4 773 [1975]

[162] A. E. Feiguin, E. Rezayi, C. Nayak, and S. Das Sarma. Density Matrix Renormalization Group Study of Incompressible Fractional Quantum Hall States. *Phys. Rev. Lett.* **100** 16 166803 [2008]

[163] T. Senthil, J. Marston, and M. Fisher. Spin quantum Hall effect in unconventional superconductors. *Phys. Rev. B* **60** 6 4245 [1999]

[164] J. Haegeman, T. Osborne, H. Verschelde, and F. Verstraete. Entanglement Renormalization for Quantum Fields in Real Space. *Phys. Rev. Lett.* **110** 10 100402 [2013]

[165] A. Flesch, M. Cramer, I. McCulloch, U. Schollwöck, and J. Eisert. Probing local relaxation of cold atoms in optical superlattices. *Phys. Rev. A* **78** 3 033608 [2008]

[166] G. Vidal. Efficient Classical Simulation of Slightly Entangled Quantum Computations. *Phys. Rev. Lett.* **91** 14 147902 [2003]

[167] G. Vidal. Efficient Simulation of One-Dimensional Quantum Many-Body Systems. *Phys. Rev. Lett.* **93** 4 040502 [2004]

[168] U. Schollwöck. The density-matrix renormalization group in the age of matrix product states. *Ann. Phys.* **326** 1 96 [2011]

[169] L. Pollet. Recent developments in quantum Monte Carlo simulations with applications for cold gases. *Reports Prog. Phys.* [2012]

[170] B. Svistunov and N. Prokof'ev. Worm Algorithm for Problems of Quantum and Classical Statistics. In L. D. Carr, ed., *Underst. Quantum Phase Transitions*, pp. 1–27. Taylor & Francis, Boca Raton [2010]

[171] A. Sandvik. Stochastic series expansion method with operator-loop update. *Phys. Rev. B* **59** 22 R14157 [1999]

[172] O. F. Syljuåsen and A. W. Sandvik. Quantum Monte Carlo with directed loops. *Phys. Rev. E* **66** 4 046701 [2002]

[173] W. Witczak-Krempa, E. Sørensen, and S. Sachdev. The dynamics of quantum criticality revealed by quantum Monte Carlo and holography. *Nat. Phys.* **10** May [2014]

[174] J. Zhang and R. Dong. Exact diagonalization: the Bose-Hubbard model as an example. *Eur. J. Phys.* **31** 3 591 [2010]

[175] K. Huang. *Statistical mechanics.* Wiley, New York [1987]. ISBN 0471815187

[176] U. Leonhardt. *Essential Quantum Optics.* Cambridge University Press, New York [2010]. ISBN 978-0-521-14505-3

[177] M. C. Bañuls, J. I. Cirac, and M. B. Hastings. Strong and Weak Thermalization of Infinite Nonintegrable Quantum Systems. *Phys. Rev. Lett.* **106** 5 050405 [2011]

[178] N. Linden, S. Popescu, A. J. Short, and A. Winter. Quantum mechanical evolution towards thermal equilibrium. *Phys. Rev. E* **79** 6 061103 [2009]

[179] J. Gibbs. *Elementary principles in statistical mechanics : developed with especial reference to the rational foundation of thermodynamics.* Ox Bow Press, Woodbridge, Conn [1981]. ISBN 9780918024206

[180] V. Flambaum and F. Izrailev. Statistical theory of finite Fermi systems based on the structure of chaotic eigenstates. *Phys. Rev. E* **56** 5 5144 [1997]

[181] S. Popescu, A. J. Short, and A. Winter. Entanglement and the foundations of statistical mechanics. *Nat. Phys.* **2** 11 754 [2006]

[182] R. Steinigeweg, J. Gemmer, and W. Brenig. Spin-current autocorrelations from single pure-state propagation. *arXiv Prepr. arXiv1312.5319* pp. 1–5 [2013]

[183] L. F. Santos, A. Polkovnikov, and M. Rigol. Weak and strong typicality in quantum systems. *Phys. Rev. E* **86** 1 010102 [2012]

[184] M. Cramer and J. Eisert. A quantum central limit theorem for non-equilibrium systems: exact local relaxation of correlated states. *New J. Phys.* **12** 5 055020 [2010]

[185] L. Néel. Propriétées magnétiques des ferrites; Férrimagnétisme et antiferromagnétisme. *Ann. Phys. (Paris).* **3** 137 [1948]

[186] W. Zurek. Decoherence, einselection, and the quantum origins of the classical. *Rev. Mod. Phys.* **75** 3 715 [2003]

[187] A. Kolovsky and A. Buchleitner. Quantum chaos in the Bose-Hubbard model. *Europhys. Lett.* **68** 5 632 [2004]

[188] A. Kolovsky. Semiclassical Quantization of the Bogoliubov Spectrum. *Phys. Rev. Lett.* **99** 2 020401 [2007]

[189] J.-S. Caux and J. Mossel. Remarks on the notion of quantum integrability. *J. Stat. Mech. Theory ...* **P02023** 1 [2011]

[190] F. Finkel and A. González-López. Global properties of the spectrum of the Haldane-Shastry spin chain. *Phys. Rev. B* **72** 17 174411 [2005]

[191] P. Anderson. Absence of diffusion in certain random lattices. *Phys. Rev.* **386** 1949 [1958]

[192] D. Basko, I. Aleiner, and B. L. Altshuler. Metal-insulator transition in a weakly interacting many-electron system with localized single-particle states. *Ann. Phys.* **321** 5 1126 [2006]

[193] A. Nanduri, H. Kim, and D. Huse. Entanglement spreading in a many-body localized system. *arXiv Prepr. arXiv1404.5216* pp. 1–7 [2014]

[194] H. Kim and D. Huse. Ballistic spreading of entanglement in a diffusive nonintegrable system. *Phys. Rev. Lett.* **1** 1 [2013]

[195] D. Huse and V. Oganesyan. A phenomenology of certain many-body-localized systems. *arXiv Prepr. arXiv1305.4915* **2** 1 [2013]

[196] C. Gogolin, M. P. Müller, and J. Eisert. Absence of Thermalization in Nonintegrable Systems. *Phys. Rev. Lett.* **106** 4 040401 [2011]

[197] M. Rigol, V. Dunjko, and M. Olshanii. Thermalization and its mechanism for generic isolated quantum systems. *Nature* **452** 7189 854 [2008]

[198] M. V. Berry. Regular and irregular semiclassical wavefunctions. *J. Phys. A* [1977]

[199] M. V. Berry. Chaotic behavior of deterministic systems. *Les Houches XXXVI* [1983]

[200] M. V. Berry. Some quantum-to-classical asymptotics. *Proc. 1989 Les Houches Summer Sch. onChaos Quantum Physicsa, Elsevier Sci. Publ. BV, Amsterdam* p. 251 [1991]

[201] M. Srednicki. Chaos and quantum thermalization. *Phys. Rev. E* **50** 2 [1994]

[202] A. Peres. Ergodicity and mixing in quantum theory. I. *Phys. Rev. A* **30** 1 504 [1984]

[203] J. Deutsch. Quantum statistical mechanics in a closed system. *Phys. Rev. A* **43** 4 4 [1991]

[204] J. von Neumann. Beweis des Ergodensatzes und des H-Theorems in der neuen Mechanik. *Z. Phys.* **57** 30 [1929]

[205] M. Rigol and M. Srednicki. Alternatives to eigenstate thermalization. *Phys. Rev. Lett.* 17 1 [2012]

[206] S. Goldstein, J. L. Lebowitz, R. Tumulka, and N. Zanghì. Long-time behavior of macroscopic quantum systems. *Eur. Phys. J. H* **35** 2 173 [2010]

[207] L. F. Santos and M. Rigol. Onset of quantum chaos in one-dimensional bosonic and fermionic systems and its relation to thermalization. *Phys. Rev. E* **81** 3 036206 [2010]

[208] A. C. Cassidy, C. W. Clark, and M. Rigol. Generalized Thermalization in an Integrable Lattice System. *Phys. Rev. Lett.* **106** 14 140405 [2011]

[209] T. Ikeda, Y. Watanabe, and M. Ueda. Eigenstate randomization hypothesis: Why does the long-time average equal the microcanonical average? *Phys. Rev. E* p. 4 [2011]

[210] P. Mazur. Non-ergodicity of phase functions in certain systems. *Physica* **43** 4 533 [1969]

[211] J. Sirker, N. P. Konstantinidis, F. Andraschko, and N. Sedlmayr. Locality and thermalization in closed quantum systems. *Phys. Rev. A* **89** 4 042104 [2014]

[212] D. Poulin, A. Qarry, R. Somma, and F. Verstraete. Quantum Simulation of Time-Dependent Hamiltonians and the Convenient Illusion of Hilbert Space. *Phys. Rev. Lett.* **106** 17 1 [2011]

[213] H. Stoof. *Ultracold quantum fields.* Springer in association with Canopus Pub, Dordrecht Bristol [2009]. ISBN 9781402087622

[214] M. Eckstein and M. Kollar. Nonthermal Steady States after an Interaction Quench in the Falicov-Kimball Model. *Phys. Rev. Lett.* **100** 12 120404 [2008]

[215] M. Kormos, A. Shashi, Y.-Z. Chou, J.-S. Caux, and A. Imambekov. Interaction quenches in the one-dimensional Bose gas. *Phys. Rev. B* **88** 20 205131 [2013]

[216] J. D. Nardis and B. Wouters. Variational solution for the interaction quench in the Lieb-Liniger Bose gas. *arXiv Prepr. arXiv . . .* 3 [2013]

[217] J. D. Nardis, B. Wouters, M. Brockmann, and J. Caux. Solution for an interaction quench in the Lieb-Liniger Bose gas. *Phys. Rev. A* **1** 1 [2014]

[218] V. N. Popov and L. Faddeev. An approach to the theory of the low-temperature Bose gas. *Sov. Phys. JETP* **1321** 890 [1965]

[219] V. N. Popov. *Functional integrals in quantum field theory and statistical physics.* Dordrecht: Kluwer Academic [1983]. ISBN 1402003072

[220] A. C. Cassidy. *Chaos and Thermalization in the one-dimensional Bose-Hubbard model in the classical-field approximation.* Phd thesis, University of Southern California [2010]

[221] E. M. Lifshits and L. P. Pitaevskii. *Physical kinetics.* Butterworth-Heinemann, Oxford England [1997]. ISBN 0750626356

[222] R. Walser, J. Williams, J. Cooper, and M. Holland. Quantum kinetic theory for a condensed bosonic gas. *Phys. Rev. A* **59** 5 3878 [1999]

[223] M. Moeckel and S. Kehrein. Interaction quench in the Hubbard model. *Phys. Rev. Lett.* **100** 17 175702 [2008]

[224] A. Kamenev and A. Levchenko. Keldysh technique and non-linear σ-model: basic principles and applications. *Adv. Phys.* [2009]

[225] C. Scheppach, J. Berges, and T. Gasenzer. Matter-wave turbulence: Beyond kinetic scaling. *Phys. Rev. A* pp. 1–18 [2010]

[226] B. Nowak and T. Gasenzer. On a new twist in the dynamics of Bose-Einstein condensation. *arXiv Prepr. arXiv1206.3181* [2012]

[227] T. Gasenzer. Ultracold gases far from equilibrium. *Eur. Phys. J. Spec. Top.* [2009]

[228] A. K. Pati and S. L. Braunstein. Impossibility of deleting an unknown quantum state. *Nature* **404** 6774 164 [2000]

[229] M. J. Ablowitz and J. F. Ladik. Nonlinear differential-difference equations and Fourier analysis. *J. Math. Phys.* **17** 6 1011 [1976]

[230] J. Paz and W. Zurek. Quantum limit of decoherence: Environment induced superselection of energy eigenstates. *Phys. Rev. Lett.* [1999]

[231] W. Zurek. Quantum Darwinism. *Nat. Phys.* **5** 3 181 [2009]

[232] W. Unruh. Notes on black-hole evaporation. *Phys. Rev. D* **14** 4 [1976]

[233] T. Kitagawa, S. Pielawa, A. Imambekov, J. Schmiedmayer, V. Gritsev, and E. Demler. Ramsey Interference in One-Dimensional Systems: The Full Distribution Function of Fringe Contrast as a Probe of Many-Body Dynamics. *Phys. Rev. Lett.* **104** 25 1 [2010]

[234] A. Polkovnikov and D.-W. Wang. Effect of Quantum Fluctuations on the Dipolar Motion of Bose-Einstein Condensates in Optical Lattices. *Phys. Rev. Lett.* **93** 7 070401 [2004]

[235] A. Polkovnikov. Quantum corrections to the dynamics of interacting bosons: Beyond the truncated Wigner approximation. *Phys. Rev. A* **68** 5 053604 [2003]

[236] A. Polkovnikov. Quantum ergodicity: fundamentals and applications. In *Lect. Notes* [2013]

[237] M. Albiez, R. Gati, J. Fölling, and S. Hunsmann. Direct observation of tunneling and nonlinear self-trapping in a single bosonic Josephson junction. *Phys. Rev. A* **40** 2 1 [2005]

[238] L. F. Santos, F. Borgonovi, and F. Izrailev. Chaos and Statistical Relaxation in Quantum Systems of Interacting Particles. *Phys. Rev. Lett.* **108** 9 1 [2012]

Published research

The following section contains research of the author published during the course of his graduate studies.

Thermalization in a one-dimensional integrable system

Pjotrs Grisins[1] and Igor E. Mazets[1,2]

[1]*Vienna Center for Quantum Science and Technology, Atominstitut, TU Wien, A-1020 Vienna, Austria*
[2]*Ioffe Physico-Technical Institute, 194021 St. Petersburg, Russia*

We present numerical results demonstrating the possibility of thermalization of single-particle observables in a one-dimensional system, which is integrable in both the quantum and classical (mean-field) descriptions (a quasicondensate of ultracold, weakly interacting bosonic atoms are studied as a definite example). We find that certain initial conditions admit the relaxation of single-particle observables to the equilibrium state reasonably close to that corresponding to the Bose-Einstein thermal distribution of Bogoliubov quasiparticles.

I. INTRODUCTION

A one-dimensional (1D) system of identical bosons with contact interactions is known to be integrable since Lieb and Liniger have solved analytically the corresponding quantum problem by means of the Bethe ansatz [1]. In the weakly interacting limit, this system can be described in the mean-field approximation by the Gross-Pitaevskii equation (GPE), also known as the nonlinear Schrödinger equation (NLSE). Zakharov and Shabat [2] have demonstrated that the NLSE with defocusing nonlinearity (which corresponds to the repulsive interactions between particles) is integrable by the inverse scattering transform (see [3] for a general review of the inverse scattering transform method). Since the number of integrals of motion in an integrable system equals to the number of degrees of freedom (infinite in the continuous mean-field description [2] or equal to the number of particles in the quantum Lieb-Liniger model [1]), one might expect that the finally attained equilibrium state must still bear signatures of the initial conditions.

One-dimensional bosonic systems have been experimentally implemented with ultracold atoms on atom chips [4,5], with the radial trapping frequency being $\sim 10^3$ times higher than the longitudinal one. The ultracold degenerate atomic system (quasicondensate, i.e., a system describable by a macroscopic wave function with a fluctuating local phase) was in the 1D regime since both the temperature and the mean interaction energy per atom were well below the energy interval between the ground and the first excited states of the radial motion. The fact that the static and dynamic correlation properties of these systems were in a very good agreement with the Bose-Einstein equilibrium distribution of quasiparticles seemed to be in contradiction with the system integrability and called for explanation. To explain the observed relaxation of single- and two-particle distribution functions for the elementary excitations (Bogoliubov quasiparticles) to the Bose-Einstein equilibrium, a mechanism of integrability breakdown via three-body effective collisions involving virtual excitations of the radial degrees of freedom has been proposed [6].

In the present paper we numerically show the existence of a certain case of nonequilibrium initial conditions of the GPE, which provide a very fast relaxation of the simplest (single-particle) observables to an equilibrium state very close to thermal equilibrium, despite the integrability of the problem.

Some indications of thermalization in 1D bosonic systems have been obtained in numerical simulations of various physical processes in quasicondensates, such as the subexponential decay of coherence between coherently split quasicondensates [7], soliton formation in a 1D bosonic system in the course of (quasi)condensation [8], in-trap density fluctuations [9], wave chaos [10], and condensate formation after the addition of a dimple to a weak harmonic longitudinal confinement of a 1D ultracold atomic gas [11]. However, a systematic study of thermalization of the GPE solution in the course of time evolution was lacking up to now. Even Ref. [12], where thermalization of the GPE solution with the initial conditions corresponding to the high-temperature limit has been numerically obtained, states that formal and systematic understanding of the problem is still incomplete. We fill this gap, at least to a certain extent, with our present study.

We also have to draw a clear distinction between our approach and that of Rigol *et al.* [13], who theoretically studied dephasing in a quantum system of hard-core bosons on a lattice, prepared initially in a coherent superposition of eigenstates, and its relaxation to a generalized Gibbs (fully constrained) equilibrium. Our aim is to demonstrate that a weakly interacting 1D degenerate bosonic gas can approach, in the course of its evolution, a state that is reasonably close to the conventional thermal Bose-Einstein equilibrium.

II. NUMERICAL APPROACH

We solve the GPE

$$i\hbar \frac{\partial}{\partial t} \Psi(x,t) = -\frac{\hbar^2}{2m} \frac{\partial^2}{\partial x^2} \Psi(x,t) + g|\Psi(x,t)|^2 \Psi(x,t), \quad (1)$$

where $\Psi(x,t)$ is a classical complex field representing a quasicondensate of atoms with mass m and g is the effective coupling constant in one dimension (we assume $g > 0$). The interaction strength is characterized by the Lieb-Liniger parameter [1] $\gamma = mg/(\hbar^2 \bar{n}) \equiv (\bar{n}\xi)^{-2}$, where ξ is the quasicondensate healing length and $\bar{n} \equiv \langle |\Psi(x,t)|^2 \rangle$ is the mean 1D number density. We consider the weak interaction limit $\gamma \ll 1$. We assume periodic boundary conditions for $\Psi(x,t)$, with the period L being long enough to ensure the loss of correlations over the half period: $\langle \Psi^*(x,t)\Psi(x + L/2,t) \rangle \ll \bar{n}$. The angle brackets denote here averaging over the ensemble of realizations. For each realization the initial conditions are prepared in a manner similar to the truncated Wigner approach [14] but

taking into account thermal fluctuations only (cf. Ref. [7]). We express the macroscopic order parameters in terms of the phase ϕ and density δn fluctuations: $\Psi = (\bar{n} + \delta n)^{1/2} e^{i\phi}$. The initial (at $t = 0$) fluctuations are expanded into plane waves as

$$\delta n(x,0) = 2\sqrt{\bar{n}/L} \sum_{k \neq 0} \beta_k \sqrt{\eta_k/\epsilon_k} \cos(kx + \varpi_k),$$

$$\phi(x,0) = (1/\sqrt{\bar{n}L}) \sum_{k \neq 0} \beta_k \sqrt{\epsilon_k/\eta_k} \sin(kx + \varpi_k), \quad (2)$$

where $\epsilon_k = \sqrt{\eta_k(\eta_k + 2g\bar{n})}$ is the energy of the elementary (Bogoliubov) excitation with the momentum $\hbar k$ and $\eta_k = (\hbar k)^2/(2m)$. The real numbers β_k and ϖ_k have the meaning of the scaled amplitude and the offset of the thermally excited elementary wave with the momentum $\hbar k$ at $t = 0$. The values of ϖ_k are taken as (pseudo)random numbers uniformly distributed between 0 and 2π. Each ensemble of realizations is also characterized by a distribution of the β_k values, with $\langle \beta_k^2 \rangle$ being equal to the main number $\mathcal{N}_0(k)$ of elementary excitation quanta (quasiparticles) in the given mode [15]. In equilibrium at the temperature T the populations of the bosonic quasiparticle modes are given by $\mathcal{N}_{BE}(k,T) = \{\exp[\epsilon_k/(k_B T)] - 1\}^{-1}$.

The use of the classical field (GPE) approach is justified, as it has been shown [16] that the noise and correlations in an atomic quasicondensate are dominated by thermal (classical) fluctuations under experimentally feasible conditions, and the observation of quantum noise is a challenging task that can be solved in particular regimes by means of involved experimental tools [17].

To integrate Eq. (1), we used the fourth-order time-splitting Fourier spectral method [18], which is rather similar to that used in Ref. [7].

We have found a set of examples of solutions of Eq. (1) that demonstrate quite a good degree of thermalization. Efficient thermalization has been observed in the cases of initial population of Bogoliubov modes within a certain momentum band around $k = 0$ [for simplicity, we assume $\mathcal{N}_0(k) = \mathcal{N}_0(-k)$], with the bandwidth being narrow enough to ensure the phononic nature of these excitations, $|k|\xi \lesssim 1$. In Fig. 1, we present our results of numerical integration of Eq. (1) for the initial conditions corresponding to the truncated classical distribution, parametrized by the effective temperature T_0 and the cutoff momentum $\hbar k_0$, i.e., for $\mathcal{N}_0(k)$ being equal to $k_B T_0/\epsilon_k$ for $|k| < k_0$ and zero otherwise. For the sake of convenience, in Fig. 1 we plot the mean energy per mode $E_k = \epsilon_k \mathcal{N}(k)$, which does not diverge at $k \to 0$, in contrast to the time-dependent population distribution $\mathcal{N}(k)$. Practically, E_k can be calculated by averaging over the ensemble of realizations the energy stored in the given mode:

$$E_k = \left\langle \frac{m}{2}\bar{n}|v_k|^2 + \left(\frac{\hbar^2 k^2}{8m\bar{n}} + \frac{g}{2}\right)|\delta n_k|^2 \right\rangle, \quad (3)$$

where δn_k and v_k are the Fourier transforms of the density $\delta n(x,t)$ and velocity $v(x,t) = (\hbar/m)\partial\phi/\partial x$ fluctuations.

Elementary excitations at different momenta are found to be uncorrelated for all propagation times, i.e., $\langle \delta n_{k'} \delta n_k^* \rangle = \langle|\delta n_k|^2\rangle \delta_{kk'}$ and $\langle v_{k'} v_k^* \rangle = \langle|v_k|^2\rangle \delta_{kk'}$, as expected for a thermal equilibrium state.
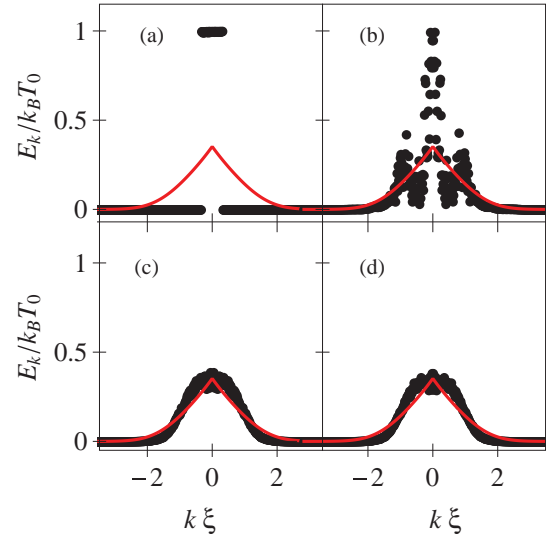

FIG. 1. (Color online) Dots: mean energy per mode (scaled to $k_B T_0$ with $k_B T_0 = 2g\bar{n}$) as the function of wave number k (scaled to ξ) for the dimensionless time $g\bar{n}t/\hbar =$ (a) 0, (b) 50, (c) 2850, and (d) 5750. The Lieb-Liniger parameter $\gamma = 5 \times 10^{-3}$, $k_0\xi = 0.33$. Solid line: mean energy per mode $\epsilon_k \mathcal{N}(k, T_{eq})$ for the equilibrium state, $T_{eq} = 0.35\,T_0$; see Eq. (4). The data are averaged over 200 realizations. Units on the axes in this figure and the subsequent figures are dimensionless.

The energy distribution approaches its equilibrium, which is quite close to the thermal Bose-Einstein distribution. The main difference is that the former is flat at $k \to 0$ and the latter has a cusp there. The equivalent temperature T_{eq} of the corresponding Bose-Einstein thermal distribution is determined from the energy conservation [19]:

$$\sum_{k \neq 0} \epsilon_k \mathcal{N}_0(k) = \sum_{k \neq 0} \epsilon_k \mathcal{N}_{BE}(k, T_{eq}). \quad (4)$$

Note that for a weakly interacting 1D system of ^{87}Rb atoms with the parameters as in Fig. 1 the time unit $\hbar/(g\bar{n}) \approx 0.1$ ms.

To check our numerical method, we performed the following tests. First, we checked the isospectrality of the (generalized) Lax operator of the inverse scattering problem [2,3]. We calculated the spectrum of the linear differential operator $\begin{pmatrix} i\partial/\partial\bar{x} & q \\ q^* & -i\partial/\partial\bar{x} \end{pmatrix}$, where $\bar{x} = x/\xi$ and $q = \bar{n}^{-1/2}\Psi(x,t)$, by substituting the numerically obtained solution for $\Psi(x,t)$ at different times and comparing the result to the spectrum that corresponds to the initial condition $\Psi(x,0)$. The spectrum of the Lax operator has been found to be time independent with a high accuracy. The maximum relative shift of an eigenvalue over more than 100 realizations was about 10^{-7} for a numerical grid consisting of 1024 points in x.

Then we checked the time independence of the numerical values of the integrals of motion of Eq. (1). The first three of them are (up to a numerical factor) the particle number, the total momentum, and the total energy of the system. Other integrals of motion can be calculated using the recurrent formula [2]. We found that they are conserved with high accuracy, with the relative error being of order of 10^{-11} for the first integral of

motion (the number of particles) and of order of 10^{-4} for the 15th integral of motion.

Following Ref. [10], we estimated the numerical error through the fidelity, defined as $\mathcal{F} = |1 - (\bar{n}L)^{-1} \int_0^L dx \, \Psi^*(x,0)\Psi_{\mathrm{fb}}(x,t,-t)|$, where $\Psi_{\mathrm{fb}}(x,t,-t)$ is the numerical solution of the GPE with the initial condition $\Psi(x,0)$ first propagated forward in time (up to time t) and then propagated backward over the same time interval. We obtained $\mathcal{F} \sim 10^{-8}$ for the propagation times t as long as $10^3 \, \hbar/(g\bar{n})$, which is sufficient for the establishment of equilibrium, with the spatial grid consisting of 512 points.

We found that our method converges if the grid contains more than 200 points for $L \approx 400\,\xi$. A coarse grid (about 100 points) yields a numerical artifact: any initial distributions rapidly smears out to the "classical-like" flat distribution of the energy over modes, i.e., to $E_k \approx$ const for all momenta $-\frac{\pi}{\Delta x} < k < \frac{\pi}{\Delta x}$ resolvable by the grid with the step Δx.

To quantify relaxation of the system toward its equilibrium, we introduce the measure

$$W = \frac{\sum_{k \neq 0} \{\epsilon_k [\mathcal{N}(k) - \mathcal{N}_{\mathrm{BE}}(k,T_{\mathrm{eq}})]\}^2}{\sum_{k \neq 0} [\epsilon_k \mathcal{N}_{\mathrm{BE}}(k,T_{\mathrm{eq}})]^2}, \tag{5}$$

which has a meaning of the normalized energy-weighted squared deviation of the quasiparticle distribution from the Bose-Einstein thermal equilibrium. For the parameters of Figs. 1 and 2, with $T_0 = 150$ nK, the thermalization time is $\tau_{\mathrm{eq}} \sim 20$ ms. If we change T_0 to 50 nK and $k_0\xi$ to 1, then τ_{eq} decreases by an order of magnitude. Note that the obtained thermalization time τ_{eq} is always shorter than the time needed for a sound wave to traverse the distance L. Therefore the thermalization observed in our simulations is a local physical effect, which is not related to specific boundary conditions. The thermalization time τ_{eq} should not be confused with the time $\tau_{\mathrm{d}} \sim m\lambda_T^2/\hbar$ [7], where $\lambda_T = 2\hbar^2\bar{n}/(mk_B T)$, of dephasing between two 1D quasicondensates initially prepared in thermal-like states with strongly mutually correlated fluctuations.
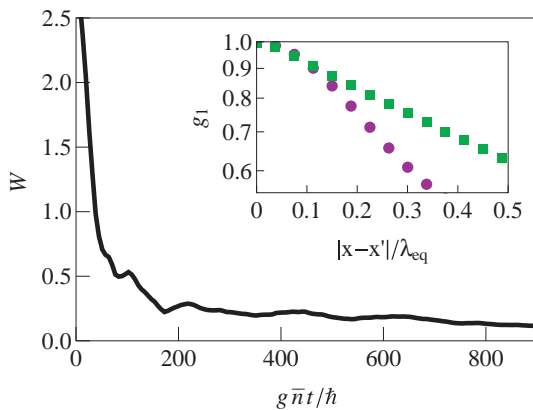

FIG. 2. (Color online) Numerically obtained energy-weighted squared deviation of the quasiparticle distribution from the Bose-Einstein thermal equilibrium as a function of time. The initial energy distribution and other parameters are the same as in Fig. 1(a). The inset shows the numerically calculated first-order correlation function $g_1(x - x')$ (shown on the logarithmic scale) for the dimensionless time $g\bar{n}t/\hbar = 0$ (circles) and 6000 (squares). The distance is scaled to λ_{eq}.
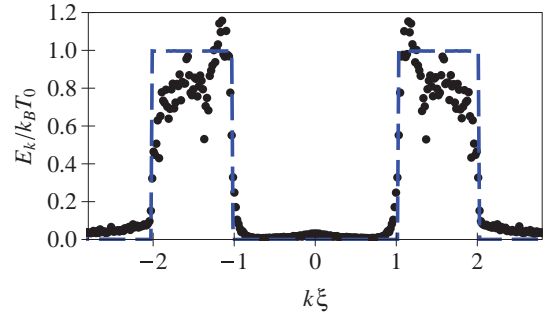

FIG. 3. (Color online) Dots: mean energy per mode (scaled to $k_B T_0$ with $k_B T_0 = 0.66 \, g\bar{n}$) as a function of wave number k (scaled to ξ) for the dimensionless time $g\bar{n}t/\hbar = 2 \times 10^4$, which is long enough to provide equilibration. The Lieb-Liniger parameter $\gamma = 5 \times 10^{-3}$, $k_1\xi = 1.0$, $k_2\xi = 2.0$. Note the closeness of the equilibrium states to the initial energy distribution (dashed line).

III. DISCUSSION AND CONCLUSIONS

Therefore we found numerically an example of the GPE solution that relaxes toward a state with practically measurable noise and correlation properties [20] well describable by a thermal Bose-Einstein ensemble of quasiparticles. As an illustration, in the inset in Fig. 2 we plot the numerically calculated first-order correlation function $g_1(x - x') = \langle \Psi^*(x',t)\Psi(x,t)\rangle/\bar{n}$ for $t = 0$ and for t large enough to provide equilibration [21]. We see that this correlation function finally approaches the exponential form $g_1(x - x') = \exp(-|x - x'|/\lambda_T)$, predicted for the thermal equilibrium [22], with $T \approx T_{\mathrm{eq}}$ [the distance in the inset in Fig. 3 is scaled to $\lambda_{\mathrm{eq}} = 2\hbar^2\bar{n}/(mk_B T_{\mathrm{eq}})$].

Not every initial distribution relaxes toward the Bose-Einstein thermal equilibrium. For example, if there are initially two oppositely propagating bunches of particle-like elementary excitations well separated in the momentum space, an equilibrium state very far from $\mathcal{N}_{\mathrm{BE}}(k,T_{\mathrm{eq}})$ is established, as seen from Fig. 3, where we assume $\epsilon_k\mathcal{N}_0(k)$ to be equal to $k_B T_0$ for $k_1 < |k| < k_2$ and zero otherwise ($k_1 \gtrsim \xi^{-1}$). This behavior can be viewed as a conspicuous example of relaxation toward the fully constrained equilibrium [13] in the weakly interacting case.

To elucidate the qualitative difference between the cases shown in Figs. 1 and 3, we calculate the time dependence of the distance $D^{(2)}[\psi_1, \psi_2] = (2\bar{n}L)^{-1} \int_0^L dx \, |\psi_1(x,t) - \psi_2(x,t)|^2$ between two solutions ψ_1, ψ_2 of the GPE, which are very close at $t = 0$. As we can see from Fig. 4, if phononic modes are initially populated, $D^{(2)}$ grows exponentially and saturates at the unity level (corresponding to the total loss of correlations at $t \to \infty$), thus signifying the chaotic regime. If only particle-like modes are initially populated, then $D^{(2)}$ grows very slowly and stays well below 1 at all experimentally relevant times (hence, the chaotic behavior is practically not observed in that case).

To conclude, we numerically observed thermalization in a 1D quasicondensate, i.e., in an ultracold atomic system described by the NLSE with a cubic repulsive nonlinearity, if only phononic modes are populated initially. The correctness of the numerical solution has been checked via the criteria of
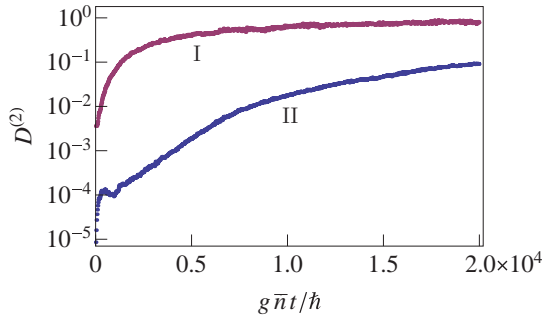
FIG. 4. (Color online) Distance $D^{(2)}[\psi_1, \psi_2]$ (on the logarithmic scale, dimensionless) as a function of scaled time for the parameters of Fig. 1 (I, upper curve) and Fig. 3 (II, lower curve).

the Lax operator isospectrality, conservation of the integrals of motion, and fidelity. Such a series of tests prevents the possible numerical artifacts that may occur in the split-step method [23]. Although the thermalization is not complete, experimentally measurable correlations are expected to be well described by the thermal equilibrium of bosonic elementary excitations. Our findings are in good agreement with the high efficiency of the evaporative cooling of ultracold atomic gases on the atom chips deeply in the 1D regime [4,5] (our work on numerical modeling of evaporative cooling of ultracold bosonic atoms in elongated traps is in progress). On the other hand, to provide full thermalization of nonequilibrium ensembles of particle-like excitations, like the one displayed in Fig. 3, we have to resort to the option of the integrability breakdown provided by the mechanism of effective three-body elastic collisions in one dimension [6].

[1] E. H. Lieb and W. Liniger, Phys. Rev. **130**, 1605 (1963); E. H. Lieb, *ibid.* **130**, 1616 (1963).

[2] V. E. Zakharov and A. B. Shabat, Zh. Eksp. Teor. Fiz. **64**, 1627 (1973) [Sov. Phys. JETP **37**, 823 (1973)].

[3] W. Eckhaus and A. van Harten, *The Inverse Scattering Transform and the Theory of Solitons* (North-Holland, Amsterdam, 1981); M. J. Ablowitz and P. A. Clarkson, *Solitons, Nonlinear Evolution Equations and Inverse Scattering* (Cambridge University Press, Cambridge, 1991).

[4] S. Hofferberth, I. Lesanovsky, B. Fischer, T. Schumm, and J. Schmiedmayer, Nature (London) **449**, 324 (2007).

[5] S. Hofferberth, I. Lesanovsky, T. Schumm, A. Imambekov, V. Gritsev, E. Demler, and J. Schmiedmayer, Nat. Phys. **4**, 489 (2008).

[6] I. E. Mazets, T. Schumm, and J. Schmiedmayer, Phys. Rev. Lett. **100**, 210403 (2008); I. E. Mazets and J. Schmiedmayer, New J. Phys. **12**, 055023 (2010); I. E. Mazets, Phys. Rev. A **83**, 043625 (2011).

[7] H.-P. Stimming, N. J. Mauser, J. Schmiedmayer, and I. E. Mazets, Phys. Rev. A **83**, 023618 (2011).

[8] B. Damski and W. H. Zurek, Phys. Rev. Lett. **104**, 160404 (2010); E. Witkowska, P. Deuar, M. Gajda, and K. Rzążewski, *ibid.* **106**, 135301 (2011).

[9] S. P. Cockburn, D. Gallucci, and N. P. Proukakis, Phys. Rev. A **84**, 023613 (2011).

[10] I. Březinová, L. A. Collins, K. Ludwig, B. I. Schneider, and J. Burgdörfer, Phys. Rev. A **83**, 043611 (2011).

[11] N. P. Proukakis, J. Schmiedmayer, and H. T. C. Stoof, Phys. Rev. A **73**, 053603 (2006).

[12] A. Nunnenkamp, J. N. Milstein, and K. Burnett, Phys. Rev. A **75**, 033604 (2007).

[13] M. Rigol, V. Dunjko, V. Yurovsky, and M. Olshanii, Phys. Rev. Lett. **98**, 050405 (2007).

[14] M. J. Steel, M. K. Olsen, L. I. Plimak, P. D. Drummond, S. M. Tan, M. J. Collett, D. F. Walls, and R. Graham, Phys. Rev. A **58**, 4824 (1998); A. Sinatra, C. Lobo, and Y. Castin, J. Phys. B **35**, 3599 (2002).

[15] In our simulations we neglect the fluctuations of β_k and always choose $\beta_k = \sqrt{\mathcal{N}_0(k)}$.

[16] H.-P. Stimming, N. J. Mauser, J. Schmiedmayer, and I. E. Mazets, Phys. Rev. Lett. **105**, 015301 (2010).

[17] J. Armijo, T. Jacqmin, K. V. Kheruntsyan, and I. Bouchoule, Phys. Rev. Lett. **105**, 230402 (2010).

[18] M. Thalhammer, M. Caliari, and C. Neuhauser, J. Comput. Phys. **228**, 3 (2009).

[19] T_{eq} is to be determined from Eq. (4) and not from $\sum_k \mathcal{N}_0 = \sum_k \mathcal{N}_{BE}$ since the total number of elementary excitations is not conserved.

[20] S. Manz *et al.*, Phys. Rev. A **81**, 031610(R) (2010); T. Betz *et al.*, Phys. Rev. Lett. **106**, 020407 (2011).

[21] The distribution of momenta of atoms (not to be confused with that of Bogoliubov quasiparticles) is given by the Fourier transform of g_1.

[22] V. N. Popov, *Functional Integrals and Collective Excitations* (Cambridge University Press, Cambridge, 1987); C. Mora and Y. Castin, Phys. Rev. A **67**, 053615 (2003).

[23] J. A. C. Weideman and B. M. Herbst, SIAM J. Numer. Anal. **23**, 485 (1986); T. I. Lakoba, Numer. Methods Partial Differ. Equations (2010).

Coherence and Josephson oscillations between two tunnel-coupled one-dimensional atomic quasicondensates at finite temperature

Pjotrs Grišins[1] and Igor E. Mazets[1,2]

[1]*Vienna Center for Quantum Science and Technology, Atominstitut, TU Wien, 1020 Vienna, Austria*
[2]*Ioffe Physico-Technical Institute, Russian Academy of Sciences, 194021 St. Petersburg, Russia*

We revisit the theory of tunnel-coupled atomic quasicondensates in double-well elongated traps at finite temperatures. Using the functional-integral approach, we calculate the relative-phase correlation function beyond the harmonic limit of small fluctuations of the relative phase and its conjugate relative-density variable. We show that the thermal fluctuations of the relative phase between the two quasicondensates decrease the frequency of Josephson oscillations and even wash out these oscillations for small values of the tunnel coupling.

I. INTRODUCTION

Systems of ultracold bosonic atoms in two parallel atomic waveguides mutually coupled via quantum tunneling (so-called extended bosonic Josephson junctions) have been a subject of intensive theoretical [1–7] and experimental [8] studies. The finite spatial extension of these systems provides much richer physics compared to the case of a pointlike bosonic Josephson junction [9]. The novel features arise due to the enhanced role of noise and correlations in low-dimensional ultracold atomic systems.

Before discussing the effects of tunneling, we recall the basic properties of a bosonic system in an isolated waveguide [10–12]. This system is effectively one-dimensional (1D) if the interaction energy per atom (we assume interatomic repulsion characterized by the effective 1D coupling strength $g > 0$) and the temperature are well below the spacing between the discrete energy levels of the potential of tight radial confinement. In this case quantum degeneracy does not lead to establishment of the long-range order; instead, atoms form a quasicondensate, i.e., a system describable by a macroscopic wave function with strong phase fluctuations. The characteristic length of the phase coherence in a quasicondensate at finite temperature T is $\lambda_T = 2\hbar^2 n_{1D}/(mk_B T)$, where m is the atomic mass and n_{1D} is the mean linear density of atoms [10] (we assume an infinite system; the thermodynamic limit implies constant $n_{1D} = N/L$, while both the atom number N and the quantization length L tend to infinity). The power-law decrease of the single-particle correlation function takes place only at $T = 0$.

If two waveguides are tunnel coupled, the system is described by the generalized Hamiltonian

$$\hat{H} = \int dz \left[\sum_{j=1}^{2} \left(\frac{\hbar^2}{2m} \frac{\partial \hat{\psi}_j^\dagger}{\partial z} \frac{\partial \hat{\psi}_j}{\partial z} + \frac{g}{2} \hat{\psi}_j^\dagger \hat{\psi}_j^\dagger \hat{\psi}_j \hat{\psi}_j - \mu \hat{\psi}_j^\dagger \hat{\psi}_j \right) \right.$$
$$\left. - \hbar J (\hat{\psi}_1^\dagger \hat{\psi}_2 + \hat{\psi}_2^\dagger \hat{\psi}_1) \right], \tag{1}$$

where $\hat{\psi}_j$ is the atomic annihilation operator for the jth waveguide ($j = 1,2$), $\mu = \hbar g n_{1D} - \hbar J$ is the chemical potential, and $2J$ is the tunnel splitting (in frequency units), i.e., the frequency interval between the two lowest eigenstates of the

radial trapping Hamiltonian (the antisymmetric and symmetric superpositions of the single-atom states localized in either $j = 1$ or $j = 2$ wells of the double-well Hamiltonian). In this case the situation changes qualitatively: the tunnel coupling mutually locks phase fluctuations in the two quasicondensates [1]. Phase locking (as we shall quantify in Sec. II) means that the distribution of the relative phase between the two quasicondensates becomes peaked around zero, while the local phase of an individual ($j = 1$ or 2) quasicondensate remains fully random (the phase-density representation for quasicondensates will be discussed in Sec. II). In the spatial correlation of the local relative phase between two quasicondensates a new length parameter appears [1,5]:

$$l_J = \sqrt{\hbar/(4mJ)}. \tag{2}$$

The length l_J sets the scale of restoration of the interwaveguide coherence due to finite tunnel-coupling strength J. The tunnel-coupling strength is usually estimated from the single-particle energy (kinetic and potential) and the overlap in the potential barrier region of the wave functions for a particle localized in the first and second waveguides. However, it is also possible to take into account atomic interactions (see Ref. [6] and references therein). Experimentally, the interwell coherence can be observed by releasing the two quasicondensates from the trap and measuring locally the contrast and the phase of their interference pattern after time of flight [13,14].

Up to now, only the theory based on linearization of the Hamiltonian (1) has been developed [1] and applied to the analysis of the experimental data [5,8]. Our work aims to develop a model of the steady-state thermal noise in tunnel-coupled quasicondensates beyond the harmonic approximation as well as to quantify the influence of the thermal noise to the macroscopic coherent dynamics of the system (Josephson oscillations).

Our paper is organized as follows. In Sec. II we summarize the harmonic approach of Ref. [1]. Section III is divided in two parts. In Sec. III A we calculate the static correlation properties of our system beyond the harmonic approximation using the transfer operator technique in the classical limit. The condition for negligibility of the quantum noise is also derived. Our way to model the equilibrium state by numerical simulation of the system's relaxation to the equilibrium after a quench is explained in Sec. III B. Section IV deals with the

noise-affected Josephson oscillations. We derive analytically the frequency of Josephson oscillations modified by the thermal noise in our extended system. We support our analysis by numerical simulations and also observe Josephson oscillations washing out as a result of thermal noise for low enough tunnel coupling. Section V contains our final remarks and conclusions. Explanations of the ways to derive the main equations of Secs. III and IV are presented in Appendices A and B, respectively.

II. HARMONIC APPROXIMATION

Following the standard procedure [11], we represent our atomic field operators through the phase $\hat{\theta}_j(z)$ and density $\hat{\rho}_j(z)$ operators, obeying the commutation relation $[\hat{\theta}_j(z), \hat{\rho}_{j'}(z')] = -i\delta(z - z')\delta_{jj'}$, as

$$\hat{\psi}_j(z) = \exp[i\hat{\theta}_j(z)]\sqrt{\hat{\rho}_j(z)}, \quad j = 1, 2. \quad (3)$$

A discussion of the way to introduce the phase operator for quasicondensates by coarse graining a lattice model on length scales containing sufficiently many atoms can be found in Ref. [11]. The density operator can be represented as $\hat{\rho}_j(z) = n_{1D} + \delta\hat{\rho}_j(z)$. Since for quantum gases with repulsive atomic interactions density fluctuations are suppressed, we can always consider the corresponding operator $\delta\hat{\rho}_j$ as a small correction. However, the same is not always true for the phase fluctuations.

Whitlock and Bouchoule [1] from the very beginning assumed the phase fluctuations to be small and thus linearized Hamiltonian (1), reducing it to $\hat{H} \approx \hat{H}_{\text{lin}}$,

$$\hat{H}_{\text{lin}} = \int dz \left[\frac{\hbar^2 n_{1D}}{m} \left(\frac{\partial \hat{\theta}_s}{\partial z} \right)^2 + \frac{\hbar^2}{16 m n_{1D}} \left(\frac{\partial \delta\hat{\rho}_s}{\partial z} \right)^2 \right.$$
$$+ \frac{g}{4} \delta\hat{\rho}_s^2 + \frac{\hbar^2 n_{1D}}{4m} \left(\frac{\partial \hat{\theta}_a}{\partial z} \right)^2 + \frac{\hbar^2}{4 m n_{1D}} \left(\frac{\partial \delta\hat{\rho}_a}{\partial z} \right)^2$$
$$\left. + g \, \delta\hat{\rho}_a^2 + \hbar J n_{1D} \hat{\theta}_a^2 \right]. \quad (4)$$

Here the symmetric (s) and antisymmetric (a) variables are introduced via canonical transformation,

$$\delta\hat{\rho}_s(z) = \delta\hat{\rho}_1(z) + \delta\hat{\rho}_2(z), \quad \hat{\theta}_s(z) = [\hat{\theta}_1(z) + \hat{\theta}_2(z)]/2,$$
$$\delta\hat{\rho}_a(z) = [\delta\hat{\rho}_1(z) - \delta\hat{\rho}_2(z)]/2, \quad \hat{\theta}_a(z) = \hat{\theta}_1(z) - \hat{\theta}_2(z).$$

Diagonalization of the Hamiltonian (4) is based on the Fourier transform $\delta\hat{\rho}_{s(a)}(z) = L^{-1/2} \sum_{k \neq 0} \delta\hat{\rho}_{s(a),k} e^{ikz}$, $\hat{\theta}_{s(a)}(z) = L^{-1/2} \sum_{k \neq 0} \hat{\theta}_{s(a),k} e^{ikz}$. The frequencies $\omega_{s(a)}(k)$ of the symmetric and antisymmetric modes with the momentum $\hbar k$ are given by the dispersion relations

$$\omega_s^2(k) = \frac{\hbar k^2}{2m} \left(\frac{\hbar k^2}{2m} + \frac{2g n_{1D}}{\hbar} \right), \quad (5)$$

$$\omega_a^2(k) = \left(\frac{\hbar k^2}{2m} + 2J \right) \left(\frac{\hbar k^2}{2m} + 2J + \frac{2g n_{1D}}{\hbar} \right). \quad (6)$$

Correlations in two tunnel-coupled quasicondensates are experimentally accessible via the two-point correlation function $g_2^a(z - z') = n_{1D}^{-2} \langle : \hat{\psi}_1^\dagger(z)\hat{\psi}_2^\dagger(z')\hat{\psi}_2(z)\hat{\psi}_1(z') : \rangle$. Since the system described by Hamiltonian (1) is translationally invariant, g_2^a depends only on the difference of the two coordinates. The symbol $\langle : \hat{O} : \rangle$ denotes the average of the normal ordered

(with respect to the atomic operators $\hat{\psi}_j$, $\hat{\psi}_j^\dagger$) form of the operator $\hat{O}$. In what follows, we omit the normal ordering notation, thus neglecting the atomic shot noise.

Since the density fluctuations for $|k| \lesssim \xi^{-1}$, with $\xi = \hbar/\sqrt{mg n_{1D}} = \hbar/(mc)$ being the healing length, are suppressed by the atomic repulsion [10,11], the main contribution to this correlation function is given by the phase fluctuations, $g_2^a(z - z') \approx \langle \exp[i\hat{\theta}_a(z') - i\hat{\theta}_a(z)] \rangle$. The experimentally accessible length scale cannot be shorter than the optical resolution length Δz_{opt}. On this scale the shot noise yields the quantum uncertainty of the relative phase, coarse grained over the distance Δz_{opt}, of the order of $1/\sqrt{2n_{1D}\Delta z_{\text{opt}}}$. For $\Delta z_{\text{opt}} \gtrsim 3 \ \mu\text{m}$ and $n_{1D} \gtrsim 30 \ \mu\text{m}^{-1}$ the shot-noise-induced phase uncertainty does not exceed 0.075 rad. This relatively small value can always be kept in mind when comparing theoretical predictions to measurement results. However, for the sake of simplicity, in what follows we assume $\langle : \exp[i\hat{\theta}_a(z') - i\hat{\theta}_a(z)] : \rangle \approx \langle \exp[i\hat{\theta}_a(z') - i\hat{\theta}_a(z)] \rangle$ and so on.

Another point related to the use of the fully classical approximation is the substitution of the Bose-Einstein statistics of the elementary excitations by its classical limit,

$$\frac{1}{\exp[\hbar\omega_a(k)/(k_B T)] - 1} \approx \frac{k_B T}{\hbar\omega_a(k)}. \quad (7)$$

One obtains strong deviations from Eq. (7) for $\hbar\omega_a(k) \gtrsim k_B T$, which corresponds, under typical experimental conditions, to the range of wave lengths shorter than Δz_{opt}, i.e., not resolvable optically. These considerations justify our method based on genuinely classical statistics.

In the harmonic approximations fluctuations are Gaussian; hence, $\langle \exp[i\hat{\theta}_a(z') - i\hat{\theta}_a(z)] \rangle = \exp\{-\frac{1}{2}\langle [\hat{\theta}_a(z') - \hat{\theta}_a(z)]^2 \rangle\}$. Expressing $\hat{\theta}_a$ through creation and annihilation operators of the elementary excitations and calculating thermal populations of the elementary modes using Eq. (7), Whitlock and Bouchoule obtained [1]

$$\langle \exp[i\hat{\theta}_a(z') - i\hat{\theta}_a(z)] \rangle = \exp\left[-\frac{2l_J}{\lambda_T}(1 - e^{-|z-z'|/l_J}) \right]. \quad (8)$$

From this expression we can see that tunnel coupling locks the relative phase between two quasicondensates. This locking means that the relative-phase correlation function (8) does not decrease to zero but even at $|z - z'| \to \infty$ has a finite value, corresponding to $\langle \hat{\theta}_a^2(z) \rangle = 2l_J/\lambda_T$. On the contrary, the phase correlations in each of the waveguides are $\langle \exp[i\hat{\theta}_j(z') - i\hat{\theta}_j(z)] \rangle = \langle \exp\{i[\hat{\theta}_s(z') \pm \frac{1}{2}\hat{\theta}_a(z') - \hat{\theta}_s(z) \mp \frac{1}{2}\hat{\theta}_a(z)]\} \rangle$, with the upper and lower signs corresponding to $j = 1$ and $j = 2$, respectively. We can evaluate them using the statistical independence of noise in the symmetric and antisymmetric modes. The result

$$\langle \exp[i\hat{\theta}_j(z') - i\hat{\theta}_j(z)] \rangle$$
$$= \exp\left\{ -\frac{1}{2}\langle [\hat{\theta}_s(z') - \hat{\theta}_s(z)]^2 \rangle - \frac{1}{8}\langle [\hat{\theta}_a(z') - \hat{\theta}_a(z)]^2 \rangle \right\}$$
$$= \exp\left[-\frac{|z - z'|}{2\lambda_T} - \frac{l_J}{2\lambda_T}(1 - e^{-|z-z'|/l_J}) \right] \quad (9)$$

decreases $\propto \exp[-|z - z'|/(2\lambda_T)]$ at $|z - z'| \to \infty$ because of the unlimited growth of the fluctuations of the symmetric component of the phase along the z direction. The correlation

properties of the symmetric mode can be experimentally measured using the density-density correlations of the ultracold gas in a time-of-flight experiment [15]; however, this subject is beyond the scope of our present paper.

The phase locking of the relative phase becomes most apparent if we treat the evolution of the relative phase along z in the harmonic approximation as the Ornstein-Uhlenbeck stochastic process [5]: while thermal excitations result in the relative phase diffusion, with the diffusion coefficient proportional to λ_T^{-1}, the tunnel coupling gives rise to the "friction" force that tends to restore a small (ultimately zero) local phase difference between the two quasicondensates.

III. CORRELATION FUNCTIONS AND THE INTERWELL COHERENCE BEYOND THE HARMONIC APPROXIMATION

A. Equilibrium theory

In the present work we make a step further with respect to the theory of Ref. [1] and abandon the assumption of small phase fluctuations (but still consider small density fluctuations, which is a reasonable approximation for quasicondensates with repulsive interactions). We evaluate the partition function [10]

$$Z = \int \mathcal{D}\delta\rho_s \int \mathcal{D}\theta_s \int \mathcal{D}\delta\rho_a \int \mathcal{D}\theta_a \, \exp[-H/(k_B T)], \quad (10)$$

where

$$H = \int dz \left[\frac{\hbar^2 n_{1D}}{m} \left(\frac{\partial \theta_s}{\partial z} \right)^2 + \frac{g}{4}\delta\rho_s^2 + \frac{\hbar^2 n_{1D}}{4m} \left(\frac{\partial \theta_a}{\partial z} \right)^2 \right.$$
$$\left. + g\,\delta\rho_a^2 + 2\hbar J n_{1D}(1 - \cos\theta_a) \right] \quad (11)$$

is Hamiltonian (1) expressed through the classical fields $\delta\rho_{s,a}$, $\theta_{s,a}$ (in the coordinate representation), over which the functional integrals are taken. For the sake of simplicity, we write Hamiltonian (11) in the phononic limit, where the fluctuation wavelengths are long compared to the healing length of the quasicondensate and Eqs. (5) and (6) are reduced to $\omega_s^2(k) \approx c^2 k^2$ and $\omega_a^2(k) \approx c^2 k^2 + 4Jgn_{1D}/\hbar$, where $c = \sqrt{gn_{1D}/m}$ is the speed of sound. Of course, the phase-density description can be extended into the short-wavelength excitation range [10,11], bringing about the Hamiltonian terms $\propto(\partial\delta\rho_{s,a}/\partial z)^2$ and thus revealing the full Bogoliubov-like spectra (5) and (6). However, we are not interested in the short-wavelength limit since the respective length scales cannot be resolved by optical imaging systems [8,13,14]. The system's description by Eq. (11) is fully consistent with Haldane's bosonization method [16]. The relative phase θ_a is accessible through interference patterns observed in time-of-flight experiments [8,13,14]. We develop here the way to evaluate its correlation properties. Since the density fluctuations are small, we can decouple symmetric and antisymmetric modes [17] and integrate out the variables of the symmetric mode. The absence of cross terms containing both $\delta\rho_a$ and θ_a in Eq. (11) allows us to integrate out $\delta\rho_a$ as well and to obtain, as an intermediate

result, the partition function in the form

$$Z = \text{const} \int \mathcal{D}\theta_a \exp\left\{ -\int dz \left[\frac{\hbar^2 n_{1D}}{4mk_B T} \left(\frac{\partial \theta_a}{\partial z} \right)^2 \right. \right.$$
$$\left. \left. + \frac{2\hbar J n_{1D}}{k_B T}(1 - \cos\theta_a) \right] \right\} \quad (12)$$

that was considered long ago [18,19] in the context of the statistical mechanics of systems describable by the sine-Gordon equation, which is known to adequately account for the low-energy physics of tunnel-coupled 1D ultracold atomic systems [17].

Note that anharmonic Hamiltonian terms, which depend on the density fluctuations neglected in our present theory, do not affect much the static properties of the quasicondensate [11]. One needs to take them into account in the analysis [20] of a slow process of the system's relaxation towards equilibrium starting from a nonequilibrium, prethermalized initial state [21], characterized by two different temperatures T_+ and $T_- \ll T_+$ for the symmetric and antisymmetric modes, respectively.

The applicability range of our fully classical approach can be determined as follows. Consider, for the sake of simplicity, distances shorter than l_J. The effects of tunnel coupling can be neglected at such short length scales, and the fully classical correlation function can be estimated [1] as $\langle \exp[i\theta_a(z') - i\theta_a(z)] \rangle \approx \exp(-2|z - z'|/\lambda_T)$. We have to compare this result to the power-law decay of correlations due to *quantum* effects, which is obtained in the limit $T \to 0$ [10,11]. Neglecting, as done previously, the contribution of the density fluctuations, we can write $\lim_{T\to 0}\langle \exp[i\hat{\theta}_a(z') - i\hat{\theta}_a(z)] \rangle \approx \lim_{T\to 0}\langle \hat{\psi}_1^\dagger(z')\hat{\psi}_1(z) \rangle \langle \hat{\psi}_2^\dagger(z)\hat{\psi}_2(z') \rangle$ and, finally,

$$\lim_{T\to 0}\langle \exp[i\hat{\theta}_a(z') - i\hat{\theta}_a(z)] \rangle \approx \left(\frac{\Lambda_{UV}}{|z - z'|} \right)^{1/\mathcal{K}}, \quad (13)$$

where the quantum-mechanical average over the ground state is taken, $\mathcal{K} = \pi\hbar\sqrt{n_{1D}/(mg)}$ is the Luttinger liquid parameter (for quasicondensates, which are weakly interacting systems, $\mathcal{K} \gg 1$), and Λ_{UV} is the ultraviolet cutoff of the theory. Equation (13) is valid if

$$|z - z'| \gg \Lambda_{UV}. \quad (14)$$

The estimation by Popov [22] yields $\Lambda_{UV} \sim \xi$.

We can fully neglect quantum fluctuations if their contribution to the decay of correlations is small compared to the contribution of the thermal noise on a given length scale. The correlation decay is dominated by the thermal noise if the classical formula $\exp(-2|z - z'|/\lambda_T)$ yields stronger decay of correlations than the quantum limit (14), i.e., if

$$2|z - z'|/\lambda_T \gtrsim \mathcal{K}^{-1}\ln(|z - z'|/\xi). \quad (15)$$

The experimentally relevant range of $|z - z'|$ is bound from below by Δz_{opt}, as we discussed in Sec. II, and $\Delta z_{opt} \gg \xi$ in a typical experiment [8]. Therefore the use of the fully classical approach is reasonable for

$$k_B T \gtrsim mc^2 \frac{\xi \ln(\Delta z_{opt}/\xi)}{\pi \Delta z_{opt}}. \quad (16)$$

We can evaluate the partition function (12) using the transfer operator technique [18,19,23]. First of all, we evaluate the

phase-correlation function as (see Appendix A for the sketch of derivation)

$$\langle \exp[i\theta_a(z') - i\theta_a(z)] \rangle$$
$$= \sum_{n=0}^{\infty} |\langle n|e^{i\theta}|0\rangle|^2 \exp[-(\epsilon_n - \epsilon_0)|z - z'|], \quad (17)$$

where

$$\langle n|e^{i\theta}|0\rangle = \int_{-\pi}^{\pi} d\theta \ \Psi_n^*(\theta) e^{i\theta} \Psi_0(\theta), \quad (18)$$

$\Psi_n(\theta)$ is the eigenfunction (normalized to 1) of the auxiliary Schrödinger-type equation,

$$\left[-\frac{2}{\lambda_T} \frac{\partial^2}{\partial \theta^2} - \frac{\lambda_T}{4l_J^2}(\cos\theta - 1) \right] \Psi_n(\theta) = \epsilon_n \Psi_n(\theta), \quad (19)$$

and ϵ_n, $n = 0,1,2,\ldots$ is the respective eigenvalue. For simplicity, we set periodic (and not quasiperiodic) boundary conditions to Eq. (19) with the period 2π, thus neglecting the band structure of its spectrum, since the zero-quasimomentum solutions define all the system properties [19] which are relevant to our present work.

In the limit of strong tunnel coupling, $l_J \ll \lambda_T$, the operator on the left-hand-side of Eq. (19) can be approximated by the harmonic oscillator Hamiltonian (in proper units), and $\epsilon_n = l_J^{-1}(n + \frac{1}{2})$, $n = 0,1,2,\ldots$ In this limit Eq. (17) reproduces the result [Eq. (8)] that holds for small phase fluctuations.

In the opposite limit, Eq. (19) can be solved perturbatively, and we obtain

$$\langle \exp[i\theta_a(z') - i\theta_a(z)] \rangle$$
$$\approx \left(\frac{\lambda_T^2}{8l_J^2} \right)^2 + \left[1 - \left(\frac{\lambda_T^2}{8l_J^2} \right)^2 \right] \exp\left(-\frac{2|z - z'|}{\lambda_T} \right),$$
$$l_J \gg \lambda_T. \quad (20)$$

In what follows, we will be interested in calculating the value of

$$\langle \cos\theta_a \rangle = \langle 0| \cos\theta |0\rangle, \quad (21)$$

which can be viewed as the mean interwell coherence. This expression can be derived in different ways, e.g., from Eq. (17) by employing the statistical independence of phase fluctuations at two very distant points, $|z - z'| \to \infty$, and recalling that $\langle \sin\hat{\theta}_a \rangle = 0$. In a general case, Eq. (21) can be evaluated from the lowest-energy solution of the Mathieu equation [24]. In the two limiting cases we obtain the asymptotics

$$\langle \cos\theta_a \rangle \approx \begin{cases} \exp(-l_J/\lambda_T), & l_J \ll \lambda_T, \\ \lambda_T^2/(8l_J^2), & l_J \gg \lambda_T. \end{cases} \quad (22)$$

A possible physical explanation of the fact that the mean interwell coherence decreases at $l_J/\lambda_T \to \infty$ much slower than the harmonic approximation [1] predicts is the large probability of thermal excitation of a soliton in this limit. Each emerging soliton decreases the number of phononic states by 1 [19], and the phononic density of states is reduced mostly in the long-wavelength range (for phonon momenta less than or of the order of $\hbar/l_J$), which gives the main contribution to the long-distance behavior of the correlation function (17) and hence to $\langle \cos\theta_a \rangle$.

B. Relaxation to the equilibrium after a quench

The results of Sec. III A are obtained at the equilibrium. However, it is interesting to investigate also the process of equilibration in the system of two 1D quasicondensates after a quench. The study of this dynamical problem is motivated by our recent numerical results [25] related to thermalization in a single 1D quasicondensate. In Ref. [25] we found that, despite the numerically confirmed integrability of the system, phononic (low-momentum) modes rapidly relaxed from their initial nonequilibrium state towards a final equilibrium state; particle-like (large-momentum) excitations, on the contrary, exhibited almost no relaxation. The equilibrium ensemble of phonons was different from the classical limit of equipartition of the thermal energy between all the degrees of freedom and was quite close to the Bose-Einstein distribution with the temperature T_{eff} determined by the total excitation energy of the initial nonequilibrium state. Observed fluctuations around this equilibrium state were due to the finite size of the system inherent in numerical modeling. Remarkably, the correlations observed at the length scales, which are large compared to the healing length, as well as to the wavelength of an elementary excitation with the energy equal to $k_B T_{\text{eff}}$, were well described by classical expressions. Note that the main contribution to the noise on these length scales stems from the low-energy excitations, which approximately exhibit classical equipartition of energy.

The need to extend the numerical approach of Ref. [25] to tunnel-coupled 1D quasicondensates can also be seen from the following considerations. Our aim is to numerically check the theoretically predicted correlations of two tunnel-coupled quasicondensates at equilibrium. This equilibrium state can be viewed as a result of the system's relaxation from its initial nonequilibrium state. Moreover, the available analytic theory predicts only averages; unlike the case of harmonic approximation, there is no way yet to generate individual realizations of the phase, obeying the necessary statistics, without simulating numerically the equilibration process. The most obvious way to obtain numerically the equilibrium solution is to observe the numerical relaxation after a quench and wait until a steady-state regime establishes. The particular type of the quench and the corresponding initial conditions are, up to a certain degree, arbitrary, as long as the system exhibits true relaxational dynamics.

Motivated by these considerations, we performed numerical modeling of the thermal equilibrium values of $\langle \cos\hat{\theta}_a \rangle$ after the dynamical process of relaxation in our system after a quench. We simulated the time evolution of two coupled Gross-Pitaevskii equations using the split-step method [26] previously used by us [25] to simulate the dynamics of a single quasicondensate and now extended it to the case of tunnel-coupled systems. As the initial conditions we took two independent quasicondensates with phonon modes populated randomly according to the Bose-Einstein thermal distribution. At $t = 0$ we quenched the system by switching on the tunnel coupling between them. We solved this coupled system for a time long enough to provide equilibration.

To juxtapose the input parameters of our numerical simulations to typical parameters of modern atom-chip experiments [8,13,14], we give the system parameters used in our simulations first in dimensional units but later show them also

in dimensionless form. The linear density for a single quasicondensate $n_{1D} = 30 \ \mu m^{-1}$ and interaction constant $g = 2\hbar\omega_\perp a_s$ with radial trapping frequency $\omega_\perp = 2\pi \times 3$ kHz and s-wave scattering length $a_s = 5.3$ nm for ^{87}Rb yields the healing length $\xi \approx 0.35 \ \mu m$ and the Luttinger liquid parameter $\mathcal{K} \approx 33$. The periodic boundary conditions were set at an interval of the length $L = 100 \ \mu m \approx 290 \xi$. The maximum integration time was $t_{max} = 0.8$ s. After a few hundred milliseconds, some kind of equilibrium was obtained. The total energy of the system was conserved in our numerical simulations with good ($\sim 10^{-3}$) accuracy; however, it was constantly redistributed in an oscillatory manner between different low-frequency elementary modes, including Josephson oscillations. The nonlinear interaction between different modes (see Sec. IV) led to excitation of Josephson oscillations of the total number imbalance $(N_1 - N_2)/2$, where N_j is the integral of the density in the jth quasicondensate over the whole length L, i.e., the number of atoms in this quasicondensate, $N_1 + N_2 \equiv 2N$. In general, the numerical stability of our split-step method was controlled using the criteria of Ref. [27]. The thermal coherence length was determined from the phase-correlation functions for each of the two quasicondensates taken *separately* by comparison of the numerically obtained value of $\langle \exp[i\theta_j(z) - i\theta_j(z')]\rangle$, $j = 1,2$, with its theoretical value $\exp(-|z - z'|/\lambda_T)$ for $|z - z'| \lesssim l_J$ [10,11] (if we trace out the phase and density variables of one of the two tunnel-coupled quasicondensates, the properties of its remaining counterpart will be described by the same temperature as of the whole system at equilibrium). The averaging is performed over statistically uncorrelated (separated by sufficiently large distances) intervals of the whole length L for $|z - z'| \lesssim \lambda_T$. We never obtain complete equilibration. In each realization, the correlation length λ_T obtained in such a way oscillates around a certain mean value and so does the value of $\langle \cos \theta_a \rangle$ (averaged over the length L). Typically, $\lambda_T \approx 8 \ \mu m$, which corresponds to $T \approx 40$ nK.

We present the results of our numerical simulations in Fig. 1. Dots represent mean values of $\langle \cos \theta_a \rangle$ obtained by

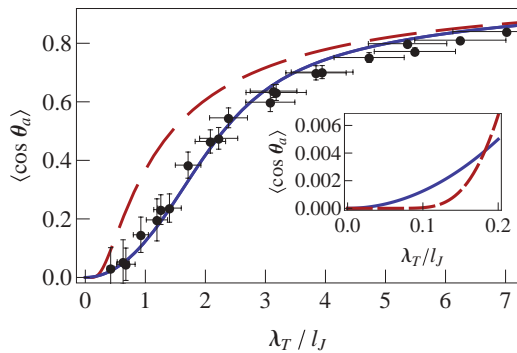FIG. 1. (Color online) Mean interwell contrast as a function of the ratio of the length scales λ_T and l_J. Solid line: exact theory given by Eq. (21). Dashed line: small-fluctuation approximation $\langle \cos \theta_a \rangle = \exp(-l_J/\lambda_T)$ following from the linearized theory [1]. Dots: results of the numerical simulations of the equilibration dynamics of two coupled condensates. Units on the axes are dimensionless. Inset: Magnified part of the main plot for small λ_T/l_J, illustrating the high-temperature asymptotics of Eq. (21) in comparison to the linearized theory result.

averaging over both the time (on the quasiequilibration stage of the system evolution) and the ensemble of realizations. The error bars in Fig. 1 show the standard deviations of $\langle \cos \theta_a \rangle$ and λ_T. These error bars indicate slow, quasiperiodic variations of $\langle \cos \theta_a \rangle$ and λ_T detected in our simulations. The range of λ_T/l_J shown in Fig. 1 corresponds to J increasing from $2\pi \times 0.1$ up to $2\pi \times 8$ Hz.

To summarize the results of the present section, we can state that we developed a theory describing the static correlation properties more precisely than the harmonic model [1]. Our approach is based on consideration of the classical partition function for the antisymmetric mode of our problem (describable by the sine-Gordon model) and application of the well-known transfer operator technique [18,19]. As one can see from Fig. 1, the difference between our results and those of Ref. [1] is most apparent for intermediate and small values of λ_T/l_J (intermediate and weak tunnel coupling).

IV. JOSEPHSON OSCILLATIONS IN A NOISY EXTENDED JUNCTION

The thermal noise effects considered in Sec. III reduce the frequency of Josephson oscillations. Consider the absolute number imbalance between two wells, $N_{12} \equiv (N_1 - N_2)/2$, and its canonically conjugate variable, the overall phase difference Φ between two quasicondensates. In the limit of the atomic repulsion energy dominating over the tunneling, $gn_{1D} \equiv gN/L \gg \hbar J$, and for small-amplitude oscillations, $|N_1 - N_2| \ll N$, the evolution of these "global" variables is described by the set of equations (see Appendix B)

$$\frac{d}{dt}\Phi = -\frac{2gN_{12}}{L\hbar}, \tag{23}$$

$$\frac{d}{dt}N_{12} = 2Jn_{1D}\int_0^L dz \ \sin\theta_a, \tag{24}$$

which is reduced, after elimination of the number-difference variable, to

$$\frac{d^2}{dt^2}\Phi = -\omega_{J0}^2 \frac{1}{L}\int_0^L dz \ \sin\theta_a, \tag{25}$$

where

$$\omega_{J0} = \sqrt{4Jgn_{1D}/\hbar} \tag{26}$$

is the frequency of the Josephson oscillations for bosonic junction unaffected by thermal noise. At zero temperature, when the thermal noise is absent, and for $\ln(L/\xi) \ll \mathcal{K}$, when the quantum noise can be neglected, spatial extension of the ultracold atomic Josephson junction plays no role, and we can derive Eq. (26) from the results of Ref. [9]. In the case of small-amplitude Josephson oscillations, the statistical properties of $\cos\theta_a$ and $\cos(\theta_a - \Phi)$ do not differ significantly, in particular, $\langle \cos\theta_a \rangle \approx \langle \cos(\theta_a - \Phi) \rangle$, i.e., the quadratic in Φ correction is negligible, and Eq. (25) reduces to

$$\frac{d^2}{dt^2}\Phi + [\omega_J^2 + \delta\omega_J^2(t)]\Phi = \zeta(t), \tag{27}$$

where

$$\omega_J^2 = \omega_{J0}^2 \langle \cos\theta_a \rangle. \tag{28}$$

In Eq. (27) we explicitly indicate the time argument of the random driving force

$$\zeta(t) = \omega_{J0}^2 \frac{1}{L} \int_0^L dz \, \sin(\theta_a - \Phi) \tag{29}$$

and the term

$$\delta\omega_J^2(t) = \omega_{J0}^2 \frac{1}{L} \int_0^L dz \, (\cos\theta_a - \langle\cos\theta_a\rangle) \tag{30}$$

that describes fluctuations of the oscillation frequency due to the noise of θ_a caused by excitations with nonzero momenta.

If we prepare some appreciable initial imbalance at $t = 0$, we obtain, to the first approximation, free Josephson oscillations governed by the equation $d^2\Phi/dt^2 + \omega_J^2\Phi = 0$, i.e., with the frequency reduced by $\sqrt{\langle\cos\theta_a\rangle}$ compared to the noise-free case of Eq. (26). The presence of the noise broadens the power spectrum of Josephson oscillations

$$S(\omega) = \left| \frac{1}{\tau} \int_{t_{max}-\tau}^{t_{max}} dt \, e^{i\omega t} \eta(t) \right|^2, \tag{31}$$

where $\eta = (N_1 - N_2)/(2N)$ is the relative number imbalance. The integration in Eq. (31) is taken over the time interval τ when the system has already reached its near-equilibrium state (typically, $\tau \approx 0.65$ s). If ω_J is high enough, the theory [28] predicts $S(\omega)$ to be a peaked function, centered at ω_J and having the half width at the half maximum of the peak height $\gamma = [\hbar L/(8gk_BT)] \, \text{Re} \int_0^\infty dt' \langle\zeta(t)\zeta(t+t')\rangle \exp(i\omega_J t')$. The latter expression, roughly evaluated as $\gamma \sim \frac{\pi}{8}k_BT/(\hbar\mathcal{K}\langle\cos\theta_a\rangle^2)$, correctly describes the order of magnitude of the bandwidth $\Delta\omega/(2\pi) \sim 10$ Hz of the numerically obtained spectra $S(\omega)$.

The presence of the random driving force is the source of excitation of Josephson oscillations in the course of the system's evolution, even if initially at $t = 0$, $\Phi = 0$, and $\eta \propto \frac{d}{dt}\Phi = 0$. Note that all the elementary excitations with nonzero momenta in the antisymmetric mode have frequencies larger than ω_J. The energy transfer between nonzero-momentum excitations and the Josephson mode is thus an essentially nonlinear process. The nonlinear structure of the right-hand side of Eq. (29) provides the presence of the frequency ω_J in the spectrum $\int_{-\infty}^\infty dt' \langle\zeta(t)\zeta(t+t')\rangle \exp(i\omega t')$ of the driving force and thus ensures the parametric excitation of the Josephson oscillations.

We confirmed our analytic estimations by the numerical simulations of two coupled 1D Gross-Pitaevskii equations already described in Sec. III B. An example of a sharp-peaked power spectrum of relative number imbalance is given in Fig. 2, together with an example of time dependence of η. If, on the contrary, $\omega_J \ll \omega_T$, where $\omega_T = 2c/\lambda_T$ is the typical time scale of fluctuations of $\zeta(t)$, then the behavior of $\eta(t)$ becomes irregular, and $S(\omega)$ does not exhibit a peak at $\omega \approx \omega_J$ any more (see Fig. 3).

The results of numerical simulations shown in Figs. 2 and 3 demonstrate a certain energy exchange, but no full equilibration between the Josephson oscillations and phononic modes. If we set $\Phi|_{t=0} = 0$ and $\eta|_{t=0} = 0$ for $J/(2\pi) = 8$ Hz (0.1 Hz), then at times t between 650 ms and 1 s the mean energy of Josephson oscillations is an order of magnitude (1.5 orders of magnitude) less than k_BT, where temperature T is determined from the phase-correlation function for a single quasicondensate and is thus associated with the phononic
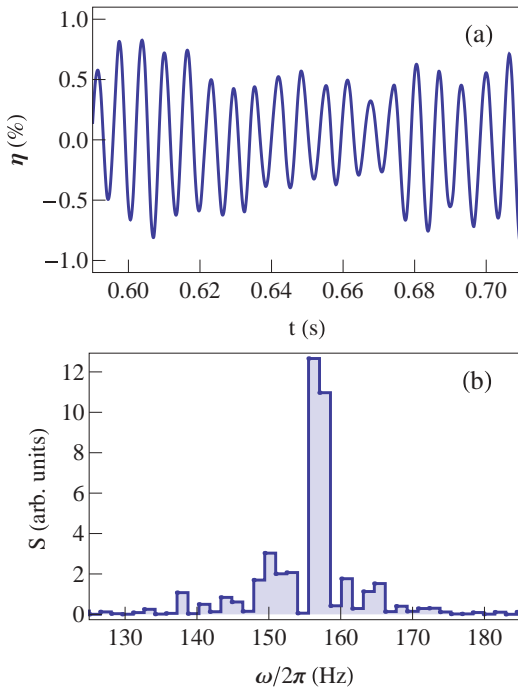

FIG. 2. (Color online) Josephson oscillations for $J = 2\pi \times 8$ Hz (for other system parameters see Sec. III). (a) The relative imbalance as a function of time. (b) The power spectrum of the atom-number imbalance (averaged over seven realizations), peaked at theoretically predicted $\omega_J/(2\pi) = 157$ Hz and broadened by thermal fluctuations.
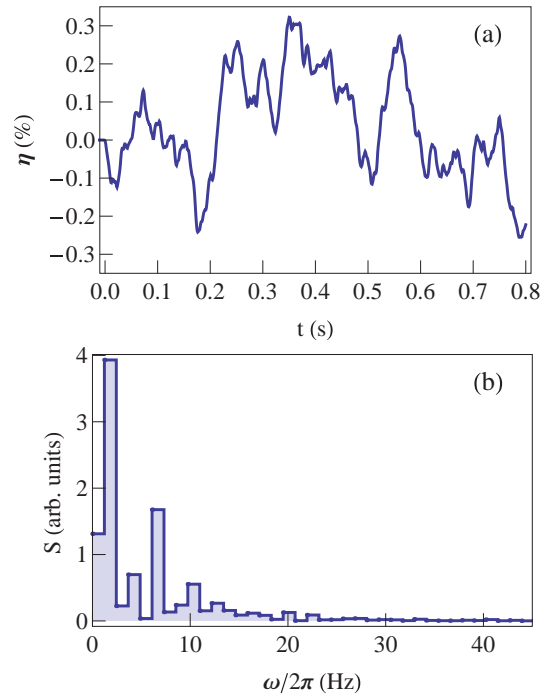

FIG. 3. (Color online) The same as in Fig. 2, but for $J = 2\pi \times 0.1$ Hz (irregular behavior). The spectral peak at theoretically predicted $\omega_J/(2\pi) = 6.5$ Hz is smeared out. $S \neq 0$ at $\omega = 0$ due to finite integration time.
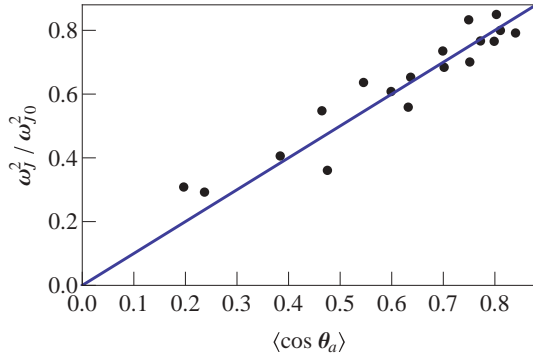
FIG. 4. (Color online) The square of the frequency of numerically obtained Josephson oscillations (normalized to its value ω_{J0}^2 for zero thermal noise) as a function of the mean interwell coherence $\langle \cos \theta_a \rangle$ (dots) and theoretical prediction given by Eq. (28) (straight line). Units on the axes are dimensionless.

modes. This may indicate an extremely long thermalization time for Josephson oscillations.

We selected our simulations that display a pronounced narrow peak of $S(\omega)$ far from zero frequency (which was the case for $J > 2\pi \times 0.7$ Hz), estimated the Josephson frequency ω_J, and analyzed the dependence of ω_J^2 on the mean interwell coherence. The resulting values are in good agreement with our theoretical prediction given by Eq. (28), as can be seen from Fig. 4.

V. CONCLUSION

To conclude, we applied the transfer operator technique to evaluate coherence and correlation properties of two tunnel-coupled 1D weakly interacting, ultracold systems (quasicondensates) of bosonic atoms. These properties are determined by the ratio of the two length scales: λ_T, which describes the spatial scale of the loss of correlations between two points, and l_J, which describes the scale for the phase locking between two quasicondensates due to interwell tunneling. In the limit $l_J \lesssim \lambda_T$ the fluctuations of the relative phase are small, and we reproduce the results of the linearized theory of Ref. [1]. In the opposite case, we found the mean interwell coherence to decrease much slower ($\propto \lambda_T^2/l_J^2$) than the exponential law predicted by the linearized theory. We interpret such a behavior as a signature of the thermal creation of sine-Gordon solitons, which provide a shift of the relative phase by 2π and thus do not contribute to the coherence loss and the corresponding decrease of the density of states for phonons (the excitations responsible for the coherence loss at large distances).

Our analytic estimations are confirmed by numerical modeling of the equilibrium state as a final state of the system's relaxational evolution after a quench. This task is solved by extending our numerical method [25] to integration of two coupled 1D Gross-Pitaevskii equations.

We demonstrate, both analytically and numerically, that thermal fluctuations of the relative phase between two quasicondensates reduce the frequency of Josephson oscillations in proportion to $\sqrt{\langle \cos \theta_a \rangle}$ and broaden their spectrum. If the theoretically predicted value of ω_J is much less than the bandwidth of the thermal fluctuation (which is of the order

of the speed of sound divided by λ_T), regular Josephson oscillations are not observed.

APPENDIX A: DERIVATION OF EQ. (17)

We briefly recall here the basics of the transfer operator technique, following Refs. [18,19,23]. We introduce a lattice with the step $\Delta z = L/M$, with M being the number of sites. We assume cyclic boundary conditions,

$$\theta_{a\,M+1} \equiv \theta_{a\,1}. \tag{A1}$$

Then the partition function (12) can be written as

$$Z = \int d\theta_{a\,1} \cdots \int d\theta_{a\,M} \int d\theta_{a\,M+1}\, \delta(\theta_{a\,M+1} - \theta_{a\,1})$$
$$\times \prod_{j=1}^{M} \exp[-f(\theta_{a\,j}, \theta_{a\,j+1})], \tag{A2}$$

where

$$f(\theta_{a\,j}, \theta_{a\,j+1}) = \frac{\hbar^2 n_{1D}}{4mk_B T \Delta z}(\theta_{a\,j} - \theta_{a\,j+1})^2$$
$$+ \frac{\hbar J n_{1D} \Delta z}{k_B T}(2 - \cos \theta_{a\,j} - \cos \theta_{a\,j+1}) \tag{A3}$$

and integrals in our case are taken from $-\pi$ to π. We omit the constant prefactor in Eq. (A2) for the sake of simplicity. Assume that eigenfunctions $\Psi_n(\theta)$ of the transfer operator

$$\int d\theta_{a\,j}\, e^{-f(\theta_{a\,j}, \theta_{a\,j+1})} \Psi_n(\theta_{a\,j}) = e^{-\epsilon_n \Delta z} \Psi_n(\theta_{a\,j+1}) \tag{A4}$$

form a set, which is complete, orthogonal, and normalized to unity, namely

$$\int d\theta\, \Psi_{n'}^*(\theta) \Psi_n(\theta) = \delta_{n'n}, \tag{A5}$$

$$\sum_n \Psi_n^*(\theta') \Psi_n(\theta) = \delta(\theta' - \theta). \tag{A6}$$

Substituting Eq. (A6) into Eq. (A2) and using Eq. (A4), we obtain

$$Z = \sum_n \exp(-\epsilon_n L). \tag{A7}$$

The eigenvalues ϵ_n are positive; in the thermodynamic limit the partition function (A7) is dominated by the lowest eigenvalue ϵ_0,

$$Z \approx \exp(-\epsilon_0 L), \quad L \to \infty. \tag{A8}$$

In the continuous limit $\Delta z \to 0$ Eq. (A4) is equivalent to the Schrödinger-type equation (19). Strictly speaking, the spectrum of Eq. (A4) is shifted with respect to the spectrum of Eq. (19) by a common offset s_0, which is related to normalization of the eigenfunctions. Since s_0 does not depend on n, we neglect it in our calculations.

To calculate correlation functions, in particular, Eq. (17), we note that $e^{i\theta_a(z')}$ and $e^{-i\theta_a(z)}$ act on Ψ_0 like quantum-mechanical perturbations, coupling Ψ_0 to the whole spectrum of eigenfunctions with the matrix elements given by Eq. (18). Therefore the leading term for $\langle \exp[i\theta_a(z') - i\theta_a(z)] \rangle$ in the limit of $L \to \infty$ is the second-order perturbative correction to the propagator for the ground state (with L playing the role of imaginary time), and we obtain thus Eq. (17).

APPENDIX B: DERIVATION OF EQS. (23) AND (24)

We begin with the lattice version of the classical sine-Gordon Hamiltonian that describes the dynamics of the antisymmetric mode of our system:

$$H_a = \sum_{j=1}^{M} \left[\frac{\hbar^2 n_{1D}}{4m\Delta z}(\theta_{aj} - \theta_{aj+1})^2 + \frac{g}{\Delta z}\delta N_{aj}^2 \right. $$
$$\left. + 2\hbar J n_{1D}\Delta z (1 - \cos\theta_{aj}) \right], \qquad (B1)$$

where the jth generalized coordinate $\delta N_{aj} = \delta\rho_a \Delta z$ is the half difference of the atomic numbers in the first and second quasicondensates at the jth site, i.e., the variable canonically conjugate to the local phase difference θ_{aj} (the jth generalized momentum). Here we neglect the nonlinear coupling between the symmetric and antisymmetric modes, as in Eq. (11) in the continuous limit.

For the sake of simplicity, we assume an odd number of sites in the lattice, $M = 2M_0 + 1$, where M_0 is a positive integer. Then we do a canonical transformation

$$\delta N_{aj} = \sum_{\ell=-M_0}^{M_0} \delta\tilde{N}_a(\ell)\eta(\ell,j), \quad \theta_{aj} = \sum_{\ell=-M_0}^{M_0} \tilde{\theta}_a(\ell)\eta(\ell,j), \quad (B2)$$

where

$$\eta(\ell,j) = \begin{cases} \sqrt{2/M}\cos(2\pi\ell j/M), & \ell = -1,-2,\ldots,-M_0, \\ 1/\sqrt{M}, & \ell = 0, \\ \sqrt{2/M}\sin(2\pi\ell j/M), & \ell = 1,2,\ldots,M_0. \end{cases} \quad (B3)$$

Then Hamiltonian (B1) reads

$$H_a = \sum_{\ell=-M_0}^{M_0} \left\{ \frac{\hbar^2 n_{1D}}{2m\Delta z}[1 - \cos(2\pi\ell/M)]\tilde{\theta}_a^2(\ell) + \frac{g}{\Delta z}\delta\tilde{N}_a^2(\ell) \right\}$$
$$+ 2\hbar J n_{1D}\Delta z \sum_{j=1}^{M} \left\{ 1 - \cos\left[\sum_{\ell=-M_0}^{M_0} \tilde{\theta}_a(\ell)\eta(\ell,j)\right] \right\}. \quad (B4)$$

From the Hamiltonian equations

$$\frac{d}{dt}\delta\tilde{N}_a(\ell) = \frac{\partial H_a}{\partial \tilde{\theta}_a(\ell)}, \quad \frac{d}{dt}\tilde{\theta}_a(\ell) = -\frac{\partial H_a}{\partial \delta\tilde{N}_a(\ell)}, \quad (B5)$$

we find, in particular,

$$\frac{d}{dt}\tilde{\theta}_a(0) = -\frac{2g\delta\tilde{N}_a(0)}{\Delta z}, \quad (B6)$$

$$\frac{d}{dt}\delta\tilde{N}_a(0) = 2\hbar J n_{1D}\Delta z \sum_{j=1}^{M} \sin\left[\sum_{\ell=-M_0}^{M_0} \tilde{\theta}_a(\ell)\eta(\ell,j)\right]. \quad (B7)$$

In the limit of $\Delta z \to 0$ the sums over j converge to integrals over z. Taking into account that $N_{12} = \int dz\,\delta\rho_a = \sum_{j=1}^{M} \delta N_{aj} = \sqrt{M}\delta\tilde{N}_a(0)$, identifying the generalized momentum conjugate to N_{12} as $\Phi = \tilde{\theta}_a(0)/\sqrt{M} = (1/M)\sum_{j=1}^{M} \theta_{aj}$, and recalling that $L = M\Delta z$, we obtain Eqs. (23) and (24). The spatially fluctuating part of the phase is then $\theta_a - \Phi$.

[1] N. K. Whitlock and I. Bouchoule, Phys. Rev. A **68**, 053609 (2003).

[2] I. Bouchoule, Eur. Phys. J. D **35**, 147 (2005).

[3] I. Lesanovsky and W. von Klitzing, Phys. Rev. Lett. **98**, 050401 (2007).

[4] R. Hipolito and A. Polkovnikov, Phys. Rev. A **81**, 013621 (2010).

[5] H.-P. Stimming, N. J. Mauser, J. Schmiedmayer, and I. E. Mazets, Phys. Rev. Lett. **105**, 015301 (2010).

[6] J. Brand, T. J. Haigh, and U. Zülicke, Phys. Rev. A **81**, 025602 (2010).

[7] T. W. A. Montgomery, R. G. Scott, I. Lesanovsky, and T. M. Fromhold, Phys. Rev. A **81**, 063611 (2010).

[8] T. Betz, S. Manz, R. Bücker, T. Berrada, Ch. Koller, G. Kazakov, I. E. Mazets, H.-P. Stimming, A. Perrin, T. Schumm, and J. Schmiedmayer, Phys. Rev. Lett. **106**, 020407 (2011).

[9] A. Smerzi, S. Fantoni, S. Giovanazzi, and S. R. Shenoy, Phys. Rev. Lett. **79**, 4950 (1997).

[10] V. N. Popov, *Functional Integrals and Collective Excitations* (Cambridge University Press, Cambridge, 1987).

[11] C. Mora and Y. Castin, Phys. Rev. A **67**, 053615 (2003).

[12] M. A. Cazalilla, J. Phys. B **37**, S1 (2004).

[13] S. Hofferberth, I. Lesanovsky, B. Fischer, T. Schumm, and J. Schmiedmayer, Nature (London) **449**, 324 (2007).

[14] S. Hofferberth, I. Lesanovsky, T. Schumm, A. Imambekov, V. Gritsev, E. Demler, and J. Schmiedmayer, Nat. Phys. **4**, 489 (2008).

[15] S. Manz, R. Bücker, T. Betz, Ch. Koller, S. Hofferberth, I. E. Mazets, A. Imambekov, E. Demler, A. Perrin, J. Schmiedmayer, and T. Schumm, Phys. Rev. A **81**, 031610(R) (2010).

[16] F. D. M. Haldane, Phys. Rev. Lett. **47**, 1840 (1981).

[17] V. Gritsev, A. Polkovnikov, and E. Demler, Phys. Rev. B **75**, 174511 (2007).

[18] J. A. Krumhansl and J. R. Schrieffer, Phys. Rev. B **11**, 3535 (1975).

[19] J. F. Currie, J. A. Krumhansl, A. R. Bishop, and S. E. Trullinger, Phys. Rev. B **22**, 477 (1980).

[20] H.-P. Stimming, N. J. Mauser, J. Schmiedmayer, and I. E. Mazets, Phys. Rev. A **83**, 023618 (2011).

[21] M. Gring, M. Kuhnert, T. Langen, T. Kitagawa, B. Rauer, M. Schreitl, I. Mazets, D. Adu Smith, E. Demler, and J. Schmiedmayer, Science **337**, 1318 (2012).

[22] V. N. Popov, Pis'ma Zh. Eksp. Teor. Fiz. **31**, 560 (1980) [Sov. Phys. JETP Lett. **31**, 526 (1980)]; see also [11].

[23] D. J. Scalapino, M. Sears, and R. S. Ferrell, Phys. Rev. B **6**, 3409 (1972).

[24] *Handbook of Mathematical Functions*, edited by M. Abramowitz and I. A. Stegun (Dover, New York, 1972), Chap. 20.

[25] P. Grisins and I. E. Mazets, Phys. Rev. A **84**, 053635 (2011).

[26] M. Thalhammer, M. Caliari, and C. Neuhauser, J. Comput. Phys. **228**, 822 (2009).

[27] J. A. C. Weideman and B. M. Herbst, SIAM J. Numer. Anal. **23**, 485 (1986).

[28] M. Gitterman, *The Noisy Oscillator* (World Scientific, Singapore, 2005), Chap. 8.

Metropolis–Hastings thermal state sampling for numerical simulations of Bose–Einstein condensates

Pjotrs Grišins [a,*], Igor E. Mazets [a,b]

[a] *Vienna Center for Quantum Science and Technology, Atominstitut TU Wien, 1020 Vienna, Austria*
[b] *Ioffe Physico-Technical Institute, Russian Academy of Sciences, 194021 St. Petersburg, Russia*

ABSTRACT

We demonstrate the application of the Metropolis–Hastings algorithm to sampling of classical thermal states of one-dimensional Bose–Einstein quasicondensates in the classical fields approximation, both in untrapped and harmonically trapped case. The presented algorithm can be easily generalized to higher dimensions and arbitrary trap geometry. For truncated Wigner simulations the quantum noise can be added with conventional methods (half a quantum of energy in every mode). The advantage of the presented method over the usual analytical and stochastic ones lies in its ability to sample not only from canonical and grand canonical distributions, but also from the generalized Gibbs ensemble, which can help to shed new light on thermodynamics of integrable systems.

© 2014 The Authors. Published by Elsevier B.V.
This is an open access article under the CC BY license
(http://creativecommons.org/licenses/by/3.0/).

1. Introduction

The recent advances in experimental methods allowed precise control and manipulation of ultracold atoms in various trap [1–3] and optical lattice geometries [4–6], including gases at temperatures much lower than the degeneracy temperature.

The effective field theory of a cold gas of neutral bosonic atoms with short-range repulsive interactions is given by the second quantized Hamiltonian (in the following we deal explicitly with a one-dimensional (1D) case, where quasicondensation takes place instead of true condensation [7])

$$\hat{H} = \hat{H}_0 + \hat{H}_{\text{int}}, \tag{1}$$

$$\hat{H}_0 = \int dz\, \hat{\psi}^\dagger(z) \left[-\frac{\hbar^2}{2m}\frac{\partial^2}{\partial z^2} + V(z) \right] \hat{\psi}(z), \tag{2}$$

$$\hat{H}_{\text{int}} = \frac{g}{2} \int dz\, \hat{\psi}^\dagger(z)\, \hat{\psi}^\dagger(z)\, \hat{\psi}(z)\, \hat{\psi}(z), \tag{3}$$

where $\hat{H}_0$ and $\hat{H}_{\text{int}}$ are respectively the free-particle and interaction Hamiltonians, $\hat{\psi}(z)$ is the field operator, which annihilates a particle at position z, m is the atomic mass, $V(z)$ is the external trap potential and g is the effective interaction strength, given in the experimentally relevant case of a harmonic transversal confinement with trapping frequency ω_r by $g = 2\omega_r a_s \hbar$, with a_s being the s-wave scattering length.

The usual experimental setups deal with thousands of atoms [1], so the quantum dynamics can be numerically simulated only using various approximations. The one approximation especially suited for studies of weakly interacting cold atomic gases is the classical field approximation, where we replace the quantum field operator of the effective field theory $\hat{\psi}(z)$ by a classical field $\psi(z)$ [8]. This approach is valid for low temperatures, where we have a range of macroscopically occupied modes $\langle \hat{\psi}_n^\dagger \hat{\psi}_n \rangle \gg 1$; the operators $\hat{\psi}_n$ are defined through the normalized eigenfunctions of the one-body non-interacting Hamiltonian $\hat{H}_0$. The evolution of this redefined classical order parameter $\psi(z)$ is then governed by the celebrated Gross–Pitaevskii equation (GPE) [9].

In experiments with cold atomic gases the system is usually prepared in thermal equilibrium, before a quench or another manipulation is applied, therefore the numerical methods for sampling the thermal initial condition $\psi_0(z)$ are of great importance. The quantum correction for the classical thermal state of a weakly interacting system can be introduced using the so-called truncated Wigner approximation (TWA), where zero-point quantum oscillations are taken into account in the initial state only, but the subsequent evolution is classical [10].

Conventional methods of initial state sampling include analytical ones [11,12], where the gas is initialized with a Bose–Einstein

* Corresponding author. Tel.: +43 158801141853.
 E-mail addresses: peter.grishin@gmail.com, pgrisins@ati.ac.at (P. Grišins).

distribution of Bogoliubov quasiparticles with random phases, as well as stochastic ones [13,14], where the thermal state is achieved during imaginary time GPE evolution with Langevin noise.

In the present paper we propose another way of sampling the initial distribution, namely using the Metropolis–Hastings algorithm. We believe that in some cases it might be preferable over the analytical methods, as it does not use Bogoliubov-type approximations, and may be used to sample states out of a generalized Gibbs ensemble, which is impossible with existing stochastic realizations.

2. Metropolis–Hastings algorithm

The Metropolis–Hastings algorithm is a Markov chain Monte Carlo method for sampling a probability distribution, especially suited for systems with many degrees of freedom [15]. For a broad overview of quantum and classical Monte Carlo methods, including the Metropolis–Hastings algorithm, see [16,17] and references therein.

In the present paper we demonstrate the implementation of the Metropolis–Hastings method for 1D Bose–Einstein quasicondensate without confinement (implying periodic boundary conditions) as well as for the experimentally relevant case of a harmonic longitudinal confinement. The method can be easily generalized to higher dimensions and other trap geometries.

This method has been already applied to classical simulations of cold Bose gases [18], but it has not been explicitly formulated as a step-by-step algorithm. In the present paper we systematically study the convergence properties of this method and outline its application to sampling the generalized Gibbs ensemble (GGE).

In our particular realization the algorithm reads as follows:

1. Initialization:
   (a) Choose an initial order parameter $\psi_0(z)$. Specific choices of $\psi_0(z)$ will be discussed in the following section.
   (b) Calculate the reduced entropy $S_0 = -\beta(\langle\psi_0|\hat{H}|\psi_0\rangle - \mu\langle\psi_0|\hat{\mathcal{N}}|\psi_0\rangle)$, where β is the inverse temperature, μ is the chemical potential (both β and μ are fixed external parameters), and $\hat{\mathcal{N}} = \int \hat{\psi}^\dagger(z)\hat{\psi}(z)\,dz$ is the particle number operator. Note that the free energy does not enter the expression for S_0, meaning that the zero-level of the latter is not defined. This is justified by the fact that we are interested only in differences of the reduced entropy, and not in its absolute value.
2. For each iteration $N \in [1, N_{\max}]$:
   (a) Generate a candidate field $\psi_N(z)$ by varying the energy. This variation of energy can be achieved by adding either a density perturbation
   $$\psi_N(z) = \psi_{N-1}(z)\left[1 + c_1 v_r \sin(k_r z + \phi_r)\right], \qquad (4)$$
   or a phase perturbation
   $$\psi_N(z) = \psi_{N-1}(z)\exp\left[i\, c_2 v_r \sin(k_r z + \phi_r)\right], \qquad (5)$$
   to the field from the previous iteration ('the seeding field'). Whether to choose the one or the other is decided at random (by a 'coin toss'). The meaning and values of the parameters are summarized in Table 1.
   (b) Vary the particle number
   $$\psi_N(z) = (1 + c_3 u_r)\psi_N(z). \qquad (6)$$
   (c) Calculate the reduced entropy of the candidate field
   $$S_N = -\beta\left(\langle\psi_N|\hat{H}|\psi_N\rangle - \mu\langle\psi_N|\hat{\mathcal{N}}|\psi_N\rangle\right). \qquad (7)$$
   (d) Calculate the acceptance ratio $a = \frac{p_N}{p_{N-1}} = \frac{e^{S_N}}{e^{S_{N-1}}} = e^{S_N - S_{N-1}}$, where $p_N = \frac{1}{Z}e^{S_N}$ is the Boltzmann probability to find the field in the state $\psi_N(z)$. The main advantage of the Metropolis–Hastings algorithm lies the fact that we have to evaluate only the ratio of probabilities, in this way avoiding to calculate the partition function Z, which is practically impossible for interacting systems with many degrees of freedom. Then we check the value of a:

Table 1
Numerical parameters of the Metropolis–Hastings algorithm.

Parameter	Description
v_r, u_r	Real random numbers, distributed normally with zero mean and unit variance.
c_1, c_2, c_3	Numerical constants governing the rate of convergence to the equilibrium state. In the presented results they have been empirically chosen to be $c_1 = 2(n_0)^{-1}$, $c_2 = 0.1$ and $c_3 = 0.001$, where $n_0 = \max|\psi_0|^2$ is the maximal initial density. This particular choice provided typical values of the acceptance ratio in each iteration $a \in [0.4, 0.6]$, which gave the fastest convergence to equilibrium. It was numerically checked that different choices of those constants did not affect the resulting state, only the rate of convergence.
ϕ_r	Random phase $\phi_r \in [0, 2\pi)$ picked from the uniform distribution.
k_r	Random wave number picked from the set $\{\pm\delta k, \pm2\delta k, \ldots, \pm k_{\max}\}$, where $\delta k = 2\pi/L$, L is the length of the simulated region and $k_{\max}$ is the cutoff wave number. It was numerically checked that the results do not depend on this cutoff as long as it is larger than the inverse healing length $\xi^{-1} = \sqrt{mg\bar{n}/\hbar^2}$, where $\bar{n}$ is the mean density. So we present results where $k_{\max} = \mathfrak{N}_z\,\delta k/2$ is the maximal allowed wave number on a lattice of $\mathfrak{N}_z$ sampling points.

   i. If $a \geq 1$, then the candidate state is more probable than the seeding state, so we keep the former.
   ii. If $a < 1$, we pick a uniform random number $r \in [0, 1]$. If $r \leq a$, the candidate state is accepted; but if $r > a$, the candidate state is discarded and the seeding state is kept for the next iteration $\psi_N(z) := \psi_{N-1}(z)$.
   (e) Proceed to the next iteration.

As a result we have a Markov chain of states $\psi_N(z)$, $N \in [0, N_{\max}]$, which can be used as thermal initial states for classical fields simulations. It is important to throw away the states obtained at early iterations (so-called 'burn-in' period), where the thermal state is not yet achieved. Neighboring states ψ_N and ψ_{N+1} are usually highly correlated (as they differ by only one elementary perturbation), so it is necessary to throw away majority of the results, picking only one state out of N_a, where N_a is calculated from the iteration-to-iteration autocorrelation length. We will return to these two issues in the results section.

Straightforward generalizations of the algorithm are easily conceivable:

1. Arbitrary trap geometry, as we can freely modify the trapping potential V in the total Hamiltonian $\hat{H}$. In general the perturbations in Eqs. (5) and (6) can be modified to be the eigenfunctions of the trapping potential (e.g. in the case of harmonic confinement $V(z) \propto z^2$ we can take harmonic oscillator eigenfunctions instead of sine-waves). But in practice using potential-specific eigenfunctions instead of plane waves did not give any speed-up to the achievement of the steady state, so the algorithm can be used without this modification.
2. Any number of dimensions. This requires representing the order parameter as a scalar field on many-dimensional space $\psi(\vec{z})$, the perturbations (Eqs. (5) and (6)) being modified accordingly as $\sin(\vec{k}_r\vec{z} + \phi_r)$.
3. Canonical state sampling. Reduced entropy becomes $S_N = -\beta\langle\psi_N|\hat{H}|\psi_N\rangle$, and we have to omit the 2b stage of the algorithm to make sure the particle number does not change.
4. Generalized Gibbs ensemble sampling. Reduced entropy now reads
$$S_N = -\beta\Bigg(\langle\psi_N|\hat{H}|\psi_N\rangle - \mu\langle\psi_N|\hat{\mathcal{N}}|\psi_N\rangle$$
$$- \sum_i \mu_i\langle\psi_N|\hat{I}_i|\psi_N\rangle\Bigg), \qquad (8)$$
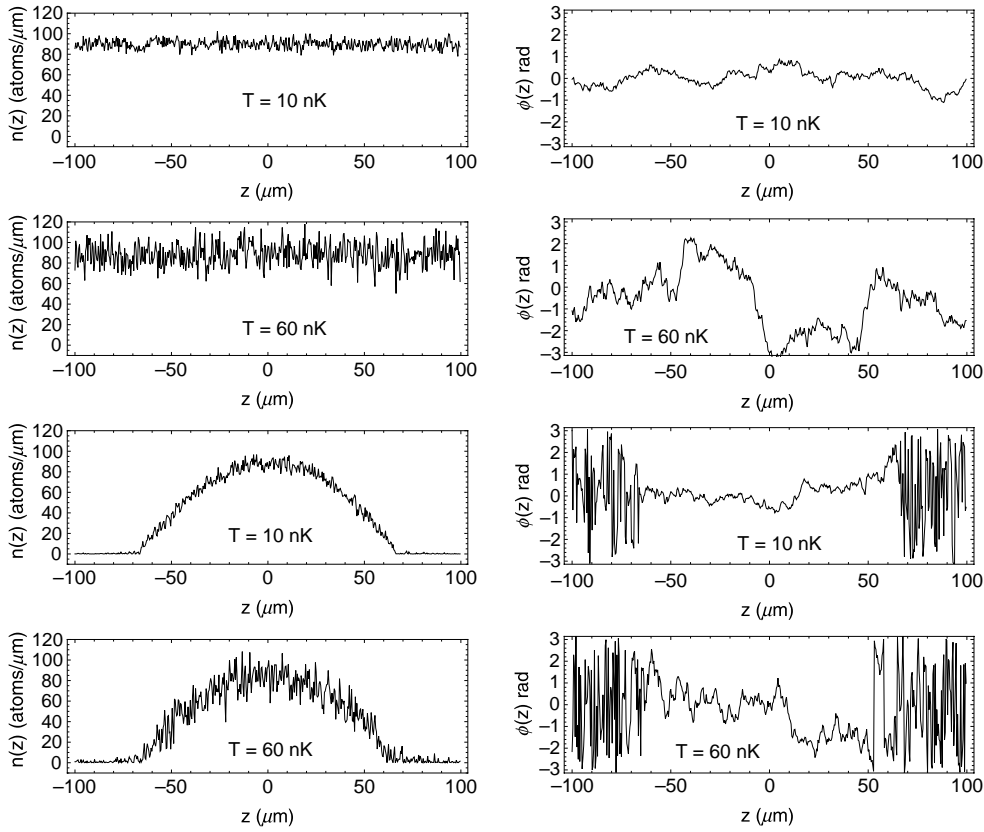
Fig. 1. Typical examples of the grand canonical thermal state with the temperatures $T = 10$ nK and 60 nK (labels on the panels) of the interacting 1D BEC, achieved after $N_{max} = 10^5$ Metropolis–Hastings iterations in the untrapped system with periodic boundary conditions (four top panels) and harmonically trapped case (four bottom panels). Quasicondensate local densities $n(z)$ (left), measured in atoms per micrometer, and phases $\phi(z)$ (right), measured in radians, as a function of the longitudinal direction z in micrometers. The initial conditions in the case of the untrapped system were taken to be the ground state of the non-interacting gas, and in the case of the harmonic confinement as a Thomas–Fermi parabolic density profile with constant zero phase. Note that achieved thermal state is not dependent on the initial conditions (see discussion in the text). Extensive fluctuations of the phase at the edges of harmonically trapped quasicondensate are due to the fact that the density there is close to zero, and the phase can take arbitrary values. Physical parameters of the simulations are summarized in Table 2.

where $\hat{I}_i$ are the local conserved charges (integrals of motion) of the system, in addition to the energy $\langle \hat{H} \rangle$ and the particle number $\langle \hat{\mathcal{N}} \rangle$, and μ_i are generalized potentials. For instance, in case of 1D GPE there exists an infinite number of local conserved charges, which can be explicitly calculated using Zakharov–Shabat construction [19]. We regard this possibility of GGE sampling as the primary advantage of the presented algorithm. In fact, simulation of the GGE requires only redefinition of the Hamiltonian to $\hat{H}' = \hat{H} - \frac{1}{\beta} \sum_i \mu_i \hat{I}_i$, to which the previously described algorithm can be applied without further modification. We reserve the detailed analysis of this case for a separate publication.

3. Results

In the following we demonstrate the application of the algorithm to generate a grand canonical thermal state for an untrapped gas of neutral ^{87}Rb atoms and an experimentally relevant case of the same gas in a harmonic confinement. The parameters of the simulation are summarized in Table 2.

Typical examples of the grand canonical thermal state of the 1D Bose–Einstein quasicondensate after $N_{max} = 10^5$ Metropolis–Hastings iterations are presented in Fig. 1.

The initial state for all the presented results was taken to be the ground state of the non-interacting gas ($n_0(z) = n_0 = $ const, $\phi_0(z) = 0$) in the untrapped case, and a Thomas–Fermi parabolic density profile with constant zero phase in the case of the harmonic confinement.

Table 2
Simulation parameters of the systems presented in the results section.

Parameter	Description
$m = 87 \cdot 1.67 \cdot 10^{-24}$ g	Atomic mass of ^{87}Rb atoms
$a_s = 5.3 \cdot 10^{-7}$ cm	s-wave scattering length
$T = 10, 60$ or 120 nK	Temperature
$\omega_r = 2\pi \cdot 2000$ s^{-1}	Transversal trapping frequency
$n_0 = 90$ atoms/μm	Maximal initial linear atom density of the cloud
$g = 2\omega_r a_s \hbar$	1D interaction strength
$\mu = g n_0$	Chemical potential
$\omega_l = 2\pi \cdot 10$ s^{-1}	Longitudinal trapping frequency in case of a harmonic confinement
$L = 200\,\mu$m	Total length of the simulation region
$\mathfrak{N}_z = 512$	Number of spatial discretization points, so the state $\psi(z)$ has $\mathfrak{N}_z$ degrees of freedom
$N_{max} = 10^5$	Total number of Metropolis–Hastings iterations
$n(z) = |\psi(z)|^2$	Local density
$\phi(z) = \arg \psi(z)$	Local phase

The achievement of the steady state is controlled by temperature measurement at the each iteration of the algorithm, calculated from the g_1 autocorrelation function

$$g_{1,N}(\Delta z) = \frac{\int \psi_N^*(z) \, \psi_N(z + \Delta z) \, \mathrm{d}z}{\int |\psi_N(z)|^2 \mathrm{d}z}. \tag{9}$$

In thermodynamic equilibrium at positive temperatures in 1D g_1 is exponentially decaying with Δz, confirming the fact that there can be no true Bose–Einstein condensate in this case

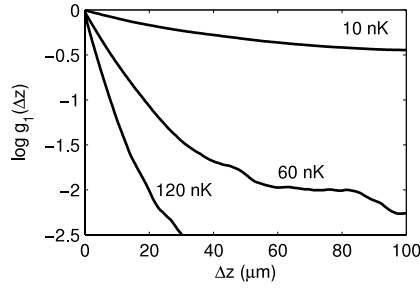$$g_1(\Delta z) = \mathrm{e}^{-|\Delta z|/\lambda_T}, \tag{10}$$

Fig. 2. Natural logarithm of the g_1 correlation function in the homogeneous case for the temperatures $T = 10, 60$ and 120 nK (from top to bottom) at the last iteration N_{max} of the algorithm, averaged over the ensemble of 70 realizations. These g_1 functions are used to calculate averaged temperatures presented in Fig. 3(a). The linear region of the logarithm spans from 0 till ≈ 15 μm, and it is used in temperature measurement. The bending and fluctuations in the subsequent region are due to the finite size effects (as the total size of the system is $L = 200$ μm) and are to be discarded.

where λ_T is thermal coherence length

$$\lambda_T = \frac{2\hbar^2 \bar{n}}{m k_B T}, \tag{11}$$

with k_B being the Boltzmann constant and $\bar{n} = \frac{1}{L'}\int_0^L |\psi(z)|^2 dz$ the mean density of the cloud. L' is the averaging length, which is the length of the integration region in Eq. (9) as well. In case of untrapped gas $L' = L$ is the total simulation region, but in case of harmonic confinement the integration region contains only the points where the local density $n(z)$ is larger than one tenth of the mean density. This helps to get rid of unessential boundary perturbations, probing the temperature of 'the bulk' of the condensate.

The Metropolis–Hastings 'evolution' of the temperature is presented in Fig. 3, with one particular example of the g_1 function in Fig. 2. It is evident that the thermal equilibrium is achieved after $N = (2-6) \cdot 10^4$ iterations.

During the initial phases of this 'evolution' the system passes through a non-equilibrium region, so temperature in general sense in not well defined until the final equilibrium is reached. Though even in the non-equilibrium case the system always possesses a well-defined energy, so we can always formally define an emergent 'non-equilibrium' temperature as the temperature of a completely thermalized system with the given average energy. This emergent temperature is then measured by g_1. We stress though that before the steady state is achieved the 'temperature' can be used as a convergence monitor only. Clearly, there is no real physical process behind the apparent 'heating' in Fig. 3 as there is no real time evolution. We also note that the temperature calculated from g_1 is independent of β in Eq. (7), the latter being an external parameter, fixing our desired temperature.

Fig. 4. Influence of the initial state on the rate of convergence to the thermal state. Temperatures during the Metropolis–Hastings 'evolution' as a function of the iteration number N in the case of untrapped gas for $T = 60$ nK, averaged over 70 realizations. Thick line: zero-temperature state of the non-interacting gas, cf. Fig. 3(a). Thin line: thermal gas of Bogoliubov quasiparticles with random phases and constant amplitudes (see explanation in the text). Both choices of initial conditions eventually lead to equilibrium, but in case of the 'Bogoliubov gas' the convergence is faster, meaning that it is a better 'initial guess' for the thermal state. In this particular realization the temperature is rising during the 'evolution', but we note that if we had chosen a higher-than-desired initial temperature, then the temperature would be dropping to the desired value. *Inset.* Temperature of the state, produced by the real-time GPE evolution starting from the achieved thermal state as a function of time. Dots: one single realization, solid line: average over 70 realizations. The stability of the temperature shows that the initial state was indeed the thermal state of the Gross–Pitaevskii Hamiltonian (see the text for further discussion).

Another independent test whether the achieved state is thermal is the real-time development of the state, as by definition the thermal state should remain thermal during such evolution. To check this criterion we prepared the thermal state of the untrapped gas with Metropolis algorithm and then propagated it in real time with Gross–Pitaevskii equation (there exist efficient algorithms for solving real-time GPE, see e.g. [20,21]). The results, presented in the inset to Fig. 4, show that indeed the temperature of the state does not change on average, assuring that the initial state was thermal with respect to the Gross–Pitaevskii Hamiltonian.

As in all realization of Metropolis–Hastings algorithm a 'good guess' of the initial state is essential for the fast convergence. In Fig. 4 we compare the beforementioned zero-temperature initial conditions with the initial state given by the thermal gas of Bogoliubov quasiparticles with random phases and constant amplitudes, given by the equilibrium Bose–Einstein distribution at the desired temperature of 60 nK [11,12]. This initial condition seems to be a much better 'initial guess', leading to faster convergence. Note that the analytical method is only an approximation (implying weak interactions and neglecting the variance of the amplitudes of the quasiparticles), meaning that it gives a non-equilibrium state, which though is expected to be close to the desired thermal equilibrium: for instance, in Fig. 4 we see that the emergent 'non-equilibrium' temperature of this initial condition is about 48 nK,
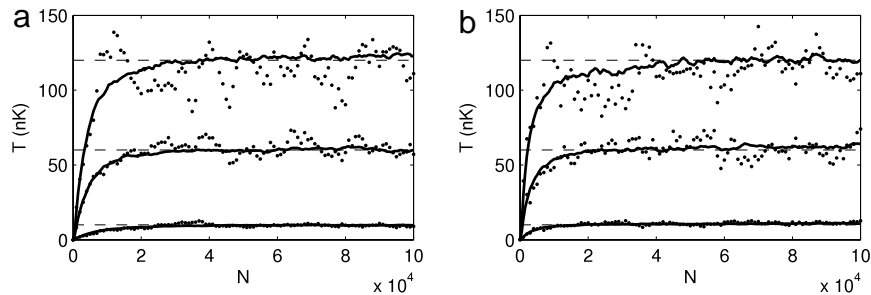

Fig. 3. Temperatures during the Metropolis–Hastings 'evolution' as a function of the iteration number N in the case of untrapped (a) and harmonically trapped (b) gas for three equilibrium temperatures (given as external parameters) $T = 10, 60$ and 120 nK. These temperatures are represented by three horizontal dashed lines serving as guides for the eye. Dots stand for one particular realization of the algorithm for the three temperatures (respectively, from bottom to top), and the corresponding solid lines show the averaged temperature over an ensemble of 70 realizations, each having the same initial conditions. Large temperature fluctuations in a single realization stem from the finite size of the simulation region, as they should converge to the equilibrium value only in thermodynamic limit. But from the ensemble averages it is evident that the thermal equilibrium is achieved after $N = 2 - 6 \cdot 10^4$ iterations.
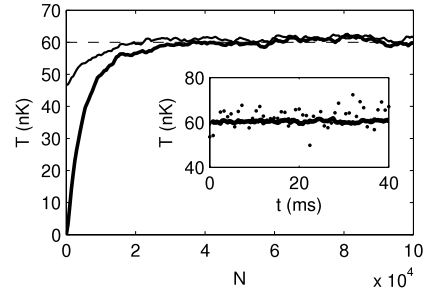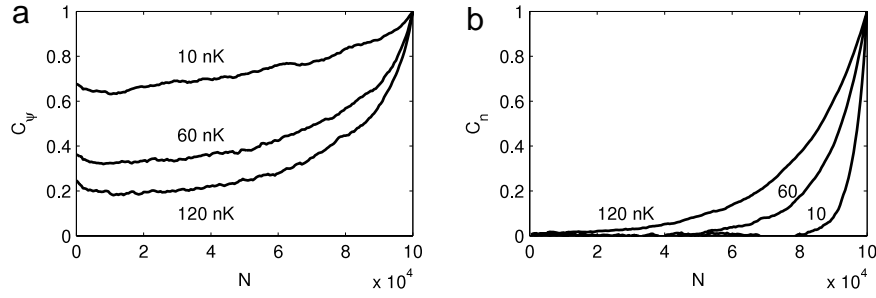
Fig. 5. (a) Order parameter correlation function C_ψ for the untrapped gas as a function of the iteration number N for temperatures 10, 60 and 120 nK (from top to bottom), averaged over 70 realizations. Remaining strong phase coherence after 10^5 iterations is due to the existence of long-range order in finite-size quasi-BEC. (b) Density fluctuation correlation function C_n for the same realizations as in subfigure (a) for temperatures 10, 60 and 120 nK (from bottom to top).

which is lower than the expected 60 nK. So this is one particular example where numerical methods are superior to the analytical ones.

It is well known that Markov chain methods give highly correlated samples from one iteration to the other. We present some correlators for the untrapped gas in Fig. 5, where C_ψ is the two-point correlation function of the last sample $\psi_{N_{\max}}(z)$

$$C_\psi = \mathrm{Re} \frac{\int \psi_N^*(z)\, \psi_{N_{\max}}(z)\, \mathrm{d}z}{\sqrt{\int |\psi_N(z)|^2 \mathrm{d}z} \cdot \sqrt{\int |\psi_{N_{\max}}(z)|^2 \mathrm{d}z}}, \quad (12)$$

and C_n is the density fluctuation correlation function of the last sample

$$C_n = \frac{\int \delta n_N(z)\, \delta n_{N_{\max}}(z)\, \mathrm{d}z}{\sqrt{\int \delta n_N(z)^2 \mathrm{d}z} \cdot \sqrt{\int \delta n_{N_{\max}}(z)^2 \mathrm{d}z}}, \quad (13)$$

where $\delta n(z) = n(z) - \bar{n}$, $n(z) = |\psi(z)|^2$, and $\bar{n} = \frac{1}{L'} \int n(z)\, \mathrm{d}z$ for the uniform gas.

It is evident that the order parameters still remain phase-correlated after 10^5 iterations, which is a consequence of the fact that we observe the system below the thermal gas to quasicondensate crossover temperature [22]: the thermal fluctuations are too weak to randomize the overall phase (note that the effects of phase diffusion are absent as there is no real-time propagation).

This remaining phase correlation has to be taken into account when performing simulations involving two or more independently prepared condensates, where a random constant overall phase difference should be added to the initial conditions at each realization. For one condensate it is not necessary, as only the phase difference is observable, and not the phase itself.

Density fluctuation correlation function C_n gives a better representation of the correlations in Metropolis–Hastings algorithm, and from the numerical simulations it follows that one should pick one state out of $N_a = (2 - 8) \cdot 10^4$ iterations (depending on the temperature) to assure statistical independence. It is always a safe choice to pick only one last realization out of the whole Markov chain, reinitializing the simulation for each 'measurement'.

The proposed Metropolis–Hastings method is generally slower (requiring more CPU time) than the analytical method of thermal Bogoliubov gas [11,12] or stochastic ones [13,14]. For instance, propagation of $N = 10^5$ steps to achieve the thermal states in Fig. 1 takes about 100 s on a 3.40 GHz Intel Core workstation, while a stochastic algorithm would require about 10 s and the analytical one would be instantaneous. Nevertheless, the proposed method is believed to be more precise in comparison with the analytical one (see Fig. 4 and discussion in the text) and more versatile in applications to generalized thermal ensembles in comparison to stochastic methods. In addition, it can be used as an independent benchmark for other numerical algorithms.

4. Conclusion

We developed an application of Metropolis–Hastings algorithm to sampling the classical thermal states of one-dimensional Bose–Einstein quasicondensates in classical field approximation in the case of untrapped gas with periodic boundary conditions and in experimentally relevant case of harmonic confinement. The achieved thermal steady state can be further used as an initial state for truncated Wigner simulations. In case when the quantum noise is important (e.g. collisions of condensates [23], prethermalization of a split quasicondensate [24]), it can be added to the thermal state using conventional methods [8,10].

The proposed algorithm can be generalized to higher dimensions and arbitrary trap geometry. We see the main advantage of the method in its ability to sample not only the conventional thermodynamic ensembles, but also the generalized Gibbs ensemble, which is believed to arise in the integrable one-dimensional bosonic gas [25,26].

Acknowledgments

References

[1] T. Berrada, S.V. Frank, R. Bücker, T. Schumm, J.-F. Schaff, J. Schmiedmayer, Integrated Mach–Zehnder interferometer for Bose–Einstein condensates, Nature Commun. 4 (2013) 2077. arXiv: arXiv:1303.1030v1. URL http://arxiv.org/abs/1303.1030.

[2] R. Desbuquois, L. Chomaz, T. Yefsah, J. Léonard, J. Beugnon, C. Weitenberg, J. Dalibard, Superfluid behaviour of a two-dimensional Bose gas, Nat. Phys. 8 (9) (2012) 645–648. http://dx.doi.org/10.1038/nphys2378. URL http://www.nature.com/doifinder/10.1038/nphys2378.

[3] C.-L. Hung, X. Zhang, N. Gemelke, C. Chin, Observation of scale invariance and universality in two-dimensional Bose gases, Nature 470 (7333) (2011) 236–239. http://dx.doi.org/10.1038/nature09722. URL http://www.ncbi.nlm.nih.gov/pubmed/21270797.

[4] I. Bloch, J. Dalibard, S. Nascimbène, Quantum simulations with ultracold quantum gases, Nat. Phys. 8 (4) (2012) 267–276. http://dx.doi.org/10.1038/nphys2259. URL http://www.nature.com/doifinder/10.1038/nphys2259.

[5] A. Reinhard, J.-F. Riou, L.A. Zundel, D.S. Weiss, S. Li, A.M. Rey, R. Hipolito, Self-trapping in an array of coupled 1D Bose gases, Phys. Rev. Lett. 110 (3) (2013) 033001. http://dx.doi.org/10.1103/PhysRevLett.110.033001. URL http://link.aps.org/doi/10.1103/PhysRevLett.110.033001.

[6] X. Zhang, C.-L. Hung, S.-K. Tung, C. Chin, Observation of quantum criticality with ultracold atoms in optical lattices, Science 335 (6072) (2012) 1070–1072. http://dx.doi.org/10.1126/science.1217990. URL http://www.ncbi.nlm.nih.gov/pubmed/22345397.

[7] F.D.M. Haldane, Effective harmonic-fluid approach to low-energy properties of one-dimensional quantum fluids, 47 (25) (1981) 2–5.

[8] P. Blakie, A. Bradley, M. Davis, R. Ballagh, C. Gardiner, Dynamics and statistical mechanics of ultra-cold Bose gases using c-field techniques, Adv. Phys. 57 (5) (2008) 363–455. http://dx.doi.org/10.1080/00018730802564254. URL http://www.tandfonline.com/doi/abs/10.1080/00018730802564254.

[9] F. Dalfovo, S. Giorgini, L. Pitaevskii, S. Stringari, Theory of Bose–Einstein condensation in trapped gases, Rev. Modern Phys. 71 (3) (1999) 463–512. URL http://rmp.aps.org/abstract/RMP/v71/i3/p463_1.

[10] A. Polkovnikov, Phase space representation of quantum dynamics, Ann. Physics 325 (8) (2010) 1790–1852. arXiv: arXiv:0905.3384v3. URL http://www.sciencedirect.com/science/article/pii/S0003491610000382.

[11] H.-P. Stimming, N. Mauser, J. Schmiedmayer, I.E. Mazets, Dephasing in coherently split quasicondensates, Phys. Rev. A 83 (2) (2011) 1–9. http://dx.doi.org/10.1103/PhysRevA.83.023618. URL http://link.aps.org/doi/10.1103/PhysRevA.83.023618.

[12] P. Grišins, I.E. Mazets, Thermalization in a one-dimensional integrable system, Phys. Rev. A 84 (053635) (2011) 1–4. http://dx.doi.org/10.1103/PhysRevA.84.053635. URL http://pra.aps.org/abstract/PRA/v84/i5/e053635, http://arxiv.org/abs/1108.5380.

[13] S. Cockburn, A. Negretti, N.P. Proukakis, C. Henkel, Comparison between microscopic methods for finite-temperature Bose gases, Phys. Rev. A 83 (4) (2011) 043619. http://dx.doi.org/10.1103/PhysRevA.83.043619. URL http://link.aps.org/doi/10.1103/PhysRevA.83.043619.

[14] R. Duine, H. Stoof, Stochastic dynamics of a trapped Bose–Einstein condensate, Phys. Rev. A 65 (1) (2001) 013603. http://dx.doi.org/10.1103/PhysRevA.65.013603. URL http://link.aps.org/doi/10.1103/PhysRevA.65.013603.

[15] N. Metropolis, A.W. Rosenbluth, M.N. Rosenbluth, A.H. Teller, E. Teller, Equation of state calculations by fast computing machines, J. Chem. Phys. 21 (6) (1953) 1087. http://dx.doi.org/10.1063/1.1699114. URL http://link.aip.org/link/JCPSA6/v21/i6/p1087/s1&Agg=doi.

[16] M. Newman, B. Gerard, Monte Carlo Methods in Statistical Physics, Oxford University Press, New York, 1999.

[17] J. Anderson, Quantum Monte Carlo: Origins, Development, Applications, Oxford University Press, New York, 2007.

[18] P. Bienias, K. Pawowski, M. Gajda, K. Rzaewski, Statistical properties of one-dimensional Bose gas, Phys. Rev. A 83 (3) (2011) 1–7. http://dx.doi.org/10.1103/PhysRevA.83.033610. URL http://link.aps.org/doi/10.1103/PhysRevA.83.033610.

[19] V. Zakharov, A. Shabat, Interaction between solitons in a stable medium, Sov. J. Exp. Theor. Phys. 37 (5) (1973) 823–828. URL http://adsabs.harvard.edu/abs/1973JETP...37..823Z.

[20] D. Vudragović, I. Vidanović, A. Balaz, P. Muruganandam, S. Adhikari, C programs for solving the time-dependent Gross–Pitaevskii equation in a fully anisotropic trap, Comput. Phys. Comm. 183 (2021) (2012) 1–8. arXiv: arXiv:1206.1361v1. URL http://www.sciencedirect.com/science/article/pii/S0010465512001270.

[21] P. Muruganandam, S. Adhikari, Fortran programs for the time-dependent Gross–Pitaevskii equation in a fully anisotropic trap, Comput. Phys. Comm. 180 (1888) arXiv: arXiv:0904.3131v4. URL http://www.sciencedirect.com/science/article/pii/S001046550900126X.

[22] I. Bouchoule, K. Kheruntsyan, G.V. Shlyapnikov, Interaction-induced crossover versus finite-size condensation in a weakly interacting trapped one-dimensional Bose gas, Phys. Rev. A 75 (3) (2007) 031606. http://dx.doi.org/10.1103/PhysRevA.75.031606. URL http://link.aps.org/doi/10.1103/PhysRevA.75.031606.

[23] A. Perrin, H. Chang, V. Krachmalnicoff, M. Schellekens, D. Boiron, A. Aspect, C.I. Westbrook, Observation of atom pairs in spontaneous four-wave mixing of two colliding Bose–Einstein condensates, Phys. Rev. Lett. 99 (15) (2007) 150405. http://dx.doi.org/10.1103/PhysRevLett.99.150405. URL http://link.aps.org/doi/10.1103/PhysRevLett.99.150405.

[24] M. Gring, M. Kuhnert, T. Langen, T. Kitagawa, B. Rauer, M. Schreitl, I.E. Mazets, D.A. Smith, E. Demler, J. Schmiedmayer, Relaxation and prethermalization in an isolated quantum system, Science 337 (6100) (2012) 1318–1322. http://dx.doi.org/10.1126/science.1224953. URL http://www.ncbi.nlm.nih.gov/pubmed/22956685, http://www.sciencemag.org/content/337/6100/1318, http://www.sciencemag.org/content/337/6100/1318.full, http://www.sciencemag.org/content/337/6100/1318.full.pdf, http://www.sciencemag.org/content/337/6100/1318.short.

[25] M. Rigol, V. Dunjko, V. Yurovsky, M. Olshanii, Relaxation in a completely integrable many-body quantum system: an ab initio study of the dynamics of the highly excited states of 1D lattice hard-core Bosons, Phys. Rev. Lett. 98 (5) (2007) 1–4. http://dx.doi.org/10.1103/PhysRevLett.98.050405. URL http://link.aps.org/doi/10.1103/PhysRevLett.98.050405.

[26] M. Kollar, F. Wolf, M. Eckstein, Generalized Gibbs ensemble prediction of prethermalization plateaus and their relation to nonthermal steady states in integrable systems, Phys. Rev. B 84 (054304) (2011) 1–11. arXiv: arXiv:1102.2117v1. URL http://prb.aps.org/abstract/PRB/v84/i5/e054304.